

Sheffield Hallam University

CNS endothelium expression of ADAM-17 and its role in multiple sclerosis pathogenesis.

HURST, Louise Anne.

Available from the Sheffield Hallam University Research Archive (SHURA) at:

<http://shura.shu.ac.uk/19848/>

A Sheffield Hallam University thesis

This thesis is protected by copyright which belongs to the author.

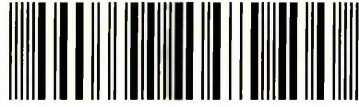
The content must not be changed in any way or sold commercially in any format or medium without the formal permission of the author.

When referring to this work, full bibliographic details including the author, title, awarding institution and date of the thesis must be given.

Please visit <http://shura.shu.ac.uk/19848/> and <http://shura.shu.ac.uk/information.html> for further details about copyright and re-use permissions.

Ausent Centre City Campus
Sheffield S1 1WB

101 930 634 3



REFERENCE

ProQuest Number: 10697154

All rights reserved

INFORMATION TO ALL USERS

The quality of this reproduction is dependent upon the quality of the copy submitted.

In the unlikely event that the author did not send a complete manuscript and there are missing pages, these will be noted. Also, if material had to be removed, a note will indicate the deletion.



ProQuest 10697154

Published by ProQuest LLC (2017). Copyright of the Dissertation is held by the Author.

All rights reserved.

This work is protected against unauthorized copying under Title 17, United States Code
Microform Edition © ProQuest LLC.

ProQuest LLC.
789 East Eisenhower Parkway
P.O. Box 1346
Ann Arbor, MI 48106 – 1346

**CNS endothelium expression of ADAM-17 and its role
in multiple sclerosis pathogenesis**

Louise Anne Hurst

A thesis submitted in partial fulfilment of the requirements of
Sheffield Hallam University for the degree of Doctor of Philosophy

May 2009

Dedication

*This thesis is dedicated to my mum,
who without her dedication to her children
this would not have been possible.
This is as much yours as it is mine.*

Abstract

Multiple sclerosis (MS) is an autoimmune disease of the central nervous system (CNS) characterised by focal lesions of inflammation and demyelination, with subsequent axonal damage. Various factors contribute to the pathogenesis of MS, including the breakdown of the blood-brain barrier (BBB), and increased local expression of inflammatory cytokines, matrix metalloproteinases (MMPs) and adhesion molecules. Upregulation of a disintegrin and metalloproteinase (ADAM)-17 has been previously reported in MS lesional white matter, associated with endothelial cells, astrocytes and macrophages. ADAM-17 is also increased in the spinal cord of rats with experimental autoimmune encephalomyelitis (EAE) (an animal model of MS), suggesting a role for the enzyme in MS pathogenesis. ADAM-17 is responsible for the proteolytic cleavage of a number of membrane-bound proteins, including tumour necrosis factor (TNF) and the chemokine and adhesion molecule, fractalkine, both of which have been implicated in MS pathogenesis. To determine the functional role of ADAM-17 in MS pathogenesis, an adult human brain endothelial cell line, hCMEC/D3 (a model of the BBB), was studied to determine the relationship between ADAM-17, its inhibitor (tissue inhibitor of metalloproteinase (TIMP)-3), fractalkine, and a number of other proteins shed by the enzyme. This work revealed that under pro-inflammatory cytokine (TNF) treatment, fractalkine expression is dramatically increased at the mRNA and protein level as determined by real-time RT-PCR and immunocytochemistry, respectively, and is shed at high concentrations from the endothelium as determined by ELISA. ADAM-17 expression was not significantly affected at the mRNA, protein, or activity level, suggesting other proteases play a role in fractalkine release, following TNF treatment of brain endothelial cells.

To further elucidate the relationship between ADAM-17 activity and fractalkine shedding, small interfering (si) RNA silencing of ADAM-17 was performed in the hCMEC/D3 endothelial cells line. This work revealed that despite knockdown of ADAM-17, fractalkine shedding was not significantly reduced. Again this suggests other mechanisms of regulating ectodomain shedding following TNF treatment are responsible for the release of fractalkine. Fractalkine expression in MS CNS tissue was observed in endothelial cells, astrocytes, macrophages and axons, however this expression was not significantly altered in comparison to control CNS white matter.

From the studies undertaken in this thesis, ADAM-17 is not the major sheddase of fractalkine from the CNS endothelium under pathological conditions. Further investigation into the mechanisms involved are required using both *in vitro* and *in vivo* methods. The observation of fractalkine shedding following cytokine treatment is another significant finding, as demonstrated here *in vitro*, which requires further investigation to understand the functional implications this may have *in vivo*.

Contents

Dedication	ii
Abstract	iii
Contents	iv
List of figures	xii
List of tables	xvi
Abbreviations	xvii
Publications related to this thesis	xxi
Acknowledgements	xxii
Quote	xxiii

Chapter 1

Introduction

1.1 Multiple sclerosis	2
1.1.1 Introduction	2
1.1.2 Clinical presentation and disease course in MS	2
1.1.3 Diagnosis	3
1.1.4 Genetic studies	5
1.1.5 Epidemiology of MS	7
1.1.6 Pathology	8
1.1.6.1 White matter pathology	8
1.1.6.2 Grey matter pathology	11
1.1.7 Axonal injury in MS	12
1.1.8 Pathogenesis of MS	13
1.2 Blood-brain barrier (BBB)	17
1.2.1 Basic structure	17
1.2.2 BBB endothelium tight junctions (TJs)	19
1.2.3 BBB disruption in MS	19
1.3 Mediators of inflammation	23
1.3.1 Cytokines in MS	23
1.3.1.1 TNF	24
1.3.1.1.1 TNF receptors	26
1.3.1.2 IL-1	29

1.3.1.3 IFN- γ	30
1.3.1.4 TGF- β 1	30
1.3.2 Chemokines	31
1.3.2.1 Fractalkine (CX3CL1)	32
1.4 Leukocyte recruitment to the endothelium	35
1.4.1 Adhesion molecules in MS	35
1.4.2 Leukocyte recruitment and extravasation	37
1.4.2.1 MMPs	38
1.5 ADAM-17	39
1.5.1 ADAM-17 structure	39
1.5.2 ADAM-17 as a sheddase	42
1.5.3 Regulation of ADAM-17 activity	42
1.5.4 Substrate specificity of ADAM-17	43
1.5.5 ADAM-17 expression	45
1.5.6 TIMP-3 and the TIMP family of proteins	45
1.5.7 ADAM-10	48
1.5.8 ADAM-17 and disease	50
1.5.9 ADAM-17 and MS	51
1.6 Hypothesis	52
1.7 Aims of this thesis	52
Chapter 2	
Optimisation of cell culture conditions for the human adult brain endothelial cell line, hCMEC/D3	
2.1 Introduction	55
2.1.1 <i>In vitro</i> models of the BBB	55
2.1.2 hCMEC/D3 cells as an <i>in vitro</i> model of the BBB	56
2.1.3 Aims of the study	57
2.2 Materials and methods	59
2.2.1 Suppliers used in this chapter	59
2.2.2 Semi-quantitative real-time reverse transcriptase-polymerase chain reaction (qRT-PCR)	59

2.2.2.1 RT-PCR	59
2.2.2.2 Semi-quantitative real-time RT-PCR (qRT-PCR)	60
2.2.2.3 Controls for RT-PCR	60
2.2.2.4 Primers	60
2.2.2.5 TaqMan probes	61
2.2.2.6 Endogenous control (housekeeping genes)	61
2.2.3 Cell culture conditions	63
2.2.3.1 Collagen coating	63
2.2.3.2 General cell culture conditions	63
2.2.3.3 Culture conditions for testing stability of housekeeping genes	63
2.2.3.4 Culture conditions to test the effects of growth factors	64
2.2.4 RNA extraction and validation	64
2.2.4.1 RNA extraction	64
2.2.4.2 Native agarose gel electrophoresis of RNA	64
2.2.5 Method	65
2.2.5.1 cDNA synthesis	65
2.2.5.2 qRT-PCR	65
2.2.5.3 Statistical analysis	66
2.2.6 BrdU proliferation assay	66
2.2.6.1 Method	66
2.2.6.2 Statistical analysis	67
2.3 Results	68
2.3.1 Optimising housekeeping genes	68
2.3.2 Testing the effects of VEGF and EGF on mRNA expression	68
2.3.3 Testing the effects of heparin on mRNA expression	68
2.3.4 Testing the effects of heparin on mRNA expression during treatment with IFN- γ	71
2.3.5 The influence of VEGF and EGF on cell proliferation	71
2.4 Discussion	74

Chapter 3

Effects of inflammatory cytokines on the expression of ADAM-17, TIMP-3 and substrates shed by the protease in the human adult brain endothelial cell line, hCMEC/D3

3.1 Introduction	79
3.1.2 Aims of the study	80
3.2 Materials and methods	81
3.2.1 Suppliers used in this chapter	81
3.2.2 Cell culture	81
3.2.3 qRT-PCR	81
3.2.3.1 Experimental conditions for testing gene expression	81
3.2.3.2 Statistical analysis for qRT-PCR data	81
3.2.4 Immunocytochemistry	82
3.2.4.1 Immunofluorescence microscopy	82
3.2.4.2 Direct immunofluorescence	82
3.2.4.3 Indirect immunofluorescence	84
3.2.4.4 Confocal laser scanning microscopy (CLSM)	84
3.2.4.5 Method	86
3.2.5 Sodium dodecyl sulphate-polyacrylamide gel electrophoresis (SDS- PAGE) and Western blotting	87
3.2.5.1 Principles of SDS-PAGE and western blotting	87
3.2.5.2 Protein extraction for western blotting	89
3.2.5.3 Protein determination	90
3.2.5.4 Optimisation of western blotting technique	90
3.2.5.5 Determination of ADAM-17 protein expression in hCMEC/D3 cells under control and pro-inflammatory conditions by SDS-PAGE and western blotting	92
3.2.5.6 Verification of protein transfer	94
3.2.5.7 Statistical analysis of western blot data	96
3.2.6 Enzyme-Linked Immunosorbant Assay (ELISA) for determining fractalkine levels	96
3.2.6.1 Principles of the ELISA assay	96
3.2.6.2 Protein extraction using CellLytic for examination by ELISA	96
3.2.6.3 Experiment to determine cell-bound and shed fractalkine levels following 24 hour treatment with TNF	98

3.2.6.4 Time course study to examine the relationship between cell-bound and shed fractalkine under TNF treatment	98
3.2.6.5 Fractalkine ELISA	98
3.2.6.6 Statistical analysis of ELISA data	100
3.2.7 Senslyte™ 520 TACE Activity Kit	100
3.2.7.1 Principles of the enzyme activity kit	100
3.2.7.2 Protein extraction for determining the activity levels of TACE under pro-inflammatory conditions using SensoLyte™ activity assay	103
3.2.7.3 Enzyme activity assay to determine the activity levels of TACE in hCMEC/D3 cells under pro-inflammatory conditions	103
3.2.7.4 Statistical analysis of enzyme activity data	103
3.3 Results	
3.3.1 qRT-PCR analysis of mRNA expression following cytokine treatment of human adult brain endothelial cells, hCMEC/D3	105
3.3.2 Immunocytochemical detection of ADAM-17, TIMP-3 and fractalkine under control and stimulatory conditions	107
3.3.3 Determination of the ability of the anti-actin antibody to distinguish between different protein concentrations on western blots	112
3.3.4 Selection of a suitable antibody for ADAM-17 detection by western blotting	112
3.3.5 Western blot analysis of ADAM-17 expression by hCMEC/D3 cells following TNF treatment	112
3.3.6 Relationship between cell-bound and shed fractalkine in endothelial cells in the presence or absence of TNF, as determined by ELISA	117
3.3.7 Time course study to determine the relationship between cell-associated and shed fractalkine following TNF treatment in hCMEC/D3 cells	117
3.3.8 Determining ADAM-17 activity in hCMEC/D3 following TNF treatment	121
3.4 Discussion	123

Chapter 4

Optimisation of ADAM-17 knockdown in hCMEC/D3 cell line using siRNA technology

4.1 Introduction	130
4.1.1 Aims of the study	131
4.2 Materials and methods	132
4.2.1 Suppliers used in this chapter	132
4.2.2 RNA interference (RNAi)	132
4.2.2.1 Basic principles of siRNA induced gene knockdown	132
4.2.2.2 Positive and negative controls to validate siRNA knockdown	134
4.2.2.3 Determining siRNA knockdown efficiency and cytotoxicity	134
4.2.3 Cell culture conditions	134
4.2.3.1 Determining the optimal volume of DharmaFECT 1 to be used for siRNA gene knockdown of ADAM-17, using qRT-PCR	134
4.2.3.2 Validation of RNA using native agarose gel electrophoresis and SYBR green as an RNA dye	136
4.2.3.3 Assessment of ADAM-17 protein expression after 72 hours of siRNA gene knockdown using western blotting	136
4.2.3.4 Assessment of fractalkine shedding by ELISA and ADAM-17 protein expression by western blotting after 72 hours siRNA gene knockdown and 24 hour TNF treatment	137
4.2.3.5 Statistical analysis of ELISA data	137
4.3 Results	138
4.3.1 Stability of cyclophilin A under siRNA treatment	138
4.3.2 Determination of the optimal volume of reagent to be used for siRNA gene knockdown of ADAM-17	138
4.3.3 Twenty four versus forty eight hour treatment with siRNA to determine the optimal concentration of DharmaFect 1	138
4.3.4 siRNA knockdown of ADAM-17, including all controls, following forty eight hour treatment with siRNA and 1µl/well of DharmaFect 1	142
4.3.5 Knockdown of ADAM-17 protein expression in hCMEC/D3 cells following 72 hour treatment with siRNA	142

4.3.6 Effects on ADAM-17 protein expression and fractalkine shedding following siRNA knockdown and TNF treatment in hCMEC/D3 cells	142
4.4 Discussion	148
Chapter 5	
Expression of ADAM-17 and fractalkine in post-mortem human control and MS brain tissue	
5.1 Introduction	153
5.1.1 Aims of the study	154
5.2 Materials and methods	155
5.2.1 Suppliers used in this chapter	155
5.2.2 Tissue	155
5.2.3 Tissue characterisation	158
5.2.3.1 Haematoxylin and eosin staining (H&E)	158
5.2.3.2 Oil red O (ORO) staining	158
5.2.3.3 Sudan black B staining (SBB)	159
5.2.4 Tissue grading	159
5.2.4.1 H&E and ORO stains	159
5.2.4.2 HLA-DR reactivity	159
5.2.4.3 MOG reactivity	163
5.2.4.4 Classification criteria using all markers	163
5.2.5 Immunohistochemistry	163
5.2.5.1 Single immunofluorescence	163
5.2.5.2 Dual immunofluorescence	165
5.2.5.3 Image analysis and capture	165
5.3 Results	167
5.3.1 Tissue classification	167
5.3.2 Determining the level of background staining	167
5.3.3 Selection of appropriate antibodies to study expression of ADAM-17 and fractalkine	171
5.3.4 Expression of ADAM-17 and fractalkine in blood vessels of MS and control CNS white matter using polyclonal antibodies	171

5.3.5 Expression of ADAM-17 and fractalkine in the parenchyma and perivascular cuffs using dual labelling	175
5.4 Discussion	187
Chapter 6	
General discussion	
6.1 General discussion	192
6.2 Addressing the hypothesis of the thesis	197
6.3 Future work	198
6.3.1 <i>In vitro</i> work using hCMEC/D3	198
6.3.2 <i>In vivo</i> work using post-mortem human brain tissue from The UK Multiple Sclerosis tissue Bank	198
6.3.3 Patient samples	199
6.4 Summary	199
Chapter 7	
References	201
Appendix I	
Ethics approval	

List of Figures

Chapter 1

1.1: Typical clinical courses of multiple sclerosis (MS)	4
1.2: Diagnostic tests for MS	6
1.3: Pathological hallmarks of MS	9
1.4: Sodium channel mediated axonal degeneration	14
1.5: The working concept of the pathogenesis of MS	16
1.6: Schematic representation of the BBB in transverse section	18
1.7: Schematic representation of the junctional proteins of the BBB	20
1.8: Types of transport across the BBB	21
1.9: Schematic representation of TNFR1 and TNFR2	27
1.10: Domain structure of fractalkine	33
1.11: Domain structure of ADAM-17	40
1.12: The three-dimensional structures of TIMPs	46
1.13: Stereo front view of the catalytic domain of ADAM-17-N-TIMP-3 complex	49
1.14: Proposed functional role of ADAM-17 in MS pathogenesis	53

Chapter 2

2.1: Human adult brain endothelial cell line, hCMEC/D3, in culture	58
2.2: TaqMan chemistry	62
2.3: qRT-PCR analysis of housekeeping genes and proliferation response in hCMEC/D3 cells under inflammatory conditions	69
2.4: Effects of VEGF and EGF on mRNA expression in hCMEC/D3 cells	70
2.5: Effects of heparin on mRNA expression in hCMEC/D3 cells	72
2.6: Effects of heparin on mRNA expression in hCMEC/D3 cells under interferon- γ (IFN- γ) treatment	73

Chapter 3

3.1: Schematic representation of immunocytochemical detection of antigens on tissue and cells using antibodies	83
3.2: Schematic diagram of the confocal laser scanning microscopy (CLSM) system	85
3.3: Representative standard curve used to determine the protein concentration of unknown samples	91
3.4: Sandwich ELISA	97
3.5: Representative standard curve used to determine the concentrations of fractalkine in cell lysates and supernatants from hCMEC/D3 cells	101

3.6: Schematic representation of the Sensolyte™ 520 TACE Activity Kit	102
3.7: qRT-PCR analysis of ADAM-17 (A), TIMP-3 (B), TNFR1 (C), TNFR2 (D), fractalkine (E) and von Willebrand factor (vWF) (F) mRNA expression under control and inflammatory conditions in the human adult brain endothelial cell line, hCMEC/D3	106
3.8: Immunocytochemical detection of ADAM-17 in hCMEC/D3 cells after fixation with ice cold acetone (i) or 4% paraformaldehyde (PFA) (ii) under control and TNF treatment conditions	109
3.9: Immunocytochemical detection of TIMP-3 in hCMEC/D3 cells after fixation with ice cold acetone (i) and 4% paraformaldehyde (PFA) (ii) under control and TNF treatment conditions	110
3.10: Immunocytochemical detection of fractalkine in hCMEC/D3 cells after fixation with ice cold acetone (i) and with 4% paraformaldehyde (PFA) (ii) under control and TNF treatment conditions	111
3.11: Determination of the sensitivity of the anti-actin antibody to distinguish different protein concentrations on western blots	113
3.12: Semi-quantitation of actin at three different protein concentrations	113
3.13: Specificity of AB19027 at detecting the pro-form and mature form of ADAM-17 in hCMEC/D3 cells	114
3.14: Western blot analysis of ADAM-17 expression in hCMEC/D3 cells under control and TNF treatment	115
3.15: Densitometric analysis of western blot of pro-ADAM-17 (A), mature ADAM-17 (B) and both pro- and mature-ADAM-17 (C) expression in hCMEC/D3 cells under control and TNF treatment	116
3.16: Enzyme-linked immunosorbant assay (ELISA) determination of fractalkine expression by hCMEC/D3 cells under control and TNF treatment	118
3.17: Time course study of the effects of TNF on cell bound and shed fractalkine in hCMEC/D3 cells	120
3.18: ADAM-17 enzyme activity in hCMEC/D3 under control and TNF treatment	122
 Chapter 4	
4.1: Basic principles of small interfering RNA (siRNA) induced gene knockdown	133
4.2: siRNA optimisation steps to ensure optimum gene knockdown and minimal cell death	135
4.3: Expression levels of cyclophilin A after 24 hour treatment with 100nM	139

non-targetting control siRNA and various concentrations of DharmaFECT 1	
4.4: Determining the optimal volume of transfection reagent, DharmaFECT 1, for gene knockdown of ADAM-17 in hCMEC/D3 cells using siRNA technology	140
4.5: Time course study on the effects of different concentrations of DharmaFECT 1 transfection reagent on ADAM-17 mRNA expression in hCMEC/D3 cells using 100nM of siRNA	141
4.6: Knockdown of ADAM-17 gene expression in hCMEC/D3 cells using 1µl/well of DharmaFECT 1 reagent for 48 hours	143
4.7: Protein expression in hCMEC/D3 cells following siRNA treatment or under control conditions	144
4.8: Protein expression in hCMEC/D3 cells following TNF treatment with siRNA knockdown or under control conditions	145
4.9: Effects on TNF-induced fractalkine shedding in hCMEC/D3 cells following siRNA knockdown of ADAM-17 expression	146
Chapter 5	
5.1: Schematic diagram explaining coronal slicing and block preparation of the cerebrum by The UK Multiple Sclerosis Tissue Bank	157
5.2: Haematoxylin and eosin (H&E) staining showing the grades of inflammation seen in CNS white matter in this study	160
5.3: Oil red O (ORO) staining showing the grades of lipid-laden macrophages observed in the white matter tissue used in this study	161
5.4: HLA-DR staining of white matter tissue showing the different grades of cellular activation	162
5.5: Myelin oligodendrocyte glycoprotein (MOG) staining of control (A and B) and MS (C-F) tissue to determine the extent of demyelination	164
5.6: Peri-lesional white matter (MS109 A1D1) showing the cell markers used to characterise the tissue and their respective isotype/negative controls	169
5.7: Peri-lesional white matter (MS109 A1D1) showing the different antibody combinations to demonstrate ADAM-17 and fractalkine expression	170
5.8: White matter control tissue (CO14 P2C3) showing the different antibody combinations to demonstrate ADAM-17 and fractalkine expression using monoclonal (red) and polyclonal (green) antibodies	172
5.9: White matter lesional border (MS090 P2B3) showing ADAM-17 and fractalkine immunoreactivity using monoclonal (red) and polyclonal (green) antibodies.	173

5.10: White matter perivascular cuff (MS130 P2F4) showing ADAM-17 and fractalkine immunoreactivity using monoclonal (red) and polyclonal (green) antibodies.	174
5.11: Expression of ADAM-17 and fractalkine in control white matter blood vessels (CO11 A1B5)	177
5.12: Expression of ADAM-17 and fractalkine in a white matter perivascular cuff (MS130 P2F4)	178
5.13: Expression of ADAM-17 and fractalkine in lesional white matter (MS090 P2B3)	179
5.14: Expression of ADAM-17 and fractalkine in peri-lesional white matter (MS090 P2B3)	180
5.15: Dual expression of ADAM-17 and fractalkine in control white matter (CO16 A2D1)	181
5.16: Dual expression of ADAM-17 and fractalkine in a white matter perivascular cuff (MS130 P2F4)	182
5.17: Dual expression of ADAM-17 and fractalkine in the white matter of an MS chronic-active lesion (MS090 P2B3)	183
5.18: Dual expression of ADAM-17 and fractalkine next to and within the white matter MS lesion (MS090 P2B3)	184
5.19: Dual expression of ADAM-17 and fractalkine in peri-lesional white matter (MS090 P2B3)	185
5.20: Dual expression of ADAM-17 and fractalkine in active white matter (MS130 P2F4)	186
Chapter 6	
6.1: Schematic representation of the role of fractalkine in MS pathogenesis	196

List of tables

Chapter 1

1.1: Cleavage sites of ADAM-17 substrates	44
---	----

Chapter 3

3.1: Determination of the optimal concentration of antibodies used in the immunocytochemical detection of ADAM-17, TIMP-3 and fractalkine in hCMEC/D3 cells, under control and pro-inflammatory conditions	88
3.2: Antibodies tested to determine their suitability to detect the pro- and mature forms of ADAM-17 using western blotting	93
3.3: Antibodies and blocking peptide used to detect ADAM-17 in hCMEC/D3 under control and pro-inflammatory conditions	95
3.4: Protease inhibitor cocktail composition used in combination with CelLytic for protein extraction	99
3.5: Tabular representation of Figure 3.5 showing the altered gene expression in hCMEC/D3 cells, under inflammatory conditions	108
3.6: Antibodies tested to determine ADAM-17 expression in hCMEC/D3 cells using western blotting	114

Chapter 5

5.1: Patient details of CNS tissue used in this study	156
5.2: Details of the antibodies used in this study	166
5.3: Tissue classification of MS and control blocks based upon H&E, ORO, HLA-DR and MOG stainings	168

Abbreviations

aa	amino acid
AD	Alzheimer's disease
ADAM	a disintegrin and metalloprotease
ADAM-17	a disintegrin and metalloprotease-17 (also known as TACE)
ANOVA	analysis of variance
APL	altered peptide ligand
APP	amyloid precursor protein
BACE	β -secretase
BBB	blood-brain barrier
BCA	bicinchoninic acid
BM	basement membrane
BMP	bone morphogenic protein
BrdU	bromodeoxyuridine (5-bromo-2'-deoxyuridine)
BSA	bovine serum albumin
cDNA	complementary DNA
CLSM	confocal laser scanning microscope
CNS	central nervous system
COS-7 cells	Fibroblast-like cells from the African green monkey
CSF	cerebrospinal fluid
CX3CL1	fractalkine
CX3CR1	fractalkine receptor
DC	dendritic cells
DD	death domain
dNTPs	deoxynucleotide triphosphates
DTT	1,6-dithiothreitol
EAE	experimental autoimmune encephalomyelitis
EBV	Epstein-Barr virus
ECM	extracellular matrix
ECV	human bladder carcinoma cells
EGF	epidermal growth factor
ELISA	enzyme linked immunosorbant assay
E-selectin	endothelial cell leukocyte adhesion molecule-1
FCS	foetal calf serum
FHL2	four and a half LIM domain 2 protein
FGF-β	fibroblast growth factor-beta
FRET	Förster Resonance Energy Transfer

GAG	glycosaminoglycan
GAPDH	glyceraldehyde 3-phosphate dehydrogenase
Gd-MRI	Gadolinium enhanced-MRI lesions
GPCR	G-protein coupled receptor
hCMEC/D3	human adult brain endothelial cell line
HBMEC	human brain microvessels
H&E	haematoxylin and eosin
HIVE	human immunodeficiency virus-1 encephalitis
HLA	human leukocyte antigen
HRP	horseradish peroxidase
HSPGs	heparan sulphate proteoglycans
HUVECs	human umbilical vein endothelial cells
IBD	inflammatory bowel disease
ICAM-1	intercellular adhesion molecule-1
ICC	immunocytochemistry
IFN-β	interferon-beta
IFN-γ	interferon-gamma
Ig	immunoglobulin
IHC	immunohistochemistry
IL-1β	interleukin-1 beta
IL-1Ra	IL-1 receptor antagonist
IL-1RI	IL-1 receptor I
iNOS	inducible nitric oxide synthase
Insulin-GF	insulin-growth factor
IPC	ischemic preconditioning
JAM	junctional adhesion molecule
KO	knockout
LFA-1	Lymphocyte function-associated antigen-1
LPS	lipopolysaccharide
MAG	myelin-associated glycoprotein
MBE	murine brain endothelial cells
MBP	myelin basic protein
MMP	matrix metalloproteinase
MOG	myelin oligodendrocyte glycoprotein
MP	methylprednisolone
MRI	magnetic resonance imaging
mRNA	messenger RNA
MS	multiple sclerosis

NAWM	normal appearing white matter
NIND	non-inflammatory neurological disease
NO	nitric oxide
nt	nucleotide
OCB(s)	oligoclonal band(s)
OD	optical density
ORO	Oil red O
PBMCs	peripheral blood mononuclear cells
PBS	phosphate buffered saline
PC	pericytes
PCR	polymerase chain reaction
PFA	paraformaldehyde
PKC	protein kinase C
PLP	proteolipid protein
PMA	phorbol-12-myristate-13-acetate
PMT	photomultiplier tube
PNGase	<i>N</i> -glycosidase F
POD	peroxidase
PPMS	primary progressive multiple sclerosis
qRT-PCR	quantitative real-time RT-PCR
RISC	RNA-induced silencing complex
RMM	relative molecular mass
RRMS	relapsing-remitting multiple sclerosis
RT	room temperature
RT-PCR	reverse transcriptase-polymerase chain reaction
SBB	Sudan black B
SDS-PAGE	sodium dodecyl sulphate-polyacrylamide gel electrophoresis
SEM	standard error of the mean
siRNA	small interfering RNA
SPMS	secondary progressive multiple sclerosis
TACE	tumour necrosis factor-alpha converting enzyme (also known as ADAM-17)
TEER	transendothelial electrical resistance
TEP	triethyl phosphate
TGF-β	transforming growth factor-beta
TJ	tight junctions
TIMP	tissue inhibitor of metalloprotease
TMB	3,3',5,5'-tetramethylbenzidine
TNF	tumour necrosis factor

TNFR1	tumour necrosis factor receptor 1
TNFR2	tumour necrosis factor receptor 2
UNG	uracil-N-glycosylase
VCAM-1	vascular cell adhesion molecule-1
VEGF	vascular endothelial growth factor
vWF	von Willebrand Factor
ZO-1	zona occludens-1
ZO-2	zona occludens-2

Publications related to this thesis

Papers

Hurst, L. A., Bunning, R. A. D., Couraud, P., Romero, I.A., Weksler, B. B., Sharrack, B., Woodroffe, M. N. (2009). Expression of ADAM-17, TIMP-3 and fractalkine in the human adult brain endothelial cell line, hCMEC/D3, following pro-inflammatory cytokine treatment. *J Neuroimmunol.* **210** (1-2): 108-112.

Published abstracts

Hurst, L. A., Bunning, R. A. D., Sharrack, B., Woodroffe, M. N. Cytokine induced shedding of fractalkine from human brain endothelial cell line, hCMEC/D3: implications for multiple sclerosis. *J Neuroimmunol* 203 (2): 146-147 October 2008. 9th International Congress of Neuroimmunology. Fort Worth, TX., USA.

Hurst, L. A., Bunning, R. A. D., Sharrack, B., Woodroffe, M. N. Upregulation of fractalkine under proinflammatory conditions: A functional role for ADAM-17 in the pathogenesis of multiple sclerosis. *Neurology* 68 (12): A397-398 Suppl. 1 March 20 2007. Boston, MA., USA.

Hurst, L. A., Bunning, R. A. D., Sharrack, B., Woodroffe, M. N. A functional role for ADAM-17 in the pathogenesis of multiple sclerosis. *Immunology* 120: 32-32 Suppl. 1 March 2007. Glasgow, Scotland, United Kingdom.

Acknowledgements

Special thanks to Professor Nicola Woodroffe and Dr. Rowena Bunning, whose support and guidance throughout my PhD have been invaluable. In addition, I am most grateful to the added support and guidance from Dr. Basil Sharrack.

I am enormously grateful to the patients and their families who gave their consent and donated their tissue which was used in the final chapter of this thesis. Without doing so, we would not have true insight into some of the pathological processes of MS.

Thanks to everyone in the BMRC, past and present, for making this a memorable 3 years. Thanks to various people for their help and technical advice, especially Alison Cross, Gail Haddock, Roger Jackson, Helen Denney and Gordon Arnott.

Thanks to Dr. Stephen McQuaid for taking me under his wing for 2 days at Queen's University Belfast to help me decipher the cellular processes that define the MS lesion. Also to his colleagues who made me feel very welcome in the lab.

Special, special thanks to my mum, Sheila, and my sister, Elizabeth, who have always supported me throughout my PhD. Thanks to my mum who has been a rock of support through the ups and downs of my PhD and to my sister who never ceases to make me laugh when things get a little difficult.

Special thanks to my hubby-to-be, Darren, who has kept me motivated throughout my PhD and known when to crack the whip, get me a coffee and most importantly when to give me a hug.

Quote

"...the chief curse of the illness...I must ask constant services of people I love most closely...it is an illness accompanied by frustration...it is an illness that inflicts awareness off loss...sporadically it is, in its manifestations, a disgusting disease"

Brigid Brophy, 1929-95

1.1 Multiple Sclerosis

1.1.1 Introduction

Multiple sclerosis (MS) is defined as an autoimmune disease of the central nervous system (CNS) which leads to demyelination, axonal damage and progressive neurological disability. These features are evident in and culminate with the plaque/lesion, which is the pathological hallmark of MS. Among the molecular components disturbed in MS are the expression of pro-inflammatory cytokines (Hofman et al., 1989; Woodroffe and Cuzner, 1993) and adhesion molecules (Bö et al., 1996), and the breakdown of the blood-brain barrier (BBB) (Kermode et al., 1990; Kirk et al., 2003; Leech et al., 2007), all of which contribute to the recruitment of immune cells into the CNS, and suggest an altered BBB is important in the pathogenesis of the disease. Most of the understanding of MS is based upon conjecture from the animal model of MS, experimental autoimmune encephalomyelitis (EAE). Despite this paradigm and other histopathological studies in MS patients, the etiology and mechanisms of the induction of MS are not fully understood. As a consequence there is not yet a cure for this disease and treatment provides limited relief for the patient (Holmoy, 2007).

1.1.2 Clinical presentation and disease course in MS

MS plaques can occur anywhere in the CNS but predominate in the white matter. Plaques have a predilection for the optic nerves, brainstem, spinal cord and periventricular white matter. Dependent upon where the plaque resides within the CNS will determine the symptoms experienced by the patient. In general the disease normally initially presents with a single symptom, which can include blurred vision, double vision, numbness or tingling, or muscle weakness. Usually the patient makes a complete recovery from the first attack, but subsequent attacks over time usually leave some disability. As the disease continues the patient usually becomes progressively disabled (Ollier and Symmons, 1992).

MS is a heterogenous disease in terms of its presentation, pathology and disease course between patients (for review see Lassmann et al., 2001). In general, however, a patient who is diagnosed with MS can be initially clinically subcategorised as either having relapsing-remitting MS (RRMS) (these account for 85-90% of MS patients) (Figure 1.1 A) or primary progressive MS (PPMS) (Figure 1.1 B). In RRMS a relapse or attack is believed to be caused by the infiltration of immune cells into the CNS, which causes inflammation and oedema. These relapses can develop over hours or days and persist for several days or weeks. Gradually these attacks dissipate and the patient goes into remission (for review see Hafler, 2004). However, over the course of many attacks the patient accumulates various disabilities due to damage and destruction of axons. As time goes on a number of patients (approximately 65%) who

were initially diagnosed with RRMS will go on to develop secondary progressive MS (SPMS) (Compston and Coles, 2008) (Figure 1.1 C). This is characterised by a significant reduction in enhanced gadolinium-diethylenetriamine penta-acetic acid (Gd-DTPA) lesions on a magnetic resonance imaging (MRI) (Gd-MRI) scan (Khoury et al., 1994), decreased brain parenchymal volume (Filippi et al., 1995), and a decreased responsiveness to immunomodulatory therapy (for review see Hafler, 2004).

As the name implies, PPMS is progressive from the outset and tends to involve one predominant part of the CNS, namely the spinal cord (for review see Thompson et al., 1997). Unlike relapsing-remitting forms of the disease, PPMS normally presents itself with progressive paraparesis (weakness affecting the lower extremities) rather than with visual and sensory disturbances (for review see Thompson et al., 1997). The frequency of enhancement in Gd-MRI scans is significantly less in PPMS and as such has raised the question as to whether inflammation is less severe in this patient subgroup. Indeed, it has been shown that inflammation in SPMS is significantly greater than in PPMS (Revesz et al., 1994). However, a more recent study has observed that active white matter lesions are indistinguishable between SPMS and PPMS in relation to the large amount of vessels with tight junction abnormalities, and in fact, tight junctional abnormality in inactive white matter lesions are more frequent in PPMS (Leech et al., 2007). The discrepancy in these findings, the authors believe, could be due to the duration of BBB damage and also lower sensitivity of the routine "single dose" Gd-MRI (Leech et al., 2007).

1.1.3 Diagnosis

Despite the heterogeneity of disease course in MS, there are a number of diagnostic tests that can be applied to diagnose MS. One defining feature is the presence of focal CNS lesions which are disseminated in space and time, i.e. events occurring within the CNS at different sites that occurred at least 30 days apart (Sobel and Moore, 2008). Normally the clinical evidence is enough to diagnose a patient, however, when cases present which have a degree of ambiguity, various tests can be performed. MRI abnormalities are not unique to MS patients, but are present in the white matter of approximately 95% of MS patients (Fig 1.2A). MRI can show both that the lesion is segregated anatomically, and also in time with the use of serial imaging which can reveal the appearance of new plaques. This can be used for diagnosis rather than waiting for the patient to have another clinical attack. The presence of oligoclonal bands (OCB) in the cerebrospinal fluid (CSF), after CSF is subjected to protein electrophoresis, represents intrathecal immunoglobulin (Ig) synthesis, which is observed in approximately 90% of MS patients and can be used as a diagnostic

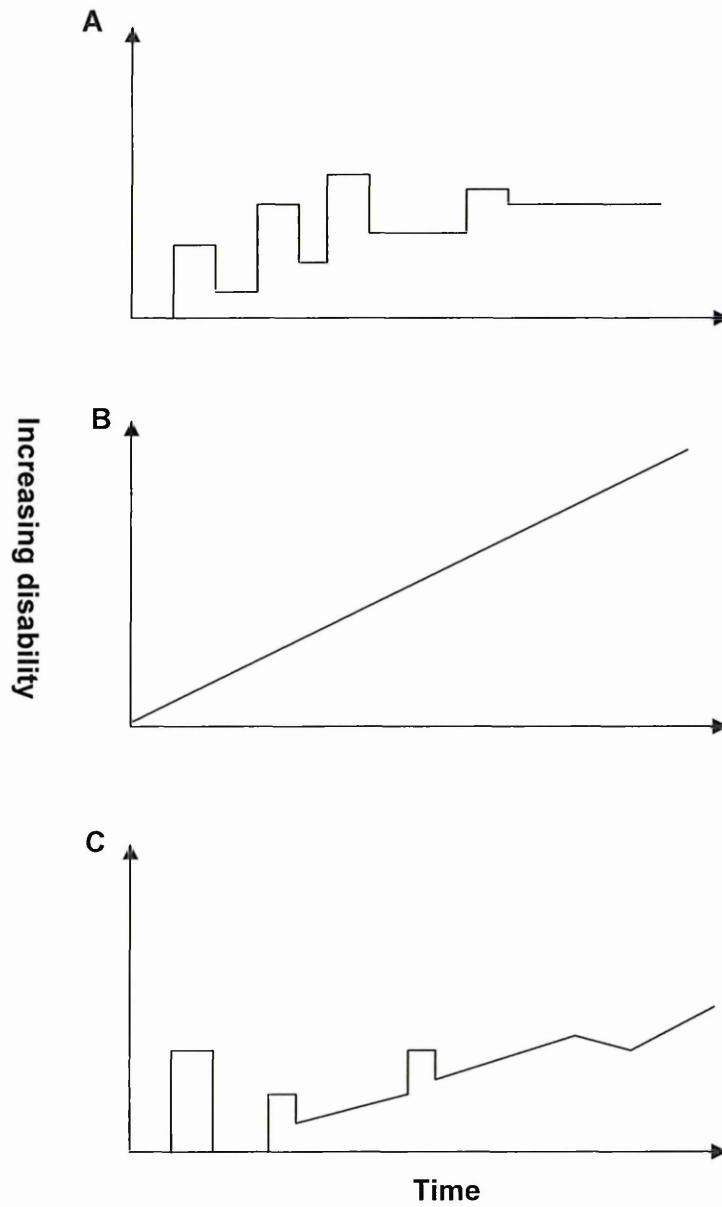


Figure 1.1: Typical clinical courses of multiple sclerosis (MS). Most patients when diagnosed with MS are either subcategorised as having relapsing-remitting MS (RRMS) (A) or primary progressive MS (PPMS) (B). As time goes on, approximately 65% of patients with RRMS will go on to develop secondary progressive MS (SPMS) (C). (Reproduced with permission from Elsevier from Lublin, 2005).

criterion (Fig 1.2B). In addition to these diagnostic criteria has been the contribution of studying evoked potentials (visual), delays of which are thought to represent the hampered saltatory conduction in demyelinated axons (Compston and Coles, 2008).

1.1.4 Genetic studies

Pedigree analysis studies have shown that MS is not inherited in a Mendelian pattern of single gene inheritance, instead it is thought several genes confer susceptibility to MS. The familial recurrence rate of MS is approximately 20%, and the affected relative is usually their sibling (Compston and Coles, 2008). The overall background age-adjusted risk of developing MS as a white northern European is 0.3% (Robertson et al., 1996). If you have an affected first-degree relative with MS you have a 3% lifetime risk of developing the disease, whereas second-/third-degree relatives have a 1% lifetime risk factor (Robertson et al., 1996; Carton et al., 1997). Concordance rates in monozygotic twins can be as high as 25-30%, and 5% in dizygotic twins (Mumford et al., 1994; Willer et al., 2003). Half-siblings have a lower age-adjusted risk of developing MS than full-siblings, and there is no change in the risk factor for half-siblings, whether they are reared together or separately (Ebers et al., 1995). Children of parents who are both affected by MS have a higher recurrence risk than children who have one parent affected by the disease (Ebers et al., 2000; Robertson et al., 1997). However, as monozygotic twins are approximately 70% discordant, genetics alone cannot explain the aetiology of the disease.

Since the 1970s it has been acknowledged that the human leukocyte antigen (HLA) genes are associated with MS. In most populations it has been found that MS is more commonly associated with DR2 (DRB1*1501 and DRB1*0602) (Olerup and Hillert, 1991; Svejgaard, 2008), however in Sardinian populations this haplotype is rare (1.5%) (Marrosu et al., 2002) and thus its contribution in this population is slight. Instead DR3 and DR4 show a stronger association with increased MS risk in the Sardinian population (Marrosu et al., 1998; 2002; Svejgaard, 2008). More recently a protective role has been reported to be conferred by HLA-C5 (Yeo et al., 2007) and HLA-DRB1*11 (Dean et al., 2008; Ramagopalan et al., 2007), and an increased susceptibility has been found to be associated with single nucleotide polymorphic (SNP) markers for the interleukin-2 (IL-2) and -7 (IL-7) receptor α chains (Gregory et al., 2007; Hafler et al., 2007; Lundmark et al., 2007). The latter SNP has been found to be located within the alternatively spliced exon 6 of IL-7R ('C' allele), which influences the amount of soluble and membrane-bound forms of the protein. The authors suggest that the 'C' allele of IL-7R associated with MS would probably decrease the expression of the membrane-bound form of IL-7R α leading to an increase in the soluble form of the

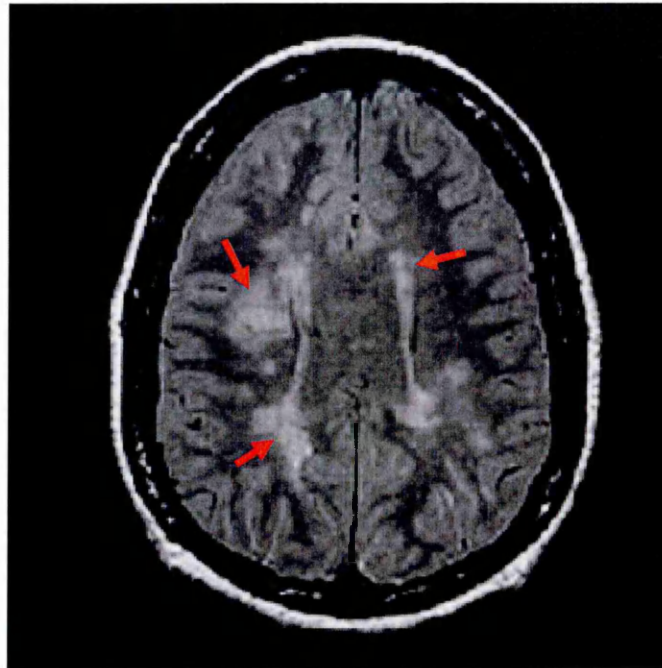
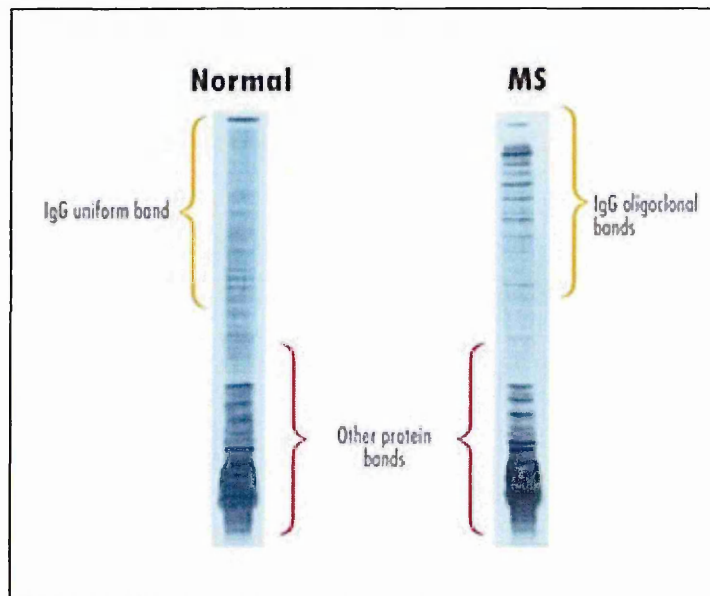
A**B**

Figure 1.2: Diagnostic tests for MS. Magnetic resonance imaging (MRI) scan from a patient with relapsing-remitting MS (RRMS) (A). Lesions can be observed in the periventricular region (red arrows) (A). Intrathecal synthesis of immunoglobulins (Ig) is a feature of approximately 90% of MS patients and can be seen as oligoclonal bands (OCBs) when cerebrospinal fluid (CSF) is subjected to protein electrophoresis (B). Normal CSF has no defined bands (monoclonal) whereas MS patients display a more restricted number of bands (oligoclonal). Images reproduced from <http://www.msstrust.org.uk>

receptor (Gregory et al., 2007). However, an increase in IL-7R and IL-7 mRNA in the cellular constituents of the CSF of MS patients, compared to other non-inflammatory neurological disorders (NIND) has been reported, which is thought could result in higher signalling that, in turn, would induce immune cell proliferation and survival (Lundmark et al., 2007). The exact role of IL-7R in MS pathogenesis has yet to be established.

1.1.5 Epidemiology of MS

Like many other autoimmune conditions, MS is more common in females than in males, having a 1.5:1 predominance in the former (Sobel and Moore, 2008). It usually presents itself in individuals in their 20s or 30s and hence can have a detrimental impact on a person's life choices, both personally and professionally (Trapp and Nave, 2008). Approximately 85,000 people in the UK currently have MS (<http://www.mssociety.org.uk/>). With increasing latitude, both in the Northern and Southern hemispheres, the incidence of MS increases. The precise cause of this equatorial resistance is unknown, however, it is postulated that the high incidence of MS in these areas coincides with the past migratory choices of Northern Europeans who have a high prevalence of MS (Bulman and Ebers, 1992). This theory is compounded by the fact that there are "resistant" groups existing in otherwise highly prevalent MS areas, such as Maoris in New Zealand (Skegg et al., 1987), and the Hutterites and Natives in western Canada (McFarlin and Lachmann, 1989). Other theories concerning the high incidence of MS in more temperate climates include the lack of vitamin D, which is thought to be linked to insufficient sunlight exposure, and/or the presence of an endemic infectious agent in these areas, which could be contributory (Miller et al., 1990; for review see Marrie, 2004; Hayes and Acheson, 2008). In addition to this, and in support of MS having an environmental risk factor influencing its development, are studies which have shown that a person who migrates before the onset of puberty will inherit the adoptive country's prevalence risk of getting MS rather than their home country's risk. After the onset of puberty the person will retain their original country's risk factor (Gale and Martyn, 1995). Epstein-Barr virus (EBV) is also thought to be associated with MS. It is thought that an immune reaction against the virus inadvertently causes an attack upon myelin through the mechanism of molecular mimicry existing between the two proteins. It has been found that myelin and EBV share four DRB1* restricted T cell receptor peptide contacts, showing that molecular mimicry exists at the structural level between the two peptides (Lang et al., 2002). Recently, it has been observed that almost 100% (21 of the 22 examined cases of MS) of MS patients brains display infiltrating B cells and plasma cells that are

reactive for EBV, and that B cell follicles within the cerebral meninges of SPMS patients are chief sites for EBV persistence (Serafini et al., 2007).

1.1.6 Pathology

1.1.6.1 White matter pathology

The pathological hallmarks of MS are distinguished from other inflammatory disorders of the nervous system by the presence of large, multifocal, demyelinated plaques with a reactive glial scar formation (for review see Hafler, 2004; Lassmann et al., 2001). Most plaques reside within the white matter of the CNS, particularly within the periventricular white matter (Lucchinetti et al., 2005). Broadly speaking two types of plaques exist: the active lesion and the chronic inactive lesion. Active lesions, which are typically localised to the white matter, can be characterised by the presence of lipid-laden macrophages, large reactive astrocytes, and an accompanying degree of perivascular inflammation (Figure 1.3). Affected areas demonstrate myelin pallor and the majority of axons are spared, however, if damage is severe enough axons will be destroyed or display irregular morphology. Macrophages that phagocytose the myelin remnants and debris are called *Gitter cells*, which are characterised by spherical nuclei, vacuolated cytoplasm, and distinct cell borders. Reactive astrocytes with prominent and polymorphic nuclei, and eosinophilic cytoplasm intermingle between these cells (Lucchinetti et al., 2005). It is believed that the actively demyelinating plaque or lesion can be defined by studying the chemical composition of the myelin degradation products and the expression of inflammatory activation antigens both within and by macrophages (Bruck et al., 1995). One to two days following phagocytosis, minor myelin proteins, such as myelin oligodendrocyte glycoprotein (MOG) or myelin-associated glycoprotein (MAG) are evident within macrophages. Whereas the major myelin proteins, such as myelin basic protein (MBP) and proteolipid protein (PLP), can be found within macrophages for six to ten days following myelin phagocytosis (Lucchinetti et al., 2005).

The chronic lesion is sharply confined, hypocellular and shows no evidence of active myelin breakdown. Fibrillary gliosis is a prominent feature of the inactive plaque, which is accompanied by a marked reduction in axonal density. Mature oligodendrocytes are either noticeably diminished or lacking in the chronic lesion. There may still be some evidence of inflammation, particularly in the perivascular region (Lucchinetti et al., 2005). Remyelination does occur in chronic lesions, however, this is usually incomplete and restricted to the plaque edge, or there may be more widespread remyelination throughout the chronic lesion. These types of lesions are referred to as *shadow plaques* and contain areas of reduced myelin staining called

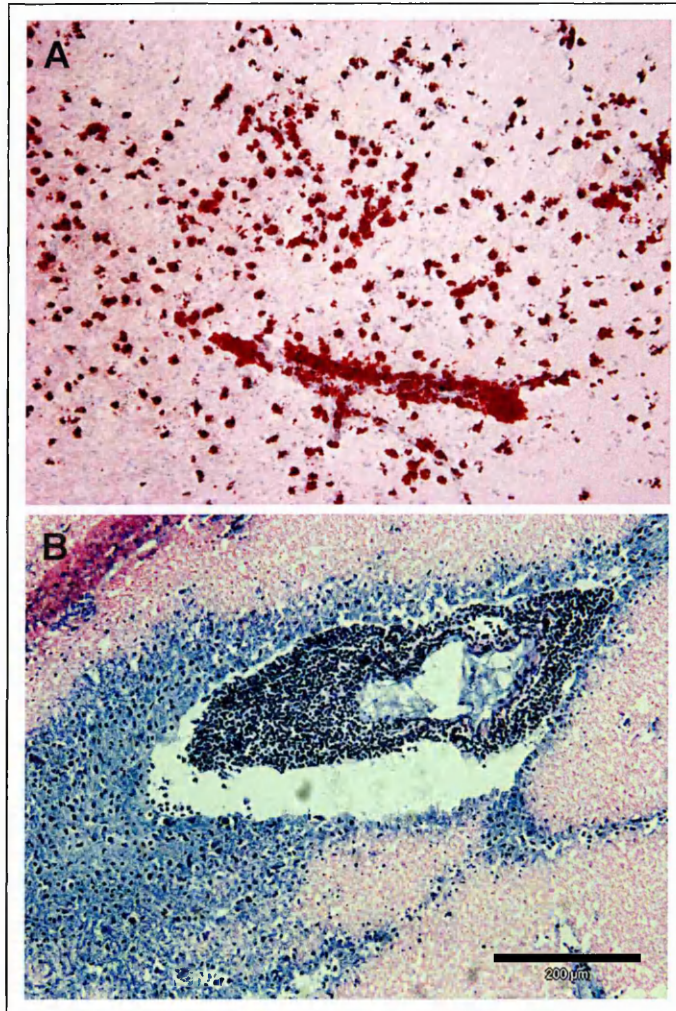


Figure 1.3: Pathological hallmarks of MS. MS lesion stained with Oil Red O (ORO) which stains lipid-laden macrophages (A) and with haematoxylin and eosin (H&E) which reveals the presence of inflammatory cuffs (B). Image A was taken at magnification $\times 100$ and was kindly provided by Dr. Helen Denney, BMRC, Sheffield Hallam University.

myelin pallor, which result from a decrease in the ratio between the myelin sheath and the axonal diameter (Lucchinetti et al., 2005).

There are two schools of thought regarding lesion classification in MS, which are based upon either the stage of the lesion (for review see van der Valk and DeGroot, 2000) or the underlying pathological mechanisms (Lucchinetti et al., 2000). So far four major staging systems for MS lesions have been described (for review see van der Valk and De Groot, 2000). The Bö/Trapp staging system relies on the cellularity of the tissue to determine the type of lesion: (1) active lesions are described as being hypercellular; (2) chronic-active lesions have a hypocellular centre with a hypercellular rim; (3) and the chronic-inactive lesion is described as being hypocellular (Bö et al., 1994; Trapp et al., 1998). This classification system works well on frozen and paraffin-embedded sections. The De Groot-van der Valk system is a modification of the Bö/Trapp system: it includes a category for (1) 'pre-active' lesions which are defined by clusters of microglial cells, (2) little inflammation and no demyelination; (3) active demyelinating; (4) active but not demyelinating; (5) chronic active (as according to the Bö/Trapp system); and (6) chronic-inactive (as according to the Bö/Trapp system) (Waesberghe et al., 1999). This system has proved more useful for MRI-sampled material (De Groot et al., 2001). The third system, called the Lassmann/Brück system, utilised a large number of biopsy tissue and hence is best suited for classifying early on-set lesions. Five lesions have been identified using this system: (1) early active; (2) late active; (3) inactive lesions; (4) early remyelinating; and (5) late remyelinating (Brück et al., 1994; 1995). The fourth staging system was brought about during a meeting in Vienna that was organised by Prof. H. Lassmann to convene experts in MS. The Vienna consensus described six lesions: (1) inflammatory and demyelinating; (2) inflammatory but not demyelinating; (3) inflammatory rim (hypocellular centre), and demyelinating; (4) inflammatory rim (hypocellular centre), not demyelinating; (5) no inflammation, but demyelinating; and (6) no inflammation, not demyelinating (Ferguson et al., 1997). The Vienna consensus has been described as being more of a descriptive system rather than a staging system (van der Valk and De Groot, 2000).

Only one group has tried to determine whether there was an underlying pathological mechanism that could define the MS lesion. The Lucchinetti group sought to determine if there was some heterogeneity in the active demyelinating plaque between and within patients using different immunohistochemical stains (Lucchinetti et al., 2000). Based on the following four criteria four different lesions were identified. They all have in common T lymphocyte and macrophage infiltrates, but were segregated on the basis of the following four criteria: (1) distribution of myelin protein loss; (2) the plaque geography and extension; (3) the pattern of oligodendrocyte destruction; (4) the presence of immunoglobulin (Ig) and activated complement

deposits (Lucchinetti et al., 2000). Pattern I were mediated by T cells and macrophages alone, pattern II by immunoglobulin (Ig) and complement, pattern III were defined by the apoptosis of oligodendrocytes and the absence of Ig, complement and remyelination, whereas pattern IV were defined by oligodendrocyte dystrophy and the lack of remyelination. Lesion heterogeneity was observed between patients but not within the same individual (Lucchinetti et al., 2000). However, this classification system was based upon the analysis of biopsy tissue ($n = 49$) and some post-mortem tissue ($n = 32$) from patients with acute MS or acute MS exacerbations, predominantly with short disease duration.

Recently Breij et al. (2008) sought to verify the Lucchinetti classification system in active lesions from patients with established MS using post-mortem tissue. Using this criterion, chronic active lesions mainly manifested as type II lesions with deposition of Ig and complement on macrophages. Pattern III and IV, based upon oligodendrocyte apoptosis, were either absent or rare. In addition, established active MS lesions displayed homogeneity and lesion heterogeneity could not be confirmed, and also there was no heterogeneity between individuals with regard to Ig and complement immunoreactivity. The authors conclude that patients with established MS display a homogenous pattern of demyelination that is associated with antibody and complement-mediated phagocytosis, which they surmise is the predominant mechanism involved in ongoing demyelination in this type of MS. Lesion heterogeneity is thought to be a characteristic of acute MS/earliest phase of MS and thus not a typical feature of patients who have had a longer disease duration (Breij et al., 2008).

1.1.6.2 Grey matter pathology

Although MS is generally described as a disease of white matter, lesions within the grey matter are also known to occur. Unlike white matter lesions, grey matter involvement in MS is typified by less inflammation (lymphocyte and macrophage infiltration), and cortical lesions are less readily detectable using conventional MRI (Newcombe et al., 1991; Kidd et al., 1999; Bö et al., 2006). Recently, studies have been performed to determine the involvement of grey matter pathology in MS. Vercellino and colleagues (2005) used whole coronal sections from MS (RRMS = 3; SPMS = 3) and control ($n = 6$) patients brains to determine the extent and distribution of demyelinating lesions within the grey matter. Demyelinating lesions were observed in various areas, including the cerebral cortex, thalamus, basal ganglia and the hippocampus. Two SPMS cases showed a significant reduction in the amount of myelination (48 and 25.5%) and all cases showed a significant reduction in neuronal density (18-23%). The authors hypothesised that these alterations in the grey matter could contribute to disability and cognitive impairment in MS, and could account for the

poor correlation between clinical disability of SPMS patients and reduced Gd-MRI. Cortical demyelination has been found to be more commonly associated with SPMS and PPMS than acute and RRMS (Kutzelnigg et al., 2005). The number of grey matter lesions ($n = 98$) has been demonstrated to be almost equal to white matter lesions ($n = 70$) using immunohistochemical staining for MBP, however, only 3% of these intracortical lesions were identified using MRI (Geurts et al., 2005).

1.1.7 Axonal injury in MS

MS is principally described as a demyelinating disease of the CNS, however, the chief cause of disability is the damage caused to the axons. Charcot, the French neurologist who first described MS, initially believed that the axons were relatively spared, but later described various axonal alterations and even destruction of the axons. He stated that the methodology of the time could not definitively exclude the presence of axonal degeneration (Kornek and Lassman, 1999). By 1915, it was generally accepted that axonal degeneration was a feature in MS lesions; this discovery was due to the establishment of Bielschowsky's silver impregnation method (Kornek and Lassman, 1999). Injury to axons leads to the transection of the axon and the formation, at their proximal ends, of spheroids defined by the presence of terminal axonal ovoids (Trapp et al., 1998). Following transection, the distal segment of the nerve will undergo Wallerian degeneration, whilst the proximal part may die due to lack of connectivity to other neurons (for review see Zaffaroni, 2003). The majority of axons, which undergo transection, are demyelinated and reside in the lesion, however, there is evidence that axonal loss also occurs in normal white matter (Davie et al., 1997; van Walderveen et al., 1998).

The causes of axonal injury, like other features of MS, remain largely hidden. The study by Bitsch et al. (2000), which sought to discern whether the pathogenesis of axonal injury was distinct from demyelination, revealed that axonal damage, defined by the accumulation of amyloid precursor protein (APP), occurs in lesions under any demyelinating condition (active or inactive), and even during remyelination. Axonal damage also correlated with the infiltration of macrophages and CD8+ T lymphocytes, but not with the expression of tumour necrosis factor (TNF) and inducible nitric oxide synthase (iNOS) mRNA. It was thus concluded that axonal damage in MS occurs, in part, independently from demyelinating activity, and its pathogenesis may be different to demyelination mechanisms. In addition to this, it has been shown that axonal loss occurs irrespective of the absence or presence of Gd-MRI lesions (indicative of increased BBB permeability and associated inflammation (Katz et al., 1993)) (Filippi et al., 2003). Although, the axonal loss in patients with enhancing lesions was greater, it was not significantly so (Filippi et al., 2003). Studies that have sought to identify a

biological marker for the neurodegenerative phase of MS have, however, found that axonal dysfunction and inflammation are not discrete processes; since L-neurofilament protein levels are higher in the CSF of MS patients when the CSF is taken the shorter the period of time after the last relapse (Lycke et al., 1998).

The timing of the majority of axonal damage has been found to occur at the early stages of the disease - within the first year of disease onset (De Stefano et al., 2001; Kuhlmann et al., 2002). It is also notable that RRMS and SPMS patients show significantly higher levels of acute axonal damage in the early stages of the disease than after a disease course of 10 years or more, whereas PPMS patients show no significant differences over time (Kuhlmann et al., 2002). It is thought that the functional recovery, that normally accompanies an attack in the early stages of MS, is a product of various compensatory mechanisms, including sodium channel redistribution (Moll et al., 1991; Black et al., 1991) and brain plasticity (Waxman, 1997; Reddy et al., 2000). Within demyelinated areas of the CNS of MS patients, axons display four times the amount of sodium channels compared to normal white matter, which could account for the fast recovery and/or silent MS lesions (Moll et al., 1991). Recent studies have revealed that the expression of sodium channels differ between acute and chronic lesions, and may suggest that the underlying mechanism of axonal damage differ in these two lesion types (Black et al., 2007). Sodium influx can lead to the overwhelm of the Na^+/K^+ pump causing an inability to extrude sodium, which in turn leads to activation of the $\text{Na}^+/\text{Ca}^{2+}$ exchanger, causing increasing and toxic levels of intra-axonal calcium; demyelinated axons are particularly vulnerable to this mode of injury (Figure 1.4). To help prevent neurodegeneration in MS patients, the use of channel blockers has been proposed and initiated in clinical trials, however, the sudden withdrawal of the channel blockers in EAE led to exacerbations of the disease, which was accompanied by an increased inflammatory infiltrate, hence some of the clinical trials were halted (for review see Waxman, 2008).

1.1.8 Pathogenesis of MS

Due to the presence of immune cell infiltrates within MS lesions and the insights from EAE, MS is regarded as an autoimmune disease. The inflammatory cuffs consist of mainly T lymphocytes, a few B cells and plasma cells, and extensive macrophage/microglial activation (Lucchinetti et al., 2005). It is believed that the disease process in MS is initiated by the increased migration of autoreactive lymphocytes across the BBB. T helper 1 cells (Th1 cells) have held most of the interest due to a number of factors, including the fact that they recognise antigens presented by HLA class II molecules, the gene that shows the strongest link with MS, Th1 cells are essential to the development of the animal model of MS, and a variety of Th1 cytokines

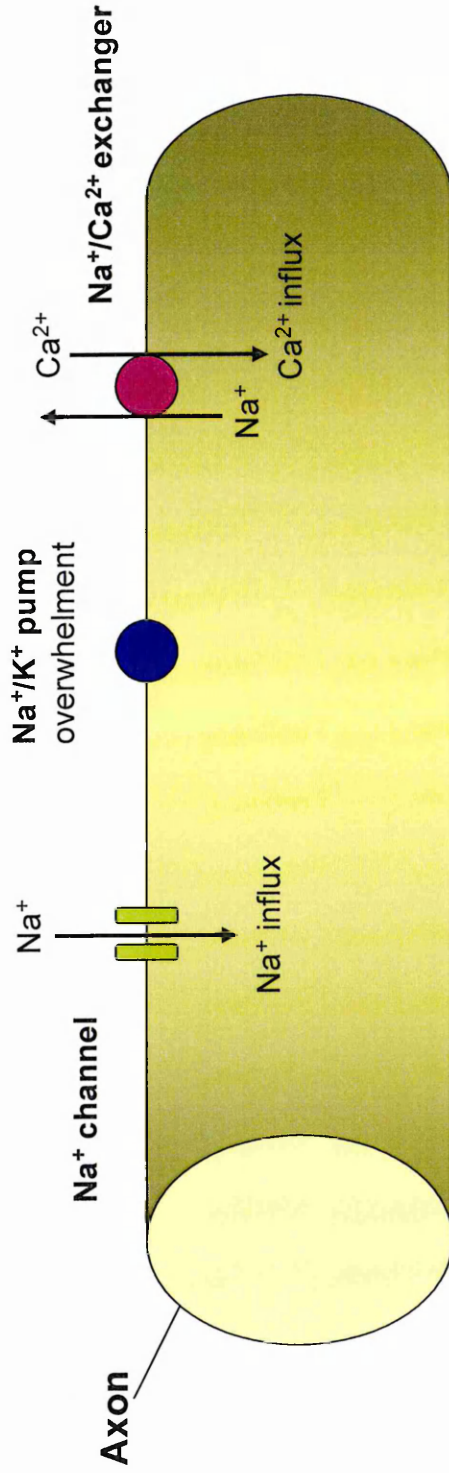


Figure 1.4: Sodium channel mediated axonal degeneration. Increasing levels of sodium (Na^+) causes overwhelm of the Na^+/K^+ pump and results in the activation of the $\text{Na}^+/\text{Ca}^{2+}$ exchanger, causing an influx of calcium (Ca^{2+}) into the cell and resulting in axonal death due to toxic levels of calcium. (Re-drawn with permission from Nature Publishing Group from Waxman, 2006).

can be observed in MS plaques (Woodrooffe and Cuzner, 1993; for review see Holmoy and Hestvik, 2008). However, due to the failure of Th1-directed therapies for MS and the identification of a new subset of CD4⁺ Th cells, Th17 cells which synthesis the pro-inflammatory cytokine IL-17, this domination of the field has been questioned. CD4⁺ cells from MS patients ($n = 30$) show increased IL-17 production in comparison to controls ($n = 14$) (Vaknin-Dembinsky et al., 2006), and IL-17⁺ T cells have been demonstrated to be significantly increased in active ($n = 11$) rather than inactive ($n = 5$) MS lesions (Tzartos et al., 2008). In addition IL-17, together with IL-22 (a cytokine product of Th17 cells), has been implicated in BBB disruption, and neuronal cell death, through the secretion of granzyme B (Kebir et al., 2007).

The antigen that is responsible for this autoimmune attack is unknown, but was thought to be myelin derived (Compston and Coles, 2008). However, what exactly initiates this attack in MS patients still remains a mystery not least because autoreactive lymphocytes can be found in healthy individuals. It is thought that immune regulation could be altered in MS (Figure 1.5), which could account for this lack of self tolerance. Subclasses of regulatory CD4⁺ T cells include, Tregs which express the transcription factor FOXP3, Tr1 cells, which secrete the cytokine IL-10, and Th3 cells, which secrete the cytokine, transforming growth factor (TGF)- β . Tregs have been reported to be functionally impaired (in terms of reducing IFN- γ production and cell proliferation of CD4⁺ CD25⁻ responder T cells in a co-culture model) in MS patients with the relapsing-remitting subtype of the disease (Haas et al., 2005 (MS/control = 73); Viglietta et al., 2004 (MS = 15; control = 21); Venken et al., 2006 (MS = 31; control = 20)), whereas secondary progressive patients have normal Treg function (Venken et al., 2006). Lower FOXP3 levels and FOXP3-expressing cells are correlated with lower Treg cell suppressive capacity in RRMS ($n = 55$) than in controls ($n = 73$) and SPMS ($n = 15$) (Venken et al., 2008). Tr1, or type 1, T regulatory cells exert their suppressive activity through the secretion of the potent immunosuppressive cytokine IL-10 (Moore et al., 2001; Roncarolo et al., 2001). Increased MRI lesion load and higher disability is associated with lower production of IL-10 in SPMS patients (MS = 37; control = 11) (Petereit et al., 2003) and CD46 (co-stimulatory molecule associated with differentiation)-induced Tr1 cells, secrete less IL-10 in MS patients ($n = 28$) compared with healthy subjects ($n = 18$) (Astier et al., 2006). Interestingly, increased IL-10 production is associated with disease remission in MS (Correale et al., 1995 (MS active/stable = 6; controls = 5; OND = 4); Clerici et al., 2001 (stable MS = 15; active MS = 27)).

Various groups have demonstrated that T cell activation responses can be initiated by various proteins including MBP (Bielekova et al., 2004), PLP (Bielekova et

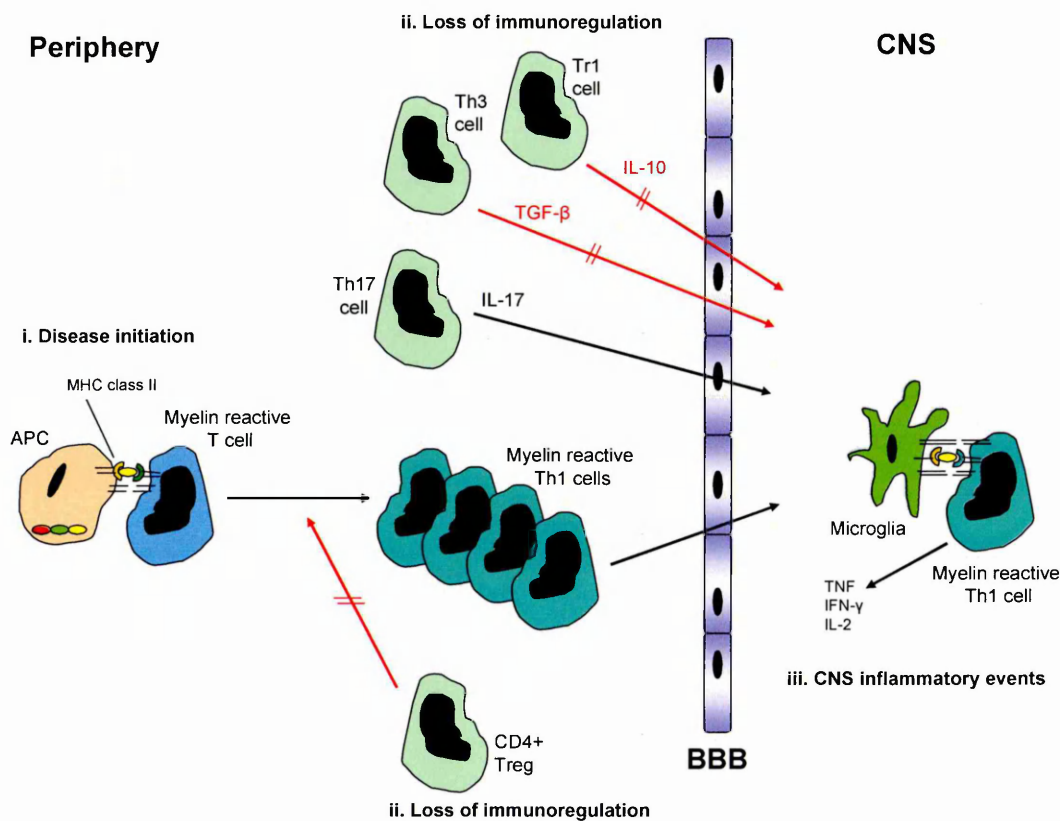


Figure 1.5: The working concept of the pathogenesis of MS. (i) Disease initiation: autoreactive T cells within the periphery become activated by antigen presenting cells (APCs) presenting myelin antigens (yellow) on major histocompatibility complexes (MHC) class II molecules. (ii) Loss of immunoregulation: reduction in immunoregulatory components of the immune system, such as CD4+ Tregs (red arrow), allows further activation of autoreactive T cells. Cells which would normally help downregulate inflammatory events, such as Tr1 and Th3 cells are reduced in MS (red arrows), whereas Th17 cells may help in mediating the inflammatory cascade with the production of IL-17 (black arrow) (iii) CNS inflammatory events: autoreactive T cells migrate into the CNS, where they recognise antigen presented by microglia, the local APCs. The production of T helper 1 cell (Th1) cytokines (TNF, IFN- γ , and IL-2) are subsequently secreted causing an inflammatory cascade (Adapted from Hafler, 2004).

al., 2004), MOG (Lindert et al., 1999; Bielekova et al., 2004) and myelin-sequestered alpha B crystallin (van Noort et al., 2000) from myelin preparations, and also that peripheral blood mononuclear cells (PBMCs) from MS patients show a higher antigen avidity than healthy controls, suggesting T cells play a vital role in MS pathogenesis (Bielekova et al., 2004). These cells were also more inclined to release pro-inflammatory cytokines when activated with myelin-specific proteins, which is appropriate if these cells are involved in the pathogenesis of MS (Bielekova et al., 2004; Hafler, 2004). Altered peptide ligand (APL) therapy using a peptide based upon MBP (amino acids (aa) 83-99), caused exacerbations of the disease in some patients, which was thought to be induced by the expansion of T cells that were specific for the APL peptide but also cross-reactive for the native MBP (Bielekova et al., 2000). Highlighting that MBP is encephalitogenic in MS.

Although MS is regarded mainly as a T-cell-mediated disease, B cells are also thought to play a role in the development of the MS plaque, as the presence of OCBs suggest an increased B cell response to an antigen present in the brain (Frohman et al., 2006). Neuropathological studies have revealed that antibodies contribute to demyelination within the MS white matter lesion (Lucchinetti et al., 2000). Studies investigating the B cells localised within the CSF have found that the most abundant cell type within this compartment in MS patients are antigen-stimulated plasma blasts (Winges et al., 2007). These cells show a biased rearrangement for the V_H4 gene segment (Qin et al., 1998; Owens et al., 2007), suggesting that the B cell response in MS is driven by the presence of antigen and is T-cell dependent (Holmoy and Hestvik, 2008). Absent or reduced numbers of OCBs in the CSF at the time of diagnosis has been associated with a better prognosis for the patient (Avasarala et al., 2001). In addition the presence of B-cell follicles within the meninges of SPMS patients has been found to be associated with younger age of MS onset, more severe disease and adjacent subpial cortical lesions suggesting soluble factors from the follicles play a direct pathogenic role (Magliozzi et al., 2007).

The following sections will deal with the mediators which are involved in regulating the invasion of the peripherally activated autoreactive immune cells across the BBB and into the CNS.

1.2 Blood-brain barrier (BBB)

1.2.1 Basic structure

The blood-brain barrier (BBB) is an important cellular barrier maintaining a balanced physiological milieu within the CNS. The BBB is composed of the capillary basement membrane (BM), astrocyte end-feet which project onto and ensheath the vessels, and pericytes (PC) which are embedded in the BM (Figure 1.6). Three characteristics of the

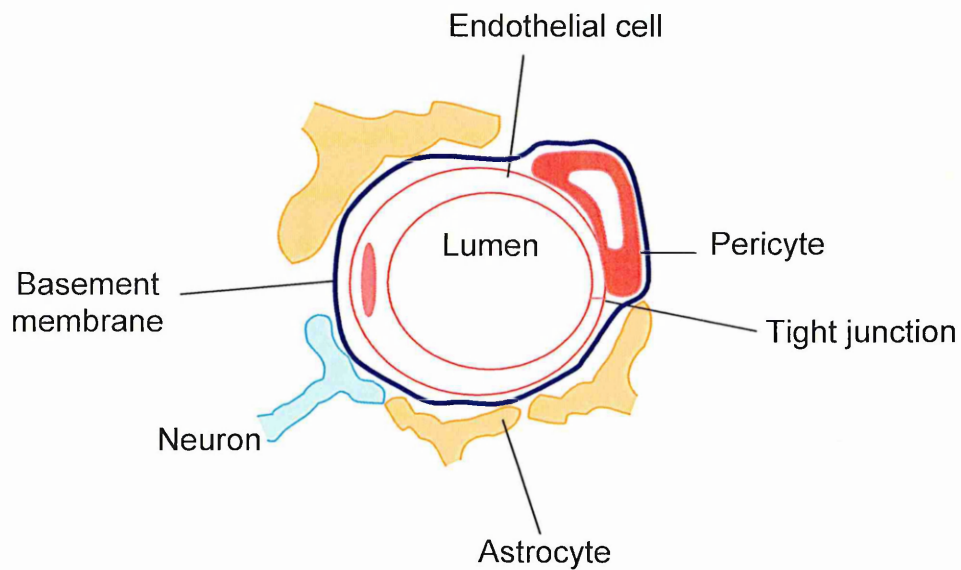


Figure 1.6: Schematic representation of the BBB in transverse section. In addition to the endothelial cell, the BBB is also comprised of astrocytic end-feet, pericytes and the basement membrane. Neurons also project onto the system. Tight junctions of the BBB endothelial cell distinguish it from other vascular endothelial cells within the periphery (Redrawn with permission from Cambridge University Press from Francis et al., 2003).

BBB endothelial cells distinguish them from peripheral endothelial cells. Firstly, they lack fenestrations, secondly, their tight junctions (TJ) are more extensive and thirdly, they have few pinocytic transport vesicles (for review see Ballabh et al., 2004).

1.2.2 BBB endothelium tight junctions (TJs)

The main components responsible for the restrictive properties of the BBB are the TJs which reside in the most apical part of the plasma membrane. Three membrane proteins comprise the TJ: claudin, occludin, and junctional adhesion molecules (JAMs) (Figure 1.7). In addition to these, there are a number of cytoplasmic accessory proteins, which include zona occludens (ZO)-1, -2, -3, cingulin, and others (for review see Ballabh et al., 2004). These tight junctions confer a high transendothelial electrical resistance (TEER) of 1500-2000 Ωcm^2 and a decreased paracellular permeability (Butt et al., 1990). In comparison, non-barrier endothelial cells such as placental cells, which have to allow the exchange of substances between mother and child, have a TEER of 22-52 Ωcm^2 (Jinga et al., 2000). At the higher end of the scale, urinary bladder epithelium have a TEER of 6000-30,000 Ωcm^2 to maintain the composition of urine (Powell, 1981). The brain still requires nutrients and oxygen and therefore employs mechanisms, which permit the exchange of substances without compromising the integrity of the system. Substances can pass through the BBB either through the endothelial cells (the transcellular pathway) or between the cells (the paracellular pathway) (Figure 1.8). The transcellular pathway involves three different mechanisms: passive diffusion, active transport and receptor-mediated endocytosis (Figure 1.8) (for review see Petty and Lo, 2002; Ballabh et al., 2004). The paracellular pathway, however, does not rely upon such mechanisms and instead, ions and solutes diffuse down their concentration gradient between cells. The paracellular space is almost completely obstructed by TJ which provide a gate function to the system. This gate function prevents substances with a molecular weight greater than 180 from passing through in such a manner (Mitic and Anderson, 1998; Stevenson and Keon, 1998; for review see Petty and Lo, 2002). Lateral diffusion between the apical and basolateral membrane is also monitored via the tight junctions and is known as the fence function. This maintains the protein and lipid polarity of the cell (Brown and Stow, 1996; Gumbiner, 1987; for review see Petty and Lo, 2002).

1.2.3 BBB disruption in MS

Disruption of the BBB, as detected by Gd-MRI scans, has been shown to precede clinicopathological evidence of new lesions, i.e. symptoms (clinical presentation) and abnormalities seen on MRI scans (pathological) (Kermode et al., 1990). Studies carried

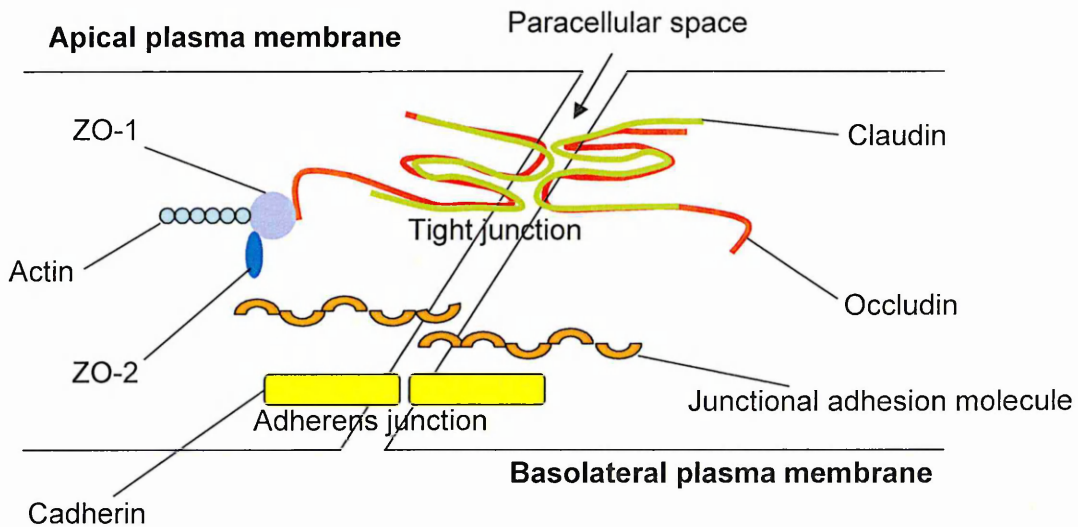


Figure 1.7: Schematic representation of the junctional proteins of the BBB. The BBB junctional complex is comprised of the tight junction (TJ) and adherens junction (AJ). Claudin, occludin and junctional adhesion molecules (JAMs) comprise the membrane bound portion of the TJ, whereas proteins such as ZO-1 and ZO-2 comprise the cytoplasmic portion (Redrawn with permission from Elsevier from Ballabh et al., 2004).

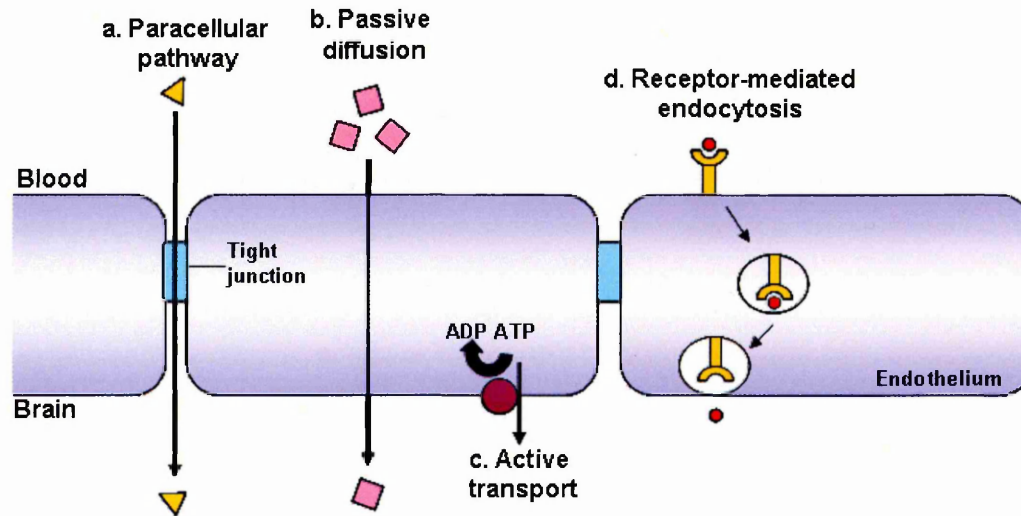


Figure 1.8: Types of transport across the BBB. Substances can either enter the brain via the paracellular pathway (a) or using three different types of transcellular passage, including: passive diffusion (b), active transport (c) or receptor-mediated endocytosis (d). (Redrawn with permission from Nature Publishing Group from Abbott et al., 2006).

out on brain capillaries in chronic silent MS lesions have suggested that BBB abnormalities persist, even in the absence of active inflammation (Kwon and Prineas, 1994; Claudio et al., 1995). This was evident in the high percentage of pinocytic vesicles and a lower percentage of mitochondria in gliotic areas, which are characteristic of the systemic endothelium (Claudio et al., 1995). Other studies using post-mortem tissue have revealed that acute plaques show leakage of plasma proteins such as fibrinogen and α -2 macroglobulin, as well as breakdown of the BM, which is evident in the fragmentation of type IV collagen and laminin. Whereas normal appearing white matter (NAWM) and chronic inactive plaques do not display any structural defect in the BM, or serum protein leakage (Gay and Esiri, 1991). Recently, dysferlin (a muscle protein involved in cell membrane repair) has been identified as a new marker of a leaky BBB in both EAE and MS. In the former inflammatory disease, dysferlin was expressed in inflamed vessel endothelium, whereas in the latter its expression was highest within active lesions but was also observed in inactive plaques. Inflammation is thought to in part be responsible for dysferlin expression as it was induced *in vitro* in brain endothelioma cells by TNF (Hochmeister et al., 2006). In contrast to the Gay and Esiri paper (1991), Kirk et al. (2003) demonstrated, using fibrinogen leakage, that TJ abnormalities in SPMS and acute MS occur in vessel segments which are more commonly associated with active plaques (42%), but are also seen in inactive plaques (23%), NAWM (13%), normal controls (3.7%) and neurological controls (8%). The authors suggest that abnormalities in inactive plaques could represent either a failure in TJ repair or a continuing pathological process. In the NAWM they believe the abnormalities could correspond to pre-lesional change or secondary damage (Kirk et al., 2003). They also demonstrated that the vessels with the most TJ abnormality also had the most fibrinogen leakage (Kirk et al., 2003). Similar levels of abnormal endothelial TJs were recently reported by the same group in PPMS patients, with regards to the active white matter lesions (42%) and the NAWM (13%) (Leech et al., 2007). They also found that chronic lesions in PPMS (37%) showed endothelial abnormalities more frequently than their SPMS (23%) counterparts (Leech et al., 2007). A similar study by Vos and colleagues (2005) showed that disruption of the blood-brain barrier takes place also in diffusely abnormal white matter (DAWM) as well as in focal lesions as determined by fibrinogen leakage and enlargement of the perivascular space.

IFN- β is one of the only successful treatments administered to RRMS patients, however, its precise mode of action is not well documented. Despite this it has been shown to reduce relapse rate, relapse severity and the progression of disability in these patients. In addition the number of Gd-MRI lesions are reduced in IFN- β treated patients (The IFNB Multiple Sclerosis Study Group, 1995; PRISMS Study Group, 1998;

Jacobs et al., 1996). One mode of action could be the stabilization of the BBB via decreasing the paracellular permeability and increasing the transendothelial electrical resistance (TEER) across the endothelial monolayer (Kraus et al., 2008). The stabilisation of the BBB by the administration of glucocorticoids, an effective treatment for MS relapses, has also been demonstrated in the newly established human brain endothelial cell line, hCMEC/D3 (Weksler et al., 2005). The application of the glucocorticoid hydrocortisone, increased the expression of occludin and claudin-5, which is thought to contribute to the three fold increase in TEER that was observed. In addition, the administration of hydrocortisone prevented TNF-induced degradation of TJ proteins (Förster et al., 2008).

1.3 Mediators of inflammation

1.3.1 Cytokines in MS

Cytokines are low relative molecular mass (RMM) proteins whose actions are generally mediated at close range and are involved in various biological processes, including cell proliferation, inflammation, immunity, migration, fibrosis, repair and angiogenesis. There are more than 100 of these small molecules, which are termed interleukins (IL), interferons (IFN), growth factors, and TNFs amongst others (Oppenheim, 2001; Vilcek and Feldmann, 2004).

A variety of cytokine mRNAs have been detected in CNS tissue of MS patients. These include IL-1 α , IL-2, IL-4, IL-6, IL-10, IFN- γ , TGF- β 1 and 2, and TNF. IL-6, IFN- γ and TNF were strongly expressed in perivascular inflammatory cuffs, whereas the other cytokines were more weakly expressed (Woodroffe and Cuzner, 1993). However, all cytokine mRNAs were more highly expressed in the perivascular cells compared to the parenchymal cells, which the authors propose, indicates that the cells that have crossed the BBB are the major source of cytokines in MS tissue (Woodroffe and Cuzner, 1993). Within actively demyelinating lesions, leukocytes and glial cells express a range of Th1-related cytokines, such as IFN- γ , TNF or IL-2, which all have pro-inflammatory effects (Merrill, 1992). The majority of cytokines detected, increase the permeability of endothelial cells, but some have an opposing influence. TNF has been shown to induce either an increase or decrease in permeability of the BBB, and this dichotomy in behaviour is thought to be cell-type dependent (for review see Walsh et al., 2000). Mayhan (2002) demonstrated the former in cerebral microvasculature of Wistar-Furth rats. It was shown that the mechanism of induction of vascular permeability involved soluble guanylate cyclase and protein tyrosine kinase as its downstream targets. Within the CSF of MS patients, IL-1 β and TNF were increased in active disease compared to inactive and other neurological diseases (Hauser et al., 1990). IL-6, however, was undetectable in most MS CSF (Hauser et al., 1990). This

contrasts with other research groups who have reported an increase in IL-6 in the CSF of MS patients, which is more prominent in acute phases of the disease (Maimone et al., 1991).

1.3.1.1 TNF

TNF is a pleiotropic cytokine that is synthesized as a 26 kDa transmembrane precursor (pro-TNF) that is cleaved into a 17 kDa soluble form by ADAM-17 (Black et al., 1997; Moss et al., 1997; Maskos et al., 1998; Milla et al., 1999; Duan et al., 2003). TNF can have negative and positive effects within the CNS: it can be a critical mediator in demyelinating and neurodegenerative diseases but can also elicit regenerative and neuroprotective effects (Loddick and Rothwell, 1999; Allan and Rothwell, 2001). It has been shown to induce oligodendrocyte cell death in *in vitro* spinal cord explants (Selmaj and Raine, 1988).

As MS is regarded as an inflammatory disorder of the CNS, various studies have been performed to investigate the TNF expression levels in MS patients. In post-mortem tissue, TNF is localised to astrocytes and macrophages at the lesional edge of the MS plaque, but is absent in brain tissue from normal and neurological control patients (Hofman et al., 1989). Significantly increased TNF levels have been observed in the CSF of chronic progressive MS patients in comparison to stable MS and other neurological disease controls. TNF levels showed a positive correlation with disease severity at the beginning of the study and also the progression of the disease, the latter suggesting that initial high levels of TNF would indicate a poor prognosis for the patient (Sharief and Hentges, 1991). An increase in TNF in the CSF of patients with active MS has also been reported by other groups (Hauser et al., 1990), however, other research has not corroborated these findings (Franciotta et al., 1989; Peter et al., 1991). Drulovic et al., (1997) studied the levels of TNF in the CSF of MS patients. TNF was detected in 60% of MS patients tested, with an average of 10.1pg/ml ($n = 15$). However, non-inflammatory neurological disease controls (NIND) showed similar levels with 9.5pg/ml ($n = 4$) of TNF. In patients with inactive MS, no TNF could be detected. However, a positive correlation was observed between the detection of TNF and the degree of disability shown in the MS patient (Drulovic et al., 1997). These discrepancies could be due to the different techniques employed and also the selection criteria for patients (Hauser et al., 1990; Sharief and Hentges, 1991). Interestingly, a high incidence of intrathecal TNF was not found to correlate with pleocytosis, thus it was concluded that TNF was CNS derived and not from the cells of the CSF (Hauser et al., 1990; Sharief and Hentges, 1991).

Serum TNF levels have been reported to be significantly lower than CSF levels in MS patients (Sharief and Hentges, 1991) or an elevated level could only be seen in a

minority of patients (16%) (Peter et al., 1991). It has been reported that serum protein levels of TNF in RRMS patients do not differ from the levels observed in healthy controls and do not correlate with clinicopathological hallmarks of the disease (Martino et al., 1997). mRNA levels were also examined in PBMCs in this study, however no correlation could be found between levels of TNF mRNA and disease activity (Martino et al., 1997).

As a consequence of the strong association between MS and TNF, studies were carried out to investigate the effects of inhibiting TNF in murine EAE. Animals treated with anti-TNF antibodies did not show any clinical manifestations of EAE, and also had no pathological signs of the disease, i.e. demyelination and inflammation (Selmaj et al., 1991). Other studies have reported a decrease in severity of EAE using anti-TNF antibodies, which is proportional to the dose of immunoglobulin administered (Ruddle et al., 1990). In addition, the over expression of TNF in the murine CNS causes a demyelinating disease, which can be neutralised by the application of an anti-TNF antibody (Probert et al., 1995). The latter study suggested TNF could have a direct role in MS pathogenesis. The application of soluble TNF receptor 1 (TNFR1, see section 1.3.1.1.1) has also been shown to inhibit the clinical and pathological manifestations of EAE (Selmaj et al., 1995). The effective prevention of EAE by TNF inhibitors led to the application of anti-TNF therapies for treatment in MS patients. cA2, a mouse monoclonal antibody, was given to two young MS patients suffering an aggressive disease course and after administration of this treatment the number of Gd-MRI lesions increased concomitantly with the number of CSF leukocytes and the IgG index, suggesting anti-TNF therapy caused immune activation and an increase in disease activity (van Oosten et al., 1996). In addition, the prescription of the anti-TNF fusion protein, Etanercept, to treat a patient with juvenile rheumatoid arthritis (RA) led to the development of MS after 9 months of treatment, suggesting anti-TNF therapy could have caused the development of MS in this patient (Siccotte and Voskuhl, 2001). This unexpected failure in TNF therapy for MS patients led some researchers to investigate the role of TNF in nerve myelination, using a neurotoxicant model of demyelination using the toxin, cuprizone, and also using transgenic mice which had either alterations in TNF, or the TNF receptors 1 and 2 (TNFR2). TNF knockout (KO) mice showed a delay in their ability to remyelinate nerve fibres, which was associated with a decrease in oligodendrocyte progenitors and subsequently the number of mature oligodendrocytes. TNFR2 KOs, but not TNFR1 KOs, showed the same reduced cell proliferation, suggesting that TNF signalling through TNFR2 is responsible for oligodendrocyte regeneration. These surprising results suggested that the failure of anti-TNF therapy in MS patients could be due to the hampered remyelination caused by the decreased bioavailability of TNF (Arnett et al., 2001).

Another protective function of TNF is its immunosuppressive ability. TNF-deficiency is associated with prolonged reactive myelin-specific T cell responses and exacerbated EAE. This study also demonstrated that the pro-inflammatory effects of TNF can be accounted for by TNFR1 and it is thus thought that blocking TNFR1 might be a more effective treatment for inhibiting the pro-inflammatory activities of TNF (Kassiotis and Kollias, 2001). More recently it has been demonstrated that transgenic mice which do not express the cleavage site of TNF and which only express the transmembrane (tm) form of TNF, show suppressed EAE onset and progression while maintaining the autoimmune suppressive properties of TNF (Alexopoulou et al, 2006). As tmTNF has a greater ability of activating TNFR2 and soluble TNF (solTNF) of activating TNFR1 (Grell et al., 1995; 1998), taken together these studies suggest that inhibiting the solTNF/TNFR1 pathway may be a more effective treatment strategy for MS patients.

1.3.1.1.1 TNF receptors

Part of the contrasting dual functionality of TNF is due to the two different TNF receptor subtypes it binds to, namely TNFR1 (also known as p55TNFR, p60, CD120a, TNFRSF1a) and TNFR2 (also known as p75TNFR, p80, CD120b, TNFRSF1b). TNFR1 is a 55 kDa protein expressed by most cell types and its activation can be mediated by both the soluble (solTNF) and transmembrane form of TNF (tmTNF), but shows a preference for solTNF. TNFR2, however, is a 75 kDa protein and is expressed by cells of the immune system (including microglia) and also by endothelial cells, and is preferentially activated by tmTNF (Grell et al., 1995; 1998).

These single transmembrane glycoproteins are structurally similar but functionally distinct. They share 28% homology, most of which is situated in the extracellular domain (Figure 1.9). Their intracellular domains share almost no homology and are mostly unrelated, suggesting that the binding of TNF to these two receptors elicits different intracellular signals (Lewis et al., 1991; Tartaglia and Goeddel, 1992; Grell et al., 1994). Two common features of the extracellular domains of TNFR1 and 2 are the four tandemly repeated cysteine-rich motifs and an extracellular pre-ligand-binding assembly domain (PLAD) (Figure 1.9). The latter pre-complexes the receptors and encourages them to trimerize, particularly under the influence of TNF, which is also presented as a trimerized complex (MacEwan, 2002). One very important and obvious distinguishing feature of TNFR1 is the presence of a death domain (DD) at the carboxyl-end of the receptor, which along with other accessory proteins, carrying the same domain, signals for cell death (Figure 1.9). Both receptors have sequences that are capable of binding TNF receptor-associating factors (TRAFs) and adaptors,

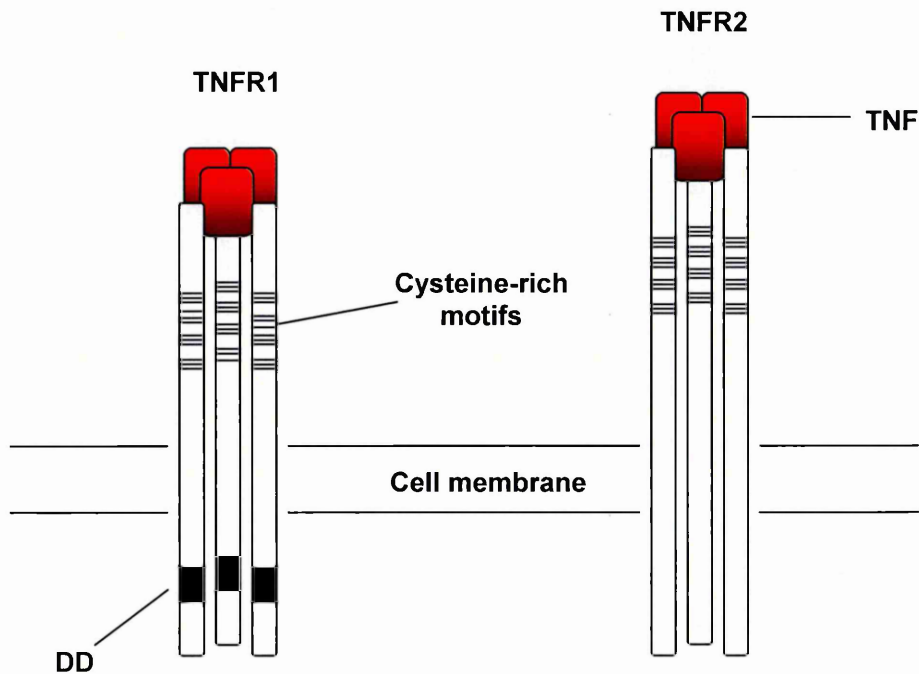


Figure 1.9: Schematic representation of TNFR1 and TNFR2. These receptors have 28% sequence homology in their extracellular domains including the presence of four tandemly repeated cysteine-rich motifs. Their cytosolic domains have almost no sequence homology. TNFR1 contains a death domain (DD) which with other adaptor proteins signals cell death when TNF binds (Redrawn with permission from Elsevier from MacEwan, 2002).

which transduce the TNF signal from the receptors to the signalling molecules within the cell (MacEwan, 2002).

The two receptors can act as transporters that chaperone TNF into the CNS. Pan and Kastin (2002) demonstrated that knocking out either of these receptors in mice reduced the influx of TNF into the brain, and if both receptors are knocked out this entry is totally abolished (Pan and Kastin, 2002). Interestingly Banks et al. (1995) demonstrated that incubating TNF with the soluble TNFR2 completely abolished transport of both human and murine TNF into the mouse brain. It was also shown that TNFR2 itself cannot cross the BBB (Banks et al., 1995). TNFR1 has been demonstrated to mediate cell death via both apoptosis and necrosis in a murine neuronal cell line, when cells are incubated with TNF and actinomycin D, which interferes with replication and transcription by binding to DNA duplexes (Sipe et al., 1996). TNFR2 mRNA was not detected in this cell line, however its expression after stimulation with TNF was not analysed (Sipe et al., 1996).

TNFR1 has been described to be constitutively expressed in barrier associated structures of the CNS, including the microvasculature. Whereas its counterpart, TNFR2, is mainly expressed when the microvasculature is activated under stimulatory conditions (Nadeau and Rivest, 1999). Microglia, which are the primary producers of TNF at CNS inflammatory sites, have been shown to express both receptors (Dopp et al., 1997). However, astrocytes and oligodendrocytes predominantly express TNFR1 (Dopp et al., 1997). TNFR2 mRNA expression in microglia is increased by both TNF and IFN- γ , and signal transduction through TNFR2 inhibits signals transduced via TNFR1, either directly or indirectly (Dopp et al., 1997). Thus, it is believed that differential expression of these two receptors can determine the response of cells to TNF i.e. whether it has a proliferative, activational, or cytotoxic effect (Dopp et al., 1997).

Martino et al. (1997) showed that the levels of soluble TNF receptors in serum of RRMS patients did not differ from the levels seen in healthy controls. However, when these molecules were examined at the molecular level i.e. the mRNA in PBMCs, both TNFR levels fluctuated significantly and peaked 6 weeks prior to clinicopathological evidence of the onset of an attack (Martino et al., 1997). In 1999, two papers were published demonstrating the shedding events of both TNFRs in MS patients. Jurewicz and colleagues (1999) measured the shedding of TNFRs from the cell surface of PBMCs, peripheral blood lymphocytes, and monocytes in three groups of MS patients: RRMS in relapse, RRMS in remission, and chronic progressive. The two receptors showed differential behaviour in MS patients in comparison to healthy volunteers. TNFR1 was shed at a lower rate, whereas TNFR2 was shed at significantly higher rates in MS patients (Jurewicz et al., 1999). The same year Franciotta et al. (1999)

investigated the levels of the soluble receptors in the plasma and CSF of MS patients before and after treatment with methylprednisolone (MP), a corticosteroid. Plasma and CSF TNFR2 levels did not vary and were similar to the levels seen in controls. CSF TNFR1 levels, however, were higher in acute MS patients in comparison to controls, and these levels increased after MP treatment (Franciotta et al., 1999). Despite the disparity in results of the previous studies, it has been demonstrated that both receptors are up-regulated in the membrane bound form in the CNS in MS patients in macrophages and microglial cells in the region of the plaque edge (Sippy et al., 1995).

1.3.1.2 IL-1

In 1984 the cDNAs for both IL-1 α and IL-1 β were cloned (for review see Feghali and Wright, 1997). Both IL-1 α and IL-1 β are synthesized as precursor proteins, however only IL-1 α is active in this form. IL-1 β , however, is inactive and must be cleaved by the cysteine-aspartate protease, caspase-1. IL-1 mediates its biological effects through its membrane-bound receptor, IL-1RI (IL-1 receptor I) (for review see Simi et al., 2007). The biological activity of IL-1 can be modulated by the IL-1 receptor antagonist, IL-1Ra, which competes for IL-1RI, preventing IL-1 from binding (for review see Feghali and Wright, 1997). An increasing body of work suggests that IL-1 may be involved in various chronic neurodegenerative diseases.

IL-1 β has been reported to be increased in CSF of patients with active MS compared to inactive MS or other neurological diseases (OND) (Hauser et al., 1990). Other studies have not corroborated this result and have only seen increased serum levels of the protein in a minority of patients (6%) (Peter et al., 1991). Certain IL-1 genotypes, or the balance between IL-1 and its receptor antagonist, IL-1Ra, have been found to be associated with disease severity/progression in MS (Mann et al., 2002). Chronic administration of IL-1 through a recombinant adenovirus vector results in BBB breakdown and extensive demyelination in rats, mimicking MS (Ferrari et al., 2004). The mechanism behind IL-1-induced BBB breakdown is associated with an induction of hypoxia inducible factor-1 (HIF-1) and vascular endothelial growth factor (VEGF)-A in astrocytes, which favour plasticity and permeability of the endothelial cells (Argaw et al., 2006). IL-1Ra has been shown to reduce disease severity in EAE (Martin and Near, 1995). Alternatively, IL-1 β knockout mice fail to remyelinate axons completely which is believed to be associated with a lack of production of insulin-like growth factor-1 (IGF-1) by microglia/macrophages and astrocytes, and a detrimental delay in mature oligodendrocyte differentiation. It was deduced from this study that IL-1 β induces the production of IGF-1 by glia and monocyte lineage cells, and may promote remyelination (Mason et al., 2001).

1.3.1.3 IFN- γ

IFN- γ is the only cytokine to belong to the type II interferon family (Pestka et al., 2004). An increased expression of IFN- γ has been shown to precede clinical attacks in MS (Beck et al., 1988; Lu et al., 1993), and also the injection of recombinant IFN- γ into MS patients was found to exacerbate the disease (Panitch et al., 1987). IFN- γ is localised within the immune cells of the perivascular cuffs in MS lesions (Woodroffe and Cuzner, 1993; Simpson et al., 2000), but has also been found, to a lesser extent, within microglia and astrocytes at the plaque edge (Traugott and Lebon, 1988).

Despite the implications of IFN- γ in MS pathogenesis, studies in EAE have revealed that IFN- γ may also have a protective role in autoimmune diseases as IFN- γ receptor KO mice experience a more severe disease than their wild-type littermates (Fabis et al., 2007). In addition, the delivery of IFN- γ through a viral vector in murine EAE prevents the development of the chronic-progressive form of the disease and is also associated with a more rapid recovery. The recovery phase of the disease was associated with an increase in apoptosis of CNS-infiltrating lymphocytes and an increased mRNA expression of TNFR1, thus the authors conclude that IFN- γ expression is protective as it helps mediate the clearance of encephalitogenic T cells (Furlan et al., 2001). IFN- γ is also thought to mediate its protective effects in EAE by inducing iNOS and hence nitric oxide (NO), which has an effect on a number of critical mediators of CNS inflammation and also apoptosis (Willenborg et al., 1999). Conversely, IFN- γ has been shown to induce the expression of the chemokines CXCL10 and CCL5 to levels associated with EAE, however, these factors by themselves are not sufficient to recruit immune cells into the CNS and require peripheral infectious agent, e.g. pertussis toxin (Millward et al., 2007). Thus within the CNS, IFN- γ appears to contribute to MS relapses, whereas in EAE, the cytokine appears to help mediate cell death of invading T cells, and is associated with recovery.

1.3.1.4 TGF- β 1

Transforming growth factors (TGF- β s) are a large family of pleiotropic cytokines which are evolutionarily conserved. Three TGF- β isoforms are known to exist in mammals: TGF- β 1, TGF- β 2, and TGF- β 3. TGF- β 1 belongs to the TGF- β superfamily, which includes activin/inhibins, bone morphogenic protein (BMP), and others which share the same structural and functional resemblances (for review see Goumans et al., 2009).

Various studies have investigated the expression of this cytokine to determine a correlation with MS (Mokhtarian et al., 1994; Söderström et al. 1995). TGF- β has been found to be significantly down-regulated in lymphocytes of patients with clinically active MS compared to stable MS, other autoimmune controls and healthy controls (Mokhtarian et al., 1994). TGF- β 2 has been observed predominantly in microglia in the

cellular border of acute active lesions, whereas all three TGF- β isotypes have been found to be associated with astrocytes in the chronic active plaque (Peress et al., 1996). TGF- β has also been observed in the extracellular matrix surrounding blood vessels and shows an association with the endothelium in acute MS lesions (Cannella and Raine, 1995), but also shows the same expression profile in normal brain, suggesting a normal regulatory role at the level of the BBB (Brosnan et al., 1995). In EAE, high plasma levels of TGF- β are associated with the recovery phase of the disease (Iwahashi et al., 1997).

1.3.2 Chemokines

The chemokine (the word is a contraction of **chemotactic cytokine**) family consists of a large number of small (8-14 kDa) proteins, which display a wide variety of biological and pathological functions. Chemokines are further classified into four subfamilies based upon the position of two cysteine residues located near the amino terminus of the protein. These are: CXC, CC, C, and CX3C chemokine families (where X represents an intervening aa). The biological effects of chemokines are induced by binding to seven-transmembrane-domain G-protein coupled receptors (GPCR) on their target cells. The nomenclature for the ligands and receptors is indicated by its subfamily then a letter 'L' or 'R', respectively, and finally its particular number, e.g. CCL2 and CCR2, and CX3CL1 and CX3CR1 (Luster, 1998; Laing and Secombes, 2004; for review see Ubogu et al., 2006).

Various chemokines have been implicated as playing a role in MS and EAE pathogenesis (Karpus and Ransohoff, 1998). The chemokine profiles in the CSF of MS patients have been shown to correspond to the cognate chemokine receptors expressed in MS lesions of post-mortem tissue. CXCL10 (IFN- γ -inducible protein of 10 kDa or IP-10), CXCL9 (monokine induced by IFN- γ or Mig) and CCL5 (regulated on activation, normal T cell expressed and secreted or RANTES) are all significantly elevated in MS CSF during a clinical attack, which corresponds with CXCR3, an CXCL10 and CXCL9 receptor, and CCR5, a CCL5 receptor, expressed by immune cells in perivascular cuffs and areas of demyelination in MS brain lesions (Sorensen et al., 1999). CXCL10 and CXCL9 have also been found to be expressed in macrophages and astrocytes in active demyelinating lesions of MS patients, which bind to CXCR3 expressing T cells in the perivascular cuffs. These two T cell chemoattractants are induced by IFN- γ secreted by the T cells within the perivascular cuff (Simpson et al., 2000). Correspondingly, within serum samples, there has been reported an increase in CXCR3⁺ T cells in RRMS patients, whereas PPMS patients showed an increase in both CXCR3⁺ and CCR5⁺ T cells, in comparison to controls (Balashov et al., 1999). Reactive hypertrophic astrocytes in post-mortem MS brain lesions have been

implicated in the recruitment of demyelinating macrophages via the expression of the potent monocyte and T cell attracting chemokine, CCL2 (monocyte chemoattractant protein-1 or MCP-1) (Van Der Voorn et al., 1999).

In EAE, inhibition of CXCR4 activation via an antagonist is associated with enhanced CNS parenchymal leukocyte infiltrates, loss of the typical perivascular cuff, the loss of CXCL12 (CXCR4 ligand) polarisation on CNS endothelial cells, and increased disease severity. It was deduced from this work that the role of CXCL12 may be to contain the leukocytes within the perivascular space and therefore limit inflammation and thus have an anti-inflammatory role within the CNS (McCandless et al., 2006).

In vitro studies have shown that the chemokine CCL3 (MIP-1 α), increases dendritic cell (DC) migration through brain microvessel endothelial cell monolayers, which in turn causes the reorganisation of occludin. However, this does not affect the barrier integrity as the TEER is not affected significantly (Zozulya et al., 2007). CCL5 has been shown to facilitate the migration of T lymphocytes across immortalised human brain microvascular endothelial cells (Man et al., 2008).

1.3.2.1 Fractalkine (CX₃CL1)

Fractalkine was the first and only chemokine identified to belong to the fourth class of chemokines, CX₃C (Bazan et al., 1997). It is distinct in terms that the two N terminal cysteine residues are interrupted by a tripeptide (compare: C, CC, CXC) (Fig 1.10). Fractalkine is dichotomous, in addition to its role as a traditional chemokine, i.e. chemoattractant for cells of the immune system when it is shed from the membrane, it also plays a role in cell adhesion in its membrane-bound form (Bazan et al., 1997). Fractalkine has also recently been shown to have angiogenic properties (Volin et al., 2001). The membrane-bound form has been localised to various cells of the body, including epithelial cells (Muehlhoefer et al., 2000; Lucas et al., 2001), endothelial cells (Bazan et al., 1997; Muehlhoefer et al., 2000), smooth muscle cells (Ludwig et al., 2002; Wong et al., 2002), dendritic cells (Papadopoulos et al., 1999; Kanazawa et al., 1999), neurons (Pan et al., 1997; Nishiyori et al., 1998; Harrison et al., 1998), astrocytes (Hulshof et al., 2003) and macrophages (Greaves et al., 2001). In 1997 the receptor for fractalkine (CX₃CR1) was identified and shown to be expressed on T cells (Bazan et al., 1997; Imai et al., 1997), natural killer (NK) cells (Imai et al., 1997), monocytes (Bazan et al., 1997; Imai et al., 1997), microglia (Nishiyori et al., 1998), astrocytes (Maciejewski-Lenoir et al., 1999) and neurons (Meucci et al., 2000). It is thus proposed to play an important role in regulating leukocyte trafficking.

Fractalkine has been found in significant levels in the CSF and serum of patients with MS (Kastenbauer et al., 2003); although its role as a CSF chemokine was

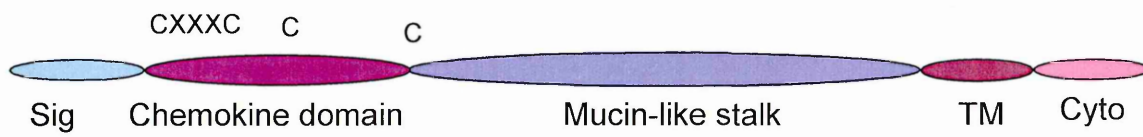


Figure 1.10: Domain structure of fractalkine. Note the CX3C motif in the chemokine domain that distinguishes it from other known chemokines. *Sig*, signal peptide; *TM*, transmembrane domain; *Cyto*, cytoplasmic domain.

not considered to be significant. Despite this, various studies have shown that blocking the fractalkine - fractalkine receptor interface could have beneficiary effects upon the course of certain diseases. Suzuki and colleagues (2005) demonstrated that applying a neutralizing monoclonal antibody directed against fractalkine significantly reduced the functional and pathological hallmarks of experimental autoimmune myositis in mice. They also witnessed reduced T cell and macrophage infiltrates in the muscle when fractalkine was immunologically silenced. The soluble form of fractalkine has also been demonstrated to interfere with arrest of CD16+ monocytes onto endothelial cells; by pre-incubating monocytes with soluble fractalkine this caused a significant decrease in the number of CD16+ monocytes that could arrest onto fractalkine expressing human umbilical vein endothelial cells (HUVEC) cells (Ancuta et al., 2003). However, it has also been shown that preventing this interaction between fractalkine and its receptor could have detrimental effects upon disease. Mice suffering from EAE and deficient in the fractalkine receptor, through gene manipulation, show reduced recruitment of NK cells into the inflamed CNS, which was associated with an increase in EAE-related mortality, non-remitting spastic paraplegia, and hemorrhagic inflammatory lesions (Huang et al., 2006).

Fractalkine expression has been shown to be influenced by a number of cytokines. Rat aortic endothelial cells show an increased expression of membrane-bound fractalkine when stimulated with inflammatory cytokines, such as IL-1 and TNF (Garcia et al., 2000). TNF significantly increases fractalkine mRNA and protein expression in HUVECs (Moon et al., 2006). Fractalkine has been shown to be regulated by IFN- γ in endothelial cells (Imaizumi et al., 2000). However, IFN- γ -induced expression of fractalkine at the mRNA and protein level in HUVECs is inhibited by heparin in a concentration dependent manner (Hatakeyama et al., 2004). Heparin binds directly to IFN- γ and partially blocks the interaction between IFN- γ and its receptor (Hatakeyama et al., 2004). Blood mononuclear cell adhesion to IFN- γ -stimulated HUVEC monolayers can be reduced by heparin (Hatakeyama et al., 2004) and is thus thought to help regulate leukocyte trafficking across the vascular endothelium (for review see Imaizumi et al., 2004). A disintegrin and metalloprotease (ADAM)-17 has been shown to mediate the inducible cleavage and shedding of fractalkine under phorbol 12-myristate 13-acetate (PMA)-stimulation (Garton et al., 2001; Tsou et al., 2001) and ADAM-10 has been implicated as the mediator of constitutive cleavage of fractalkine (Hundhausen et al., 2003) (see section 1.5.7).

1.4 Leukocyte recruitment to the endothelium

1.4.1 Adhesion molecules in MS

Adhesion molecules and chemokines (see 1.3.2) mediate the recruitment of immune cells into tissues through post-capillary venules (Man et al., 2007). Adhesion molecules include selectins, integrins, the JAM family and the endothelial cell-selective adhesion molecule (ESAM). Selectins expressed on the endothelium mediate the capture of leukocytes by interacting with glycosylated ligands on the leukocyte in a process known as *tethering*. This is a transient process, as cells under the shear forces of blood flow begin to roll, a process known as *rolling*. Under an activated state, the endothelial cells begin to express chemokines and adhesion molecules which in turn activate GPCR on the leukocyte, causing a conformational change in the leukocytes' integrins. These integrins can then interact with their cognate protein, e.g. vascular cell adhesion molecule-1 (VCAM-1), intracellular adhesion molecule-1 (ICAM-1), or JAM-1. This process results in the leukocyte attaching onto the endothelium (Man et al., 2007).

It has been well documented that normal human CNS microvessels do not express endothelial cell activation markers, but MS patients do, including VCAM-1, endothelial cell leukocyte adhesion molecule-1 (E-selectin) and ICAM-1 (Washington et al., 1994; Brosnan et al., 1995). The amount of inflammation in these areas shows a positive correlation with the increased expression levels of the adhesion molecules (Canella and Raine, 1995; Sobel et al., 1990; Washington et al., 1994). In addition, increased levels of soluble adhesion molecules have been reported during the relapse phase of RRMS, and SPMS (Baraczka et al., 1999; McDonnell et al., 1999; Dore-Duffy et al., 1995; Droogan et al., 1996; Kraus et al., 1998; Sharief et al., 1993; Tsukada et al., 1993). Recently, it has been reported that various adhesion molecules show variability in their expression profiles between different clinical MS subtypes and controls. The cell surface expression, on mononuclear cells, of very late antigen 4 (VLA-4), lymphocyte function-associated antigen 1 (LFA-1) and ICAM-1 are increased in the blood and CSF of PPMS patients ($n = 25$) compared to controls ($n = 11$). ICAM-1 also shows a higher expression in PPMS patients in comparison to SPMS patients ($n = 18$) (Ukkonen et al., 2007).

MS patients treated with IFN- β -1b show a significant increase in the levels of soluble VCAM-1 which correlate with a concomitant decrease in MRI lesions (Jensen et al., 2005). Levels of soluble ICAM-1, E-selectin, L-selectin and TNFR1 were not significantly altered during treatment (Calabresi et al., 1997). Cleavage and shedding of this receptor and adhesion molecules, apart from E-selectin, have been shown to be mediated by ADAM-17 (Peschon et al., 1998; Borland et al., 1999; Reddy et al., 2000; Garton et al., 2003). However ADAM-17 was not discovered until 1997 (Black et al., 1997) and therefore was not investigated in the work by Calabresi and colleagues

(1997). The fact that other targets of ADAM-17, apart from VCAM-1, are unaffected by IFN- β -1b suggests that the mechanism of action of this cytokine is distinct from the other ligands. It has been shown that the method of action of IFN- β -1b upon VCAM-1 expression in endothelial cells is indirect via its' effect upon T cells (Calabresi et al., 2001).

Endothelial cells isolated from human brain microvessels (HBMEC) showed significantly greater surface expression of VCAM-1, under inflammatory conditions produced using lipopolysaccharide (LPS), TNF or IL-1 β . With LPS proving the most potent at inducing this effect, followed by TNF and then IL-1 β . IFN- γ did not influence VCAM-1 expression (Wong and Dorovini-Zis, 1995).

As a proof of concept of adhesion molecules being implicated in MS, in 2004 a humanised monoclonal antibody called Natalizumab (Tysabri, Biogen Idec Inc., Cambridge, MA and Elan Pharmaceuticals, Inc., San Diego, CA) directed against α 4-integrin of VLA-4 was approved for treating RRMS. The antibody was designed to interfere with the interaction between VLA-4 and its ligand, VCAM-1, and thus prevent the migration of immune cells across the BBB (Yednock et al., 1992). Unfortunately the drug was withdrawn and the trials had to be stopped after two MS patients and one Crohn's disease patient treated with Natalizumab went on to develop progressive multifocal leukoencephalopathy (PML) after its co-administration with IFN- β (Stuve et al., 2007). The drug has since been approved to treat MS and Crohn's patients as a monotherapy in the US and European Community (Engelhardt and Kappos, 2008). Recent investigations into the effects of Natalizumab on immune cell responses in MS patients has revealed that each patient responds differently to the treatment, Natalizumab (standard intravenous infusion of 300mg) does not fully block surface expression of VLA-4, and the drug can also alter the activation threshold of the immune cells (Niino et al., 2006).

Studies are in agreement that ICAM-1 is increased in MS pathology. Bö et al. (1996) showed that MS brains ($n = 11$) had a significant increase in ICAM-1-positive vessels and that this increase was greater in MS lesions (81%) than in non-lesion areas (37%). Immunohistochemical examination of microvessels in MS patients have shown more numerous ICAM-1 positive vessels in white matter in comparison to control samples and normal-appearing, uninvolved MS white matter (Sobel et al., 1990). Immortalized HUVECs (ECV304) subjected to cerebral microvasculature conditions, i.e. co-cultured with C6 astrogloma cells, show decreased barrier integrity and up-regulated ICAM-1, nine-fold more when exposed to TNF for 6-18 hours (Dobbie et al., 1999). Most recently, it has been reported that ICAM-1 null mutant mice experience significantly attenuated EAE, which is characterised by a reduced spinal cord infiltrate with a concomitant reduction in IFN- γ production (Bullard et al., 2007). This indicated

that ICAM-1 is critical in the development of demyelinating diseases as other adhesion molecules e.g. VCAM-1, which were still expressed, could not compensate for its loss (Bullard et al., 2007). More recently, the combined knockdown of ICAM-1 and C3 (the central complement component) in mice with MOG-induced EAE have shown significantly worse disease severity than C3^{-/-} mice alone and only a modest attenuation compared to wild-type mice (Smith et al., 2008). Emphasising that removal of factors implicated in MS will not necessarily ameliorate the disease.

Riekmann and colleagues (1995) found that soluble ICAM-1 inhibits attachment of lymphocytes to cerebral endothelial cells *in vitro*. A positive correlation was found in RRMS patients with Gd-MRI negative scans and high soluble ICAM-1 serum levels compared to patients who had Gd-MRI positive scans (Trojano et al., 1996). Both suggest that soluble adhesion molecules play an important role by restricting leukocyte extravasation across the BBB and the basis for this is a competitive mechanism with their membrane-bound counterparts (for review see Avolio et al., 2003).

1.4.2 Leukocyte recruitment and extravasation

Under normal physiological conditions lymphocyte trafficking into the CNS is limited, however, in MS and its animal model, EAE, there is increased migration of immune cells. Leukocyte migration across the BBB is a multi-step process, whereby cells of the immune system firstly have to penetrate the endothelial cells and the underlying endothelial BM, followed by a transient stop in the perivascular space, before finally penetrating the parenchymal/astroglia BM to reach the brain parenchyma.

Bolton and colleagues (1998) demonstrated that leukocyte recruitment results in junctional disorganization and the subsequent breakdown of the BBB. This was associated with the loss of certain TJ proteins such as occludin and ZO-1 and the redistribution of vinculin, the adherens junctional protein. Immunocytochemical examination of human immunodeficiency virus-1 encephalitis (HIVE) brains (Dallasta et al., 1999) and brains from patients with cerebral malaria (Brown et al., 1999) also showed the same abnormalities in TJ proteins as described by Bolton et al. (1998). Recently it has been reported that in EAE mononuclear cells traverse the endothelium via the transcellular pathway, leaving the TJs undisturbed. It was also reported that the endothelial cells form filipodia-like protrusions which envelope the mononuclear cell, creating a pore through which the immune cell can reach the abluminal side of the endothelium (Wolburg et al., 2005). Various ECM proteins have been observed in the inflammatory cuffs of MS patients, including heparan sulphate proteoglycans (HSPGs) and heparan sulphate glycosaminoglycan sidechains (HS GAGs), which are thought to help mediate the influx/efflux of leukocytes by acting as a conduit network or reservoir

for chemokines (van Horssen et al., 2005). Leukocytes penetrate the endothelial BM using integrin β 1-mediated processes. It was recently shown that macrophages are responsible for penetration of the second BM, the parenchymal/astroglial BM, using gelatinases (MMP-2 and MMP-9), which degrade dystroglycan (a protein which anchors astrocytic endfeet onto the BM). Inhibition of the proteolytic cleavage of this transmembrane receptor via knockout of MMP-2 and -9 confers resistance to EAE in mice (Agrawal et al., 2006).

1.4.2.1 MMPs

The MMPs belong to a large family of zinc-dependent metalloproteinases called the metzincins which are all structurally related. Other metzincin subfamilies include the ADAMs, bacterial serralysins and the astacins. Based upon substrate specificity and certain protein domains, the MMPs can be further subdivided into groups, which include the gelatinases, stromelysins, collagenases, membrane-type (MT)-MMPs and others (for review see Yong et al., 2001). MMPs are thought to be involved in facilitating the migration of immune cells into the CNS in MS by degrading extracellular components associated with the BBB.

Various MMPs have been found to be increased in the serum, CSF and CNS tissue of MS patients (Anthony et al., 1997; Agrawal et al., 2008). MMP-9 is of particular interest due to its increased expression in the serum of MS patients, especially during relapse and levels also correlated with the number of Gd-MRI lesions (Lee et al., 1999; Waubant et al., 1999). Recently, the activity of MMP-9 has been studied in MS patients and has shown that MMP-9 activity is increased in CSF and serum compared to controls. Also, an increase in serum MMP-9 activity and active MMP-9/TIMP-1 ratio corresponded to clinicopathological signs of disease activity, suggesting that this assay could be used as a biomarker for disease activity in MS patients (Fainardi et al., 2006).

Concordantly, increased MMP levels have been observed in mice with EAE (Pagenstecher et al., 1998; Yong et al., 2007), and the application of MMP inhibitors can block the onset of the disease and can even reverse EAE (Hewson et al., 1995; Liedtke et al., 1998). Toft-Hansen et al. (2006) showed that the application of a broad-spectrum MMP inhibitor, Batimastat, in a mouse model of neuroinflammation, prevented the migration of leukocytes across the astroglial BM into the surrounding parenchyma. Instead the leukocytes accumulated in the perivascular space and there were no signs of disease, indicating that MMPs are essential for breaching the astroglial BM. Interestingly, leukocytes could still enter the perivascular space, indicating that MMPs are possibly not essential for migration across the endothelial cells and BM. In addition, dendritic cells (DC) are also not completely blocked from transmigrating

across murine brain endothelial cell cultures in the presence MMP inhibitors (Zozulya et al., 2007), highlighting that MMPs are somewhat redundant in endothelial cell/BM transmigration of DCs also. The MT-MMPs have also been investigated by the Toft-Hansen group in EAE and observed that the regulation of expression of this subtype of MMPs in two models of the disease, i.e. immunization with MOG and adoptive transfer of MOG specific T cells, shows the same pattern. Whereby, MMP-14 and -25 were significantly up-regulated and MMP-15, -16, -17 and -24 were significantly down-regulated in both disease types. This pattern of expression was not found to be associated with the pro-inflammatory cytokines TNF, IL-1 β or IFN- γ (Toft-Hansen et al., 2007).

In vitro studies in rat primary CNS microvascular endothelial cells have revealed that MMP-2 and MMP-9 are constitutively expressed by these cells and that upon 24 hour cytokine treatment with the pro-inflammatory cytokines, TNF and IL-1 β , there was an up-regulation in MMP-9 activity, which was partially inhibited by the steroid, dexamethasone. In addition, this study also investigated the effects of active MMP-9 on the expression of the junctional protein, ZO-1, which after 1-6 hours treatment with the enzyme, resulted in a decrease in the intensity of the staining. This could be prevented by the addition of dexamethasone or an MMP inhibitor (KB8301) (Harkness et al., 2000). An increase in MMP expression has also been observed in primary human brain microvascular endothelial cells under oxidative stress, a hallmark of neurodegenerative disorders, which has been shown to augment BBB permeability and monocyte migration. This was paralleled with the degradation of BM protein, collagen IV, and increased tyrosine phosphorylation of the TJ proteins: occludin, claudin-5 and ZO-1 (Haorah et al., 2007).

1.5 ADAM-17

1.5.1 ADAM-17 structure

ADAM-17 was first identified in 1997 as the principal convertase of TNF and was thus named TNF- α converting enzyme or TACE (Black et al., 1997; Moss et al., 1997). ADAM-17 also belongs to the ADAM family of membrane-bound proteins (Killar et al., 1999; Schlöndorff and Blobel, 1999; Schlöndorff et al., 2001) which together with snake venom metalloproteinases (SVMPs) make up the reprotin family of zinc metalloproteinases. The ADAM family of proteins currently consists of more than 30 members (for review see Mezyk et al., 2003). ADAM-17 shares a number of facets belonging to the majority of ADAMs. It is a multi-domain type I transmembrane protein that relies upon zinc for its catalytic activity, and also has a disintegrin-cysteine rich sequence (Fig 1.11) (Schlöndorff and Blobel., 1999). The catalytic domain has a zinc-binding consensus motif (HELGHNFGAEHD), which coordinates the interaction of zinc

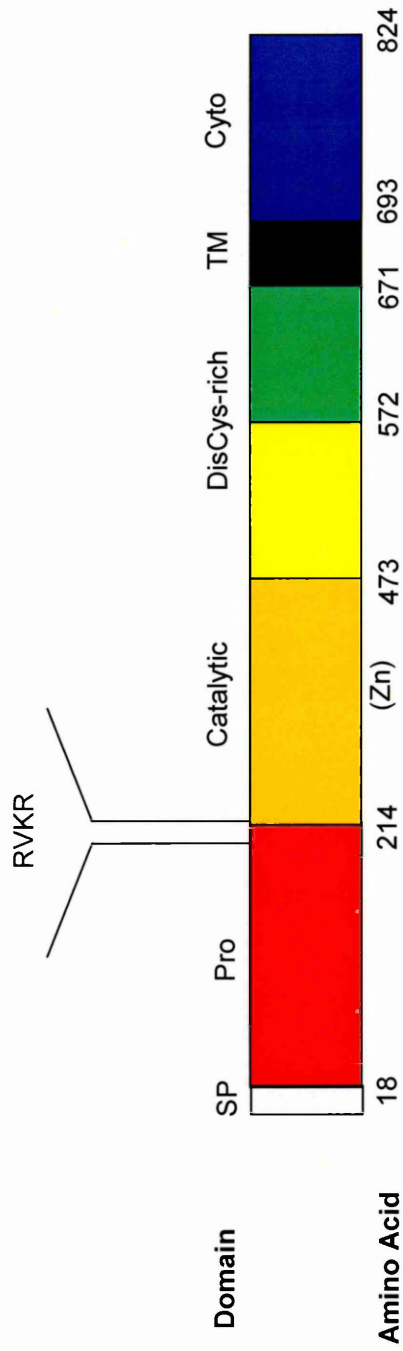


Figure 1.11: Domain structure of ADAM-17. The pro-domain (Pro) is cleaved to yield the mature protein. The catalytic site (Catalytic) of the enzyme relies upon zinc (Zn) for its catalytic activity. The other domains highlighted are the signal peptide (SP), disintegrin-cysteine rich domain (DisCys-rich), the transmembrane domain (TM) and the cytoplasmic domain (Cyto). (Adapted with permission from Elsevier from Black (2002)). The amino acid numbers also highlight where the particular domains reside within the protein (Mezyk et al. 2003).

with histidine residues, thus creating the active site of ADAM-17 (Black et al., 1997; Moss et al., 1997). The disintegrin-cysteine rich domains have been shown to play important roles in cell adhesion and migration (Zhang et al., 1998; Iba et al., 1999, 2000; Wild-Bode et al., 2006). However, the disintegrin region of the ADAMs has recently been shown to be unavailable for protein binding, due to the conformation of the enzyme (Takeda et al., 2006). It is thus thought to play more of a structural role rather than as an integrin ligand (for review see Rocks et al., 2008). Like the MMPs, ADAM-17 is synthesized as an inactive pro-form, or zymogen, that is cleaved between its cysteine switch and catalytic domain to yield a mature, active enzyme (Figure 1.11) (Moss et al., 1997). Consistent with other ADAM proteases (Lum et al., 1998; Roghani et al., 1999), ADAM-17 has been shown to possess a furin-cleavage motif (RVKR²¹⁴) between the pro-domain and the catalytic domain and is thus presumed to be activated by removal of the pro-domain by a furin-type proprotein convertase (Moss et al., 1997). However, a direct involvement of furin in the proteolytic processing of ADAM-17 was not demonstrated until 2003 when Peiretti and colleagues showed that upon furin inhibition, ADAM-17-processed substrates were reduced, which was subsequently rectified by the over-expression of furin. This is in agreement with immunocytochemical studies that have shown the intracellular localisation of ADAM-17 to be predominantly confined to perinuclear regions, which is indicative of the late Golgi compartment, which is also the subcellular localisation of furin (Schlöndorff et al., 2000). It has also been recently shown that ADAM-17 is incorporated into lipid-rafts during transport through the Golgi apparatus where furin performs cleavage of the pro-domain (Tellier et al., 2006).

ADAM-17 is reported to be an 85kDa protein (Black et al., 1997; Moss et al., 1997) expressed in various cell types, including monocytes, peripheral blood T cells, neutrophils, endothelial and smooth muscle cells (Black et al., 1997). Black and colleagues (1997) found no evidence of the pro-enzyme, however Schlöndorff and colleagues (2000) reported a 100kDa form in THP-1 cells (monocytic cell line) that represented ADAM-17 with its pro-domain, which was later converted to a 70kDa protein in its mature state. The differences in RMM between the Black and Schlöndorff studies could be due to the fact that the latter study deglycosylated ADAM-17 with a peptidase: *N*-glycosidase F (PNGase), whereas the former did not. Also, Black and colleagues (1997) mention that there are slight variations in the RMM they observed on western blots for ADAM-17, which they credit to differential glycosylation of the protein, but could also represent the pro-form. Only the mature form of ADAM-17 is expressed on the cell surface, but not the zymogen (Doedens and Black, 2000; Schlöndorff et al., 2000).

1.5.2 ADAM-17 as a sheddase

In addition to its ability to cleave TNF from its pro-form to its active soluble form, ADAM-17 also has been demonstrated to be the major physiological sheddase responsible for the ectodomain cleavage of some 50 transmembrane proteins including: TNFR2 (Peschon et al., 1998), TNFR1 (Reddy et al., 2000), macrophage colony-stimulating factor receptor (Rovida et al., 2001), and interleukin 1- receptor 2 (IL1-R2) (Reddy et al., 2000), CD40 (Contin et al., 2003), VCAM-1 (Garton et al., 2003), L-selectin (Peschon et al., 1998), the chemokine and adhesion molecule fractalkine (Garton et al., 2001), TNF-related activation-induced cytokine (TRANCE) (Lum et al., 1999), transforming growth factor- α (TGF- α) (Peschon et al., 1998), and APP (Buxbaum et al., 1998). In 2006, it was demonstrated that ADAM-17 performs its shedding activities within the cholesterol-rich membrane microdomains, lipid rafts, and that upon cholesterol depletion this process is increased. This highlights the fact that cholesterol plays a significant role in regulating ADAM-17's shedding activities. The precise mechanism of this process was not investigated, but disruption of the lipid raft displaced the mature form of ADAM-17 into non-raft areas where the majority of ADAM-17 substrates were situated. Under normal physiological conditions, these substrates would not be available to the protease and the cleavage of substrates would be dependent upon the entry of ADAM-17 into the lipid-raft. Also, different proportions of substrates were found to be localised within the rafts, and it is believed protein partitioning, in such a manner, may be involved in regulating ADAM-17 substrate proteolysis (Tellier et al., 2006). Recently, it has been demonstrated that high-density lipoproteins (HDL) activate ADAM-17 dependent shedding by decreasing the cholesterol content of lipid rafts (Tellier et al., 2008).

1.5.3 Regulation of ADAM-17 activity

The exact system employed to regulate shedding of membrane-bound proteins by ADAM-17 is still not clearly understood, however, experiments utilising cells which have a mutated ADAM-17 have provided useful tools to investigate ADAM-17 protease activity. Cells lacking the transmembrane portion (TM) of the protein and instead have a glycosylphosphatidylinositol (GPI)-binding polypeptide or a miscellaneous receptor show a great reduction in the shedding of TGF- α , but not TNF and L-selectin. The authors observed from this that the TM portion of ADAM-17 is important as a transmembrane anchor to bring about the cleavage of a broad diversity of substrates and also in terms of the amino acid sequence it carries, as different TM sequences differentially influence the substrates that are cleaved, e.g. TGF- α compared to TNF and L-selectin (Li et al., 2007). PMA has been found to be a general inducer of shedding for all ADAM-17 substrates, as have growth factors, ionophores and

cholesterol depletion for the substrates examined (Pandiella and Massague, 1991; Fan et al., 2003; Matthews et al., 2003). So far, two intracellular signalling pathways have been cited as being important in regulating ectodomain shedding of transmembrane proteins: Erk and p38 MAP kinase. PMA-induced shedding involves the Erk-dependent mechanism, whereas the basal shedding of TGF- α and TNF requires the activity of p38 MAP kinase (Fan and Derynck, 1999; Gechtman et al., 1999; Montero et al., 2002). As ectodomain shedding of transmembrane proteins involves intracellular activity some researchers deduced that the cytoplasmic domain of ADAM-17 must be an important facilitator of this process. However, constructs of ADAM-17 lacking the cytoplasmic domain show no loss of functional shedding ability (Fan et al., 2003; Reddy et al., 2000; Li and Fan, 2004). Surprisingly, especially in the context of the previous report, is the fact that the cytoplasmic domain of ADAM-17 is phosphorylated in response to shedding activators (Fan et al., 2003; Diaz-Rodriguez et al., 2002).

Interestingly, the disintegrin-cysteine rich domain has been implicated as an important regulator of ectodomain shedding: mutagenesis and functional studies using mutant Chinese hamster ovary (CHO) cells revealed that a point mutation in this region (Cys⁶⁰⁰) was detrimental to the shedding of TGF- α and TNF, either in the presence or absence of PMA. Amino acid substitution experiments, whereby this cysteine residue was replaced with one of the other 19 amino acids, did not restore shedding ability to this cell line. Suggesting that Cys⁶⁰⁰ is essential for the proteolytic activity of ADAM-17, perhaps through participating in disulfide bonding, which would be essential for both the processing and catalysis of ADAM-17 (Li and Fan, 2004).

1.5.4 Substrate specificity of ADAM-17

As ADAM-17 can induce the shedding of approximately 50 substrates this has raised the question of what common properties do these proteins hold in their cleavage regions that they can all be shed by ADAM-17. ADAM-17 has been shown to preferentially cleave peptides that resemble the processing sites of TNF and TGF- α , but also cleaves peptides that are unlike these two proteins very efficiently (Black et al., 2003). Peptide cleavage assays have revealed that a 20-residue peptide, which spans the cleavage site of TNF is cleaved solely between Ala⁷⁶ and Val⁷⁷ (Mohler et al., 1994) (Table 1.1). Other proteins shed by ADAM-17, however, are cleaved at sites discrete from the alanine-valine preference site of TNF. L-selectin is reported to be cleaved between lysine and serine amino acids (Kahn et al., 1994), APP is cleaved at a site between residues lysine and leucine (Buxbaum et al., 1998), whereas TNFR1 is cleaved between asparagine and valine (Reddy et al., 2000), and TNFR2 is shed by the cleavage between glycine and serine (Crowe et al., 1995) (Table 1.1). Threonine

Table 1.1: Cleavage sites of ADAM-17 substrates. The arrow indicates where ADAM-17 cleaves the protein.

Substrate	Cleavage site		
TNF	PLAQA	↓	VRSSS
L-selectin	QKLDK	↓	SFSMI
APP	VHHQK	↓	LVFFA
TNFR1	PQIEN	↓	VKGTE
TNFR2	MGPSPPAEG	↓	STGDFAL

and leucine are also acceptable substitutes for alanine and valine (Black et al., 2003). How ADAM-17 is able to cleave substrates with different primary sequences in the cleavage site is not exactly known, but suggests that there is not a common consensus motif which signals cleavage (Mezyk et al., 2003). In the case of L-selectin it has been shown that amino acid substitution in the cleavage site does not affect the cleavage process (Chen et al., 1995; Migaki et al., 1995; Stoddart et al., 1996). However, if amino acids are deleted in the proximal membrane region shedding will be eliminated, highlighting that the length of the proximal region is of more importance (Zhao et al., 2001). Thus the conformation of the proteins could be an important factor influencing the type of substrates cleaved by ADAM-17. In addition to this, the extensive surface loops of ADAM-17 have also been hypothesised as being important factors influencing the substrate cleavage by ADAM-17 (Black et al., 2003).

1.5.5 ADAM-17 expression

ADAM-17 mRNA has been found in most tissues, for example, in the adult heart, skeletal muscle, thymus, small intestine and in the foetal brain, lung, liver and kidney and is said to be largely constitutively expressed (Black et al., 1997). ADAM-17 has been found to be predominantly localised to intracellular perinuclear compartments in COS-7 cells, which are fibroblast-like cells from the African green monkey (Schlöndorff et al., 2000). Some diffuse staining, consistent with surface and endoplasmic reticulum staining patterns, was also observed (Schlöndorff et al., 2000). However, no dual labelling experiments to confirm this co-localization were performed. ADAM-17 has also been reported to be co-localized with the actin cytoskeleton, along with FHL2 (four and a half LIM domain 2 protein), a LIM domain protein that is involved in multiple protein-protein interactions (adaptor/docking protein and regulation of transcriptional events), in cardiomyoblast cells. Subcellular fractionation experiments revealed that the mature form of ADAM-17 had a higher tendency to cosediment with the cytoskeleton rather than the pro-form. FHL2 deficiency resulted in the increased expression of ADAM-17, which in turn resulted in the reduced production of TNFR1 and TNFR2 under PMA-treatment. Thus, FHL2 is involved in the regulation of activity and localisation of ADAM-17 (Canault et al., 2006).

1.5.6 TIMP-3 and the TIMP family of proteins

The tissue inhibitors of metalloproteases or TIMPs are a family of proteins that are made up of four members, TIMP-1, -2, -3, and -4. They share the same secondary structure of six loops that are held together by 6 disulphide bonds, which secure the protein into a wedge shape, that is similar to the Fab portion of immunoglobulins (for

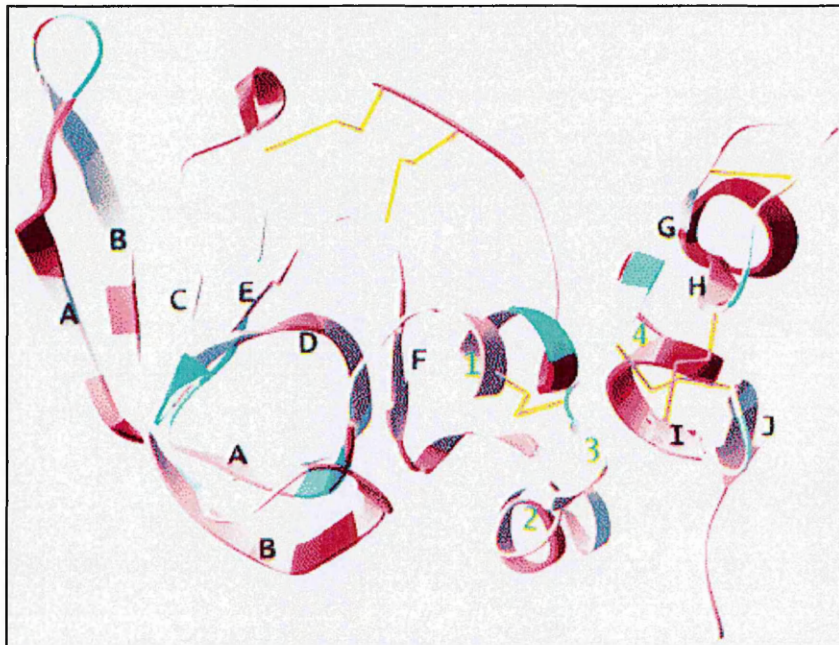


Figure 1.12: The three-dimensional structures of TIMPs. Here the ribbons secondary structure of TIMP-2 is used to demonstrate the wedge shaped conformation of the TIMPs. Disulphide bonds are shown in yellow. (Reproduced with permission from Elsevier from Brew et al., 2000).

review see Crocker et al., 2004) (Figure 1.12). The TIMPs all bind tightly, although with varying affinity, to MMPs. They inhibit MMPs via noncovalent interactions in a 1:1 stoichiometry (Gomis-Ruth et al., 1997). TIMP-3 is distinct in that it is the only TIMP to bind to the extracellular matrix (ECM) through sulphated glycosaminoglycans (GAGs) such as heparan- and chondroitin-sulphate (Yu et al., 2000). TIMP-3 is also unique in terms that it is the only TIMP to inhibit members of the ADAM family and has been found to be the endogenous inhibitor of ADAM-17 (Amour et al., 1998). TIMP-3 has been found to be highly expressed in the heart, kidney and thymus (for review see Crocker et al., 2004). Its' mRNA is also expressed in ventricular zones and subventricular zones of the embryo and postnatal rat brain, respectively (Jaworski and Fager, 2000). TIMP-3 expression coincides with areas of neurogenesis, such as along the rostral migratory stream (RMS) to the olfactory bulb, where it is expressed by astrocytes (Jaworski and Fager, 2000). In addition, an abundance of TIMP-3 mRNA in neocortical endothelial cells was also observed (Jaworski and Fager, 2000). TIMP-3 expression has been described in Purkinje cell somata and processes in the adult rat cerebellum (Vaillant et al., 1999).

TIMP-3 has been shown to inhibit the inducible shedding of L-selectin from leukocytes (Borland et al., 1999) and VCAM-1 from cardiac endothelial cells through actions on ADAM-17 (Singh et al., 2005). The latter study also reported a down-regulation of TIMP-3 mRNA following simultaneous cytokine stimulation with TNF and IL-1 β (Singh et al., 2005). This is in agreement with Li and colleagues (1999) who previously demonstrated that protein and mRNA levels of TIMP-3 are down-regulated 15 hours after TNF and IL-1 β simultaneous administration to cardiac cells, which could result in an equilibrium that is in favour of degradation of the ECM under inflammatory conditions. Bugno and colleagues (1999) also showed that administering TNF and IL-1 β simultaneously almost completely blocked TIMP-3 expression in endothelial cells, and was down-regulated by TNF or IFN- γ in astrocytes.

Mutations in the coding region of TIMP-3, that lead to alterations in the quantity of cysteine residues, have been found in Sorsby's fundus dystrophy (Weber et al., 1994), which is a rare inherited degenerative disorder of the retina. Chong and colleagues (2003) showed there was a reduction in the mRNA expression of TIMP-3 in Sorsby retinal pigment epithelium cells. TIMP-3 also inhibits VEGF coordinated angiogenesis by hindering the association of VEGF to VEGF receptor-2 and thereby stopping downstream signalling, which would induce angiogenesis (Qi et al., 2003). Over expression of TIMP-3 results in a type II apoptotic pathway which is mediated via a Fas-associated death domain-dependent mechanism (Bond et al., 2002). It is thought that this inhibits shedding of death receptors (unidentified) by inhibiting MMPs that usually mediate the cleavage of death receptors and their ligands from cell surfaces

(Wetzel et al., 2003). A positive cooperativity has been demonstrated between the extracellular region of ADAM-17 and the inhibitory domain of TIMP-3 (N-TIMP-3) (Wei et al., 2005) (Figure 1.13). Mutations such as amino acid substitutions or elongation of side chains, that prevent the interaction of the cysteine switch region with the catalytic zinc, proved to have insignificant effects upon the ADAM-17-TIMP-3 complex (Figure 1.13), but interfered in the interaction of their matrix counterparts and TIMP-3. As such it was suggested that the mechanism of inhibition of ADAM-17 by TIMP-3 is possibly distinct from that of inhibiting MMPs (Wei et al., 2005).

1.5.7 ADAM-10

ADAM-10 (also known as MADM, mammalian disintegrin-metalloproteinase) shows a significant amount of sequence and structural homology to ADAM-17 (Black et al., 1997; Rosendahl et al., 1997; Moss et al., 1997), and like ADAM-17 has also been studied for its ability to mediate ectodomain shedding of membrane-bound substrates. ADAM-10 is responsible for the constitutive shedding of a number of substrates which are also shed by ADAM-17, including fractalkine (Hundhausen et al., 2003) and APP (Allinson et al., 2004). ADAM-10 has been shown to mediate vascular permeability and transmigration of T-cells through HUVECs via vascular endothelial (VE)-cadherin proteolysis. Over expression of ADAM-10 in HUVECs, using a viral vector, resulted in the increased permeability for FITC-dextran of the endothelium (Schulz et al., 2008). ADAM-10 activity has been shown *in vitro* to be inhibited by TIMPs -1 and -3 (Amour et al., 2000). ADAM-10 is homologous to the neurogenic drosophila protein, *kuzbanian* (*kuz*), and is involved in neurogenesis itself via the shedding of various Notch ligands (Howard and Glynn, 1995; Rooke et al., 1996; Muraguchi et al., 2007). There has only been one study examining the expression of ADAM-10 in MS lesions (Kieseier et al., 2003) and one in the EAE model of MS, the latter, however found that ADAM-10 was not dysregulated significantly at the mRNA level using quantitative real-time RT-PCR (qRT-PCR) and further investigation into this protein was not performed (Toft-Hansen et al., 2004). ADAM-10 has been found to be expressed by astrocytes in MS and in non-inflammatory CNS tissue as determined by immunohistochemistry. In chronic-active MS lesions, ADAM-10 was also found to be expressed by a few perivascular macrophages (Kieseier et al., 2003). ADAM-10 has been shown to be able to degrade MBP *in vitro* (Howard and Glynn, 1995; Amour et al., 2000), however its exact role in the pathogenesis of MS is not yet known.

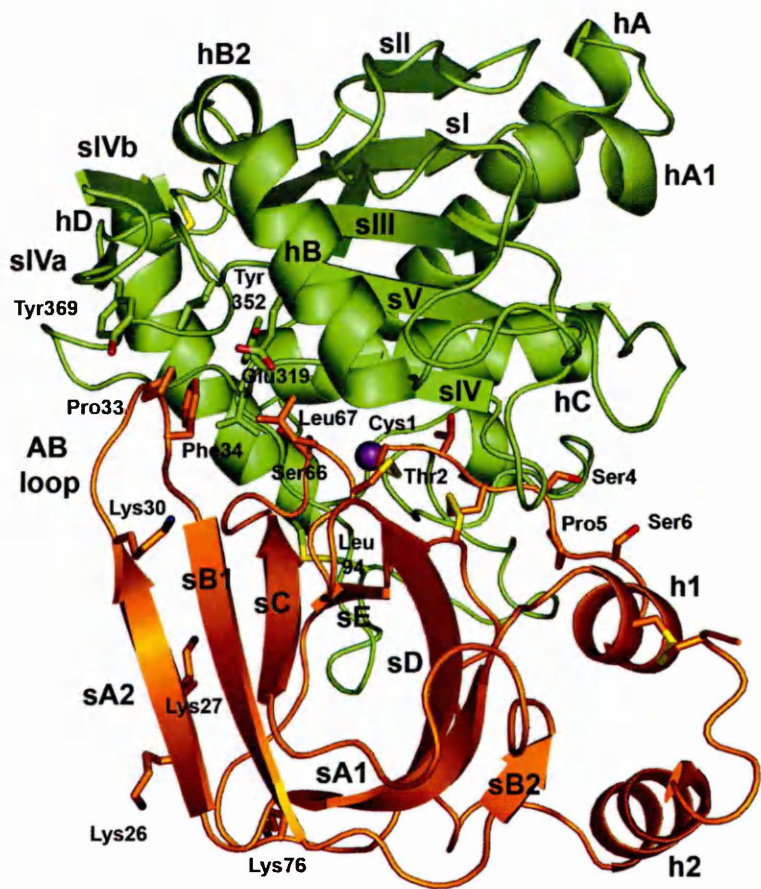


Figure 1.13: Stereo front view of the catalytic domain of ADAM-17-N-TIMP-3 complex. Green ribbon, catalytic domain of ADAM-17; purple sphere, catalytic site; orange ribbon, N-TIMP-3 domain. (Reproduced with permission from Elsevier from Wisniewska et al., 2008).

1.5.8 ADAM-17 and disease

ADAM-17 has been implicated in diseases both as a detrimental and/or protective influence. In ulcerative colitis, functional ADAM-17 activity is increased, particularly in patients with clinically active disease (Brynskov et al., 2002). Patients were classed as being clinically active based upon the number of bowel movements per day, and/or the presence of pus or blood in the stool, with or without systemic symptoms such as weight loss or fever (Langholz, et al 1994). This increase in ADAM-17 activity has also been shown to increase TNF and iNOS in the animal model of inflammatory bowel disease (IBD). The increase of both these factors (TNF and iNOS) coincides with colonic damage, which can be ameliorated by B-1101, a preferred ADAM-17 inhibitor (Colón et al., 2001). Prostatic cancer cell lines show an inverse expression of ADAM-17 and its natural inhibitor, TIMP-3, whereby the former is up-regulated and the latter was not detected at all (Karan et al., 2003).

ADAM-17's protective role is seen in the brain in ischemic preconditioning (IPC) experiments whereby protein expression is increased after IPC which coincides with a reduction in infarct volume that is inhibited by B-1101 or anti-TNF- α (Cárdenas et al., 2002). It has been shown that this neuroprotection is provided by shedding of TNF- α (Cárdenas et al., 2002) which activates NF- κ B, which in-turn could increase the expression of anti-apoptotic proteins such as Bcl-2 or decrease the activation of pro-apoptotic caspase-3. It has been subsequently shown by the same group that the up-regulation of TNF- α in IPC also induces the up-regulation of glutamate uptake and glutamate transporters *in vitro* (Romera et al., 2004). The high concentrations of glutamate released in cerebral infarction that usually lead to excitotoxic cell death (Choi and Rothman, 1990; Castillo et al., 1996) are therefore "mopped-up" during this process. This up-regulation of TNF- α is partially mediated by ADAM-17 and is thus credited with this neuroprotective mechanism in cortical neurons (Romera et al., 2004). In contrast Wang and colleagues (2004) found that *inhibiting* ADAM-17 with the novel inhibitor, DPH-067517, actually provided a neuroprotective effect that reduced infarct size and neurological deficits and was credited to the reduced expression of soluble TNF- α in the rat brain. However, the latter study used different inhibitors and different models to induce stroke from the former two studies and thus this could account for the discrepancy in results.

There have been numerous studies investigating the involvement of ADAM-17 in the proteolytic processing of APP. ADAM-17 has been identified as one of the metalloproteinases responsible for APP's cleavage along the α -pathway and is therefore classed as an α -secretase (Slack et al., 2001; Allinson et al., 2004; for review see Kojro and Fahrenholz, 2005). ADAM-17 has been shown to play a minor role in APP shedding in SH-SY5Y (neuroblastoma cells) and HeLa cells (cervical cancer cells),

whereas ADAM-10 is thought to be responsible for the constitutive shedding of APP. When ADAM-17 and ADAM-10 were independently reduced, with antisense oligonucleotides, APP shedding was reduced by 30% and 60%, respectively (Allinson et al., 2004). It has been shown that α -secretase APP cleavage occurs in the trans-Golgi network and that both ADAM-17 and -10 compete with β -secretase (BACE, the enzyme responsible for the amyloidogenic pathway) for cleavage of APP (Skovronsky et al., 2000; 2001). Alzheimer's diseased brains show ADAM-17 expression in close proximity to amyloid plaques. However, normal brains show no significant up- or down-regulation of ADAM-17 expression in comparison to AD brains as might be expected if it is involved in the pathological processes of AD (Skovronsky et al., 2001).

1.5.9 ADAM-17 and MS

Despite the fact that ADAM-17 was first described as the major protease for cellular release of TNF- α in 1997 (Black et al., 1997) and, that TNF- α is a major immunomodulatory and pro-inflammatory cytokine, having a pathogenic role in a variety of CNS inflammatory diseases, including MS (Brosnan et al., 1988; Cimini et al., 2003; Raine, 1995) there are few studies on the role of ADAM-17 in the pathogenesis of MS. The studies that have been reported have certain disparities in terms of the cellular localisation of ADAM-17, but they all report the expression of this protein in MS. ADAM17 mRNA has been found to be up-regulated in PBMCs in the blood of RRMS patients, which preceded the disruption of the BBB as assessed by MRI (Seifert et al., 2002). Eleven RRMS patients were used in this study and it was found that patients that were positive for ADAM-17 mRNA in PBMCs had significantly higher mean numbers of lesions one month after sampling the cells (Seifert et al., 2002). More recently Comabella and colleagues (2006) investigated the protein expression of ADAM-17 in PBMCs of patients with different clinical subtypes of MS. No distinct trend of ADAM-17 expression was identified between PPMS, SPMS or RRMS patients (PPMS=20, SPMS=20 and RRMS=40). The main findings included a down-regulation of the enzyme in healthy controls and PPMS patients in comparison to patients with SPMS, and RRMS patients who were in clinical remission. Interestingly no significant differential expression of the protease was witnessed between RRMS patients who were in relapse ($n = 20$) compared to those who were in remission ($n = 20$) (Comabella et al., 2006).

T lymphocytes have been reported to be the primary producers of the enzyme in acute and chronic active MS plaques at post-mortem ($n = 7$) as detected by immunohistochemistry. ADAM-17 was also detected in the CSF of MS patients ($n = 10$), but not in NIND controls ($n = 5$) (Kieseier et al., 2003) by western blotting. Conversely, immunoreactivity for ADAM-17 was found to be associated with blood vessel

endothelium, activated macrophages/microglia and parenchymal astrocytes in MS white matter (n = 19) by Plumb et al. (2006). The disparity in results between Kieseier et al (2003) and Plumb et al. (2006) has been discussed by Plumb and colleagues (2006) to be due to the use of different tissue fixation methods and the antibodies used to detect ADAM-17. Plumb et al. (2006) also showed an increase in the levels of ADAM-17 immunoreactivity in active lesions of patients with MS, which was associated with recent myelin breakdown as proven by the presence of lipid-laden activated macrophages (Plumb et al., 2006). The latter group also found ADAM-17 expression in endothelial cells in the naive and pre-diseased spinal cords of rats with EAE, which extends to astrocytes and macrophages during the peak and recovery phases of the disease (Plumb et al., 2005). TIMP-3 was down regulated in the latter model (Plumb et al., 2005).

1.6 Hypothesis

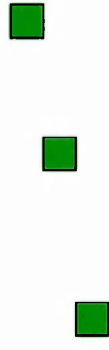
The increased expression ratio of ADAM-17 to its inhibitor, TIMP-3, in MS favours shedding of membrane bound proteins which could be beneficial or detrimental to the disease (Figure 1.14).

1.7 Aims of this thesis

The overall aim of this thesis is to elucidate the role of ADAM-17 in MS pathogenesis, in particular ADAM-17s relationship with its inhibitor and proteins shed by the protease in an *in vitro* model of the BBB. This work will be expanded to determine the expression levels of ADAM-17 and its substrates in post-mortem human MS CNS tissue to see whether the expression levels witnessed *in vitro* replicate the *in vivo* situation. This will be determined by carrying out the following:

- (i) Optimise culture conditions for the human brain endothelial cell line, hCMEC/D3.
- (ii) Determine the expression levels of ADAM-17 and counterparts by hCMEC/D3 under control and inflammatory conditions.
- (iii) Develop a method to knockdown ADAM-17 using small interfering RNA (siRNA) and to assess the functional effects this will have.
- (iv) Determine the *in vivo* expression of ADAM-17 and fractalkine in control and MS CNS tissue by immunohistochemistry in relation to markers of inflammation and demyelination.

iii. The ADAM-17/TIMP-3 expression ratio favours shedding of proteins under the inflammatory conditions of MS

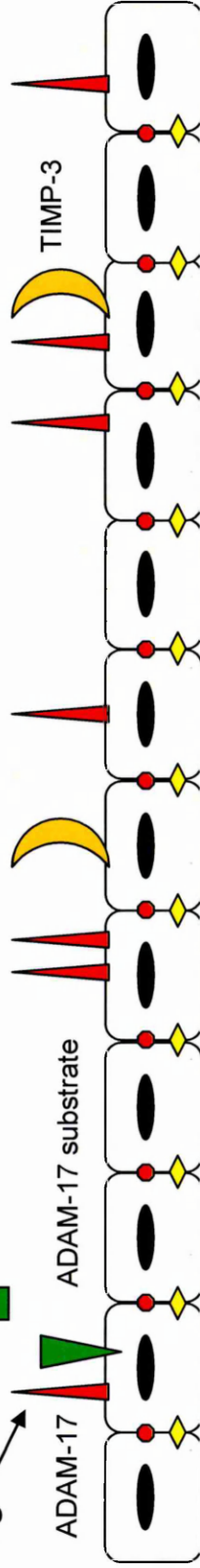


Blood

i. Increased expression of ADAM-17

cleavage

ii. Decreased expression of TIMP-3



Endothelium

CNS

Figure 1.14: Proposed functional role of ADAM-17 in MS pathogenesis. i. Increased expression of ADAM-17 (red triangle): increased expression levels are observed in MS white matter and EAE. ii. Decreased expression of TIMP-3 (yellow crescent): decreased expression levels of TIMP-3 have been observed in EAE. iii. The ADAM-17/TIMP-3 expression ratio favours shedding of proteins (green squares) under the inflammatory conditions of MS: the previous two points suggest that an increased level of ADAM-17 and a decreased level of TIMP-3 might favour shedding of membrane-bound substrates of ADAM-17 (green triangle).

Chapter 2

Optimisation of cell culture conditions for the human adult brain endothelial cell line, hCMEC/D3.

2.1 Introduction

2.1.1 *In vitro* models of the BBB

Various parameters distinguish the endothelial cells that constitute the BBB from those that make up the other blood vessel walls within the periphery. The two most important factors include the presence of TJs, which confer an extremely high electrical resistance (Butt et al., 1990), and a slow rate of fluid-phase endocytosis (Rubin et al., 1991). These have the overall effect of limiting paracellular and transcellular movement, respectively.

One of the major interests of BBB biology is understanding the regulation of BBB permeability. This is for several reasons: firstly, the development of candidate therapeutics that are able to cross the BBB freely. Secondly, understanding the mechanisms of undesired cell-trafficking into the brain in conditions, such as MS, HIV, and metastatic cancer, so that they can be manipulated *in vivo*. Thirdly, understanding neurological disorders which involve a compromised BBB, such as vasogenic brain oedema and MS (Rubin et al., 1991). Recapitulating the BBB *in vitro* must thus involve reproducing the structural and functional properties of the BBB *in situ*. As such, various attempts have been made to establish an *in vitro* model of the BBB. These have included the use of brain endothelial cells from various animal species, including rodent, porcine, and bovine (Rubin et al., 1991; Gaillard et al., 2001; Bzowska et al., 2004), as human brain endothelial cells are difficult to obtain due to ethical issues and post-mortem delay. Studies that do use human tissue usually involve the use of endothelial cells from various sources including, the umbilical vein (HUVEC), appendix, aorta and lymph node (Chapman et al., 2000; Ancuta et al., 2003; Harkness et al., 2003; Bzowska et al., 2004; Brueckmann et al., 2006). Some studies do involve the use of human brain microvascular endothelial cells (HBMEC) prepared as primary cultures from patients (Cucullo et al., 2007), however, this type of cell culture can sometimes contain contaminant cell types and is not always reproducible.

Highlighting the importance of establishing a suitable *in vitro* model of the BBB, from an appropriate vascular bed, are various studies that have examined protein expression by different endothelial sources. The chemokine expression profile of endothelial cells has been shown to be tissue specific. This has been demonstrated by the Male group at The Open University who studied chemokine, chemokine receptor and adhesion molecule expression in primary HUVECs, lung, dermal, saphenous (leg vein) endothelial cells and a bone-marrow cell line (Hillyer et al., 2003). All cells expressed different chemokines and chemokine receptors, and did so at a stereotypical level for the endothelial type studied. However, the adhesion molecules that were examined showed inter-individual variability in their expression profiles, highlighting that some of the variability in expression in primary cells is due to the different donors

and not typical of the cell source (Hillyer et al., 2003). In a recent study by the Ransohoff group, who investigated certain properties of an immortalised human brain microvascular endothelial cell line (THBMEC) in comparison to HUVECs, demonstrated the following: HUVECs show a punctate pattern of ZO-1 expression at cell contacts only, whereas THBMECs showed continuous occludin and ZO-1 expression; THBMECs also had a significantly higher TEER and lower solute permeability than their umbilical counterparts; THBMECs utilise the chemokine, CCL5, to facilitate T lymphocyte migration, whereas HUVECs did not (Man et al., 2008). In addition other groups have also described differences in behaviour concerning barrier function and responsiveness to TNF application in endothelial cells dependent upon their derivation, i.e. aortic versus brain endothelial cells, whereby brain endothelial cells are more responsive to TNF, and aortic to IL-1 β and IFN- γ (Harkness et al., 2003). In this present study a novel human brain endothelial cell line called hCMEC/D3 was used as a model of the BBB.

2.1.2 hCMEC/D3 cells as an in vitro model of the BBB

The human brain endothelial cell line, hCMEC/D3 (Fig. 2.1), was developed by Weksler and colleagues (2005). Preconfluent primary brain endothelial cells in passage 0 were infected with a lentivirus. The cell line hCMEC/D3 was selected from one clonal population. hCMEC/D3 maintained a non-transformed phenotype, with no signs of senescence or de-differentiation, a normal diploid karyotype and the ability to form capillary-like cords on Matrigel (reconstituted extracellular matrix) for more than 100 population doublings (33 passages). This cell line shows a number of phenotypic characteristics of endothelial and/or BBB cells including:

1. Formation of a tightly packed monolayer of elongated cells (Fig. 2.1);
2. Expression of a number of TJ proteins, including PECAM-1, VE-cadherin, β - and γ -catenins, ZO-1, JAM-A, and claudin-5;
3. Expression of a number of adhesion molecules and chemokine receptors either under basal conditions or after treatment with the pro-inflammatory cytokines IFN- γ and TNF- α , including ICAM-1, ICAM-2, PECAM-1, and CD40;
4. Expression and functionality of various multidrug resistant proteins belonging to the ATP binding cassette (ABC) transporter family, including MDR1 (multidrug resistance 1 or P-glycoprotein), MRP1 (multidrug resistance associated protein), and BCRP (breast cancer resistance protein);
5. Greater restriction properties than other endothelial cell culture models of the BBB, including primary bovine brain endothelial cells and rat brain endothelial cell line, GPNT.

This cell line recapitulates most of the unique properties of the BBB, despite the absence of coculturing with glial cells. It is the first example of an extensively characterised human brain endothelial cell line (Weksler et al., 2005).

2.1.3 Aims of the study

The aims of this study were to develop a suitable cell culture system for the human brain endothelial cell line, hCMEC/D3, which could be used to study gene expression of this cell line, under inflammatory conditions in subsequent experiments. This involved the identification of a suitable housekeeping gene and also determining whether growth factors in the media used to culture the cells could interfere with the expression of the genes of interest.

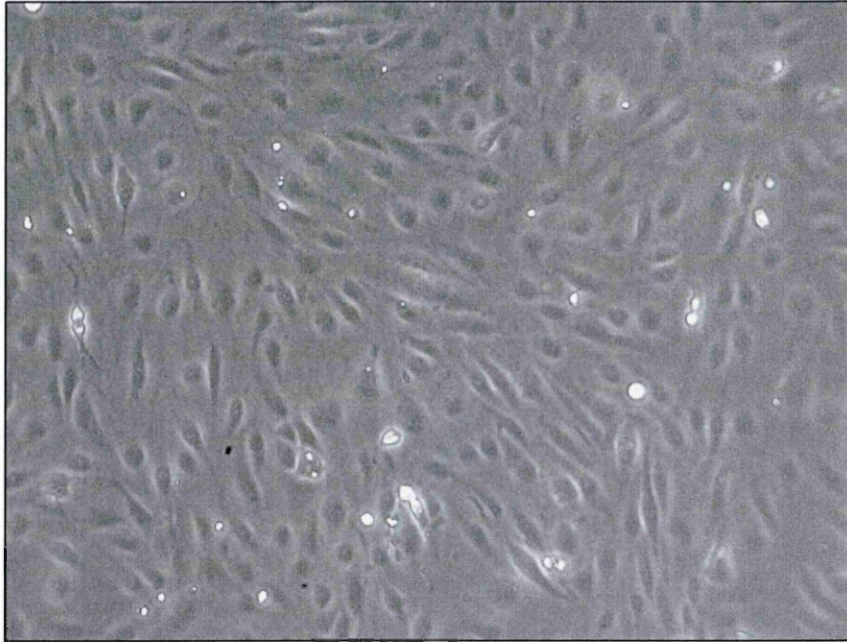


Figure 2.1: Human adult brain endothelial cell line, hCMEC/D3, in culture. The cells have an elongated shape and form a tight monolayer when confluent. *Magnification x100.*

2.2 Materials and methods

2.2.1 Suppliers used in this chapter

Applied Biosystems, Lingley House, 120 Birchwood Boulevard, Warrington, WA3 7QH, UK; **Greiner Bio-One Ltd**, Brunel Way, Stroudwater Business Park, Stonehouse, GL10 3SX, UK; **Invitrogen**, 3 Fountain Drive, Inchinnan Business Park, Paisley, PA4 9RF, UK; **Lonza**, Muenchensteinerstrasser 38, CH - 4002, Basel, Switzerland; **PeproTech EC Ltd**, PeproTech House, 29 Margravine Rd., London, W6 8LL, UK; **Roche Diagnostics Ltd**, Bell Lane, Lewes, East Sussex, BN7 1LG, UK; **Sigma-Aldrich**, The Old Brickyard, New Rd., Gillingham, Dorset, SP8 4XT, UK; **VWR International**, Hunter Boulevard, Magna Park, Lutterworth, Leicestershire, LE17 4XN.

2.2.2 Semi-quantitative real-time reverse transcriptase-polymerase chain reaction (qRT-PCR)

2.2.2.1 RT-PCR

This technique allows the reverse transcription of RNA to DNA using an enzyme called reverse transcriptase (RT). Using random primers which anneal to the 3' end of a single strand of mRNA, the enzyme elongates the sequence using deoxynucleotide triphosphates (dNTPs) to produce a complementary DNA (cDNA) sequence. This is based upon RNA bases (A, U, G, C) pairing with their DNA counterparts (T, A, C, G). In terms of RT-PCR this can be described as the first step or the "first strand reaction".

PCR is a method which permits the amplification of DNA exponentially. Each cycle of the reaction causes exponential growth of the DNA product so that 2 DNA copies produce 4, which then produce 8, which then produce 16 etc. The DNA fragment that is amplified is dependent upon the primers used. Primers are short synthetic oligonucleotide strands that anneal to their complementary target DNA. Primers are designed to sit at the 3' and 5' ends of a specific DNA sequence, which when synthesised will be approximately 100 bases in length. This is termed the amplicon. The primers are thus called the forward and reverse primer. The DNA is heated to 95°C to break the hydrogen bonds and separate the DNA alpha-helix. The temperature is then reduced (to approximately 60°C) to allow annealing of the primers and a thermostable DNA polymerase to the DNA. The first heat-stable enzyme to be discovered to withstand PCR conditions was Taq polymerase and was first isolated from the bacterium *Thermus aquaticus* (hence the name Taq). Approximately 40 cycles of melting (heating) and cooling (annealing) allow millions of copies of the target DNA to be synthesised. This stage of the RT-PCR reaction can be described as the second step or "second strand reaction" (<http://pathmicro.med.sc.edu/pcr/realtime-home.htm>).

2.2.2.2 Semi-quantitative real-time RT-PCR (qRT-PCR)

Real-time RT-PCR allows the quantification of mRNA in biological samples by analysing the kinetics of the PCR experiment. Whereas traditional PCR analyses the end-point of the reaction on an agarose gel. End-point PCR relies upon band size discrimination and due to the insensitivity of the ethidium bromide stain, that is used to visualise the DNA product, it is difficult to discern any differences that may be present. Real-time RT-PCR allows the quantification of PCR products based upon fluorescence emitted at every cycle of the reaction for each biological sample. However, in order to collect comparative values between samples it is important to take readings at the exponential phase of amplification of the DNA product for each sample. This is the most reproducible phase of the reaction. However, the abundance or rarity of the target will determine at which point readings are taken. This threshold, where all samples fluorescence intensity crosses, is called the threshold cycle or Ct value, and can be analysed in various mathematical equations to extrapolate the relative mRNA levels between the samples

http://www3.appliedbiosystems.com/cms/groups/mcb_marketing/documents/general/ocuments/cms_042484.pdf.

2.2.2.3 Controls for RT-PCR

When performing reverse transcription of RNA, two controls should be used. A "no template control" (NTC) should be performed, where RNase-free water is substituted for RNA to rule-out cross contamination of reagents and surfaces with RNA. Also, a "no amplification control" (NAC) should be performed, which involves substituting the reverse transcriptase enzyme with RNase-free water. This is to ensure there is no contamination of the sample with the final product

<http://www.ambion.com/techlib/tn/102/17.html>.

2.2.2.4 Primers

Primers are designed to be the reverse complement of a section of DNA, which will allow DNA polymerase binding and initiate DNA synthesis. When designing primers it is important to consider the sequence composition of the primers for the following reasons. The melting temperature (T_m) is the temperature below which primers associate with the template DNA and above which they disassociate from the template DNA. Primers should be between 18-25 bases, as the T_m increases with primer size. The primers should also not be too GC rich, but contain 40-60% G and C bases as this will also increase the T_m . To prevent primer dimers from forming, 3' ends should not be complementary. Primer self-complementary sequences should not reside in the oligonucleotide as these form secondary structures, such as hairpins. The 3' ends of

the primers should also not contain runs of 3 or more G or C bases as this may result in mispriming and the wrong section of DNA being synthesised. The primers should be designed so that the amplicon crosses an exon-exon boundary, thus ensuring only DNA transcribed from mRNA is amplified. Thus, preventing any amplification of contaminating genomic DNA

(http://www.premierbiosoft.com/tech_notes/PCR_Primer_Design.html).

2.2.2.5 TaqMan probes

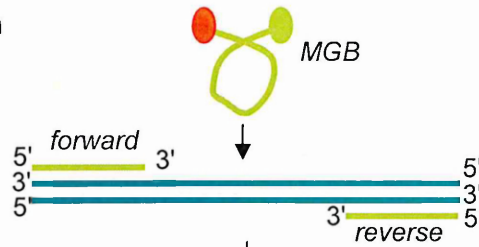
In addition to using forward and reverse primers to initiate DNA polymerase binding, TaqMan also utilises another oligonucleotide that binds an internal region of the amplicon between the forward and reverse primer (Fig 2.2). At the 5' end of the internal oligonucleotide a fluorescent reporter dye is attached and at the 3' end a quencher moiety. The proximity of these two molecules in the unhybridised state prevents fluorescence emission through a phenomenon known as Förster Resonance Energy Transfer (FRET). When PCR begins, and DNA polymerase binds the target amplicon on which there is a TaqMan probe bound, the 5' to 3' nuclease activity of the enzyme hydrolyses the probe. This results in the decoupling of the reporter and quencher and abolishing FRET. Thus, cleavage of the probe is directly proportional to the amount of fluorescence emitted, which increases with each cycle. There are many advantages to using the TaqMan system. Firstly, the use of three hybridization probes (forward and reverse primers, and internal oligonucleotide) instead of only two (forward and reverse primers) abolishes amplification of ambiguous DNA sequences. Secondly, if there are any primer-dimers in the system these will not result in the emission of false fluorescence as the TaqMan probe cannot bind

(<http://www.ambion.com/techlib/basics/rtqcr/index.html>).

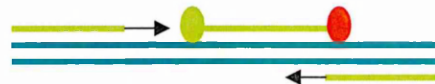
2.2.2.6 Endogenous control (housekeeping genes)

An endogenous control is required to act as a reference to normalise quantitation of a cDNA target for the amount of cDNA added to each reaction. Housekeeping genes are used as they are constitutively expressed and normally show little variability under most experimental conditions. Traditionally β -actin, glyceraldehyde-3-phosphate (GAPDH) and ribosomal RNA (rRNA) are used as endogenous controls because they show relatively stable expression (Mullis and Faloona, 1987). However, many housekeeping genes have been shown to be more abundantly expressed than others, e.g. β -actin and 18 Svedberg Units (S) rRNA (18S rRNA), or show altered expression in certain diseases, e.g. GAPDH under hypoxic conditions (Zhong and Simons, 1999).

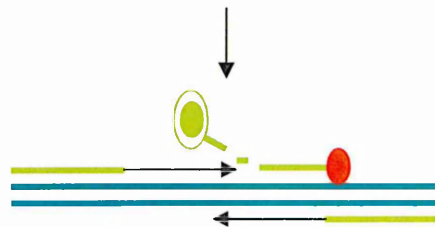
Step 1: Hybridisation



Step 2: Polymerisation



Step 3: Displacement and cleavage



Step 4: Fluorescence

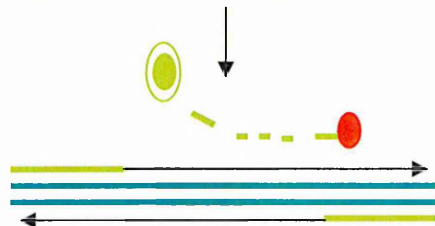


Figure 2.2: TaqMan chemistry. Taqman chemistry, unlike conventional PCR, uses three hybridization probes: a forward primer, a reverse primer, and a minor groove binding (MGB) probe (Step 1). During polymerization, DNA polymerase (horizontal black arrow) synthesises the complementary strand of DNA (cDNA) (Step 2). As 5' to 3' nuclease activity of the enzyme continues along the DNA strand, the probe is displaced (strand displacement) and cleaved (cleavage) (Step 3). This results in the reporter (green) becoming detached from the quencher (red) and fluorescence being emitted and polymerization is completed (Step 4) (Adapted with permission from http://www3.appliedbiosystems.com/cms/groups/mcb_marketing/documents/generaldocuments/cms_042484.pdf).

2.2.3 Cell culture conditions

2.2.3.1 Collagen coating

Collagen type I from rat tail (3.41mg/ml) (VWR, U.K.) was used to coat plasticware for culturing hCMEC/D3. The solution was prepared by diluting the collagen 1:30 in autoclaved distilled H₂O (dH₂O) and then filtering through a 0.2µm filter. This was done as previous culturing experiments had encountered contamination problems. Enough collagen solution was then placed on the plasticware to cover the bottom of the plate or flask. After 1 hour incubation at 37°C the solution was removed and the plasticware ready for direct seeding of cells.

2.2.3.2 General cell culture conditions

The human adult brain endothelial cell line, hCMEC/D3 (Weksler et al., 2005), was cultured on collagen type I from rat tail in EGMTM-2 endothelial cell medium-2 basal media supplemented with hydrocortisone (1x10⁻⁴µl/ml), EGF vascular, gentamycin, ascorbic acid, human EGF, long R insulin-GF, heparin (all 2.5x10⁻⁴µl/ml), human FGF-β (1µl/ml) (Lonza, U.K.), penicillin (50units/ml) and streptomycin (50µg/ml) (Invitrogen, U.K.), and 2% heat inactivated foetal calf serum (HI FCS) (Invitrogen, U.K.). Exact concentrations of the supplements used in the media are unknown as EGMTM-2 endothelial cell medium-2 basal media and supplements is a commercial product of Lonza, U.K. Supplements were added at a concentration recommended by Dr. Ignacio Romero (Open University, Milton Keynes). The cells were maintained at 37°C with 5% CO₂/95% air in a humidified environment. Media was replaced every 2-3 days until confluence was reached. Cells were subcultured using 0.5% trypsin and 0.2% EDTA (Sigma-Aldrich, U.K.).

2.2.3.3 Culture conditions for testing stability of housekeeping genes

For qRT-PCR, cells were seeded in complete media at 1x10⁵/500µl/well of a 24 well plate. After 24 hours the media was aspirated, cells washed with calcium and magnesium free-phosphate buffered saline (PBS, Invitrogen, U.K.), and fresh serum-free media containing 1, 10 or 100ng/ml TNF, IL-1β, IFN-γ or TGF-β1 (PeproTech, U.K.) was added. The cytokines were prepared according to the company that supplied them and stored at various stock solutions (TNF at 100µg/ml; IL-1β at 100µg/ml; IFN-γ at 100µg/ml and TGF-β1 at 50µg/ml). Serum-free media, without cytokine, was used as a control. Each condition was represented in triplicate and the experiments were repeated three times. After 24 hours of cytokine treatment, the cells were washed twice with PBS and RNA was extracted using TRI Reagent (Sigma-Aldrich, U.K.) following the manufacturer's guidelines (see section 2.2.3.1). β-actin, GAPDH and cyclophilin A

housekeeping genes were tested for their stability under the experimental conditions used later (see Chapter 3).

2.2.3.4 Culture conditions to test the effects of growth factors

1×10^5 cells/ml/well were seeded in 24 well plates in complete media containing FCS. After culturing for 24 hours, the media was aspirated and the cells washed twice with PBS. The media was replaced with either complete media or media containing all factors except VEGF and EGF, or heparin. In both instances FCS was absent. After 24 hours, the cells were washed twice and mRNA was extracted using TRI Reagent (Sigma-Aldrich, U.K.) according to the manufacturer's guidelines. The experiment was carried out in triplicate and repeated three times.

2.2.4 RNA extraction and validation

2.2.4.1 RNA extraction

TRI® Reagent is a phenol-based homogenous solution used to isolate RNA, protein and DNA. The reagent contains a number of denaturants and RNase inhibitors. RNA was extracted according to the manufacturer's guideline (Sigma-Aldrich, UK). Briefly, approximately 1ml of TRI Reagent per 10cm^2 of the cell culture dish was added, the cell lysate passed through a 1ml pipette (Gilson) several times and allowed to stand at RT for 5 minutes. 0.2ml of chloroform per ml of TRI Reagent was then added, mixed, allowed to incubate at RT for approximately 10 minutes and then centrifuged at $12,000 \times g$ for 15 minutes at 4°C to facilitate the separation into the three organic phases. The colourless RNA phase was then transferred to a clean tube and 0.5ml of isopropanol per 1ml of TRI Reagent was added, mixed, incubated at RT for 7 minutes, and then centrifuged at $12,000 \times g$ for 10 minutes at 4°C . The supernatant was removed and the RNA pellet washed by adding 1ml of 75% ethanol/ml of TRI Reagent used in the initial sample preparation, vortexed and centrifuged at $7,500 \times g$ for 5 minutes at 4°C . The pellet was then air-dried for 5-10 minutes, 10-20 μl RNase-free water added and the sample stored at -80°C .

2.2.4.2 Native agarose gel electrophoresis of RNA

In order to test the quality of the RNA extracted from the cells, RNA can be run on a native agarose gel and the 28S and 18S bands examined. The 28S rRNA band should be twice as bright as the 18S rRNA. A 2:1 (28S:18S) ratio of the RNA is a good indication that the RNA is intact (http://www.ambion.com/techlib/append/supp/rna_gel.html).

To form the agarose gel, 0.5g of agarose (Bioline, U.K.) was dissolved in 50ml TBE buffer (Tris base, boric acid, and EDTA) (89 mM Tris-HCl pH 7.8, 89 mM borate,

2 mM EDTA) with 0.5µl of ethidium bromide (10mg/ml) (Sigma-Aldrich, U.K.). Loading dye (Bioline, U.K.) was diluted 1:1 with each RNA sample and 2µl of the sample loaded onto the gel. Using TBE as the buffer, the gel was run at 100V for 30min. Serial images were captured using a UVP epi II dark room and using Labworks version 4.0.

2.2.5 Method

2.2.5.1 cDNA synthesis

1µl of RNA was reverse transcribed to cDNA using the following reagents: 4µl of 5x first strand buffer, 2µl of 1,6-dithiothreitol (DTT), 1µl deoxynucleotide triphosphates (dNTP), 0.5µl of RNase inhibitor, 0.5µl of random hexamers (A, T, G, C), 1µl Superscript II (all Invitrogen, UK) and 9µl of RNase and DNase free water (Sigma-Aldrich, UK). As controls, to ensure there was no genomic DNA or RNA contamination of the reagents, negative controls were also included with RNA or superscript II absent. 15µl of mineral oil (Sigma-Aldrich, UK) was pipetted over the samples to create a layer that would prevent evaporation in the heating step. Samples were heated for 1 hour at 42°C, followed by a step to heat inactivate the enzyme at 95°C for 5 minutes. Samples were then diluted with 10µl of water and stored at -20°C until analysis by qRT-PCR was performed.

2.2.5.2 qRT-PCR

Using the fluorescent TaqMan 5' nuclease assay (Applied Biosystems, U.K.) each cDNA sample was analyzed for expression of ADAM-17, TIMP-3, TNFR1, TNFR2, fractalkine, von Willebrand Factor (vWF), β-actin, cyclophilin A and GAPDH by qRT-PCR. ADAM-17, TIMP-3 and substrates of the enzyme (TNFR1, TNFR2 and fractalkine) were studied here to determine whether their expression levels were affected by the culture conditions as their relationship to one another was to be studied in the following chapter (Chapter 3). vWF was studied as a phenotypic marker for endothelial cells. Each 10µl reaction consisted of 2x TaqMan Universal PCR Master Mix (Applied Biosystems, U.K.), 3.6µM for each primer, 1µM for the FAM labelled probe and 1µl of template cDNA. Each primer and probe set was designed by Applied Biosystems (U.K.) and selected on the basis that they crossed an exon-exon boundary, to prevent any amplification of contaminating genomic DNA. To ensure there was no genomic DNA or RNA contamination, negative controls were run in parallel without either superscript II or RNA. Reactions were carried out in a 384-well reaction plate (Greiner Bio-One, U.K.) using the Applied Biosystems 7900HT fast real-time PCR system (Applied Biosystems, U.K.). The thermal profile of the reaction was as follows: 50°C for 2 minutes, 95°C for 2 minutes, and 40 cycles of denaturation at 95°C for 15 seconds and annealing/elongation at 60°C for 1 minute. The 2 minute heating step at 50°C, at the

beginning of the process, is used to activate uracil-N-glycosylase (UNG), which will degrade any contaminating PCR product, containing uracil. At each stage of the process, emitted fluorescence was measured to later construct an amplification plot using ABI Prism 7900HT Sequence Detection System software version 2.2.1. Relative mRNA levels of the above genes were determined using the threshold cycle (C_T) and the $2^{-\Delta C_T}$ method (Livak and Schmittgen, 2001). Where ΔC_T is calculated using the following formulae: C_T (target gene) - C_T (Housekeeping gene) = ΔC_T

2.2.5.3 Statistical analysis

qRT-PCR data was analysed using the non-parametric Mann Whitney U test. To carry out this test, $2^{-\Delta C_T}$ for each sample was calculated to determine the relative gene expression. For housekeeping gene analysis the C_T value was normalised to proliferation data and a Mann Whitney U test performed on the data. Each treated condition was then compared to the control. Statistical significance was set at $p < 0.05$ and data are represented as mean \pm SEM for the indicated number of experiments.

2.2.6 BrdU proliferation assay

Proliferation assays allow the assessment of cell numbers following cell division and to assess whether cytokines or growth factors influence cell proliferation. 5-Bromo-2'-deoxyuridine (BrdU) is a thymidine analogue which can be incorporated into the DNA of dividing cells instead of endogenous thymidine. Through the use of antibodies, and a DNA denaturing step, the BrdU can be detected in the cells that have proliferated and incorporated BrdU. This particular system relies upon the same methodology as an ELISA assay, whereby peroxidase linked to the anti-BrdU-POD (POD, peroxidase) reacts with the substrate 3,3',5,5'-tetramethylbenzidine (TMB) to create a colorimetric reaction (Roche).

2.2.6.1 Method

Using the Cell Proliferation ELISA BrdU kit (Roche, U.K.) cells were assessed for proliferation capacity under certain treatment regimes. Cells were seeded in complete media at 2×10^4 cells/200 μ l/well of a 96-well plate (including growth factors and FCS). After 24 hours incubation, cells were washed twice with PBS and 200 μ l of the appropriate media, e.g. with test growth factors or cytokine, was added. Media without cells served as a blank control, which would be subjected to the complete BrdU procedure. The plate was incubated for a further 22 hours and then 10 μ M (20 μ l/well) of BrdU was added to each well. Following 2 hours incubation with BrdU, the media was removed and the plate dried at 60°C for 60 minutes. Cells were then fixed and denatured in a single step with 200 μ l/well of FixDenat and incubated at room

temperature for 30 minutes. After removal of the FixDenat solution, 100µl/well of the anti-BrdU-POD was added and left to bind for 90 minutes at room temperature. The antibody conjugate was then removed and the wells were rinsed 3 times with 200µl/well of wash solution. Following the final wash, 100µl/well of substrate solution was added and left to develop for 30 minutes at room temperature. In order to stop the reaction, 25µl/well of sulphuric acid (2N H₂SO₄) was added and left for 1 minute before the absorbance was read at 450nm in a Wallac Victor²_{TM} 1420 Multilabel Counter using Wallac 1420 software version 2.00 release 8. Absorbance values were calculated with the following formula: absorbance of test samples - blank control (culture medium + BrdU + anti-BrdU-POD).

2.2.6.2 Statistical analysis

Proliferation data was analysed using an unpaired student's *t*-test. Statistical significance was set at $p < 0.05$.

2.3 Results

2.3.1 Optimising housekeeping genes

Of the 3 housekeeping genes tested only cyclophilin A and GAPDH could be detected by qRT-PCR technology. β -actin was not found in any of the samples analysed. Following treatment with TNF, IL-1 β , IFN- γ or TGF- β 1 at 1, 10 or 100ng/ml both cyclophilin A and GAPDH fluctuated in comparison to their respective controls (Fig. 2.3 A and B, respectively). Data was normalised to the proliferation response of hCMEC/D3 cells to the different cytokines and concentrations (Fig. 2.3 C). Both housekeeping genes responded similarly to the cytokine treatments with significant increases in expression after treatment with TNF at 10 and 100ng/ml, and IFN- γ at 1, 10 and 100ng/ml ($p < 0.05$) (Fig. 2.3.A and B). Both housekeeping genes showed a significant decrease in expression following treatment with TGF- β 1 at 100ng/ml ($p < 0.05$) (Fig 2.3 A and B). Only cyclophilin A was down regulated at the mRNA level when treated with IL-1 β at 1ng/ml (Fig. 2.3 A).

2.3.2 Testing the effects of VEGF and EGF on mRNA expression

To determine whether VEGF and EGF influenced the expression levels of the genes of interest, qRT-PCR was performed on hCMEC/D3 cells treated for 24 hours with media either +/- supplements. VEGF and EGF caused a decrease in the expression level of ADAM-17, which was significantly different from cells treated with media without these factors ($p < 0.05$) (Fig. 2.4 A). VEGF and EGF also caused a decrease in expression of TIMP-3, TNFR1 and TNFR2, however, none of these changes were significantly different from the cells not exposed to these factors ($p > 0.05$) (Fig 2.4 B-D). Fractalkine and vWF were up-regulated by the application of VEGF and EGF, but this increase was not significantly different from endothelial cells treated with media without VEGF and EGF ($p > 0.05$) (Fig 2.4 E and F, respectively).

2.3.3 Testing the effects of heparin on mRNA expression

To determine whether heparin influenced the expression of the genes of interest, qRT-PCR was performed on hCMEC/D3 cells treated +/- heparin in the media for 24 hours. Removing heparin from the cell media caused a decrease in mRNA expression of all genes tested: ADAM-17, TIMP-3, TNFR1, TNFR2, fractalkine and vWF (Fig 2.5). This decrease in mRNA expression however, was only significantly different for TNFR1 in comparison to cells that had heparin in the cell culture media ($p \leq 0.05$) (Fig 2.5 C).

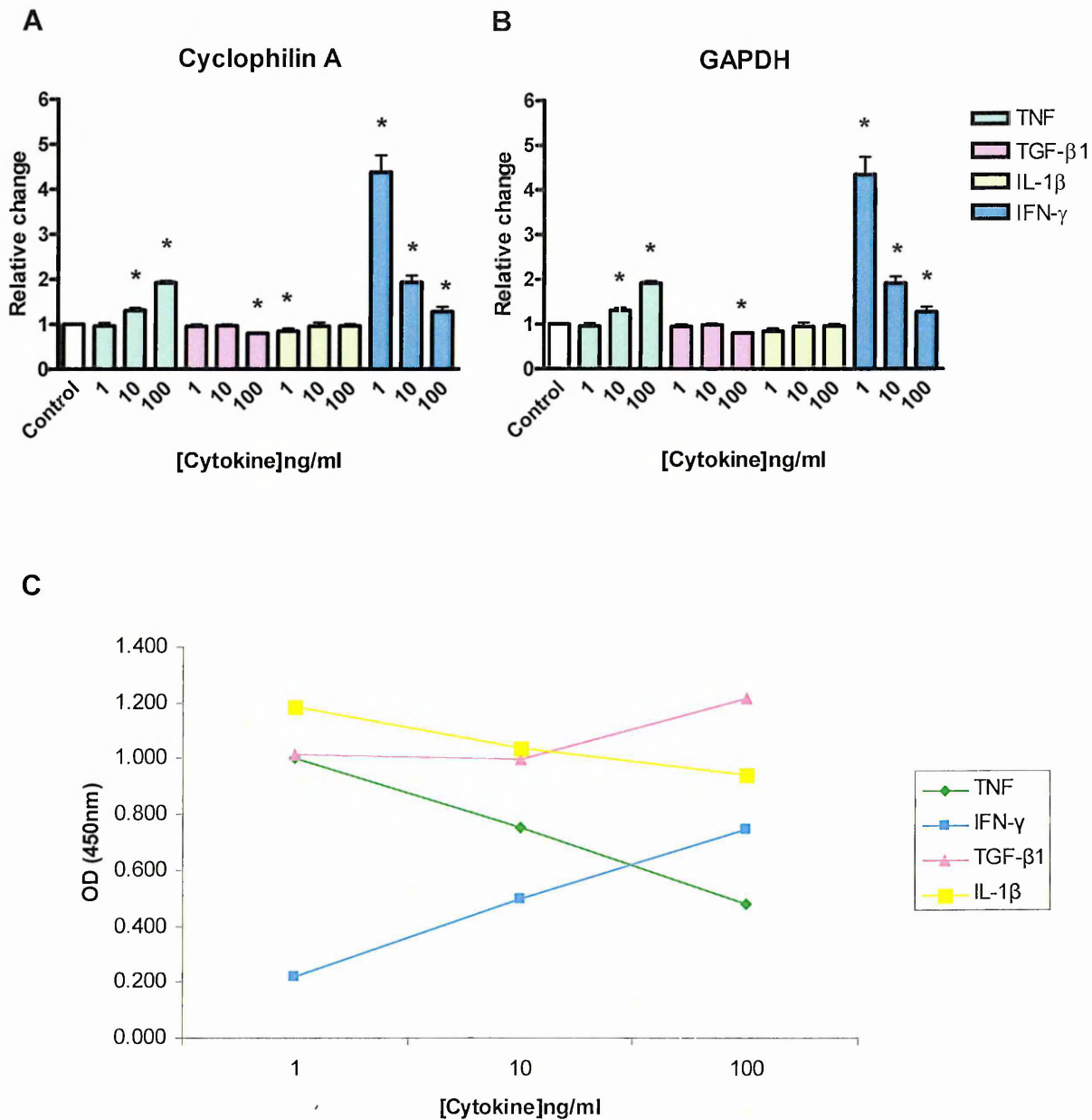


Figure 2.3: qRT-PCR analysis of housekeeping genes and proliferation response in hCMEC/D3 cells under inflammatory conditions. Cyclophilin A (A) and GAPDH (B) mRNA expression was analysed under control and inflammatory conditions in the human brain endothelial cell line, hCMEC/D3. Data are represented as the mean ($n = 3$) \pm SEM. Significant differences are indicated by an asterisk ($p < 0.05$) and were analysed using the non-parametric Mann Whitney U test. Data was normalised to proliferation data obtained using the cell proliferation ELISA BrdU kit (Roche, U.K.) (C).

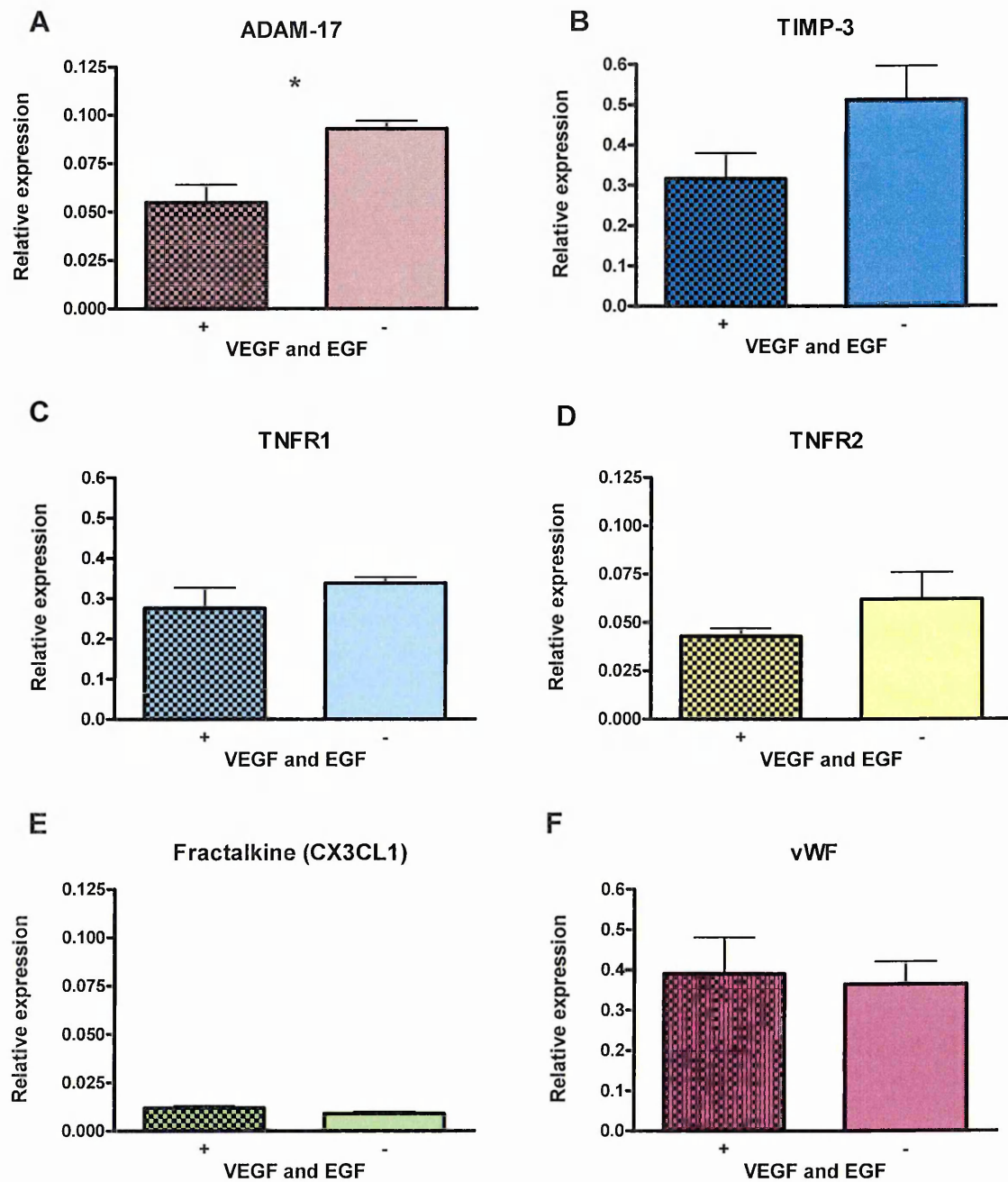


Figure 2.4: Effects of VEGF and EGF on mRNA expression in hCMEC/D3 cells. Relative mRNA expression of ADAM-17 (A), TIMP-3 (B), TNFR1 (C), TNFR2 (D), fractalkine (E) and von Willebrand Factor (vWF) (F) with either vascular endothelial growth factor (VEGF) and epidermal growth factor (EGF) in the media (+) or lacking from the media (-). Relative mRNA levels were calculated using the housekeeping gene, cyclophilin A, and the $2^{-\Delta CT}$ method, and using a non-parametric Mann Whitney U test. Data are presented as the mean ($n = 3$) \pm SEM. Asterisk (*) denotes statistically significant differences ($p < 0.05$). Note the differences in scale.

2.3.4 Testing the effects of heparin on mRNA expression during treatment with IFN- γ

When endothelial cells were treated with IFN- γ for 24 hours with heparin included in the cell culture media they showed lower mRNA expression levels for all genes tested except fractalkine compared to when they were treated with the cytokine without heparin in the cell culture media (Figure 2.6). This increase in gene expression without heparin occurred at all concentrations of IFN- γ treatment. Fractalkine, however, showed a decrease in mRNA expression when treated with IFN- γ at all concentrations when heparin was absent from the media (Figure 2.6 E). The increase in expression without heparin was significant ($p \leq 0.05$) for three of the genes tested: ADAM-17 at 100ng/ml IFN- γ , TNFR1 at 1 and 100ng/ml IFN- γ , and TNFR2 at 1ng/ml IFN- γ (Figure 2.6 A, C and D, respectively).

2.3.5 The influence of VEGF and EGF on cell proliferation

Cells treated with VEGF and EGF in the media had a significantly higher proliferation rate than cells treated with media lacking these components ($p < 0.05$) ($n = 3$). Cells treated with VEGF/EGF had an optical density (OD) of 1.35 (SEM \pm 0.05) and cells lacking these supplements had an OD of 1.14 (SEM \pm 0.04), suggesting these supplement are necessary for cell division.

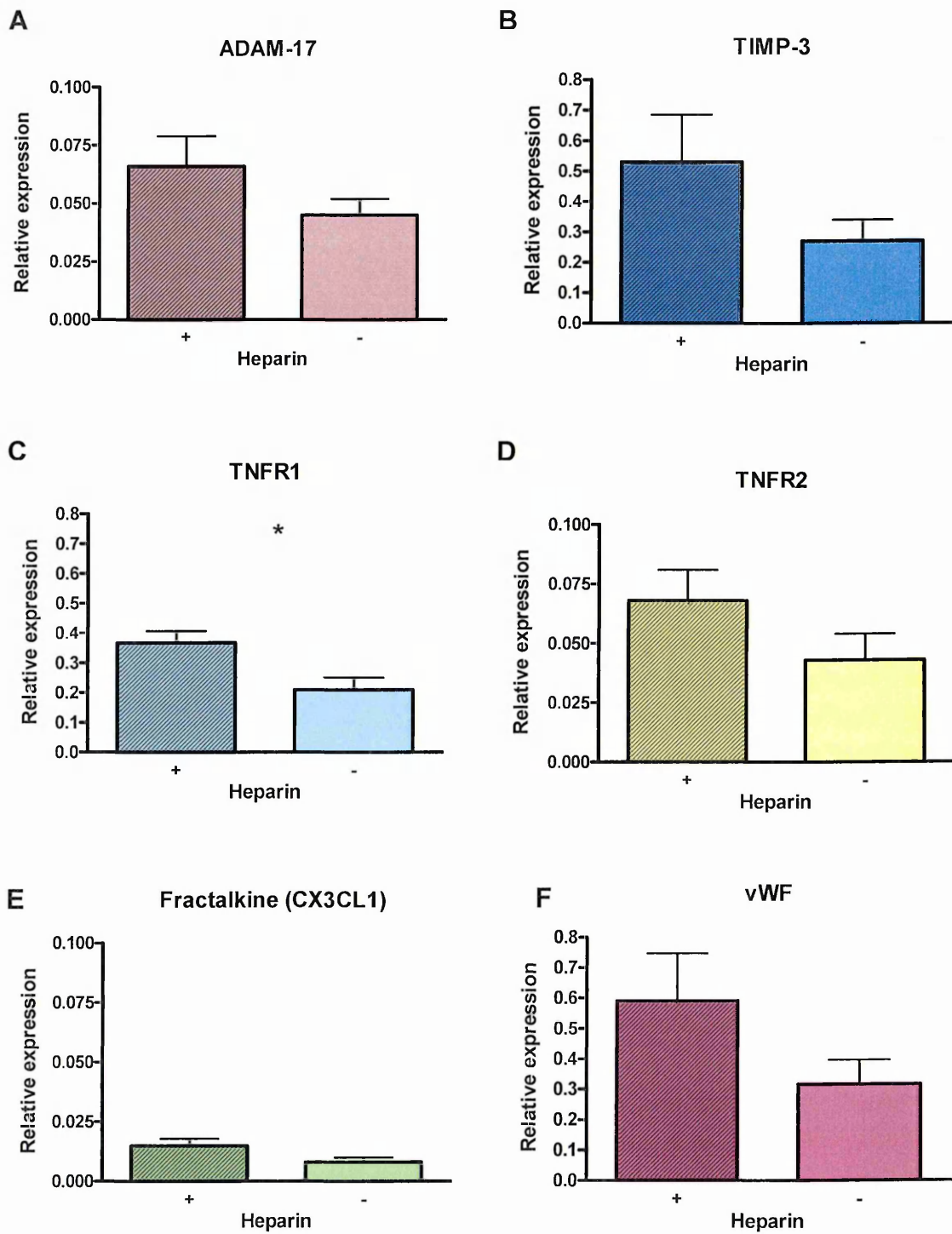


Figure 2.5: Effects of heparin on mRNA expression in hCMEC/D3 cells. Relative mRNA expression of ADAM-17 (A), TIMP-3 (B), TNFR1 (C), TNFR2 (D), fractalkine (E) and von Willebrand Factor (vWF) (F) with either heparin in the media (+) or lacking from the media (-). Relative mRNA levels were calculated using the housekeeping gene, cyclophilin A, and the $2^{-\Delta CT}$ method, and using the non-parametric Mann Whitney U test. Data are presented as the mean ($n = 3$) \pm SEM. Asterisk (*) denotes statistically significant differences ($p < 0.05$). Note the differences in scale.

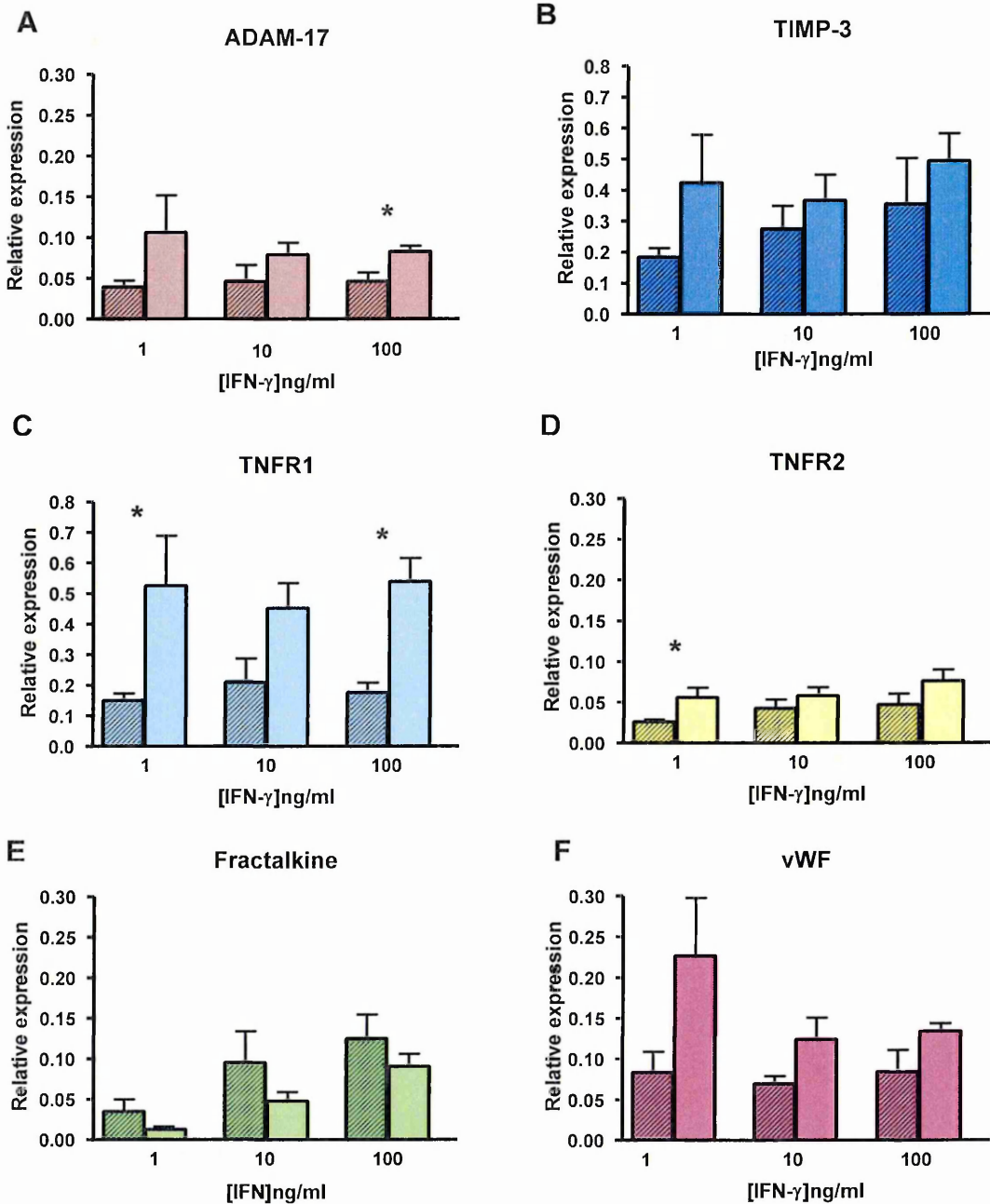


Figure 2.6: Effects of heparin on mRNA expression in hCMEC/D3 cells under interferon- γ (IFN- γ) treatment. Relative mRNA expression of ADAM-17 (A), TIMP-3 (B), TNFR1 (C), TNFR2 (D), fractalkine (E) and vWF (F) under IFN- γ treatment with heparin (hatched bars) and without heparin (blank bars). Relative mRNA levels were calculated using the housekeeping gene, cyclophilin A, and the $2^{-\Delta C_T}$ method, and using the non-parametric Mann Whitney U test. Data are presented as the mean ($n = 3$) \pm SEM. Asterisk (*) denotes statistically significant differences ($p < 0.05$). Note the differences in scale.

2.4 Discussion

In standard PCR, up to eight housekeeping genes can be selected to test primer efficiency and stability under the various experimental conditions. The TaqMan system negates the need to test efficiency as the primers have already been optimised by the company (Applied Biosystems, U.K.). In this present study the stability of three housekeeping genes (β -actin, cyclophilin A and GAPDH) was tested. β -actin could not be detected in the cell line, hCMEC/D3. Other studies have also reported the lack of expression of β -actin in newly isolated primary HUVECs and primary human placental microvascular endothelial cells (HPMEC) (Galustian et al., 1995). However, prolonged passage of immortalized human microvascular cell-line, HGTEN 21, and HPMEC, caused β -actin to be expressed (Galustian et al., 1995). The cells used in this present study were used at high passages, between 27 and 33, but β -actin could not be detected at any of these stages of the cell culture. It could be that the primer was faulty in some manner or that the cells contain a polymorphism for this gene which prevented annealing of the primer. Both cyclophilin A and GAPDH showed similar expression profiles under the various treatments in comparison to the control. Although there were some changes in expression of cyclophilin A and GAPDH under the different treatment regimes, these were minimal. The exception to this was the expression levels following treatment with 1ng/ml IFN- γ , which caused a large increase in expression of both genes. After careful examination of this result it was decided that it was an anomaly, possibly due to an anomalous optical density reading in the BrdU assay. The increase in expression was observed in both genes, and only at 1ng/ml, not 10 or 100ng/ml. It is unlikely that IFN- γ was having the same effect on both these unrelated genes. Thus Cyclophilin A was selected because it has been used in previous studies by a number of groups studying gene expression in a number of cell types, including endothelial cells, under various treatment regimes, e.g. VEGF (Gerritsen et al., 2003; Grenett et al., 1999; Yang et al., 2002).

This part of the study was devised to determine whether various supplements could have an affect on ADAM-17, fractalkine and the other genes of interest mRNA expression in hCMEC/D3 cells. Previous studies have reported various effects due to the application of growth factors, which might mask the effects seen from applying cytokines (Majka et al., 2001; Bzowska et al., 2004; Hatakeyama et al., 2004). Culturing of endothelial cells requires a specific system consisting of many growth factors and supplements for their growth and maintenance. The particular endothelial cells used in these experiments required the addition of VEGF, EGF and heparin (Lonza, U.K.). In 2001, Majka et al. found that ADAM-17 and one of its ligands, TNFR1, were up-regulated at the mRNA level by VEGF at 10ng/ml, however, only ADAM-17 was significantly up-regulated. In 2004, Bzowska et al. reported that ADAM-17 in

endothelial cells (murine brain microvascular, and human appendix and lymph node) is up-regulated at both the transcriptional and translational level when stimulated with VEGF or EGF. In addition they reported that this up-regulation of ADAM-17 mRNA was increased when VEGF (at 30ng/ml) or EGF (at 25ng/ml) was combined with TNF- α (10ng/ml); highlighting the synergistic effects of the growth factors with the cytokine.

VEGF is a secreted homodimeric 45kD glycoprotein (Ferrara, 1995; Senger et al., 1993) whose receptors are exclusively expressed on endothelial cells (Pepper et al., 1992; Goto et al., 1993). As well as stimulating endothelial cell growth, VEGF also increases the permeability of the microvasculature by disassembling tight junctions via reducing occludin expression and disrupting ZO-1 and occludin organisation (Ferrara, 1995; Senger et al., 1993; Stephan and Brock, 1996; Thomas, 1996; Wang et al., 2001). Here we have shown that VEGF and EGF modulate the mRNA expression of a number of proteins, however, only ADAM-17 was significantly altered in its expression. When treated with VEGF and EGF, ADAM-17 mRNA expression was significantly decreased ($p < 0.05$). This is contrary to other research groups who reported that upon VEGF or EGF treatment, ADAM-17 expression is increased at both the mRNA and protein level (Majka et al., 2001; Bzowska et al., 2004). However, these two studies did not determine the effects of both these growth factors administered at the same time, which could have a synergistic effect upon the expression of ADAM-17. This could account for the decrease in expression rather than the reported increase in expression of ADAM-17. In addition, it is not known at which concentration these factors are added to the growth media (company copyright laws). One vial of growth factor is recommended per bottle of media, however, the cells in this present study were cultured with a quarter of this amount. Private communication with the company (Lonza, UK) has confirmed that if the growth factors are added to the growth media at the recommended amount, the final concentration of VEGF would be around 10ng/ml and EGF would be less than 25ng/ml: both concentrations that elicit increased expression of ADAM-17 (Bzowska et al., 2004). Thus, as we used a quarter of the recommended amount the concentrations of VEGF and EGF were not sufficient to elicit increases in mRNA and protein expression of ADAM-17.

In addition, it has been shown that treatment of immortalised murine brain endothelial cells (MBE-SV) with TNF induces the secretion of VEGF from the cells; after 24 hours incubation with TNF the concentration of VEGF can reach 1ng/ml (Bzowska et al., 2004). Thus, it is impossible to exclude VEGF from the culture of endothelial cells when investigating the expression of genes under TNF treatment. Removal of VEGF and EGF from the media also caused a decrease in cell proliferation, thus to prevent this and to retain the phenotype of the cells these factors were kept in the media for subsequent experiments.

It has been previously reported that IFN- γ stimulates the expression of fractalkine in HUVEC endothelial cells (Imaizumi et al., 2000; 2004). However, in 2004 it was found that this expression is inhibited in a concentration-dependent manner by heparin (Hatakeyama et al., 2004), which is believed to bind to IFN- γ preventing it from interacting with its receptor. Heparin was administered at 4, 20 and 100 μ g/ml, however, the greatest concentration (100 μ g/ml) showed the most significant inhibitory effects. Heparin is an N-sulphated polysaccharide which is frequently used as an anticoagulant. In addition to this function, heparin and heparin-related molecules inhibit leukocyte-endothelial interactions by binding inflammatory proteins (Strunk and Colten, 1976; Matzner et al., 1984), chemokines (Miller and Krangel, 1992), and adhesion molecules (Skinner et al., 1991; Watt et al., 1993; Diamond et al., 1995; Koenig et al., 1998). These include the cytokines IL-1 (Ramsden and Rider, 1992) and IFN- γ (Lortat-Jacob and Grimaud, 1992). The binding of heparin and heparan sulphate to IFN- γ has been shown to result in reduced bioavailability and activity at the cell surface of this cytokine (Daubener et al., 1995).

A dense layer of proteoglycans cover the luminal surface of the vascular endothelium, the main functional components of which are polyanionic GAGs. The most abundant endothelial GAG is heparan sulphate, which is structurally and biosynthetically related to heparin and chondroitin sulphate (Kjellen and Lindahl, 1991). Heparin has been shown to inhibit IFN- γ -induced expression of fractalkine in HUVEC monolayers, but has no effect on the IL-1 β -induced expression of fractalkine (Hatakeyama et al., 2004). Similarly, heparin reduces adhesion of blood mononuclear cells to IFN- γ -stimulated HUVEC monolayers, but has no effect on the IL-1 β -induced adhesion of mononuclear cells (Hatakeyama et al., 2004). Heparin prevents the action of IFN- γ by either directly binding IFN- γ , or by partially blocking the binding of IFN- γ to its receptor, which in turn prevents downstream signalling via STAT1 (Hatakeyama et al., 2004). To determine whether heparin in the cell culture media could affect the expression levels of fractalkine and the other genes of interest induced by IFN- γ treatment, the mRNA expression levels of the genes of interest either in the presence or absence of heparin were investigated. Heparin caused an increase in mRNA expression in the genes of interest in the endothelial cells in comparison to cells not treated with heparin. However, this increase in expression was only significantly different in TNFR1 mRNA expression ($p \leq 0.05$). Next, to determine whether heparin could interfere with IFN- γ -induced mRNA expression levels, IFN- γ was applied to cells with or without heparin in the media. For all genes, apart from fractalkine, the absence of heparin under IFN- γ treatment caused an increase in mRNA expression, indicating that heparin could be interfering with the action of IFN- γ on the cells, either by binding to the cytokine itself or by partially blocking the binding of IFN- γ to its receptor

(Hatakeyama et al., 2004). This increase in mRNA expression, however, was only significant in three of the genes studied. It is not known at what concentration heparin is used in the present system, however, personal communications with the company (Lonza, UK) that supplies the media and supplements has confirmed that the concentration of heparin is below 100µg/ml, the concentration that significantly reduced mononuclear cell adherence and abolished fractalkine mRNA expression under IFN-γ treatment (Hatakeyama et al., 2004). A quarter of the recommended concentration supplied was used in this study and it is thus presumed that the final concentration in this system is greatly below that used by Hatakeyama and colleagues (2004). In conclusion, heparin itself increased mRNA expression levels of the genes of interest, however, during IFN-γ treatment it reduced the effects of the cytokine. However, heparin's effect on the system was not significantly different for the majority of genes examined. Thus a greater increase in the expression levels of the genes of interest may be observed had heparin been removed from the system.

This chapter of the thesis was undertaken to establish a cell culturing system for the human brain endothelial cell line, hCMEC/D3, which would be suitable for subsequent experiments involving this cell line. This entailed identifying a suitable housekeeping gene for qRT-PCR and determining the effects of growth factors on the expression of the genes of interest. From this work the major findings can be thus summarised:

- Cyclophilin A is a stable housekeeping gene under inflammatory conditions and is suitable for the analysis of gene expression using qRT-PCR.
- Removal of VEGF and EGF from the media only elicited a significant increase in mRNA expression of ADAM-17.
- Removal of heparin from the media caused a significant decrease in mRNA expression of TNFR1.
- Retaining heparin in the media during IFN-γ treatment reduced the effects of the cytokine in all genes analysed except fractalkine. This was significant for ADAM-17, TNFR1, and TNFR2.

In conclusion, Cyclophilin A is a suitable housekeeping gene for qRT-PCR experiments to analyse gene expression under inflammatory conditions. As VEGF, EGF and heparin did not consistently significantly affect the expression levels of the genes of interest, and in the case of heparin, even under an IFN-γ treatment regime, these factors were retained in the cell culture medium under the experimental conditions described in subsequent chapters 3 and 4.

Chapter 3

Effects of inflammatory cytokines on the expression of ADAM-17, TIMP-3 and substrates shed by the protease in the human adult brain endothelial cell line, hCMEC/D3.

3.1 Introduction

ADAM-17 protein expression has previously been demonstrated *in vivo* in endothelial cells in normal human brain (Goddard et al., 2001) and is up-regulated in MS white matter (Plumb et al., 2006). An up-regulation of ADAM-17 mRNA in endothelial cells and astrocytes in spinal cords of rats with EAE has also been reported (Plumb et al., 2005). BBB endothelial cells are specialised to act as a physical and physiological barrier between the CNS and the circulation. Diffusion of substances and cell migration across the BBB is regulated by both tight junctions and the low expression of adhesion molecules on the endothelium. In MS, endothelial cells demonstrate TJ abnormalities (Kirk et al., 2003) and increased levels of cell adhesion molecules (Sobel et al., 1990; Washington et al., 1994; Bö et al., 1996).

The breakdown of the BBB has been associated with the actions of various cytokines, including TNF. *In vitro* studies have revealed that TNF increases the expression of various adhesion molecules (Wong and Dorovini-Zis, 1995; Dobbie et al., 1999) and causes a decrease in barrier integrity, resulting in increased permeability of the endothelial cell monolayer (Dobbie et al., 1999; for review see Walsh et al., 2000). TNF is produced by an array of cells including monocytes, macrophages and NK cells (Delves et al., 2006). TNF has been found to be localised to astrocytes and macrophages within the MS plaque border (Hofman et al., 1989) and is also expressed by leukocytes within the perivascular cuff (Merrill, 1992; Woodroffe and Cuzner, 1993). An increased expression of TNF in the CSF of patients with active disease (Hauser et al., 1990) and in progressive forms of the disease, compared to stable MS (Sharief and Hentges, 1991) has been reported. Other pro-inflammatory cytokines implicated in MS pathogenesis include: IL-1 β , which is secreted by monocytes and macrophages amongst others (Delves et al., 2006), and has been found to be increased in the CSF of MS patients with active disease (Hauser et al., 1990) and is associated with BBB breakdown and demyelination in rats (Ferrari et al., 2004); and IFN- γ , which is produced by T lymphocytes (Delves et al., 2006), has been found to be increased preceding relapses (Beck et al., 1988; Lu et al., 1993) and is found within the inflammatory cuffs of MS patients (Woodroffe and Cuzner, 1993; Simpson et al., 2000). Dysregulation of cytokine expression in MS is not restricted to pro-inflammatory mediators but is also observed in anti-inflammatory cytokines: TGF- β has been shown to be significantly down-regulated in lymphocytes of MS patients with clinically active disease compared to stable MS (Mokhtarian et al., 1994), and has been observed in microglia within the plaque edge of acute active lesions (Peress et al., 1996) and surrounding the blood vessels within the ECM of acute lesions (Cannella and Raine, 1995). Increased expression of TGF- β is associated with the recovery phase in EAE (Iwahashi et al., 1997).

ADAM-17 is the major convertase of pro-TNF, however, the function of ADAM-17 in the pathogenesis of MS is unknown. In other neurological conditions, ADAM-17 has been described as having beneficial and/or deleterious effects. In AD, the protease acts as an alpha-secretase, which produces the neuroprotective species of APP (Allinson et al., 2004). In stroke, however, ADAM-17's role is speculative; increased expression of ADAM-17 in the animal model of stroke coincides with reduced brain infarction, due to increased production of TNF, which is prevented with inhibition of ADAM-17 (Cárdenas et al., 2002). Ischemic preconditioning (IPC) was induced in this model using transient middle cerebral artery occlusion (tMCAO) followed by occlusion of the ipsilateral common carotid artery (CCA). ADAM-17 expression was examined following IPC using western blotting, and the levels of TNF in brain homogenates examined following IPC using an ELISA assay (Cárdenas et al., 2002). TNF has been shown *in vitro* to induce the up-regulation of glutamate transporters and glutamate uptake which prevented excitotoxic cell death (Romera et al., 2004). However, other studies have found inhibiting ADAM-17 and thereby reducing TNF, has a neuroprotective effect in the animal model of stroke (Wang et al 2004). In the latter study a blood clot was introduced in the CCA to induce stroke, 24 hours later, the brain was removed and homogenised in lysis buffer and the supernatant subjected to an ELISA assay for TNF. ADAM-17 was not examined directly in this study, but the application of an ADAM-17 inhibitor (DPH-067517) resulted in a reduction in TNF and reduced infarct size. The differences between the latter study and that of Cárdenas and colleagues (2002) is discussed as possibly being due to the different models used to study ischemic stroke, i.e. IPC versus ischemic injury, and the use of different ADAM-17 inhibitors (Wang et al 2004).

3.1.2 Aims of the study

The aims of this chapter were:

- (i) to investigate gene expression of ADAM-17, TIMP-3, fractalkine and other proteins shed by the protease, under control and various inflammatory conditions at the mRNA level using qRT-PCR in the human adult brain endothelial cell line, hCMEC/D3;
- (ii) to investigate the protein expression of ADAM-17, TIMP-3 and fractalkine using immunocytochemistry, and also the expression of ADAM-17 pro- and mature forms by western blotting in hCMEC/D3;
- (iii) to elucidate the functional role of ADAM-17, by studying the shedding activities of ADAM-17 by hCMEC/D3 using an ELISA assay for fractalkine (one of the membrane-bound substrates of ADAM-17);
- (iv) to elucidate the enzyme activity of ADAM-17 in hCMEC/D3 under control and pro-inflammatory conditions using a bioassay.

3.2 Materials and methods

3.2.1 Suppliers used in this chapter

Abcam, 332 Cambridge Science Park, Cambridge, CB4 0FW, UK; **Chemicon**, supplied through Millipore; **Anaspec**, Cambridge Bioscience, 24/25 Signet Court, Newmarket Rd., Cambridge, CB5 8LA, UK; **Fischer Scientific Inc**, Bishop Meadow Rd., Loughborough, Leicestershire, LE11 5RG, UK; **GE Healthcare UK Ltd.**, Pollards Wood, Nightingales Lane, Chalfont Street Giles, Buckinghamshire, UK; **Millipore**, The Science Centre, Eagle Close, Chandlers Ford, Hampshire, SO53 4NF, UK; **Molecular Devices**, 1311 Orleans Drive, Sunnyvale, CA 94089-1136, U.S.A; **Molecular Probes**, supplied through Invitrogen; **NUNC**, supplied through Fischer Scientific Inc; **R&D Systems**, 19 Barton Lane, Abingdon Science Park, Abingdon, Oxon, OX14 3NB, UK; **Vector Laboratories**, 3 Accent Park, Bakewell Rd., Orton Southgate, Peterborough, UK; **Whatman**, 27 Great West Rd., Brentford, Middlesex, TW8 9BW, UK; or as otherwise stated in Chapter 2 section 2.2.1.

3.2.2 Cell culture

For full details see Chapter 2 (see section 2.2.3).

3.2.3 qRT-PCR

For full details see Chapter 2 (see section 2.2.5.2).

3.2.3.1 Experimental conditions for testing gene expression

For qRT-PCR, cells were seeded in complete media at $1 \times 10^5/500\mu\text{l}$ /well of a 24 well plate (Fischer Scientific, U.K.). After 24 hours the media was aspirated, cells washed with 1ml of PBS (Invitrogen, U.K.), and fresh serum-free media containing 1, 10 or 100ng/ml TNF, IL-1 β , IFN- γ or TGF- β 1 (PeproTech, U.K.) was added. Cells cultured in serum-free media without cytokine were used as a control. Each condition was performed in triplicate and the experiments were repeated three times. After 24 hours of cytokine treatment, the cells were washed twice with PBS, and RNA was extracted using TRI Reagent (Sigma-Aldrich, U.K.) following the manufacturer's guidelines (see Chapter 2 section 2.2.4.1).

3.2.3.2 Statistical analysis for qRT-PCR data

qRT-PCR data was analysed using the non-parametric Mann Whitney *U* test. To carry out this test, $2^{-\Delta C_T}$ for each sample was calculated to determine the relative gene expression. Each treated condition was then compared to the control. Significance was

set at $p < 0.05$ and the data are presented as mean \pm SEM for the indicated number of experiments.

3.2.4 Immunocytochemistry

3.2.4.1 Immunofluorescence microscopy

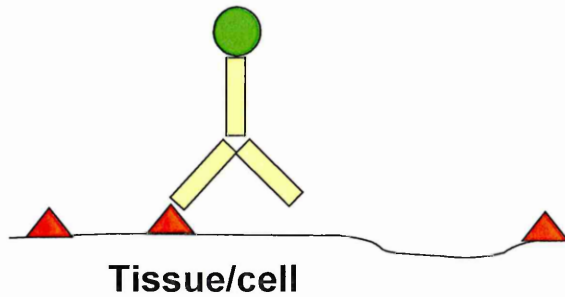
Antibodies have been employed to detect the subcellular localisation of proteins (or antigen) in cells and tissues. The detection of antigens using antibodies in cultured cells is known as immunocytochemistry (ICC), whereas the detection of antigens in tissues is known as immunohistochemistry (IHC). Immunofluorescence relies upon the coupling of fluorophores/fluorochromes to antibodies, which when bound to the antigen of interest and excited by a light source (usually UV light) reveal the subcellular location of the antigen of interest (Figure 3.1). Before antibody application, the cells/tissue must be prepared by fixation, permeabilization and sometimes blocking with a protein such as albumin. Fixatives preserve the cellular morphology and the antigenicity of the protein/antigen of interest. Fixatives can work in two main ways: the formation of crosslinkages (e.g., aldehydes such as glutaraldehyde or formalin) or protein denaturation by coagulation (e.g., acetone and methanol). Permeabilization, using a detergent such as Triton X-100 or Tween-20 (fixatives such as acetone or methanol do not require a permeabilization step), allows free passage of the antibodies across the plasma membrane. A blocking step using an irrelevant protein such as albumin or using serum from the secondary host (see Indirect immunofluorescence) is sometimes used to block non-specific binding of IgG to the tissue or cells, particularly to Fc receptors (FcR). In between each step the cells/tissue are washed with an appropriate buffer to remove unbound reagents. Antigens can be detected by this method using antibodies that are labelled either directly or indirectly (Figure 3.1). Appropriate controls should be run in parallel which can include the omission of a primary antibody to determine the non-specific staining pattern of the secondary antibody or an isotype control which will reveal the non-specific binding of the primary antibody (Delves et al., 2006).

3.2.4.2 Direct immunofluorescence

In this method the antibody used to locate the antigen of interest is directly coupled to the fluorophore/fluorochrome (Figure 3.1). This technique is limited as only a certain amount of antibodies can access the antigen of interest. However, this technique is employed in flow cytometry, which is a more sensitive technique for the detection of antigens.

A

Direct method



B

Indirect method

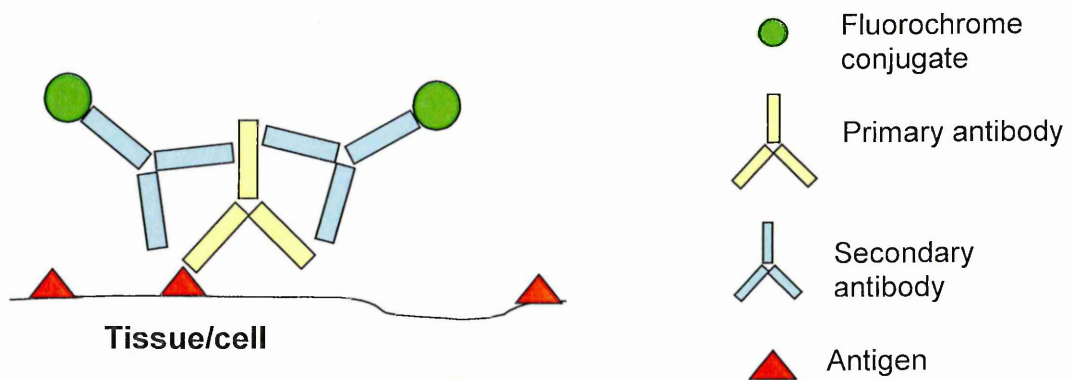


Figure 3.1: Schematic representation of immunocytochemical detection of antigens on tissue and cells using antibodies. Antigens can be detected with the use of either a directly (A) or an indirectly (B) conjugated antibody, whereby an unlabelled primary antibody is used to detect the antigen and then a secondary antibody is used to detect the primary antibody.

3.2.4.3 *Indirect immunofluorescence*

This type of immunofluorescence, called the double-layer technique, is most commonly employed. Two antibodies are used to visualise the target antigen: the primary antibody, which is directed against the target antigen; the secondary antibody, which is directed against the species Ig that was used to raise the primary antibody (Figure 3.1). So for example, a monoclonal mouse anti-ADAM-17 antibody will be applied to cells or tissue, which is then visualised using a fluorochrome-conjugated rabbit anti-mouse immunoglobulin (Ig) serum. This technique has a number of advantages: in the first instance, several fluorescently labelled secondary antibodies can bind the primary antibody, and thus the fluorescence intensity is brighter than the direct method; secondly, the purchase of one secondary antibody can be sufficient to suit an array of primary antibodies, thus limiting cost; thirdly, more than one protein can be detected within the same cell in the same experiment. The primary antibodies, however, must be raised/generated in different species, otherwise the secondary antibody will not be able to discriminate between the two primary antibodies and hence the antigens of interest. The fluorophores, which are conjugated to the secondary antibodies must also have distinct emission wavelengths when carrying out labelling of different antigens within the same sample so as to avoid overlapping otherwise discrimination between the antigens will not be possible. For example, to simultaneously detect ADAM-17 and fractalkine within the same cell, one antibody could be generated in mouse and one in rabbit. Fluorescently labelled species-specific Ig (e.g., goat anti-rabbit and goat anti-mouse) can then be used to compare the relative positions and/or expression levels of the two different proteins (Delves et al., 2006).

3.2.4.4 *Confocal laser scanning microscopy (CLSM)*

Unlike fluorescence microscopy, which utilises a UV light source and a number of different reflectors to view the fluorescently-tagged proteins, confocal laser scanning microscopy (CLSM) utilises a different system. The overall effect of this system is to exclude any out of focus light that is emitted from the surrounding cells/tissue in the planes above and below the target object. This allows the user to obtain a high-resolution optical image. This is achieved in two ways: firstly, the microscope uses a concentrated light source, a laser, which excites the fluorochromes at a specific wavelength; secondly, the placement of "pinholes" in front of the laser and the detector excludes "out of focus" light (Figure 3.2). The CLSM consists of a conventional fluorescence microscope which is attached to a confocal scanning unit. The confocal scanning unit consists of scanning mirrors, a laser, wavelength-selective filters, a pinhole aperture, and a photomultiplier detector. Light from the laser is directed through

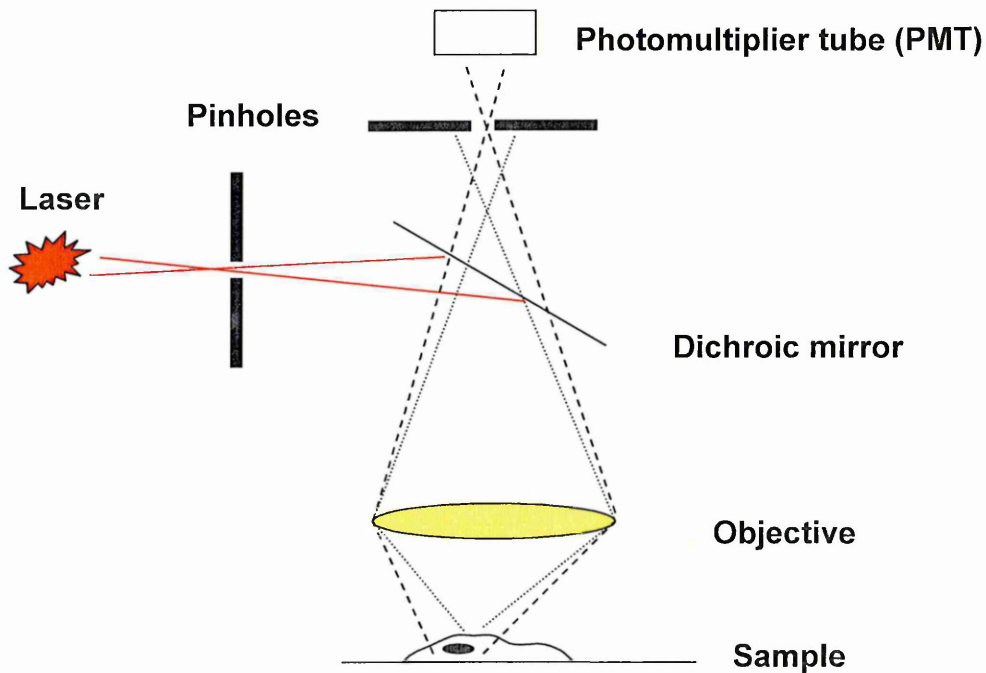


Figure 3.2: Schematic diagram of the confocal laser scanning microscopy (CLSM) system. Lasers and the use of two appropriately placed pinholes have the overall effect of rejecting out-of-focus light and create a sharp confocal image. Illumination from the laser is directed down the phototube to the sample by a number of *scanning* mirrors (not shown). Fluorescence light emitted by the sample passes back up through the phototube, "descanned" by the scanning mirrors and passes through the dichroic mirror (reflected laser light is removed here) to the pinhole aperture. Light emitted from the focal plane (----) passes through the pinhole to the photomultiplier tube (PMT) (detector), but all other light (.....) is rejected (Adapted from Murray, 2005).

the phototube of the microscope. Rapidly oscillating scanning mirrors deflect the laser light so that it sweeps across the specimen in a "raster" pattern. Emitted fluorescent light from the sample passes back up the phototube where it is "descanned" by the scanning mirrors. The light then passes through a dichromatic beam splitter, which removes any reflected laser light, and then to the pinhole aperture. After passing through the pinhole, the light is collected by a detector (photomultiplier tube (PMT)) and converted into an electrical signal, which is recorded by a computer (Figure 3.2). Visual (nonconfocal) inspection of the specimen is provided by use of the usual binocular eyepieces with a sliding prism and the use of a UV lamp. A confocal microscope only differs from a light microscope in that both the field of view of the objective lens and the region of illumination have been limited to a single point in the same focal (*confocal*) plane (Murray, 2005). Another advantage of the CLSM is that it can perform a Z-stack, which allows an organelle/cell/tissue to be reconstructed in 3D. By carrying out a series of automated X-Y scans in the Z-axis, a series of images can be compiled to view, for example, a cell from its apical to its basal surface, which can then be manipulated and rotated (Delves et al., 2006; for review see Stephens and Allan, 2003).

3.2.4.5 Method

As TNF at 100ng/ml elicited the most potent response in hCMEC/D3 cells at the mRNA level, in three of the genes of interest, namely ADAM-17, TIMP-3 and fractalkine, the protein expression under this treatment regime was assessed. TNFR2 was also significantly increased but not as great as fractalkine, thus expression of the protein was restricted to the three genes. For ICC, cells were seeded at 5×10^4 cells/250 μ l/well of an 8-well glass chamber slide (NUNC, Labtech International, U.K.) in complete media for 24 hours. Following two wash steps with PBS, the media was replaced with serum-free media, with or without 100ng/ml TNF. Following 24 hours stimulation, cells were processed for ICC analysis of proteins. Each condition was performed in triplicate for each protein examined. Cells were washed with PBS and fixed with either ice-cold acetone for 10 minutes or fresh 4% paraformaldehyde (PFA) for 15 minutes. Fresh 4% PFA was prepared by dissolving 2g of PFA powder (Sigma-Aldrich, U.K.) in 25ml of dH₂O and heated to 60°C whilst stirring with a magnetic stirrer on a hot plate. Before the solution reached 60°C a couple of drops of NaOH (1M) were added to alter the pH to aid dissolving. Once heated to 60°C, the solution was removed from the hot plate, and filtered through filter paper (Whatman) into 25ml 0.2M phosphate buffer. Once cooled the pH was adjusted to 7.2. The solution was stored at 4°C for a maximum of 2 weeks.

Cells fixed with acetone were air dried for 15 minutes and then washed. Cells fixed with 4% PFA were washed 3 times for 5 minutes each with PBS after aspirating the PFA. Cells were treated with blocking solution containing 1% bovine serum albumin (BSA) (Sigma-Aldrich, U.K.) and 3% goat serum (Sigma-Aldrich, U.K.) for 30 minutes at RT. Cells fixed with 4% PFA were permeabilised with 0.2% Triton X-100 during the blocking step. The cells were stained for ADAM-17, TIMP-3 and fractalkine using monoclonal mouse anti-human ADAM-17 (R&D Systems, U.K.), polyclonal rabbit anti-human TIMP-3 (Abcam, U.K.) and monoclonal mouse anti-human fractalkine (R&D Systems, U.K.), respectively. Preliminary experiments were performed to determine the optimum concentration required for ICC; each antibody was diluted within a range of that recommended by the supplier (Table 3.1). All antibodies were diluted 1:200 in blocking solution and incubated overnight at 4°C. Cells were washed and bound primary antibody visualised using Alexa Fluor® 568 conjugated to either goat anti-mouse IgG (for monoclonal antibodies) or goat anti-rabbit IgG (for polyclonal antibodies) secondary antibodies (Molecular Probes, USA) diluted 1:500 in PBS and incubated at RT for 90 minutes. Following three wash steps in PBS, the cells were mounted in Vectashield™ hardset mounting media with 4',6-diamidino-2-phenylindole (DAPI) (Vector Laboratories, U.K.) as a nuclear counterstain. Images were captured using a Zeiss 510 laser-scanning confocal microscope. Omission of the primary antibody served as a negative control.

3.2.5 Sodium dodecyl sulphate-polyacrylamide gel electrophoresis (SDS-PAGE) and western blotting

3.2.5.1 Principles of SDS-PAGE and western blotting

SDS-PAGE is a technique which allows the separation of proteins based upon their RMM by passing a current through the matrix in which they are loaded. SDS is an anionic detergent, which means when it is dissolved, its molecules carry a negative charge. For every 1g of protein, 1.4g of SDS binds to it, thus the amount of SDS which binds is proportional to the size of the protein. When SDS binds to the protein it denatures it and allocates a net negative charge, which will cause the protein to migrate towards the positively charged electrode in an electric field. Polyacrylamide gels contain a cross-linker such as bisacrylamide, which forms bonds between two polyacrylamide molecules, forming a porous matrix through which the proteins migrate. The concentration of the acrylamide determines the speed at which the proteins move through the gel. Lower concentrations of acrylamide are better at resolving high RMM proteins and higher concentrations are better at resolving low RMM. Once a current is

Table 3.1: Determination of the optimal concentration of antibodies used in the immunocytochemical detection of ADAM-17, TIMP-3 and fractalkine in hCMEC/D3 cells, under control and pro-inflammatory conditions. The optimum concentration for each antibody used in this experiment is highlighted in bold.

Antibody	Antibody type (Species)	Supplier	Cat No.	Antibody dilutions tested
ADAM-17	Monoclonal (mouse)	R&D Systems	MAB9302	1 in 10 1 in 20 1 in 50 1 in 100 1 in 200
TIMP-3	Polyclonal (rabbit)	Abcam	ab2169	1 in 50 1 in 100 1 in 200
Fractalkine	Monoclonal (mouse)	R&D Systems	MAB3651	1 in 10 1 in 20 1 in 50 1 in 100 1 in 200
Alexa fluor 568 goat anti-mouse IgG	N/A	Molecular Probes	A-11004	1 in 500
Alexa fluor 568 goat anti-rabbit IgG	N/A	Molecular Probes	A-11011	1 in 500

passed through the gel, proteins migrate based upon their size due to the constant mass to charge ratio. In order to determine the size of the migrated proteins, standards of known mass are separated on each gel alongside the sample. Comparisons can then be drawn as to the RMM of the protein under investigation.

Western blotting is a technique which employs the same principles as ICC to detect specific proteins within a complex mixture of proteins. Once proteins are separated via SDS-PAGE, proteins are transferred onto a membrane (typically nitrocellulose or polyvinylidene difluoride (PVDF)) by passing a current through the gel. The membrane is then probed using antibodies specific for a certain antigen of interest. As with ICC, membranes must be blocked to prevent non-specific binding of the antibodies. This is usually done using 5% non-fat milk powder or BSA. To ensure any differences in protein concentration between samples does not affect semi-quantitative analysis of protein expression, a control antibody to a commonly expressed protein, e.g. actin, is used to normalise loading of samples (Delves et al., 2006).

3.2.5.2 Protein extraction for western blotting

For the western blots, protein was extracted according to the manufacturer's guidelines using TRI Reagent (Sigma-Aldrich, U.K.). TRI Reagent was used for protein extraction for western blotting as previous work within this laboratory has detected ADAM-17 expression in tissue using this method (Plumb et al., 2005; 2006). Following the separation of the solution into the three organic phases (see Chapter 2 section 2.2.4.1) the RNA was removed and the DNA precipitated by adding 0.3ml of 100% ethanol/ml of TRI reagent, mixed, left to incubate for 2-3 minutes at RT and then centrifuged at 2,000 x g for 5 minutes at 4°C. The protein containing supernatant was then removed to a fresh tube and 1.5ml of isopropanol/ml of TRI Reagent was added, mixed and allowed to stand for at least 10 minutes at RT. Following a centrifugation step at 12,000 x g for 10 minutes at 4°C, the supernatant was aspirated, and the protein pellet was washed 3 times with 0.3M guanidine hydrochloride/95% ethanol solution, using 2ml/ml of TRI Reagent. During each wash step the pellet was stored in wash solution for 20 minutes at RT and then centrifuged at 7,500 x g for 5 minutes at 4°C. Following 3 washes, 2ml of 100% ethanol was added and the protein pellet vortexed. The sample was allowed to stand at RT for 20 minutes and subsequently centrifuged at 7,500 x g for 5 minutes at 4°C. The pellet was dried for 5-10 minutes and dissolved in 1% SDS. Any insoluble material was removed by centrifugation of the mixture at 10,000 x g for 10 minutes at 4°C and the supernatant was transferred to a clean eppendorf tube and stored at -20°C.

3.2.5.3 Protein determination

The protein concentration of each sample was determined using the bicinchoninic acid (BCA) assay. This method relies upon the formation of a Cu^{2+} -protein complex under alkaline conditions, followed by the reduction of the Cu^{2+} to Cu^{1+} . Various amino acids and the peptide bond within the protein are responsible for the reduction of Cu^{2+} to Cu^{1+} including cysteine, cystine, tryptophan and tyrosine. Under alkaline conditions, BCA forms a purple-blue complex with Cu^{1+} and provides a method of monitoring the reduction of Cu^{2+} by proteins at an absorbance of 570nm. The amount of protein in the sample is proportional to the amount of reduction. A protein of known concentration, such as BSA is used as a standard at different concentrations (0-4mg/ml for example). This can then be used to construct a standard curve and the unknown protein concentrations of the samples can be extrapolated from the standard curve using the formula of the gradient of the curve. There are a number of advantages in using the BCA assay, such as the stable formation of the colour complex, its compatibility with a number of detergents, and it is applicable to a broad range of protein concentrations (http://www.sigmaaldrich.com/Area_of_Interest/Life_Science/Proteomics_and_Protein_Expr_/Protein_Analysis/Protein_Quantitation/Bicinchoninic_Acid_Kit.html).

BCA provided as a solution (Sigma-Aldrich, U.K.) was mixed with copper sulphate solution ($\text{CuSO}_4 \cdot 5\text{H}_2\text{O}$) (4% w/v) (Sigma-Aldrich, U.K.) at a ratio of 50:1. Using a 96 well plate, 20 μl of sample or standard, diluted in an appropriate buffer, was added per well followed by 200 μl of the BCA: CuSO_4 solution. Standards (BSA) were assayed in triplicate, whereas the samples were assayed in duplicate. Following a 30 minute incubation, the plate was read at a wavelength of 570nm. Data was then plotted in Microsoft® Office Excel 2003 SP3 to construct a standard curve (Figure 3.3).

3.2.5.4 Optimisation of the western blotting technique

Various parameters had to be altered in order to optimise the western blotting detection method. These included:

1. Using actin as a standard to normalise protein loading. Recent publications claimed that β -actin is an unsuitable loading control for western blot analysis as it cannot detect differences in actin protein levels (between the ranges of 1.88 and 7.5 μg) (Dittmer and Dittmer, 2006). To ensure this was not the case with the antibody used in these experiments, serial dilutions of hCMEC/D3 protein at similar concentrations that would be used in the experiment (0.75, 1.5 and 3 μg) were separated by SDS-PAGE and probed for actin on a western blot.

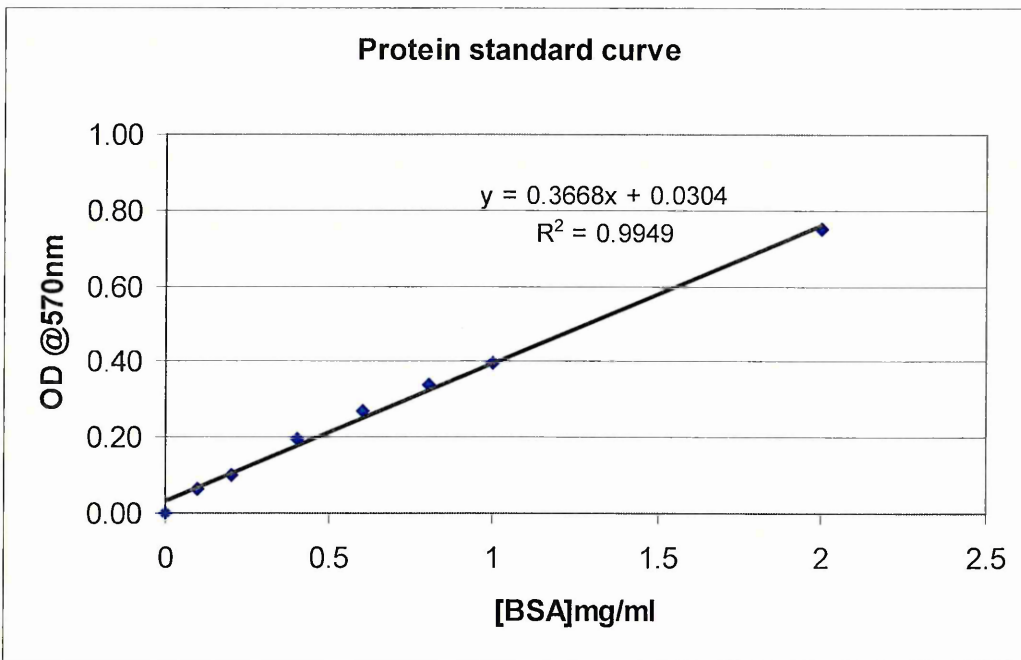


Figure 3.3: Representative standard curve used to determine the protein concentration of unknown samples. BSA was used as a standard. Using the optical density (OD) of the unknown protein sample which corresponds to y in the formula for the gradient of the curve, the concentration (x) can be determined by rearranging the equation to $x = (y-0.0304)/0.3668$.

2. Finding a suitable antibody to detect ADAM-17. Various antibodies against ADAM-17 were tested (Table 3.2) for their ability to detect the mature and pro-form of the protease. Protein extracted from human peripheral blood leukemia T cell line (JURKAT), or the human hepatocellular carcinoma cell line (HepG2) (kindly provided by S. Turner, BMRC), were used as positive controls.

3.2.5.5 Determination of ADAM-17 protein expression in hCMEC/D3 cells under control and pro-inflammatory conditions by SDS-PAGE and western blotting

In order to prepare the protein sample for SDS-PAGE, 100µl sample was mixed with 50µl NuPAGE LDS (Lithium Dodecyl Sulfate, this is used instead of SDS as it is less viscous) sample buffer (4x concentrate), 20µl NuPAGE sample reducing agent (both Invitrogen, U.K.) and 30µl water. The samples were then boiled for 4 minutes at 99°C. 3µg of sample or 3µl of protein ladder (SeeBluePlus2 molecular weight marker, Invitrogen, U.K.) were loaded per well of a NuPAGE 10% Bis-Tris gel and run in NuPAGE MOPs SDS running buffer using an Invitrogen Novex Mini-Cell (Invitrogen, UK) at 150V for approximately 60 minutes, until the dye reached 1cm from the end of the gel.

To transfer the proteins to a nitrocellulose membrane, wet-blotting was performed using a TE Series transfer tank (Hoefer®) at approximately 100V for 60 minutes in NuPAGE transfer buffer containing 10% methanol and 0.1% NuPAGE antioxidant (Invitrogen, U.K.). Following transfer, blots were immediately placed in blocking solution consisting of Tris-buffered saline (TBS; 20mM Tris, pH 7.4/0.9% NaCl; Sigma), 5% non-fat dry milk powder and 0.05% Tween 20 for 90 minutes at room temperature on a platform shaker. Blots were then washed with TBS-Tween (TBS-T) three times for 10 minutes each, with shaking.

To determine a suitable ADAM-17 antibody various antibodies were tested at different concentrations: T-5442 (Sigma-Aldrich, U.K.), Ab39162 (Abcam), MAB9302 (R&D Systems), AB19027 (Chemicon, U.K.) (Table 3.2). Each membrane was then probed overnight at 4°C with different antibodies diluted in TBS-T containing 5% milk powder. The following day, the blots were washed again three times for 10 minutes each in TBS-T to remove any unbound antibody. The blots were incubated at room temperature for 120 minutes with goat anti-rabbit IgG (Sigma; at 1:80,000; for polyclonal antibodies) conjugated to horseradish peroxidase (HRP). The blots were then subjected to two intervals of three washes each for 5 minutes, firstly with TBS-T and then with TBS alone. Antibody binding was detected using an enhanced chemiluminescence Plus (ECL) kit (GE Healthcare, U.K.), which was left to develop for 5 minutes at room temperature. Blots were then placed in a UVP epi II dark room and

Table 3.2: Antibodies tested to determine their suitability to detect the pro- and mature forms of ADAM-17 using western blotting. Each antibody was tested at various concentrations in line with those recommended by the supplier.

Antibody	Antibody type and Species	Company	Cat No.	Dilutions tested
ADAM-17	Polyclonal (rabbit)	Sigma-Aldrich	T-5442	1 in 500 1 in 1000 1 in 2000
ADAM-17	Polyclonal (rabbit)	Abcam	Ab39162	1 in 1000 1 in 2000 1 in 5000 1 in 10,000
ADAM-17	Monoclonal (mouse)	R&D Systems	MAB9302	1 in 250 1 in 500 1 in 1000
ADAM-17	Polyclonal (rabbit)	Chemicon	AB19027	1 in 250 1 in 500 1 in 1000

10 serial images were captured at every 1 minute 30 seconds interval using Labworks version 4.0. Following visualisation of the experimental protein the membranes were washed with TBS and stripped using stripping solution (Millipore, U.K.) for 15 minutes at RT. Following a blocking step, the membranes were probed for actin using the same method as described above. The rabbit anti-actin antibody (1:1000, Sigma-Aldrich, U.K.) was visualised with the same goat anti-rabbit IgG antibody described above. Actin was used to normalise protein loading.

Once the optimal antibody was selected (AB19027, polyclonal anti-ADAM-17, Chemicon, CA, at 1:250) the protein from cells treated under control and pro-inflammatory conditions were subjected to SDS-PAGE and western blotting. At any one time, three gels with the same samples were run in parallel, one gel was probed using the anti-ADAM-17 antibody, one was used as a negative control (omission of the primary antibody) and the final gel was used as a blocking peptide control (Table 3.3). The latter was used to confirm the specificity of the anti-ADAM-17 antibody. This peptide (200µg/ml) was used at the same volume as the antibody (as recommended by the supplier; both adding the same concentration or volume as the antibody elicited the same outcome). The antibody and the peptide were diluted together in 200µl TBS and placed in a 37°C incubator for 30 minutes. The solution was then centrifuged at 9,200 x g for 15 minutes at 4°C. The supernatant was then diluted in 4.8ml TBS-T with 5% milk powder and added to the membrane. The membrane was then subjected to the same immunostaining protocol as detailed above. Semi-quantitative analysis of the bands was carried out by densitometry using Labworks version 4.0, and the data normalised to actin and then the respective control using the following formulae: $(target\ band/actin\ band)/control\ target\ band$.

3.2.5.6 Verification of protein transfer

In order to verify protein transfer, the membrane was stained with Ponceau S (3-Hydroxy-4-(2-sulfo-4-[4-sulphophenylazo]phenylazo) -2, 7-naphthalenedisulfonic acid sodium salt) (0.1% Ponceau S (w/v) in 5% (v/v) acetic acid) (Sigma Aldrich, UK) for 5 minutes, which allows the reversible staining of protein bands on the membrane. The bands are not apparent until the membrane is rinsed with deionised water. An image was then captured. To completely remove the staining and proceed with the immunostaining, the membrane was washed with TBS-T (0.05%) twice for 10 minutes each. As a positive control for the presence of protein before transfer, another gel with the same samples was run in parallel and stained with Coomassie blue (0.25%) (Sigma-Aldrich, U.K) dissolved in a mixture of methanol (45%) (Fisher Scientific, UK) and acetic acid (10%) for several minutes and then de-stained with a mixture of

Table 3.3: Antibodies and blocking peptide used to detect ADAM-17 in hCMEC/D3 under control and pro-inflammatory conditions. The antibody titre of each antibody was determined in preliminary experiments. The optimum concentration for each antibody used in this thesis is highlighted in bold.

Antibody/Peptide	Antibody type and Species	Company	Cat No.	Dilutions tested
ADAM-17	Polyclonal (rabbit)	Chemicon	AB19027	1 in 250 1 in 500 1 in 1000
Blocking peptide	N/A	Chemicon	AG909	1 in 250
Actin	polyclonal (rabbit)	Sigma	A5060	1 in 1000*
HRP goat anti-rabbit IgG	polyclonal (goat)	Sigma	A9169	1 in 80,000*

* dilutions previously determined and described in Haddock et al., 2006.

methanol (5%) and acetic acid (7%) for several hours until bands were visible. The transferred gel is also stained in the same manner to ensure all separated proteins had been transferred to the nitrocellulose membrane.

3.2.5.7 Statistical analysis of western blot data

Densitometric data was analysed using a parametric one-way ANOVA followed by Dunnett's multiple comparison test. Each treated sample was compared to the control. Significance was set at $p < 0.05$ and the data are presented as mean \pm SEM for the indicated number of experiments.

3.2.6 Enzyme-Linked Immunosorbent Assay (ELISA) for determining fractalkine levels

3.2.6.1 Principles of the ELISA assay

ELISAs also utilise specific antibodies, but in this technique they are used to determine the presence and concentration of a protein in a sample, e.g. in cell culture supernatants, serum or CSF. Like ICC and IHC the process involves a series of blocking and wash steps and relies upon the fact that antibodies, as with all proteins, can attach to the plastic 96-well microtitre plate. The most used immunoassay is the two antibody 'sandwich ELISA' also known as an antigen-capture assay (Fig 3.4). Following immobilization of the antibody on the microtitre plate, unbound protein-binding sites on the plate are blocked using an appropriate protein. Following a wash step, the sample containing the antigen to be measured is added and incubated for a few hours to allow the antibody to capture the protein of interest. Following further wash steps to remove unbound sample, a detection antibody, which is also directed against the protein of interest, is applied. The capture and detection antibodies must detect discrete epitopes on the protein of interest so that they do not compete for the same binding sites. The detection antibody in this instance is biotinylated and will thus bind the streptavidin-HRP complex. Upon application of an appropriate substrate a colourimetric product is created. By using a range of standards of known concentration of the particular protein to be assayed, the concentration of the unknown samples can be determined (Delves et al., 2006; http://www.millipore.com/drugdiscovery/dd3/elisa_kits).

3.2.6.2 Protein extraction using CellLytic for examination by ELISA

For the ELISA assay, CellLytic™ (Sigma-Aldrich, U.K.), proprietary detergent of Sigma-Aldrich, was used to extract total cell protein from the cells, so as to determine the cell bound fractalkine as this solubilises proteins and can be used for such protein capture methods. Protein extraction requires efficient cell lysis and solubilisation of proteins, whilst preventing protein degradation and/or reagent interference with protein

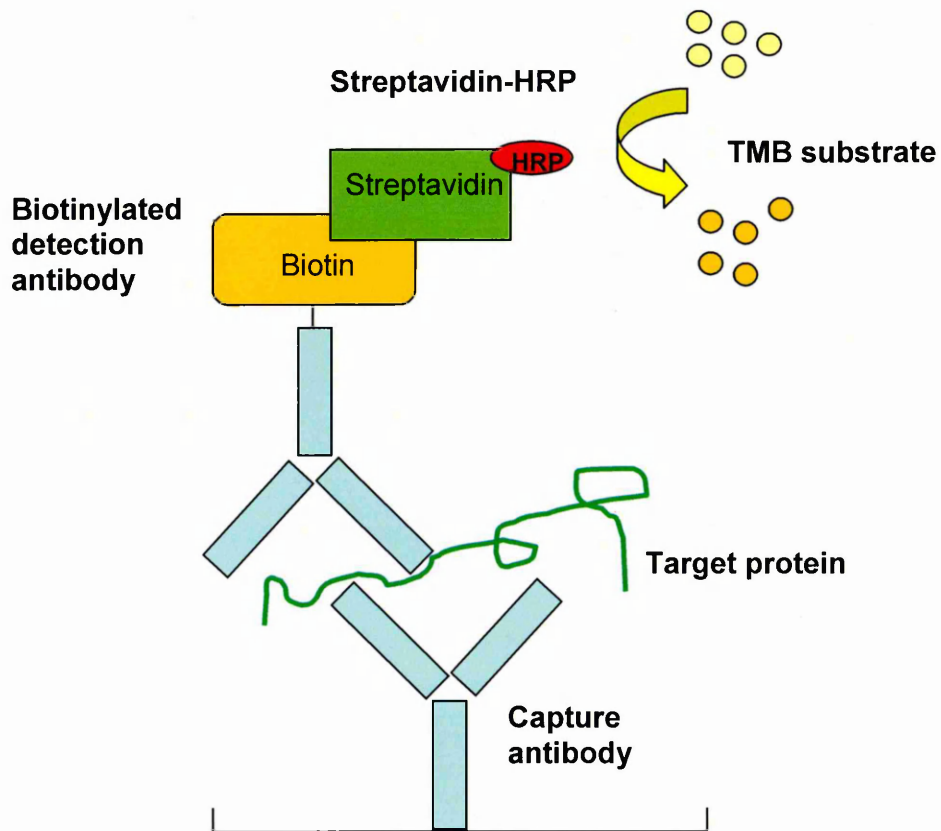


Figure 3.4: Sandwich ELISA. Capture antibodies bind the target protein, which is subsequently detected using a biotinylated detection antibody. Streptavidin-HRP (horseradish peroxidase) is applied and then upon the application of a substrate solution (tetramethyl benzidine (TMB)) a colorimetric product is created. The level of colour is an indicator of the quantity of target protein in the sample (image adapted from http://www.bendermedsystems.com/bm_images/29/high-sensitivity-figure-1.jpg and <http://www.cellsignal.com/ddt/elisa.html>).

immunoreactivity. Protease inhibitors can be added to lysis buffers, which inhibit a broad range of proteases and phosphatases; this prevents the action of endogenous enzymes that are capable of degrading proteins present in the extract. The protease inhibitor cocktail used in combination with CelLytic in this study included inhibitors of serine, cysteine and metalloproteinases (Sigma-Aldrich, U.K.) (see Table 3.4).

3.2.6.3 Experiment to determine cell-bound and shed fractalkine levels following 24 hour treatment with TNF

For the ELISA, cells were seeded at 5×10^5 cells/2.5ml/well of a collagen coated 6-well plate and treated as previously described with either serum-free medium or, TNF at 1, 10 or 100ng/ml. Each treatment was performed in triplicate. Following 24 hour treatment, the supernatant was collected, pulse centrifuged at 200 x g and stored at -20°C for subsequent analysis of secreted fractalkine by ELISA. Total protein from the cells was extracted using 450µl of CelLytic™ with 50µl protease inhibitor cocktail following the manufacturers' guidelines. Cells were washed twice with PBS and 500µl of lysis buffer was added. The plates were then placed on a rocking shaker at room temperature (RT) for 15 minutes. Following this, cells were scraped from the cell culture plate and the cell suspension collected in a microcentrifuge tube and centrifuged for 15 minutes at 13,400 x g. The protein containing supernatant was then transferred to a chilled tube and stored at -80°C until analysis by ELISA.

3.2.6.4 Time course study to examine the relationship between cell-bound and shed fractalkine under TNF treatment

To study the expression levels of fractalkine following 1 to 48 hours of TNF treatment, 2×10^5 cells/ml/well of a collagen coated 12-well plate were seeded in complete media. Cells were left for 24 hours, washed with PBS and then treated with serum-free media or serum-free media with 1, 10, or 100ng/ml TNF and left to incubate for 1, 6, 12, 24, or 48 hours. Following the appropriate incubation period, the cell supernatant was collected, centrifuged and the supernatant from this stored at -20°C until analysis by ELISA could be performed. The cells were washed twice with PBS, 225µl with 25µl protease inhibitors was added and the protein extracted as described above (see 3.2.5.3).

3.2.6.5 Fractalkine ELISA

Fractalkine in cell supernatants and extracts from cells was measured using a fractalkine DuoSet ELISA assay (R&D Systems, U.K.) (Figure 3.4). The DuoSet is designed to detect the chemokine domain of human fractalkine (N terminus). The assay was performed as recommended by the manufacturer. To prepare the 96 well

Table 3.4: Protease inhibitor cocktail composition used in combination with CellLytic for protein extraction.

Inhibitor	Type of protease	Example
AEBSF - [4-(2-Aminoethyl)benzenesulfonyl fluoride hydrochloride]	Serine	Trypsin, chymotrypsin, plasmin, kalikrein, thrombin
Aprotinin	Serine	Trypsin, chymotrypsin, plasmin, and kalikrein; human leukocyte elsatase, but not pancreatic elastase
Bestatin hydrochloride	Aminopeptidase	Leucine aminopeptidase and alanyl aminopeptidase
E-64 - [N-(trans-Epoxy succinyl)-L-leucine 4-guanidinobutylamide]	Cysteine	Calpain, papain, cathepsin B, and cathepsin L
EDTA	Metalloprotease	
Leupeptin hemisulphate salt	Serine and cysteine	Plasmin, trypsin, papain, and cathepsin B

plate for the ELISA assay, 100µl/well of the capture antibody (4µg/ml) was added, the plate sealed and left to incubate overnight at RT. The following day the unbound antibody was aspirated and the plate washed three times with PBS-Tween 20 (0.05%, PBS-T). After the final wash, the plate was inverted and blotted against a paper towel to ensure the removal of any remaining wash buffer. The plates were then blocked with 1% BSA in PBS for 1 hour at RT. After another wash step, 100µl/well of samples or standards were added in duplicate, the plate sealed and left to incubated at RT for 2 hours. Following another wash step, 100µl/well of the detection antibody (500ng/ml) was added, the plate sealed and left to incubate for 2 hours at RT. Following washing, 100µl/well of streptavidin-HRP was added, the plate sealed and left to incubate at RT for 20 minutes. After aspiration and washing, 100µl/well of substrate solution was added and left to incubate at RT for 20 minutes. To stop the reaction, 50µl/well of 2N H₂SO₄ was added and the plate gently shaken to ensure thorough mixing. The optical density of each well was read at 450 and 570nm in a Wallac Victor²_{TM} 1420 Multilabel Counter using Wallac 1420 software version 2.00 release 8. Absorbances at 570nm were subtracted from absorbance values at 450nm to correct for optical imperfections in the plate, which would affect the test optical density readings. Each standard and sample was assayed in duplicate and the mean value taken. Fractalkine concentrations were then calculated from a seven point standard curve (Figure 3.5) using 2-fold serial dilutions and a minimum standard of 0.625ng/ml and a maximum of 20ng/ml fractalkine. Fractalkine expression levels were calculated per mg of total cellular protein, which was determined using the BCA method (see section 3.2.5.3).

3.2.6.6 Statistical analysis of ELISA data

ELISA data was analysed using a parametric one-way ANOVA followed by Tukey multiple comparison test, so that comparisons could be made between the groups. Significance was set at $p < 0.05$ and the data are presented as mean \pm SEM for the indicated number of experiments.

3.2.7 SensolyteTM 520 TACE Activity Kit

3.2.7.1 Principles of the enzyme activity kit

The SensolyteTM 520 TACE activity kit consists of a QXLTM520/5-FAM FRET substrate whose sequence is derived from the cleavage site of TACE (LAQAVRSSSR) (Jin et al., 2002) (Figure 3.6). In its intact form, the peptides' 5-FAM fluorescence is quenched by QXLTM520, however, upon cleavage by active TACE, these two molecules separate resulting in an increase in 5-FAM fluorescence. Fluorescence can be measured at excitation/emission wavelength of 490nm/520nm, respectively.

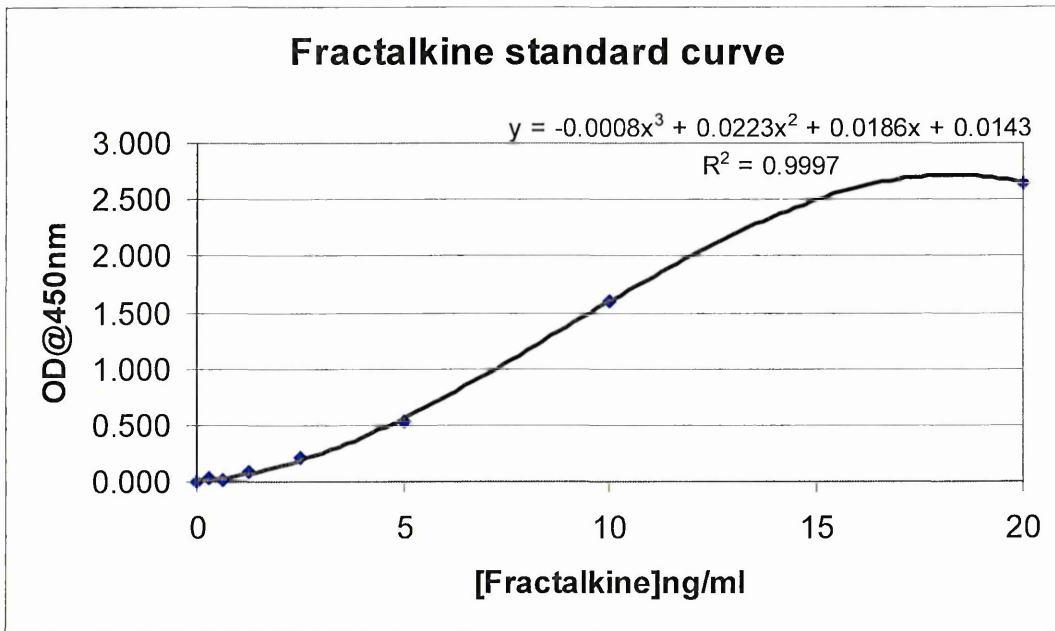


Figure 3.5: Representative standard curve used to determine the concentrations of fractalkine in cell lysates and supernatants from hCMEC/D3 cells.

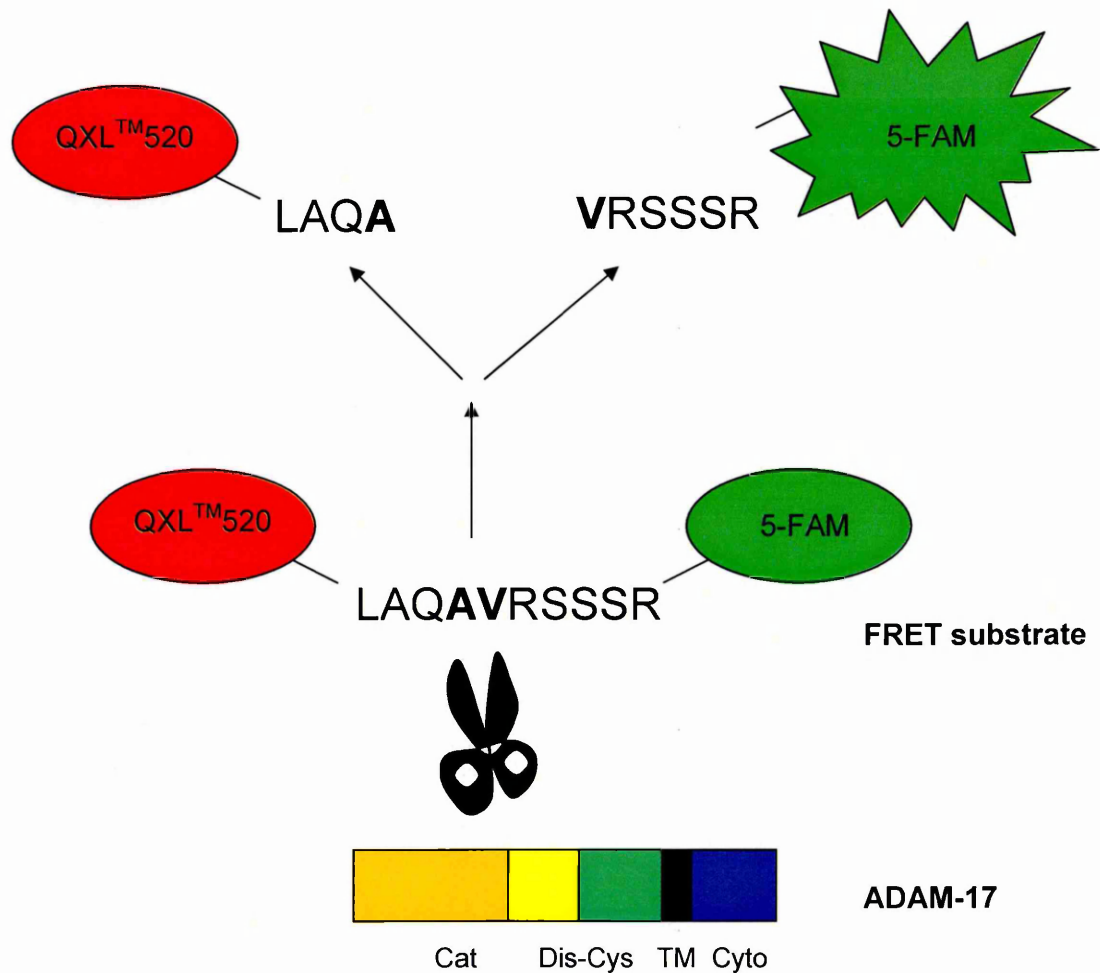


Figure 3.6: Schematic representation of the Sensolyte™ 520 TACE Activity Kit. The QXL™520/5-FAM FRET substrate, whose sequence is derived from the cleavage site of TACE, is cleaved by active ADAM-17 to release the 5-FAM molecule from the quenching QXL™520 molecule. Thus, enzyme activity in the sample is directly proportional to the level of fluorescence produced. Domains of ADAM-17: *Cat*, catalytic site; *Dis-Cys*, disintegrin-cysteine rich domain; *TM*, transmembrane domain; *Cyto*, cytoplasmic domain.

3.2.7.2 Protein extraction for determining the activity levels of TACE under pro-inflammatory conditions using SensoLyte™ TACE activity assay

To determine the levels of ADAM-17 enzyme activity in total cell lysates and membrane fractions of hCMEC/D3 cells, 5×10^5 cells /2ml/well of 6-well plate and 1.3×10^6 cells/6ml in a T25 flask, respectively, were seeded for 24 hours in complete media. After 24 hours, the media was aspirated and the cells washed twice with PBS. Cells were treated with either serum-free media or serum-free media supplemented with TNF at 1, 10, or 100ng/ml for 24 hours. After 24 hours treatment, total protein was extracted using assay buffer (AnaSpec, Inc., CA, USA) containing 0.1% Triton X-100 (Sigma-Aldrich, U.K.) and by scraping the cells from the culture plate. The cell suspension was collected in a microcentrifuge tube and placed on a shaker for 10 minutes at 4°C. Following this, the cell suspension was centrifuged for 10 minutes at 2,500 x g at 4°C and the supernatant collected and stored at -80°C until use. To extract protein from membrane fractions, the cells were washed twice with PBS and 1ml of ice cold PBS with 10% protease inhibitors (Sigma-Aldrich, U.K.) (Table 3.4) was added. Following 5 freeze-thaw cycles, the cells were scraped from the culture flask and centrifuged at 16,000 x g at 4°C for 20 minutes. The pelleted membranes were then washed with PBS, centrifuged at 16,000 x g at 4°C for 10 minutes and resuspended in assay buffer. Protein concentrations were determined using the BCA method (see section 3.2.5.3).

3.2.7.3 Enzyme activity assay to determine the activity levels of TACE in hCMEC/D3 cells under pro-inflammatory conditions

To determine the levels of ADAM-17 enzyme activity, 50µl of lysates or membrane fractions from cells, either treated with TNF at various concentrations or without, were added to a 96-well black plate (Fisher Scientific, U.K.). Following a 10 minute incubation at RT to allow the samples to equilibrate to RT, 50µl of substrate solution was added per well and the reagents were gently mixed for 30 seconds on a shaker. Following a 60 minute incubation step, the fluorescence intensity of each sample was measured at an excitation/emission wavelength of 490nm/520nm using a SpectraMax M5[®] using SoftPro version 5.2 (Molecular Devices, U.K.) (University of Sheffield). Each control and sample were assayed in duplicate and the mean value taken. Purified TACE (Millipore, U.K.) was used as a positive control. RFU levels were normalised against protein concentrations to take into account any differences in cell numbers between culture flasks.

3.2.7.4 Statistical analysis of enzyme activity data

Enzyme activity data was analysed using a parametric one-way ANOVA followed by Tukey's multiple comparison test. Comparisons were made between each of the

groups. In all instances, significance was set at $p < 0.05$ and the data are presented as mean \pm SEM for the indicated number of experiments.

3.3 Results

3.3.1 qRT-PCR analysis of mRNA expression following cytokine treatment of human adult brain endothelial cells, hCEMC/D3.

In order to understand the functional activity of ADAM-17 in endothelial cells, ADAM-17, TIMP-3 and a number of substrates of ADAM-17 (TNFR1, TNFR2, and fractalkine) were selected for testing mRNA expression levels in hCEMC/D3 cells, under different cytokine treatment regimes. vWF was selected as a marker for endothelial cells. To this end a number of cytokines known to be dysregulated in MS, and also to be produced by T cells and macrophages, which are stereotypical of the perivascular cuffs in MS pathology, were selected to determine which elicited the greatest effects. qRT-PCR analysis revealed that all genes examined, ADAM-17, TIMP-3, TNFR1, TNFR2, fractalkine and vWF were constitutively expressed in the human adult brain endothelial cell line, hCEMC/D3. Some of these genes were differentially expressed when cells were treated with TNF, IL-1 β , IFN- γ and TGF- β 1 at 1, 10 and 100ng/ml.

ADAM-17 mRNA expression increased, but not significantly upon cytokine treatment with TNF and TGF- β 1, but remained at control levels when treated with IL-1 β and IFN- γ ($p > 0.05$) ($n = 3$) (Figure 3.7 A). There was an apparent, but non-significant, increase in TIMP-3 mRNA expression when stimulated with TNF and IFN- γ , whereas it decreased non-significantly when cells were treated with IL-1 β and TGF- β 1 ($p > 0.05$) ($n = 3$) (Figure 3.7 B).

TNFR1 showed little fluctuation under any of the treatment conditions in comparison to the control. Treatment with IL-1 β at 100ng/ml, however, caused a small, but significant down-regulation by 14% (± 0.05 SEM) of TNFR1 mRNA compared to the control ($p < 0.05$) ($n = 3$) (Figure 3.7 C). TNFR2 mRNA expression was significantly up-regulated 3.6 fold (± 0.38 SEM) when cells were treated with TNF at 100ng/ml ($p < 0.05$) ($n = 3$). IFN- γ non-significantly increased TNFR2 mRNA expression, whereas IL-1 β and TGF- β 1 caused a non-significant down-regulation in mRNA expression at all concentrations (Figure 3.7 D). Fractalkine mRNA expression was significantly increased when cells were stimulated with TNF and IFN- γ at all concentrations ($p < 0.05$) ($n = 3$) (Figure 3.7 E). Means of 52.0 (± 3.69 SEM), 143.0 (± 49.43 SEM) and 170.8 (± 23.69 SEM) fold were detected at 1, 10 and 100ng/ml TNF, respectively. IFN- γ at 1, 10 and 100ng/ml caused fractalkine mRNA expression to increase to means of 6.3 (± 2.68 SEM), 17.5 (± 6.99 SEM) and 23.2 (± 5.76 SEM) fold, respectively (Figure 3.7 E). Fractalkine mRNA levels were unaffected by treatment with IL-1 β and TGF- β 1 ($p > 0.05$). vWF mRNA expression levels fluctuated slightly under cytokine treatment (Figure 3.7 F), however, none of these fluctuations reached significance ($p > 0.05$) ($n = 3$).

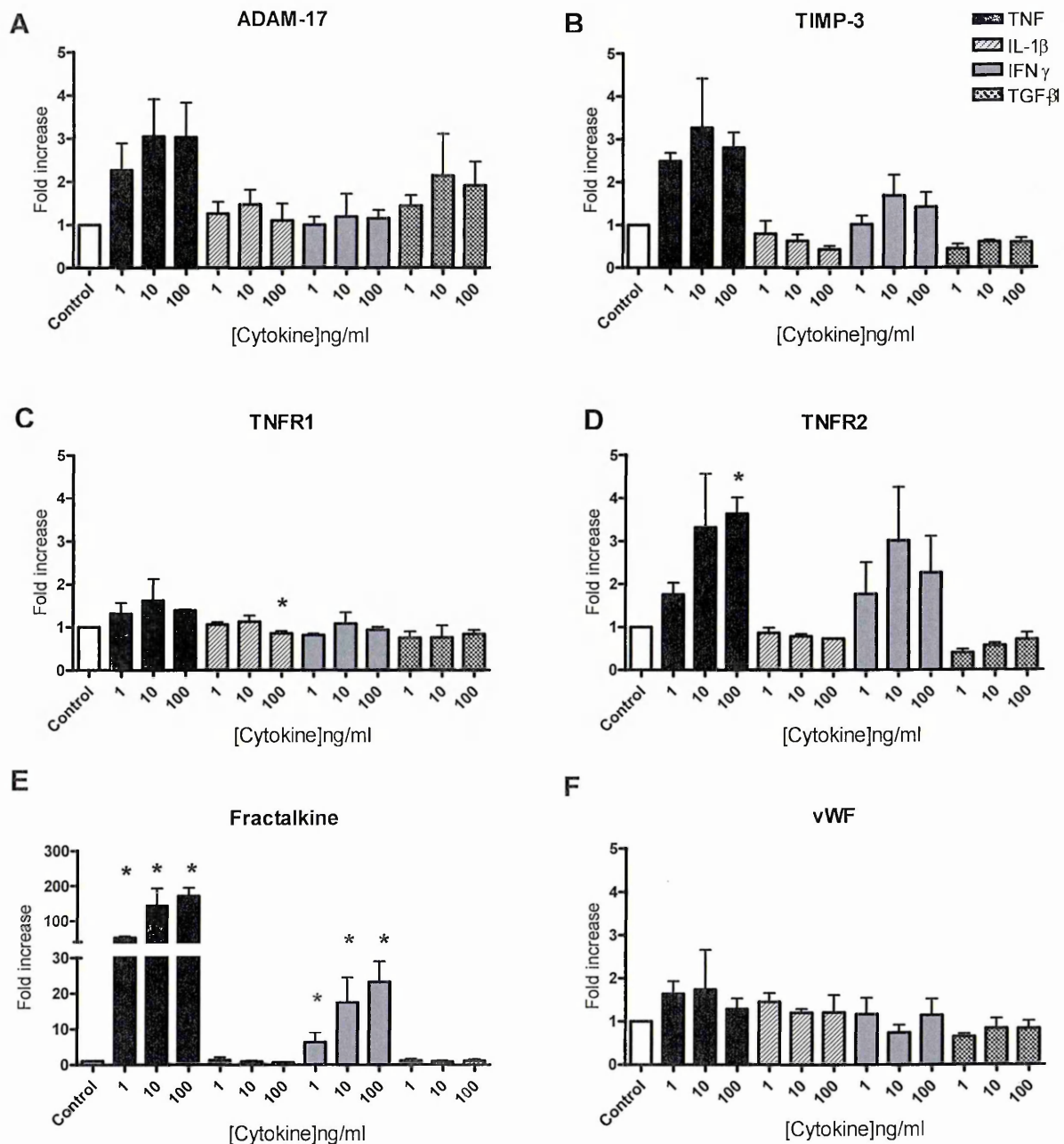


Figure 3.7: qRT-PCR analysis of ADAM-17 (A), TIMP-3 (B), TNFR1 (C), TNFR2 (D), fractalkine (E) and von Willebrand factor (vWF) (F) mRNA expression under control and inflammatory conditions in the human adult brain endothelial cell line, hCMEC/D3. Data are represented as the mean ($n = 3$) \pm SEM. Statistically significant differences are indicated by one (*) asterisks which denotes a significance of $p < 0.05$. Note scale of figure E.

In summary, TNF elicited the most prominent effects upon hCMEC/D3 cells causing an up-regulation in mRNA expression in the majority of genes studied, highlighting that the cells were more responsive to this cytokine. IFN- γ also elicited significant increases in mRNA expression in hCMEC/D3 cells whereas IL-1 β and TGF- β 1 were very limited in their effects upon the endothelial cell line and tended to cause a down-regulation in the expression of the genes of interest. In summary hCMEC/D3 cells are responsive to TNF > IFN- γ > IL-1 β > TGF- β 1 (Table 3.5).

3.3.2 Immunocytochemical detection of ADAM-17, TIMP-3 and fractalkine under control and stimulatory conditions

As treatment with TNF at 100ng/ml (Table 3.5) caused an increase in mRNA synthesis of some of the genes of interest in this study, particularly fractalkine, protein expression in cells after treatment with this concentration of TNF was assessed by ICC.

When cells were fixed with acetone, ADAM-17 was found to be located diffusely within the cell cytoplasm (Figure 3.8 i A-D). Under control conditions, ADAM-17 was also observed to cluster in perinuclear compartments which, upon TNF treatment (100ng/ml), appeared to disperse (compare Figure 3.8 i A and C with B and D). The intensity of ADAM-17 staining did not appear to alter under TNF treatment (Figure 3.8 i B and D), however, it did induce a filamentous distribution (arrows, Figure 3.8 i D). When the cells were fixed with 4% PFA, ADAM-17 expression was observed to occur in a pattern that resembled a cytoskeletal distribution (Figure 3.8 ii A-D). Upon TNF application the amount and pattern of expression did not alter (Figure 3.8 ii B and D).

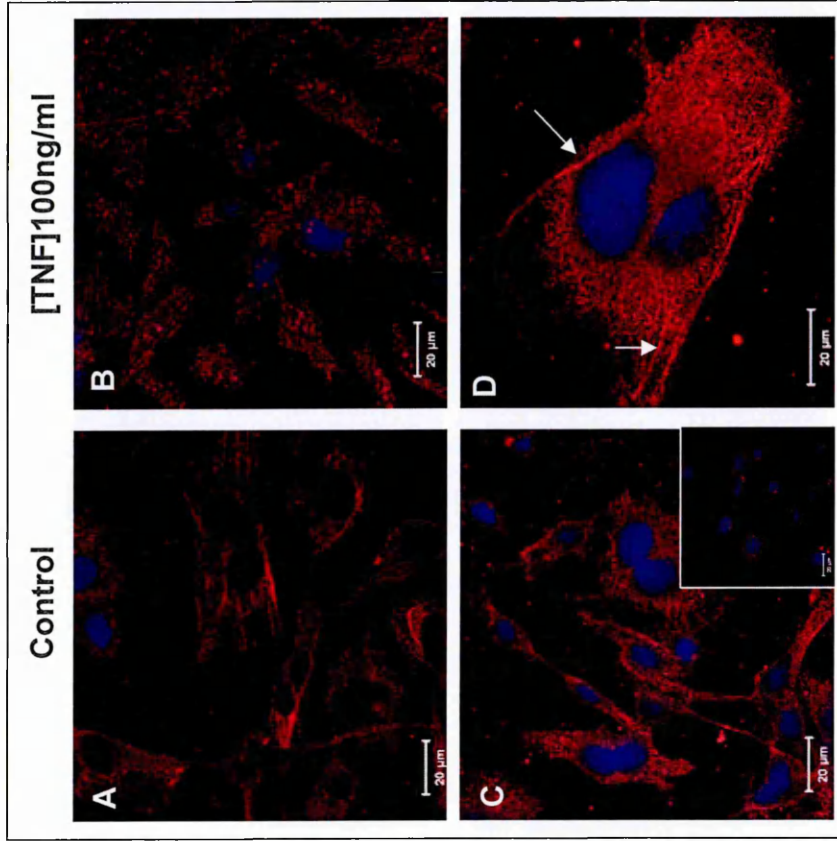
TIMP-3 expression appeared in a punctate pattern throughout the cell regardless of the fixative used to prepare the cells for ICC (Figure 3.9 i A-D and Figure 3.9 ii A-D). Upon TNF treatment, TIMP-3 showed no change in expression levels or in distribution (Figure 3.9 i B and D, and Figure 3.9 ii B and D).

Both acetone and PFA induced a diffuse fractalkine staining pattern within the endothelial cells, both under control and TNF conditions (Figure 3.10 i A-D and Figure 3.10 ii A-D). Following TNF treatment the expression levels of fractalkine increased greatly which was apparent after acetone fixation (Figure 3.10 i B and D), but not after PFA fixation (Figure 3.10 B and D). The background staining shown in Figure 3.10 i A-D and Figure 3.10 ii A-D could be due to shedding of fractalkine from the cells and its subsequent attachment to the chamber slide whilst in culture, which was then subsequently immunocytochemically stained, since there was no non-specific background seen when staining with the other antibodies, and also in the negative controls in the absence of the primary antibody.

Table 3.5: Tabular representation of Figure 3.5 showing the altered gene expression in hCMEC/D3 cells, under inflammatory conditions. Each gene is represented showing the cells response following the application of each cytokine for 24 hours. The responses are summarised as either increases (↑), decreases (↓) or no response (-) to the individual cytokine. Significant fluctuations are indicated by an asterisks (*).

	TNF	IL-1 β	IFN- γ	TGF- β 1
ADAM-17	↑	-	-	↑
TIMP-3	↑	↓	↑	↓
TNFR1	-	↓*	-	-
TNFR2	↑*	↓	↑	↓
Fractalkine	↑*	-	↑*	-
vWF	-	-	-	-

i. Acetone fixation



ii. 4% PFA fixation

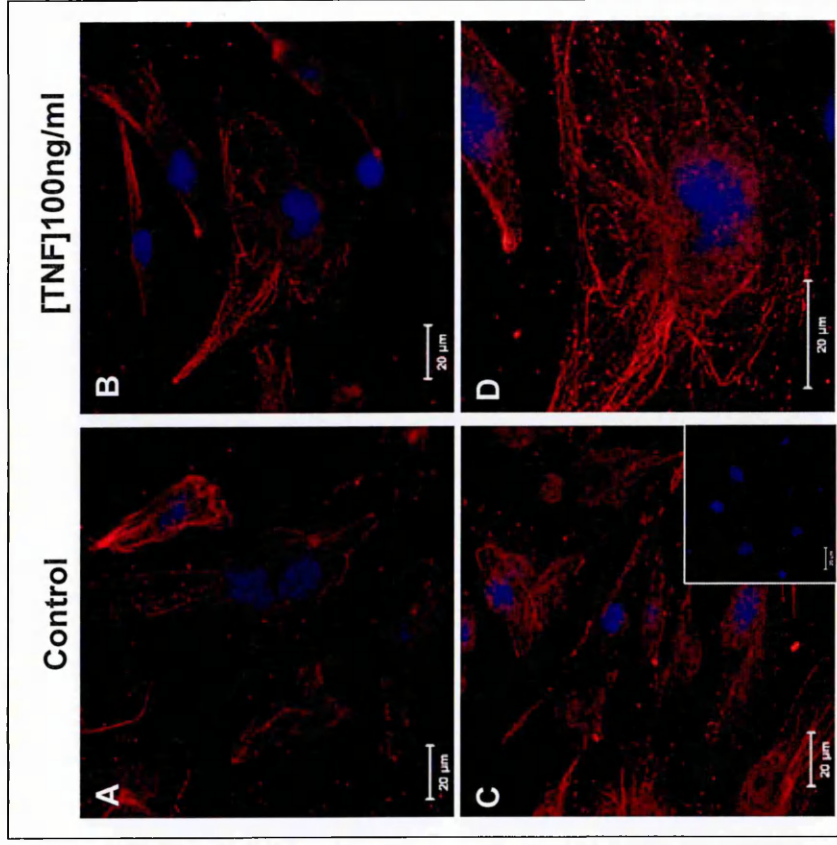
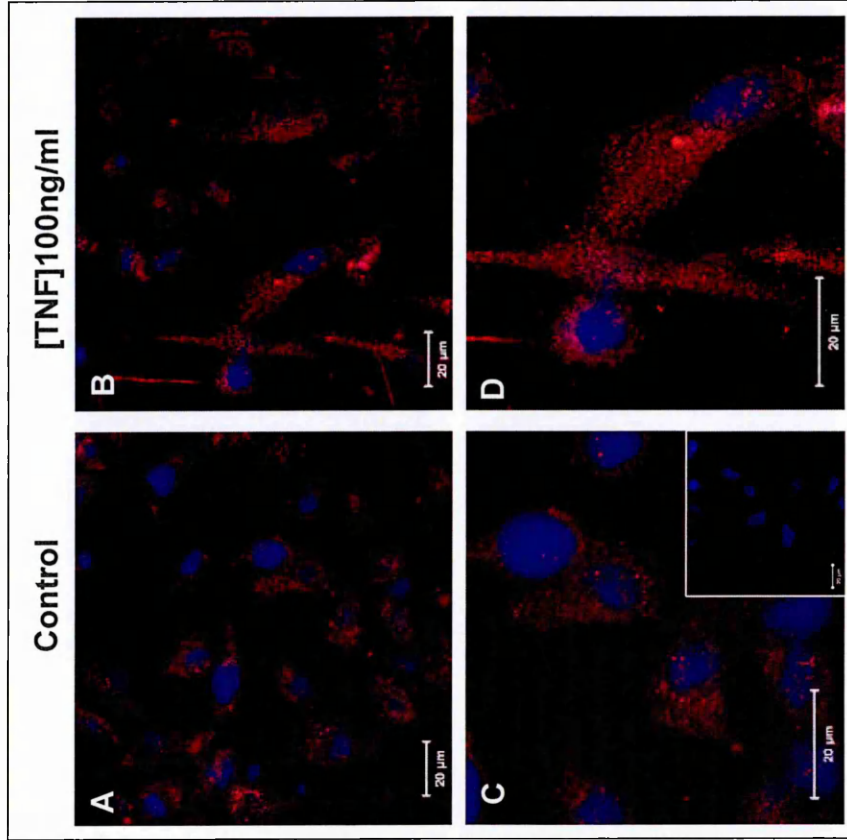


Figure 3.8: Immunocytochemical detection of ADAM-17 in hCMEC/D3 cells after fixation with ice cold acetone (i) or 4% paraformaldehyde (PFA) (ii) under control and TNF treatment conditions. ADAM-17 expression under control (A and C) and inflammatory (B and D) conditions in the human adult brain cell line, hCMEC/D3. Upon TNF treatment ADAM-17 expression demonstrated a filamentous distribution (D, arrows). Data are representative of three experiments. Omission of the primary antibody served as a negative control (insert in C). Scale bar is 20µm.

i. Acetone fixation



ii. 4% PFA fixation

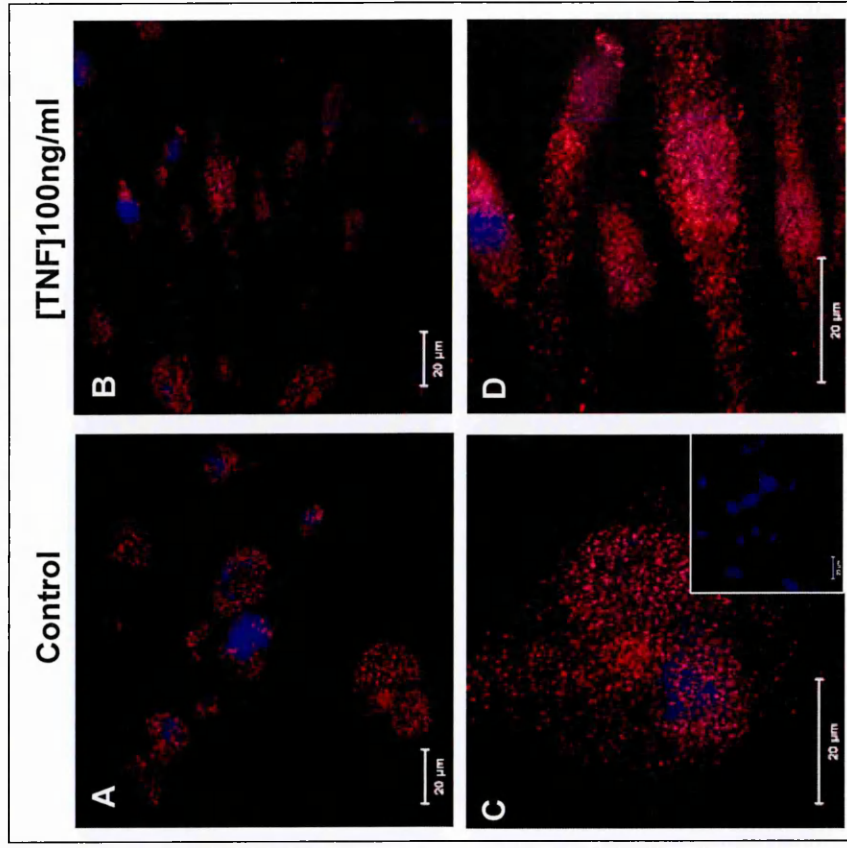


Figure 3.9: Immunocytochemical detection of TIMP-3 in hCMEC/D3 cells after fixation with ice cold acetone (i) and 4% paraformaldehyde (PFA) (ii) under control and TNF treatment conditions. TIMP-3 expression under control (A and C) and inflammatory (B and D) conditions in the human adult brain cell line, hCMEC/D3. Data are representative of three experiments. Omission of the primary antibody served as a negative control (insert in C). Scale bar is 20μm.

i. Acetone fixation

ii. 4% PFA fixation

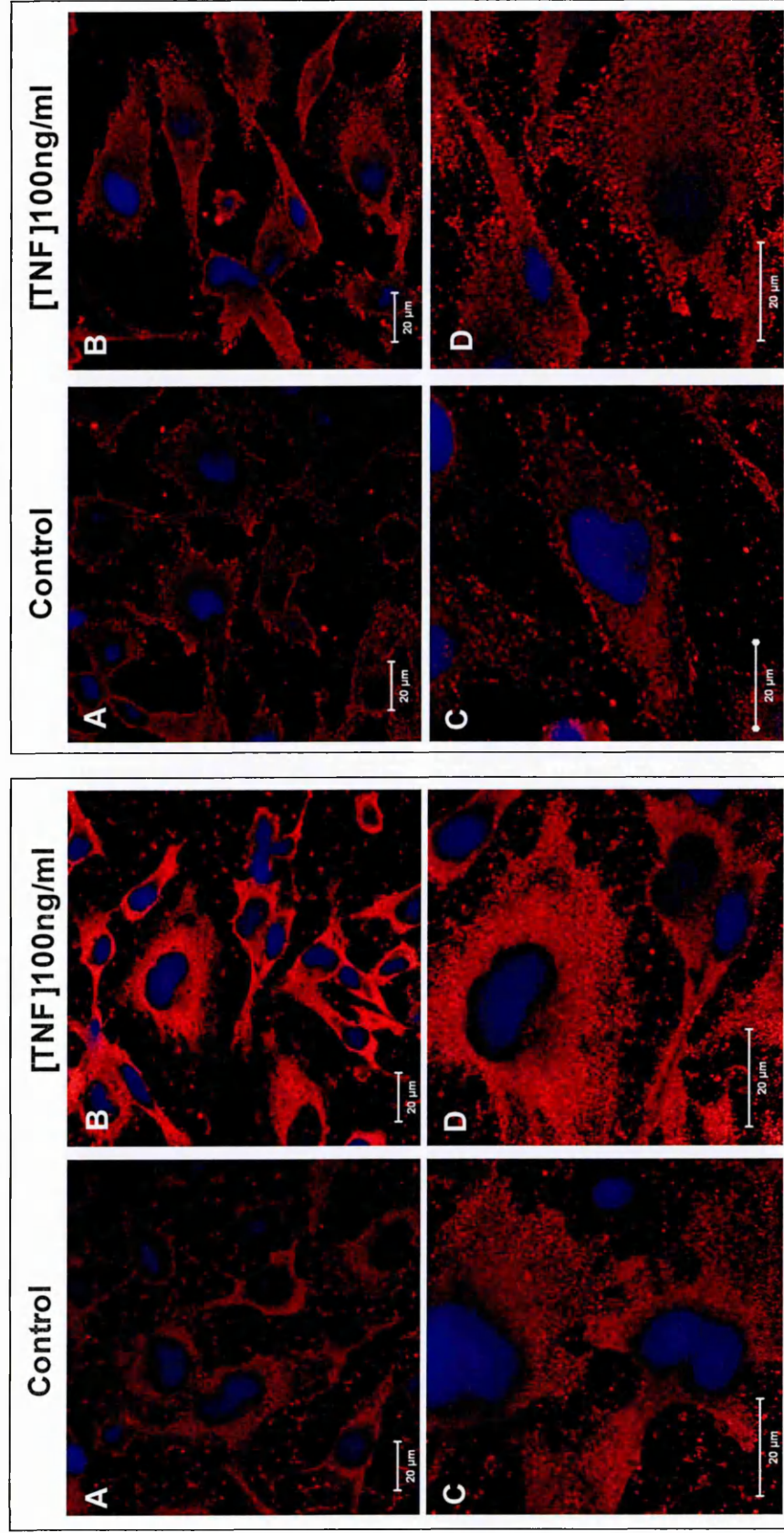


Figure 3.10: Immunocytochemical detection of fractalkine in hCMEC/D3 cells after fixation with ice cold acetone (i) and with 4% paraformaldehyde (PFA) (ii) under control and TNF treatment conditions. Fractalkine expression under control (A and C) and inflammatory (B and D) conditions in the human adult brain cell line, hCMEC/D3. Data are representative of three experiments. Omission of the primary antibody served as a negative control (see inserts in Figure 3.7Ci and ii). Scale bar is 20μm.

3.3.3 Determination of the ability of anti-actin antibody to distinguish between different protein concentrations on western blots

Western blot analysis of actin in protein extracted from hCMEC/D3 cells revealed that the antibody distinguished between the different concentrations of protein within the sample (Figure 3.11 and 3.12). When 0.75µg/ml of protein was loaded only a faint band appeared, and as the concentration of protein increased to 1.5 and 3µg/ml the band intensity also increased. Thus, this actin antibody was able to differentiate protein concentrations and was therefore used as a loading control for the western blotting analysis to confirm equal protein loading between sample lanes.

3.3.4 Selection of a suitable antibody for ADAM-17 detection by western blotting

To find a suitable antibody which would detect the pro- and mature forms of ADAM-17, various antibodies from different suppliers were tested (Table 3.2). However, most of the antibodies tested appeared to produce multiple or unexpected protein bands (Table 3.6). It was found that AB19027 was a suitable antibody for detecting the pro- and mature form of ADAM-17. However, as well as detecting the pro- and mature forms of the protein, a band of approximately 60kDa was also detected. To determine whether this was either specific or non-specific a blocking peptide was used. After incubation of the antibody with its cognate peptide and applying it to the membrane, the band of 60kDa remained visible, whereas the other two bands corresponding to the two forms of ADAM-17 disappeared (Figure 3.13). This antibody was thus used in the western blotting detection of ADAM-17, however, the band at 60 kDa was not included in the analysis. .

3.3.5 Western blot analysis of ADAM-17 expression by hCMEC/D3 cells following TNF treatment

Western blot analysis of ADAM-17 expression in hCMEC/D3 cells revealed bands at approximately 100 and 80kD (Figure 3.14), which correspond to the pro- and mature form of ADAM-17, respectively (Moss et al., 1997; Schlondorff et al., 2000; Peiretti et al., 2003). Both these bands disappeared when the antibody was incubated with its cognate blocking peptide or when the primary antibody was omitted, demonstrating that the staining for ADAM-17 was specific. Densitometric analysis of the two forms of ADAM-17, independently or combined, showed no significant increase in the pro-form (Figure 3.15 A), mature form (Figure 3.15 B) or both isoforms (Figure 3.15 C) of ADAM-17 with increasing cytokine concentration, although there was a trend to suggest that protein levels increase at 100ng/ml TNF (Figure 3.15) ($p > 0.05$).

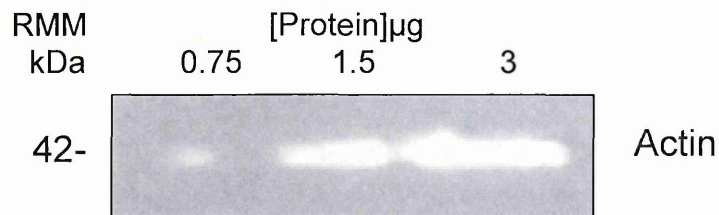


Figure 3.11: Determination of the sensitivity of the anti-actin antibody to distinguish different protein concentrations on western blots. Total cell protein from human adult brain endothelial cells, hCMEC/D3, was loaded at three different amounts and separated by SDS-PAGE, and the membrane probed with a rabbit polyclonal antibody against actin. An increase in band intensity can be seen with increasing concentrations of protein.

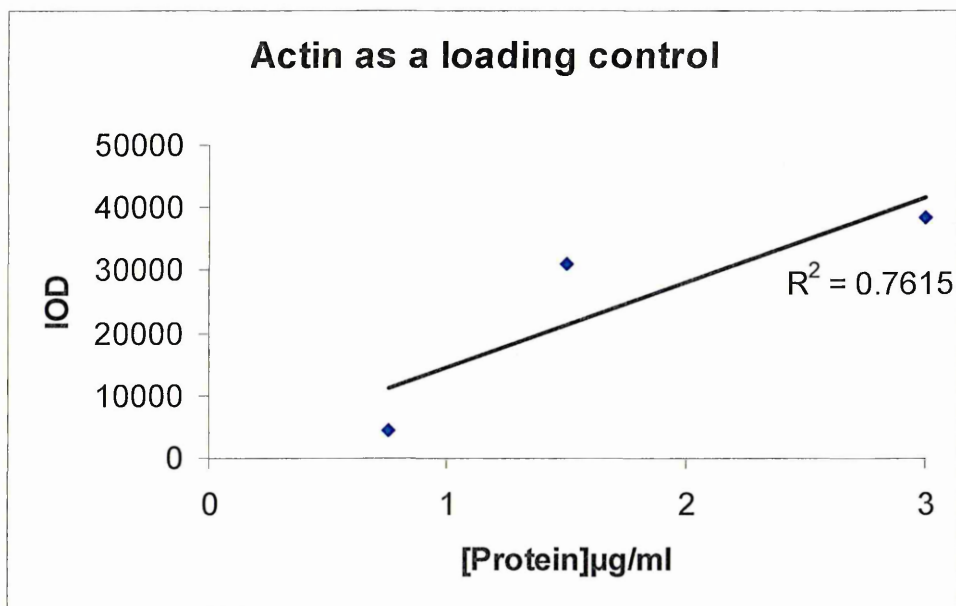


Figure 3.12: Semi-quantitation of actin at three different protein concentrations. Different amounts of total protein from hCMEC/D3 cells were separated by SDS-PAGE, following western blotting for actin using a polyclonal antibody the integrated optical density was calculated (IOD).

Table 3.6: Antibodies tested to determine ADAM-17 expression in hCMEC/D3 cells using western blotting.

Antibody Cat No.	Company	Antibody type and Species	Dilution	Expected bands (kDa)	Outcome (kDa)
Ab39162	Abcam	Polyclonal (rabbit)	various	93-110	Multiple 60-100
MAB9302	R&D Systems	Monoclonal (mouse)	various	ectodomain	40-60
T-5442	Sigma	Polyclonal (rabbit)	various	80-130	80, 100 and 191
AB19027	Chemicon	Polyclonal (rabbit)	various	80-130	60, 80 and 100

NB: Each antibody was individually tested at a range of concentrations (see section 3.2.5.5).

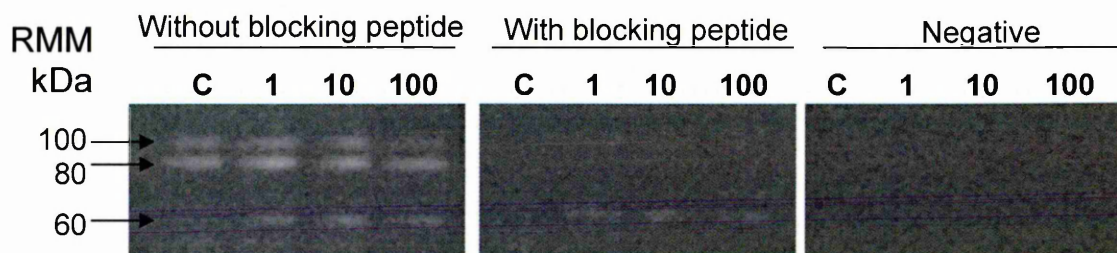


Figure 3.13: Specificity of AB19027 at detecting the pro-form and mature form of ADAM-17 in hCMEC/D3 cells. In the absence of the blocking peptide the antibody detected three bands at 60, 80 and 100kDa. However, when the antibody was incubated with its cognate blocking peptide prior to application to the blotting membrane, the two bands at 80 and 100kDa disappear whereas the 60kDa band is still apparent. Thus, detection of the higher molecular mass proteins are specific, whereas the lower band represents non-specific binding. A negative control was also included to show there was no non-specific binding of the secondary antibody. Total protein was extracted from cells under control (C) and TNF treatment at 1 (1), 10 (10), and 100ng/ml (100).

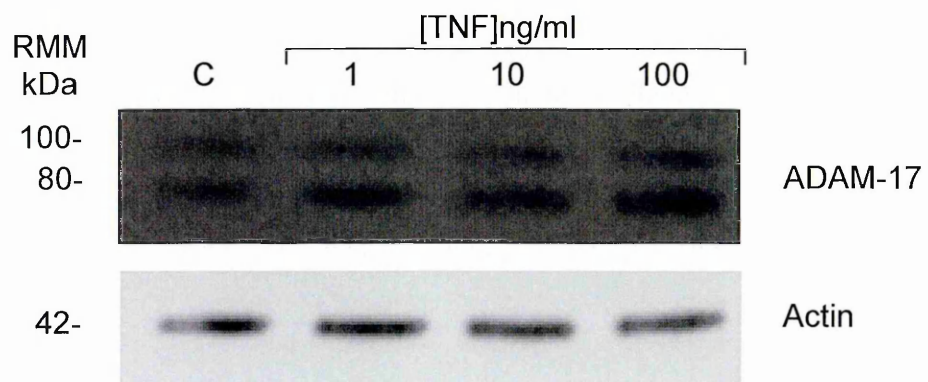


Figure 3.14: Western blot analysis of ADAM-17 expression in hCMEC/D3 cells under control and TNF treatment. Both the pro-form (100kD) and the mature form of ADAM-17 (80kD) can be seen. Actin was used as a loading control. Data are representative of three replicate experiments.

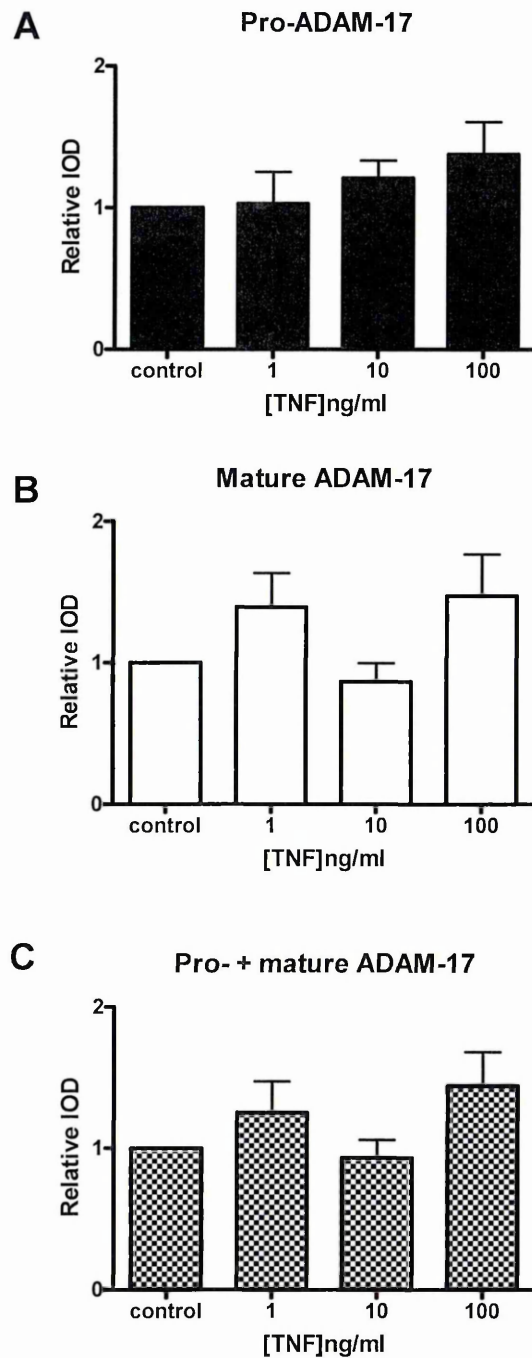


Figure 3.15: Densitometric analysis of western blot of pro-ADAM-17 (A), mature ADAM-17 (B) and both pro- and mature ADAM-17 (C) expression in hCMEC/D3 cells under control and TNF treatment. The integrated optical density (IOD) of each band was normalised to actin and then to their respective controls. Data are represented as the mean of individual blots from three separate experiments ($n = 3$) \pm SEM. No significant difference was observed between cells under control conditions and those treated with TNF, at all concentrations.

3.3.6 Relationship between cell-bound and shed fractalkine in endothelial cells in the presence or absence of TNF, as determined by ELISA

With increasing concentrations of TNF, the amount of cell associated fractalkine increased in hCMEC/D3 cells, measured in cell extracts by ELISA. Under control conditions a mean of 23.7ng fractalkine/mg total cell protein was detected in the cell lysates ($n = 3$) (Figure 3.16 A). This was not significantly different from cells treated with 1ng/ml TNF ($p > 0.05$). However, when cells were treated with 10 or 100ng/ml TNF, significant increases were observed with mean values of 73.5 ($p < 0.001$) and 78.3 ($p < 0.001$) ng fractalkine/mg total cell protein, respectively ($n = 3$). Significant differences were also observed between cells treated with 1ng/ml of TNF and cells treated with 10 and 100ng/ml TNF ($p < 0.001$). No significant difference was observed between cells treated with 10 and 100ng/ml TNF ($p > 0.05$) (Figure 3.16 A).

The amount of fractalkine shed into the supernatant by cells also increased with increasing concentrations of TNF (Figure 3.16 B). Under control conditions, fractalkine levels were below the detection limit of the assay. Treatment with 1, 10, or 100ng/ml TNF caused significant levels of fractalkine to be shed; mean values of 210.4 ($p < 0.05$), 472.2 ($p < 0.001$), and 775.7 ($p < 0.001$) ng fractalkine/mg total cell protein were detected, respectively ($n = 3$). Significant differences were also observed between cells treated with TNF at 1ng/ml and cells treated with 10ng/ml ($p < 0.05$) and 100ng/ml ($p < 0.001$) of TNF. A significant difference was also observed between cells treated with 10 and 100ng/ml of TNF ($p < 0.01$).

The ratio of cell associated to shed fractalkine was calculated. Under control conditions the mean ratio of cell associated to shed fractalkine was 1:0. Treatment with TNF at 1, 10, or 100ng/ml caused significant increases in this ratio to 1:5.8 ($p < 0.01$), 1:6.4 ($p < 0.01$), and 1:9.9 ($p < 0.001$), respectively. No significant difference was observed between cells treated with 1 and 10ng/ml TNF ($p > 0.05$), however there was a significant difference between cells treated with 1 and 100ng/ml TNF ($p < 0.05$). No significant differences were observed between cells treated with 10 and 100ng/ml TNF ($p > 0.05$).

3.3.7 Time course study to determine the relationship between cell-associated and shed fractalkine following TNF treatment in hCMEC/D3 cells

Following TNF treatment over the different time periods the levels of cell-associated and shed fractalkine showed a trend to increase with increasing concentrations of the cytokine. After 1 hour treatment with TNF at 1, 10, 100ng/ml, 23.5, 43.1 and 47.2ng fractalkine/mg protein were detected in cell lysates, compared to 30.2ng fractalkine/mg protein under control conditions; there was a slight decrease in the amount of cell-

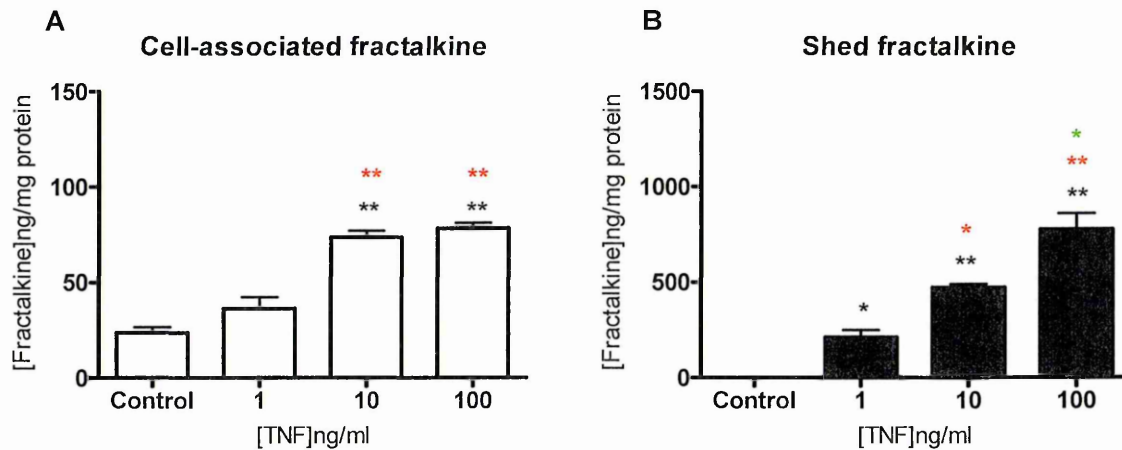


Figure 3.16: Enzyme-linked immunosorbant assay (ELISA) determination of fractalkine expression by hCMEC/D3 cells under control and TNF treatment. Cell associated (A) and shed (B) fractalkine data are represented as the mean ($n = 3$) \pm SEM. To analyse significant differences between the groups data were analysed by ANOVA followed by a Tukey post-hoc test. Statistically significant differences are indicated by one (*) or two (**) asterisks where the former denotes significance of $p < 0.05$ and 0.01, and the latter significance of $p < 0.001$ compared to control conditions. The black asterisks indicate differences between the controls, the red indicate differences between groups and treatment with 1ng/ml of TNF, and the green asterisk differences between groups and treatment with 10ng/ml of TNF. Note the scale difference between the figures.

associated fractalkine in comparison to the control after 1 hour treatment with 1ng/ml TNF (Figure 3.17). Significant differences were detected between cell lysates from cells treated with 1 and 100ng/ml TNF ($p < 0.05$). At this same time point, 17.2ng fractalkine/mg protein was detected in cell supernatants from the same cell cultures. These levels increased to 48.6, 74.8, and 93.3ng fractalkine/mg protein following treatment with TNF at 1, 10 and 100ng/ml of TNF, respectively (Figure 3.17). Significant differences were detected between cells under control conditions and cells treated with 10 ($p < 0.01$) and 100ng/ml ($p < 0.001$), and between cells treated with 1 and 100ng/ml TNF ($p < 0.05$).

Following 6 hours treatment with TNF, cell lysates from cells under control conditions expressed 22.0ng fractalkine/mg protein, which increased to 34.7, 45.1, and 78.7ng fractalkine/mg protein following treatment with 1, 10, and 100ng/ml TNF, respectively (Figure 3.17). The amount of fractalkine shed into supernatants at this time point under control conditions was below the detectable limit of the assay as too were the levels after treatment with TNF at 1ng/ml; however, following 6 hours treatment with TNF at 10 and 100ng/ml 105.5 and 185.9ng fractalkine/mg protein were detected, respectively (Figure 3.17). Both the cell associated and shed fractalkine showed the same pattern of statistically significant differences: levels of fractalkine under control conditions significantly differed from cells treated with TNF at 10 ($p < 0.01$) and 100ng/ml ($p < 0.001$); in addition, cell associated and shed fractalkine in cells treated with 100ng/ml TNF was significantly higher than cells treated with 1ng/ml TNF ($p < 0.001$); and in cells treated with 100ng/ml TNF significantly more fractalkine was detected in comparison to cells treated with 10ng/ml TNF ($p < 0.05$). In addition to these differences, the amount of shed fractalkine was significantly higher in cells treated with TNF at 10ng/ml in comparison to cells treated with 1ng/ml ($p < 0.01$).

Due to an experimental error, the data for the 12 hour treatment group was not analysed.

Following 24 hour treatment with TNF, 19.4ng fractalkine/mg protein were detected in cell lysates under control conditions, which increased to 24.2, 54.9 and 76.6ng fractalkine/mg protein following treatment with 1, 10 and 100ng/ml of TNF, respectively (Figure 3.17). The amount of shed fractalkine in cell supernatants after 24 hours TNF treatment was below the detectable limit of the assay under control conditions, but was detected at 47.7, 194.3 and 325.5ng fractalkine/mg protein following treatment with 1, 10 and 100ng/ml of TNF, respectively (Figure 3.17). Again the same patterns of significant difference were observed in cell associated and shed fractalkine at this time point: cells treated with 10 and 100ng/ml TNF showed significantly higher levels of fractalkine in comparison to control conditions (both $p <$

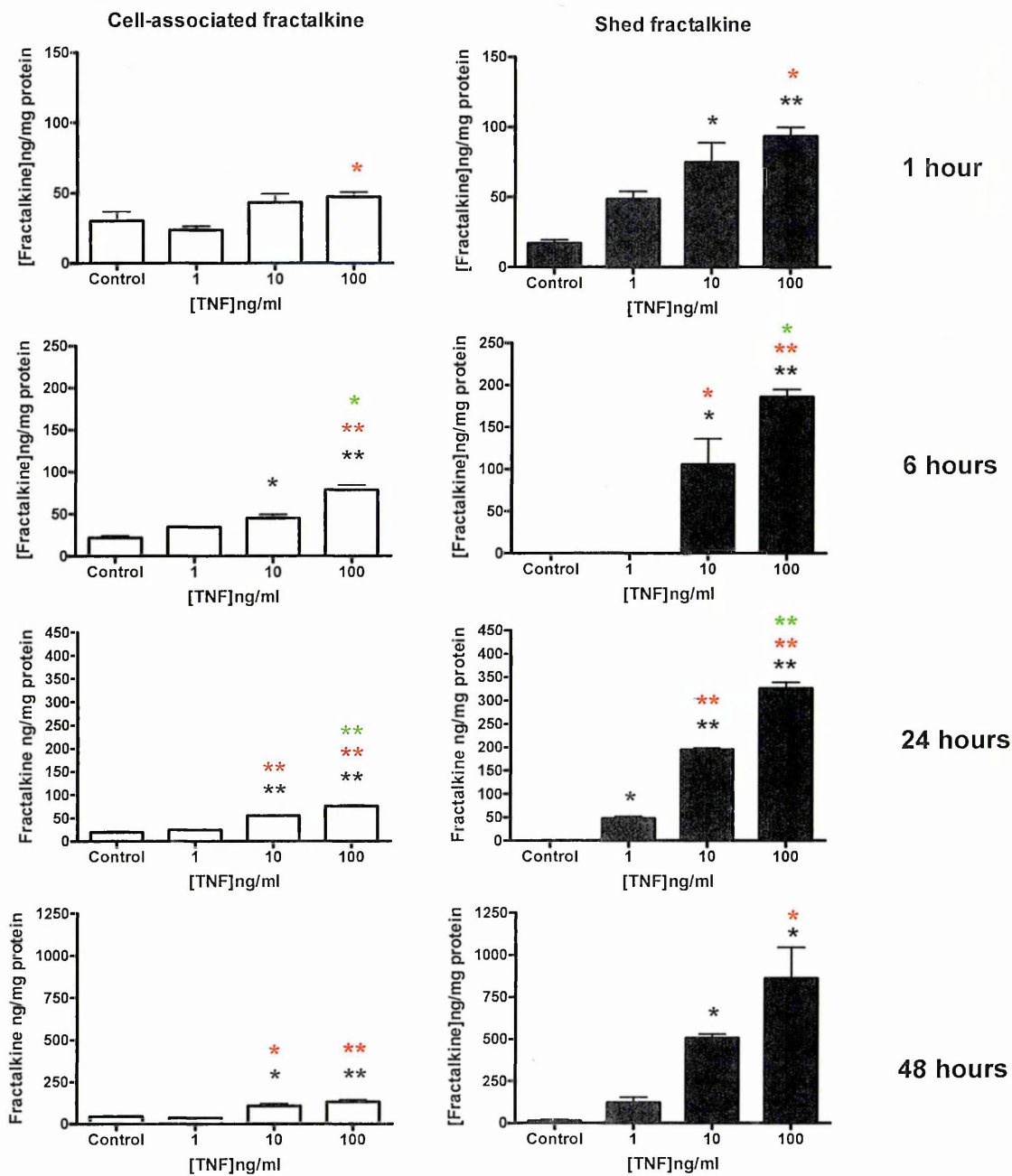


Figure 3.17: Time course study of the effects of TNF on cell bound and shed fractalkine in hCMEC/D3 cells. Cells were cultured for 1hr, 6hr, 12hr, 24hr and 48hr with TNF at various concentrations. Following this period the cell supernatant was harvested and the total cell protein extracted, and both were subjected to a fractalkine ELISA assay. Results from the 12 hour time course are absent due to an experimental error. Data are represented as the mean ($n = 3$) \pm SEM. Statistically significant differences are indicated by one (*) or two (**) asterisks, where the former denotes significance of $p < 0.05$ or 0.01 , and the latter significance of $p < 0.001$ compared to control conditions. Note the scale difference between graphs.

0.001) and treatment with TNF at 1ng/ml (both $p < 0.001$); and significant differences were also detected between cells treated with TNF at 10 and 100ng/ml (both $p < 0.001$). In addition, significantly higher levels of fractalkine were detected in cell supernatants in cells treated with TNF at 1ng/ml in comparison to control conditions ($p < 0.01$).

After 48 hours under control conditions 44.7ng fractalkine/mg protein were detected in cell lysates. Following 48 hour treatment with TNF at 1, 10, and 100ng/ml, 36.2, 107.2, and 130.4ng fractalkine/mg protein were detected in the cell lysates, respectively (Figure 3.17). In comparison to cells under control conditions, the levels of fractalkine, which were cell associated, was significantly increased after 48 hours treatment with TNF at 10 ($p < 0.01$) and 100ng/ml ($p < 0.001$); this trend in significance levels was also observed in comparison to cells treated with TNF at 1ng/ml. The amount of fractalkine detected in the cell supernatant under control conditions was low at 15.6ng/mg protein, however following TNF treatment with 1, 10, and 100ng/ml of TNF, this rose to 121.0, 505.8, and 860.1ng fractalkine/mg protein, respectively (Figure 3.17). Significant differences in the amount of shed fractalkine were observed in comparison to the control and cells treated with 10 ($p < 0.05$) and 100ng/ml TNF ($p < 0.01$), and also between cells treated with 1 and 100ng/ml TNF ($p < 0.01$).

3.3.8 Determining ADAM-17 activity in hCMEC/D3 cells following TNF treatment

ADAM-17 activity was determined in membrane fractions and total cell lysates from human adult brain endothelial cells treated with TNF at various concentrations for 24 hours using a FRET assay. Purified ADAM-17 served as a positive control and the lysis buffer as a negative/background control. Under control conditions 14.5 RFU/ μ g protein was observed in cell membrane fractions (Figure 3.18 A). After treatment with TNF at 1, 10, and 100ng/ml the activity levels of ADAM-17 in membrane fractions decreased non-significantly to 11.5, 11.6 and 11.8 RFU/ μ g protein, respectively, in comparison to cells under control conditions ($p > 0.05$) (Figure 3.8 A). This decrease in enzyme activity was also observed in total cell lysates, where an RFU of 58.6 was observed under control conditions, which decreased non-significantly in comparison to the control to 52.9, 46.4, and 52.3 upon treatment with TNF at 1, 10 and 100ng/ml, respectively ($p > 0.05$) (Figure 3.18 B). Any differences in cell numbers were accounted for by correcting values for activity by total cellular protein and could not be responsible for the decrease in ADAM-17 activity.

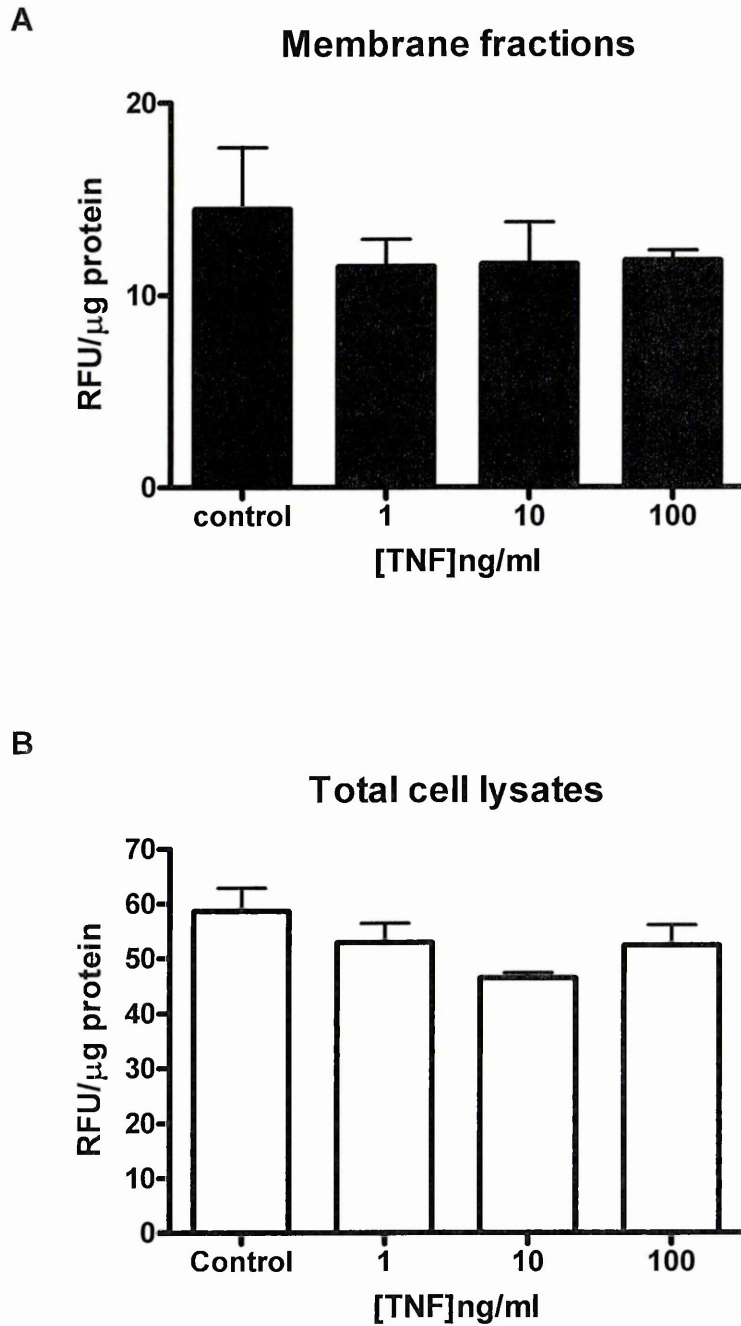


Figure 3.18: ADAM-17 enzyme activity in hCMEC/D3 cells under control and TNF treatment. Membrane fractions (A) and total cell lysates (B) show a non-significant decrease in ADAM-17 enzyme activity under TNF treatment when compared to control conditions ($p > 0.05$).

3.4 Discussion

In this present study, qRT-PCR revealed that ADAM-17, TIMP-3, TNFR1, TNFR2, fractalkine and vWF were all constitutively expressed in the human adult brain endothelial cell line, hCMEC/D3. Under inflammatory conditions, each gene showed differential expression, however, TNF elicited the greatest response on three of the genes of interest, namely ADAM-17, TIMP-3 and fractalkine, the latter being substantially and significantly up-regulated under these conditions. Thus, further analysis at the translational level was restricted to these genes and this cytokine. ADAM-17 mRNA and protein expression increased upon TNF treatment, as detected by qRT-PCR and western blotting, respectively, however neither of these increases reached significance. Another group has reported an increase in ADAM-17 at the mRNA level using Northern blot analysis and also at the protein level using western blot analysis following 24 hour TNF treatment (10ng/ml) in murine brain endothelial cells (Bzowska et al., 2004). Conversely, Majka et al. (2002) did not observe an increase in ADAM-17 mRNA in murine retinal endothelial cells following 24 hour TNF treatment (1ng/ml) as analysed by RT-PCR. The immunocytochemical analysis of ADAM-17 under control and TNF conditions revealed a cytoplasmic staining which was diffuse after acetone fixation and cytoskeletal after PFA fixation. Previous reports have reported that ADAM-17 is localised within perinuclear compartments in COS-7 cells (Schlöndorff et al., 2000), but it also associates with actin in cardiomyoblast cells (Canault et al., 2006), which is in agreement with the present findings after acetone and PFA fixation, respectively. ADAM-17 has also been reported to associate with, and carry out its shedding activities, in lipid rafts (Tellier et al., 2006). Further assessment of hCMEC/D3 cells using dual labeling for ADAM-17 and antibodies against lipid rafts (e.g. Flotillin, a lipid raft-associated protein) could be performed to ascertain if this association exists in hCMEC/D3 cells.

TIMP-3 mRNA levels increased, but the protein levels did not change after TNF treatment, as shown by qRT-PCR and immunocytochemistry, respectively. Another study has reported a decrease in TIMP-3 mRNA and protein expression in endothelial cells upon cytokine treatment (Singh et al., 2005). However, this study used different treatment periods and different combinations of cytokines. Singh and colleagues used a cardiac endothelial cell line, which was co-treated with TNF (10ng/ml) and IL-1 β (10ng/ml). qRT-PCR analysis after 8 and 24 hours treatment revealed that TIMP-3 expression was down-regulated under these conditions. However, they did not study the effects of single cytokine treatment. An antagonistic relationship has been demonstrated between TNF and IFN- γ in endothelial cells, whereby the latter can depress the effects of the former when administered together (Hillyer et al., 2003). *In vivo* studies from this laboratory have also reported a down-regulation of TIMP-3

mRNA in peak EAE rat spinal cord white matter (Plumb et al., 2005). In this thesis, TIMP-3 expression in endothelial cells alone was examined whereas *in vivo* other cells types, including neurons and astrocytes, contribute to TIMP-3 expression levels (Jaworski and Fager, 2000; Vaillant et al., 1999). Despite this, it does not appear as though the increase in TIMP-3 mRNA and protein has had a significant inhibitory influence on the shedding activities of ADAM-17 or other sheddases, as evidenced by the shedding of fractalkine following TNF treatment.

TNF caused a significant increase in fractalkine mRNA and protein expression, and a significant increase in shedding from endothelial cells. It has been well documented that fractalkine expression increases in endothelial cells that are treated with inflammatory cytokines (Garcia et al., 2000; Imaizumi et al., 2004; Moon et al., 2006). Moon et al. (2006) demonstrated significant increases in mRNA and protein expression of fractalkine in HUVECs when treated with TNF (10ng/ml). An induction of membrane-bound fractalkine, as determined by western blotting, has also been observed in rat aortic endothelial cells after TNF treatment, which was found to be dependent upon the transcription factor, NF- κ B. However, shed fractalkine was not detected in the supernatant of these cultures (Garcia et al., 2000). Cell-associated fractalkine was observed in this present study without cytokine treatment, and was increased by the application of TNF and also significant increases in the amount shed into the supernatant under TNF treatment was observed. These discrepancies between this present study and that of Garcia and colleagues (2000) could be due to the different systems used to detect fractalkine at the protein level, i.e. western blotting versus an ELISA assay. The immunocytochemical detection of fractalkine in hCMEC/D3 cells, revealed a vesicular and cytoplasmic staining under control conditions, which was increased upon TNF treatment. Previous studies have shown that fractalkine inhabits two distinct compartments in human bladder carcinoma cells (ECV) cells: diffusely on the plasma membrane and in a punctate perinuclear compartment (Liu et al., 2005). The cell surface expression of fractalkine could not be achieved by ICC methods in this present study, however the punctate pattern of distribution was witnessed when cells were fixed with acetone.

ADAM-17 has been shown to be responsible for the induced shedding of fractalkine from the cell membrane of ECVs, HUVECs and murine fibroblast cells (Garton et al., 2001; Tsou et al., 2001), which can be accounted for by an accompanying increase in ADAM-17 enzymatic activity that occurred under stimulatory conditions (Doedens et al., 2003). A peptide-cleavage assay revealed that under basal conditions enzymes other than ADAM-17 were responsible for processing of a TNF processing-site peptide (DNP-SPLAQAVRSSSR-amide), a similar peptide was used in this thesis to determine ADAM-17 enzyme activity. However, upon stimulation with

PMA an increase in peptide cleavage, that was ADAM-17-dependent, was observed (Doedens et al., 2003). The authors proved that ADAM-17 was responsible for this increase in peptide cleavage in a number of ways. Firstly, they utilized an immortalized mouse monocytic cell line which had a deletion for the Zn⁺⁺-binding site in the catalytic domain of ADAM-17. This mutation had no effect on the cleavage rate in untreated cells, and treatment with PMA did not increase the generation of the cleavage product. Thus, the authors deduced that the PMA-induced activity must be ADAM-17-dependent. They also deduced from their work that peptide processing can be divided into two components: non-ADAM-17-dependent basal activity and PMA-induced activity that is ADAM-17-dependent. Secondly, treatment of ADAM-17 expressing cells with hydroxamate IC-3, a metalloprotease inhibitor that inhibits ADAM-17, slightly reduced the production of the peptide-cleavage product under basal conditions. However, under PMA treatment, IC-3 completely blocked the production of the peptide-cleavage product. Thirdly, the addition of TIMP-1 which inhibits most MMPs and in particular, ADAM-10, but not ADAM-17, had no effect on the basal or the PMA-induced peptide cleavage. However, treatment with ADAM-17's endogenous inhibitor, TIMP-3, produced similar effects as IC-3 (Doedens et al., 2003).

The authors also performed surface biotinylation experiments to determine the abundance of ADAM-17 on the cell surface under basal and PMA-treatment. PMA-treated cells displayed similar levels of ADAM-17 expression on the cell surface, which was reduced upon longer treatment with PMA (Doedens et al., 2003). Thus, an increase in ADAM-17-dependent cleavage does not necessarily equate to an increase in protein expression, but instead could be due to an increase in enzyme activity. Indeed, protein levels of ADAM-17 could be decreased due to internalisation and subsequent degradation (Doedens et al., 2000). ADAM-17 is decreased on the cell surface of THP-1 and JURKAT cells under PMA treatment, which is also a feature of other cell lines, and not merely restricted to hematopoietic cell lines, and is not due to shedding of the metalloprotease but due to internalisation, which could be a regulatory mechanism to control the shedding activity of ADAM-17 (Doedens et al., 2000). The overall level of ADAM-17 within the cells under PMA treatment was reduced in these experiments, as shown through western blotting, which thus suggests that ADAM-17 is degraded once it is endocytosed (Doedens et al., 2000). Thus this could explain why ADAM-17 protein expression was not significantly increased in hCMEC/D3 cells under TNF treatment. However, when cells were assessed for their levels of ADAM-17 activity under TNF treatment conditions in the current study, an increase in enzyme activity could not be found.

SensoLyte™ is sold as an ADAM-17 enzyme activity assay, however, the specificity of the assay is questionable as other ADAMs, such as ADAM-10 also have

similar substrate specificity as ADAM-17. The substrate is described as being derived from a sequence surrounding the cleavage site of ADAM-17, however, MMPs such as MMP-1, -9 and -13 have also been shown to cleave this substrate (Jin et al., 2002). However, the consumption of the substrate by these proteases was found to be less than 10% (Jin et al., 2002). Another enzyme activity assay (InnoZyme TACE Activity Kit, Merck Chemicals Ltd., U.K.), which utilised a monoclonal antibody to capture ADAM-17 in the cell homogenate lysate, before addition of the substrate was tested in this study, but was incompatible with various plate readers and could not be used. It is also notable that an increase in shedding could be dependent upon an increase in substrate availability and concentration, not merely the enzyme; fractalkine protein expression was increased upon TNF treatment, which could have caused a shift in the reaction rate to favour the enzyme reaction. However, despite the limitations of the enzyme activity assay used in this study, it is notable that PMA-induced shedding could be different to TNF-induced shedding of fractalkine. PMA has been widely used as a tumour promotor in cancer research and as an activator of Protein Kinase C (PKC) (Saitoh and Dobkins, 1986), whereas TNF-induced expression of fractalkine is mediated through NF- κ B, and not PKC or PKA (Garcia et al., 2000; Ahn et al., 2004; Moon et al., 2006). Hence the activation of fractalkine shedding seems likely to be mediated through the same pathway, however, previous reports in rat aortic endothelial cells have not observed an increase in shed fractalkine under TNF treatment and the involvement of NF- κ B (Garcia et al., 2000). Recent work has revealed that protease activity is stimulation type-dependent; treatment of COS-7 cells with the ionophore, ionomycin, causes fractalkine to be shed by ADAM-10 (Hundhausen et al., 2007). It is therefore possible that TNF-induced shedding could activate ADAM-10 protease activity or another enzyme. To further investigate the involvement of ADAM-10 and/or -17 in fractalkine shedding, inhibition studies could be performed using TIMP-1 and -3 to determine whether fractalkine shedding is reduced. TIMP-1 should inhibit ADAM-10, whereas TIMP-3 should inhibit both ADAM-10 and -17. Although this would not exclusively prove the involvement of these proteases, as these inhibitors have other substrates, e.g. MMPs, it may help give some insight into the mechanism of fractalkine shedding.

ADAM-10 has been reported to cleave fractalkine in ECV, murine and primate fibroblast cells, however it has been shown to be responsible for constitutive, not PMA-induced shedding (Hundhausen et al., 2003). The mechanism of TNF-induced shedding of fractalkine in hCMEC/D3 may be regulated by cathepsin S, the latter has recently been identified as a protease for fractalkine shedding in dorsal root ganglia neurons (Clark et al., 2007). MMP-2 has also been found to mediate the shedding of fractalkine in murine embryonic fibroblasts (Dean and Overall, 2007). ADAM-17 has

recently been implicated as a mediator in the conversion of MMP-2 from its inactive form to its active form (Gööz et al., 2009), thus although MMP-2 could be involved in fractalkine shedding it does not appear that ADAM-17 activity has increased under TNF treatment conditions, to increase the production of the active form of MMP-2. Although TIMP-3 protein was detected and it inhibits ADAM-17 in a 1:1 stoichiometry, it also acts on other metalloproteinases including ADAM-10 (Amour et al., 2000; Kashiwagi et al., 2001), and thus from the evidence reported here it appears the levels expressed are not sufficient to inhibit the shedding of fractalkine.

It is notable that an increase in fractalkine mRNA under IL-1 β treatment was not observed in hCMEC/D3 cells, as reported by other groups in other endothelial cells (Bazan et al., 1997; Garcia et al., 2000). This could be due to the different endothelial cell types used in previous studies. Indeed other authors have described differences in behaviour concerning barrier function and responsiveness after TNF application in endothelial cells, which is dependent upon their source e.g. aortic versus brain endothelial cells. Brain endothelial cells were shown to be more responsive to TNF treatment, whereas aortic endothelia were more sensitive to IL-1 β and IFN- γ (Harkness et al., 2003). Recent work on hCMEC/D3 cells has shown that the cells are responsive to IL-1 α , and therefore must express the IL-1RI and have the ability to react to IL-1 β as they act upon the same receptor (Afonso et al., 2007). IL-1 β also induced a significant down-regulation of TNFR1 at 100ng/ml in this work, so the lack of responsiveness is not due to an inability of the cells to respond to IL-1 β .

Fractalkine's dual functionality allows it to interact with cells of the immune system via its membrane-bound form and/or shed form through its receptor, CX3CR1. In EAE, microglial and peripheral leucocytes positive for CX3CR1 are recruited to the inflamed lesions of the CNS via membrane-bound CX3CL1 (Sunnemark et al., 2005). However, in MS patients, membrane-bound fractalkine is not increased in brain tissue (Hulshof et al., 2003), but is shed at significant levels into the CSF and serum (Kastenbauer et al., 2003). Shedding of fractalkine from cell membranes in the CNS of MS patients could have a deleterious or protective mechanism. Fractalkine, in its shed form, is a potent chemoattractant for monocytes and T cells (Bazan et al., 1997). In addition, it can have autocrine effects on CX3CR1-expressing HUVEC endothelium by increasing the expression of ICAM-1, which in turn facilitates adhesion of neutrophils to the endothelium (Yang et al., 2007). Cell-bound and shed fractalkine also initiate platelet degranulation and surface expression of P-selectin, which promotes recruitment of leukocytes (Schäfer et al., 2004; Schulz et al., 2007). Indeed, various studies have shown that blocking or abolishing the fractalkine - CX3CR1 interaction has beneficial effects upon the course of animal models of stroke and idiopathic inflammatory myopathy (Soriano et al., 2002; Suzuki et al., 2005). Generation of mice

deficient in fractalkine and subjected to transient focal cerebral ischemia had a 28% reduction in infarct size and a lower mortality rate, in comparison to their wild-type littermates (Soriano et al., 2002). Using a monoclonal antibody against fractalkine significantly reduces the histopathological myositis score, the number of necrotic muscle fibres, and the infiltration of CD4+ and CD8+ T cells and macrophages in mice with experimental autoimmune myositis (Suzuki et al., 2005). Treatment with this antibody also down-regulated mRNA expression of TNF, IFN- γ , and perforin in the muscles (Suzuki et al., 2005). These reports would thus support a role for fractalkine in cell recruitment.

Alternatively, shed fractalkine could act to reduce inflammation by masking CX3CR1-expressing leukocytes, preventing them from binding to the activated endothelium. Saturating the receptor with fractalkine, results in reduced immune cell infiltrates (e.g. monocytes, NK cells) as these cells cannot attach the fractalkine expressed on HUVECs or ECV monolayers (Ancuta et al., 2003; Chapman et al., 2000b; Imai et al., 1997). Shedding of other adhesion molecules has also been shown to have a protective role in MS. Soluble ICAM-1 (sICAM-1) reduces lymphocyte attachment to cerebral endothelial cells *in vitro* (Riekmann et al., 1995) and high sICAM-1 serum levels correlate with Gd-MRI negative scans in relapse-remitting MS patients (Trojano et al., 1996). A recent report has also revealed that fractalkine could modulate leukocyte diapedesis by shedding from the endothelium which would facilitate the detachment of bound PBMCs (Hundhausen et al., 2007). However, silencing the fractalkine receptor in EAE results in increased EAE-related mortality, non-remitting spastic paraplegia and hemorrhagic inflammatory lesions, which is thought to be due to impaired recruitment of NK cells (Huang et al., 2006). Thus the protective or pathogenic role of fractalkine in MS and other inflammatory disorders requires further investigation.

In conclusion, increased expression and shedding of fractalkine by human adult brain endothelial cells following TNF activation of the endothelium, as demonstrated here, could regulate the attraction and T cell/monocyte load in CNS inflammation in MS. Whether fractalkine is beneficial (leukocyte blocking) or detrimental (chemoattractant) to this process in MS will require further investigation, e.g. migration assays. Evidence provided here suggests that this process is not regulated by an increased activity of ADAM-17, but instead could be due to regulatory mechanisms discrete from this system.

Chapter 4

Optimisation of ADAM-17 knockdown in hCMEC/D3 cell line using siRNA technology

4.1 Introduction

TNF is one of the major pro-inflammatory cytokines implicated in a number of inflammatory diseases including, RA, Crohn's disease and MS. As such it has been targeted by therapeutic agents to "treat" a number of these diseases. Anti-TNF treatment has been shown to be effective in the animal model of MS, EAE, whereby blocking the actions of TNF reduced or alleviated symptoms of the disease (Ruddle et al., 1990; Selmaj et al., 1991). However, when this treatment was translated to treat MS patients it resulted in compounding the disease rather than alleviating it (Van Oosten et al., 1996). ADAM-17 mediates the release of TNF, and is increased in MS white matter (Plumb et al., 2006) and in the spinal cord of EAE rats (Plumb et al., 2005), however, the exact role of ADAM-17 in MS pathogenesis is unknown. Another mechanism of reducing the bioavailability of TNF would be to knockdown the expression of ADAM-17, its natural convertase. However, as ADAM-17 sheds a number of substrates not only implicated in disease pathogenesis, e.g. immune modulation through cytokines and chemokines (Black et al., 1997; Moss et al., 1997; Garton et al., 2001; Tsou et al., 2001), but also normal physiological functions, e.g. development and angiogenesis (for review see Reiss and Saftig, 2009), this must be investigated first *in vitro* to understand the effects of reduced ADAM-17 activity on endothelial cell function.

Ectodomain shedding is involved in a number pathophysiological processes, including inflammation, cell degeneration and apoptosis, and oncogenesis (for review see Dello Sbarba and Rovida, 2002) and can be induced by a number of factors including PMA, ionophores, growth factors, cholesterol depletion and cytokine treatment (Pandiella and Massague, 1991; Fan et al., 2003; Matthews et al., 2003; Singh et al., 2005). Ectodomain shedding provides a post-translational mechanism by which membrane protein's surface expression can be down-regulated and their function modulated. In the case of fractalkine, ectodomain release determines whether the molecule acts as an adhesion molecule or as a chemokine. Cytokine-induced ectodomain shedding has not been investigated extensively, which with regards to MS, is surprising given that a number of pro-inflammatory cytokines have been found to be expressed within the inflammatory cuffs (Woodroffe and Cuzner, 1993) and therefore can directly activate the CNS endothelium inducing the shedding of a number of membrane-bound molecules, which are reported to be increased in MS patient serum, e.g. fractalkine (Kastenbauer et al., 2003). Fractalkine has been found to be proteolytically cleaved by ADAM-17 under PMA-induction (Garton et al., 2001; Tsou et al., 2001), whereas ADAM-10 is responsible for its constitutive shedding (Hundhausen et al., 2003). The physiological counterpart of PMA is unknown however, and previous work (Chapter 3) has shown that following TNF administration, an increase in

fractalkine shedding is not associated with an increase in ADAM-17 activity, suggesting that under cytokine treatment, ADAM-17's role as a fractalkine sheddase is limited (Hurst et al., 2009).

4.1.1 Aims of the study

To investigate the functional role of ADAM-17 in fractalkine shedding from hCMEC/D3 cells, under pro-inflammatory conditions by knocking down the expression of the gene at the mRNA and protein level using siRNA technology.

4.2 Materials and methods

4.2.1 Suppliers used in this chapter

Bioline Ltd, 16 The Edge Business Centre, Humber Road, London NW2 6EW; **Dharmacon**, Unit 9 Atley Way, North Nelson Industrial Estate, Cramlington, Northumberland, NE23 1WA, UK; **Dako UK Ltd.**, Denmark House, Angel Drove, Ely, Cambridgeshire, CB7 4ET, UK; or as otherwise stated in Chapter 2 section 2.2.1 or Chapter 3 section 3.2.1.

4.2.2 RNA interference (RNAi)

RNAi is a naturally occurring phenomenon in eukaryotic cells involved in cellular defense against viral invasion, transposon expansion, and post-transcriptional regulation (Zamore, 2001; Tuschl, 2001; Sharp, 2001; McManus and Sharp, 2002; Hannon, 2002; Hutvagner and Zamore, 2002). RNAi is also known as gene silencing, and is a technique which allows the down-regulation of a gene of interest, by incorporating double stranded RNA (dsRNA), which has a complementary sequence to the target mRNA into a living cell. There are various dsRNAs that can initiate gene silencing in mammalian cells using RNAi, including synthetic small interfering RNAs (siRNAs), endoribonuclease-prepared siRNAs (esiRNAs), and short hairpin RNAs (shRNAs) (Snove and Rossi, 2006). Gene regulation using siRNA machinery has not been found to occur naturally within mammals, but appears to be controlled by microRNAs (miRNAs), which bind miRNA binding sites, predominantly located on the 3' untranslated region (UTR) on mRNAs (Pillai, 2005).

4.2.1.1 Basic principles of siRNA induced gene knockdown

Small interfering RNAs (siRNAs) are synthetic dsRNA duplexes which are 21-23 nucleotides (nt) long that are base-paired with 2-nt 3' overhangs at each end (Figure 4.1). They are usually designed to be fully complementary to their target mRNA. One strand of the dsRNA duplex is selectively incorporated into the **RNA-induced silencing complex (RISC)** by RNase III and/or other components of the RNAi machinery. This strand is known as the guide strand, as it acts as a guide RNA to direct the RISC to the complementary mRNAs. It is also the antisense strand to the targeted mRNA. Its base-paired complementary sense strand, known as the passenger strand, is degraded upon incorporation of the guide strand into RISC (Figure 4.1). mRNAs with a perfect or near-perfect complementary sequence to the guide strand are recognised by the catalytic RISC and are cleaved. Cleavage occurs at a site exactly 10 nt upstream from the nt opposite the most 5' nt of the guide strand. The target mRNA fragments are then subsequently degraded by cellular nucleases, which results in knockdown in the expression of the corresponding gene (Figure 4.1) (Pei and Tuschl, 2006).

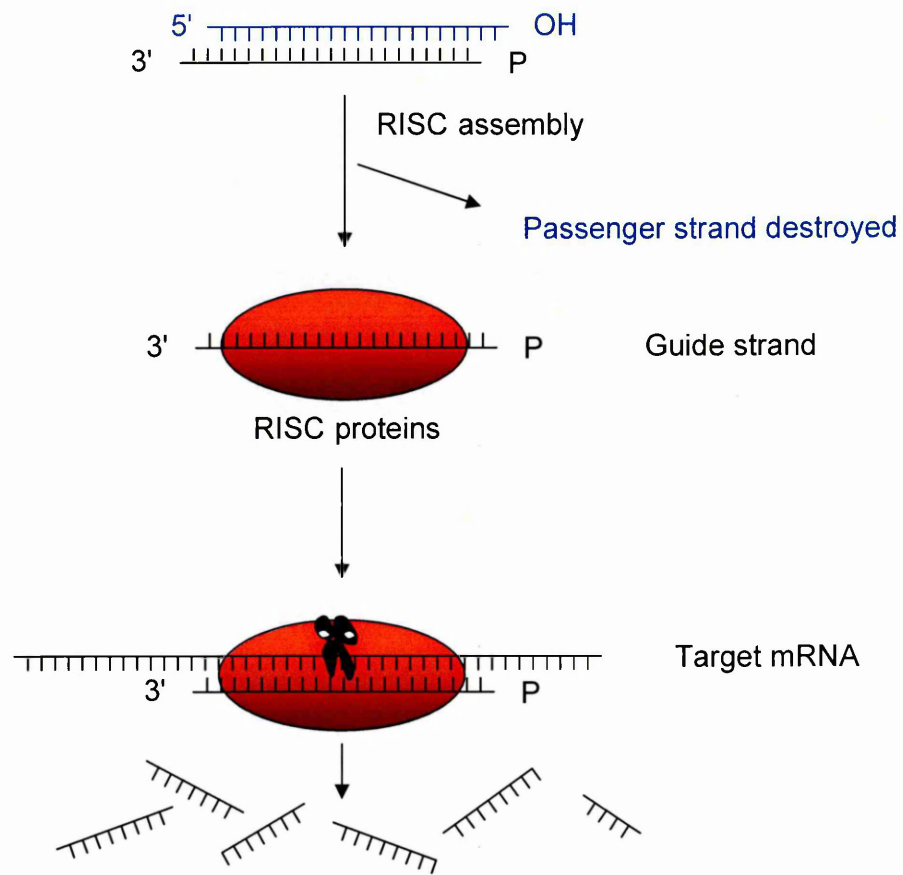


Figure 4.1: Basic principles of small interfering RNA (siRNA) induced gene knockdown. The siRNA duplexes consist of a guide strand (black) and a passenger strand (blue), which have 2-nucleotide (nt) 3' overhangs at each end. Upon selective incorporation of the guide strand into the RNA-induced silencing complex (RISC) the passenger strand is degraded. The guide strand then directs the RISC to the complementary mRNA, which is then cleaved by the catalytic RISC at a site precisely 10 nt upstream from the most 5' nt of the guide strand (scissors). The mRNA fragments of the target gene are then subsequently degraded by cellular nucleases, resulting in knockdown of the gene of interest (Adapted from Pei and Tuschl, 2006).

4.2.1.2 Positive and negative controls to validate siRNA knockdown

For each experiment, controls should be run. As a positive control for siRNA knockdown, cells are transfected with siRNA directed towards a housekeeping gene, such as GAPDH. The negative control or off-target control is a scrambled sequence, which bears no homology to the human, mouse or rat genome. The negative control should have no effect on GAPDH expression, both at the transcriptional and translational level, and acts as a baseline for measuring the effects of the GAPDH siRNA. As the negative control contains the same reagents as the samples with specific siRNA, it can be used to determine any nonspecific effects such as off-target siRNA effects, cytotoxicity of the transfection agent and/or the siRNA, or inadequate transfection conditions. In addition to these two controls, a buffer-only control should also be included in the experiment. This consists of media containing siRNA buffer, but lacking transfection agent and siRNA.

4.2.1.3 Determining siRNA knockdown efficiency and cytotoxicity

Two parameters are essential when determining transfection efficiency: mRNA levels and also cell viability. In addition to this, protein levels of the gene of interest can also be assessed. A $\geq 70\%$ gene knockdown with $\leq 15\%$ cell death should be expected from a successful transfection experiment. In cases where insufficient gene knockdown is observed and cytotoxicity is high, the protocol should be adjusted by altering the concentration of the transfection agent and siRNA, altering the exposure time of the cells to the reagents, and also by determining the optimal cell density (optimal confluency for transfection is 30-80%) (Figure 4.2) (<http://www.ambion.com/techlib/tn/121/9.html>).

4.2.2 Cell culture conditions

4.2.2.1 Determination of the optimal volume of DharmaFECT 1 to be used for siRNA gene knockdown of ADAM-17, using qRT-PCR

In order to determine the optimal volume of transfection reagent required to facilitate ADAM-17 gene knockdown in hCMEC/D3 cells, 5×10^4 cells/500 μ l/well of a 24 well plate were seeded in complete media without antibiotics. After 24 hours in culture, the media was aspirated, the cells washed twice with PBS, and antibiotic-free media with 100nM of siRNA and either 0.5, 1.0, or 1.5 μ l/well of DharmaFECT 1 was added. Antibiotic-free media with an appropriate amount of siRNA dilution buffer (1x siRNA buffer (100mM KCl, 30mM HEPES-pH 7.5, 1.0mM MgCl₂), Dharmacon) was used as a control. DharmaFECT is a lipid transfection reagent, which complexes with siRNAs to facilitate their transfer into cells. DharmaFECT 1 was selected on the basis that it has

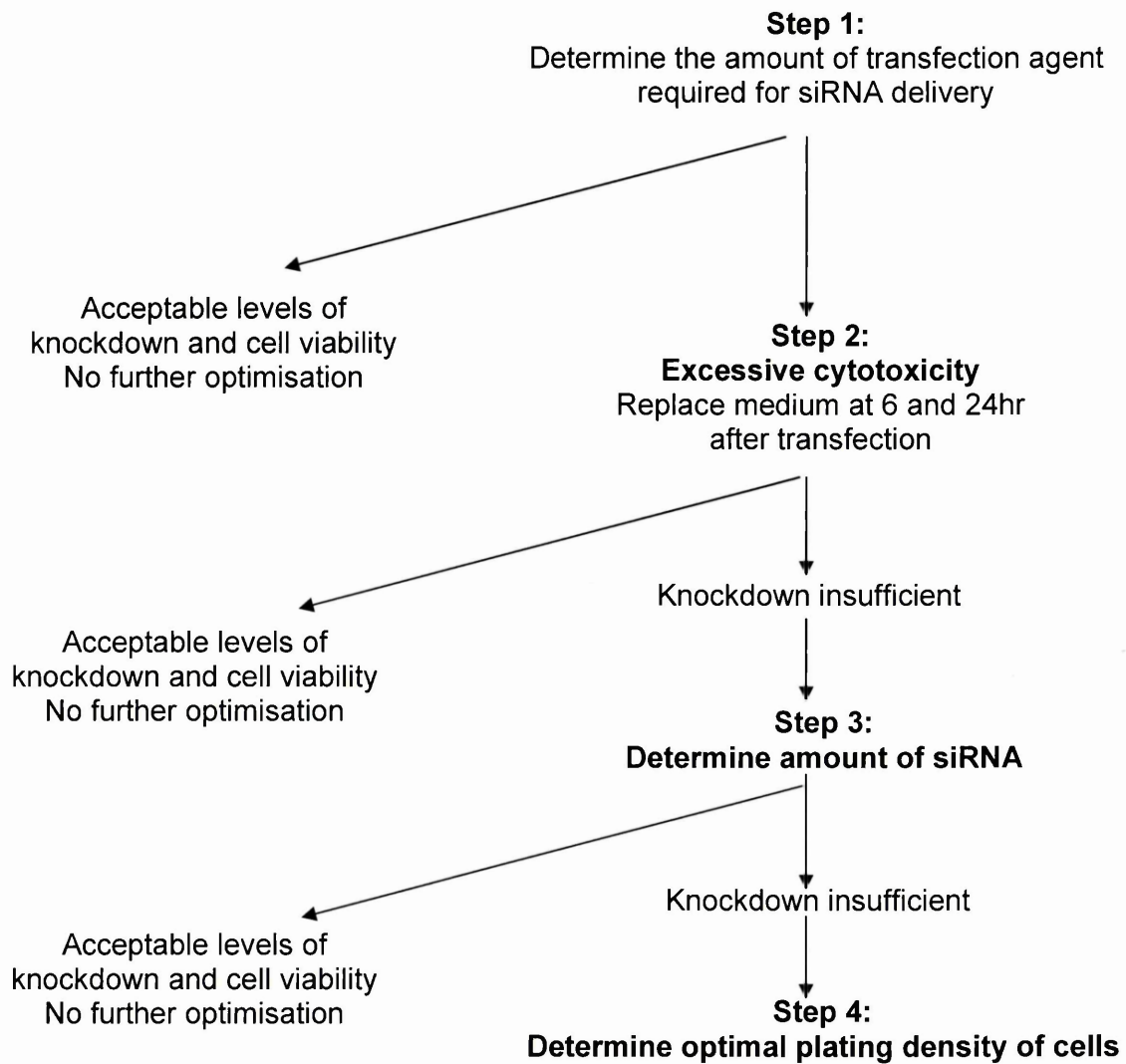


Figure 4.2: siRNA optimisation steps to ensure optimum gene knockdown and minimal cell death. At each step the level of gene knockdown and cytotoxicity was assessed. Only if acceptable knockdown and cytotoxicity levels are obtained can the experimental protocol proceed.

been previously used to transfect HUVEC cells with siRNA (Dharmacon, Lafayette). The siRNA oligonucleotides were supplied from the siGENOME™ collection (Dharmacon) and designed to target either ADAM-17 (ON-TARGETplus SMARTpool; accession number NM_003183) or GAPDH (accession number NM_002046) mRNA sequence. As negative controls, a siGENOME non-targeting siRNA pool (Dharmacon) (catalogue number D-001206-14-05) and siGENOME RISC-free control siRNA (Dharmacon) (catalogue number D-001220-01-05) were selected. RISC-free controls are non-targeting siRNAs with an impaired ability for RISC interaction. After 24 hours culturing, either the media was aspirated and replaced with antibiotic-free media so that the cells could be cultured for a further 24 hours (this limits cell death due to exposure to the siRNA reagents), or the media was aspirated and the cells rinsed twice with PBS and the RNA extracted using TRI Reagent (Sigma-Aldrich, U.K.) (see Chapter 2 section 2.2.4.1). qRT-PCR was carried out as explained previously (see Chapter 2 section 2.2.5.2) using primer and probe sets designed against ADAM-17, Cyclophilin A and GAPDH (Applied Biosystems, U.K.). Each experiment was carried out in triplicate. Cyclophilin A expression was also examined to determine its suitability as housekeeping gene.

4.2.2.2 Validation of RNA using native agarose gel electrophoresis and SYBR green as an RNA dye

To determine the integrity of the RNA extracted from the cells, native agarose gels were run after each RNA extraction. In this case, however, SYBR green (Sigma-Aldrich, U.K.) was used as an RNA dye instead of ethidium bromide. The agarose gel was prepared as previously described (see Chapter 2 section 2.2.4.2), however, instead of adding ethidium bromide to the gel, 2µl of SYBR green was added to 1µl of RNA and 2µl of DNA loading dye (Bioline, U.K.). The total 5µl was then loaded into a well of the agarose gel. The RNA was then electrophorised for 15 minutes at 100V. Serial images were captured using a UVP epi II dark room on the SYBR green setting and using Labworks version 4.0.

4.2.2.3 Assessment of ADAM-17 protein expression after 72 hours of siRNA gene knockdown using western blotting

In order to determine the optimal volume required to facilitate ADAM-17 gene knockdown in hCMEC/D3 cells, 2.5×10^5 cells/2ml/well of a 6 well plate were seeded in complete media without antibiotics. Each experiment was performed in triplicate. After 24 hours, the media was aspirated, the cells washed twice with PBS, and antibiotic-free media with 100nM siRNA against ADAM-17, GAPDH, non-target control, RISC-free were added. Antibiotic-free media and media with buffer alone served as controls. After

24 hours, the media was aspirated and replaced with antibiotic-free complete media (this limits cell death due to exposure to the siRNA reagents) and the cells cultured for a further 48 hours, at which point the cells were washed twice and the total cell protein was extracted using TRI Reagent (Sigma-Aldrich, U.K.) (see Chapter 3 section 3.2.5.2). SDS-PAGE and western blotting was performed as previously described (see Chapter 3 section 3.2.5.5). GAPDH was detected using a monoclonal antibody (Abcam, U.K., Ab8245) at 1:5000 in TBS-T with 5% non-fat milk powder overnight at 4°C, and subsequently using a polyclonal rabbit anti-mouse Ig HRP secondary antibody at 1:1000 (Dako, U.K., P0161).

4.2.2.4 Assessment of fractalkine shedding by ELISA and ADAM-17 protein expression by western blotting after 72 hours siRNA gene knockdown and 24 hour TNF treatment

To determine whether the protein knockdown of ADAM-17 had had an effect on fractalkine shedding, an ELISA assay on shed fractalkine in the cell supernatant was performed. However, as fractalkine shedding was previously shown to be optimally induced following TNF treatment (Chapter 3 section 3.3.6 and 3.3.7) the cells were subsequently treated with TNF at 100ng/ml for a further 24 hours following 72 hour siRNA treatment. hCMEC/D3 cells were seeded at 2.5×10^5 cells/2ml/well of a 6 well plate in complete media without antibiotics. After 24 hours, the media was aspirated, the cells washed twice with PBS, and antibiotic-free media with 100nM siRNA against ADAM-17, GAPDH, non-target control was added. Antibiotic-free media and media with buffer alone served as controls. Each experiment was performed in triplicate. After 24 hours, the media was aspirated and replaced with antibiotic-free complete media so that the cells could be cultured for a further 48 hours, at which point the cells were washed twice with PBS and the media replaced with 100ng/ml TNF in serum- and antibiotic-free media. Following 24 hours, the cell supernatant was collected, centrifuged at 300 x g and the supernatant stored at -20°C until analysis by ELISA could be performed (see Chapter 3 section 3.2.6.5). The total cell protein was extracted using TRI Reagent (Sigma-Aldrich, U.K.) and analysed by western blotting (see Chapter 3 section 3.2.5).

4.2.2.5 Statistical analysis of data

qRT-PCR data was analysed using $2^{-\Delta C_T}$ relative expression values and the non-parametric Mann Whitney *U* test. ELISA data was analysed using a parametric one-way ANOVA followed by Tukey multiple comparison test, so that comparisons could be made between each of the groups. Significance was set at $p < 0.05$ and the data are presented as mean \pm SEM for the indicated number of experiments.

4.3 Results

4.3.1 Stability of cyclophilin A under siRNA treatment

To determine whether cyclophilin A would be a suitable housekeeping gene under siRNA treatment, the gene was analysed following treatment with 100nM non-targetting siRNA and various volumes of DharmaFECT 1. This revealed that following 24 hours treatment with DharmaFECT 1 at 0.5-1.5 μ l/well of a 24 well plate, cyclophilin A expression levels fluctuated compared to the buffer-only control, but not significantly so ($p > 0.05$) (Figure 4.3). Thus, cyclophilin A was used to normalise data.

4.3.2 Determination of the optimal volume of reagent to be used for siRNA gene knockdown of ADAM-17

To determine the optimal volume for gene knockdown in hCMEC/D3 cells, cells were initially treated for 24 hours with siRNA against ADAM-17, GAPDH and a non-target control with 0.5, 1, or 1.5 μ l/well of DharmaFECT 1 transfection reagent. Cells treated with buffer alone were used as a control. Following 24 hours treatment with the siRNA and 0.5, 1, or 1.5 μ l/well of transfection reagent, ADAM-17 mRNA expression decreased significantly by 25%, 55%, and 60%, respectively ($p < 0.05$) (Figure 4.4 A). GAPDH decreased significantly by 55%, 83%, and 85% using the same volumes of DharmaFECT 1 ($p < 0.05$) (Figure 4.4 B). The non-target control fluctuated but remained at around the buffer control levels, with non-significant increases of 111%, 105%, and 111%, respectively ($p > 0.05$) (Figure 4.4 C).

4.3.3 Twenty four versus forty eight hour treatment with siRNA to determine the optimal concentration of DharmaFECT 1

As the silencing of ADAM-17 did not reach a 70% reduction with any of the concentrations of transfection reagent after 24 hours of culturing with the siRNA in hCMEC/D3 cells, an experiment was performed to determine whether 48 hours siRNA treatment would elicit a greater effect. As such, cells were treated with the same concentration of siRNA against ADAM-17 and between 0.5 and 1.5 μ l/well of DharmaFECT 1 reagent. After 24 hours culturing with the siRNA, ADAM-17 mRNA expression decreased significantly by 50%, 70% and 69% with 0.5, 1.0 and 1.5 μ l/well of transfection reagent, respectively ($p < 0.05$) (Figure 4.5 A). After 48 hours treatment with siRNA, ADAM-17 mRNA expression was significantly reduced by 64%, 73%, and 69% using 0.5, 1.0 and 1.5 μ l/well of transfection reagent, respectively ($p < 0.05$) (Figure 4.5 B). As ADAM-17 mRNA expression decreased by 73% using 1 μ l/well of DharmaFECT 1 after 48 hours in culture, this concentration of transfection reagent and time period for incubation with the siRNA were chosen for subsequent analysis of mRNA.

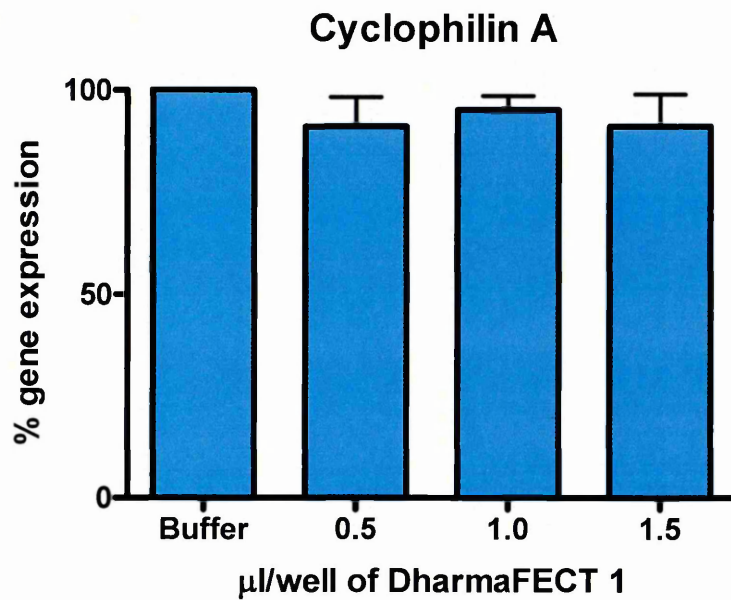


Figure 4.3: Expression levels of cyclophilin A after 24 hour treatment with 100nM non-targetting control siRNA and various concentrations of DharmaFECT 1. The cells were treated for 24 hours and then the RNA extracted and analysed by qRT-PCR. Data are represented as the mean ($n = 3$) \pm SEM. Cyclophilin A expression was not significantly affected by any of the amounts of transfection reagent compared to the buffer-only control ($p > 0.05$).

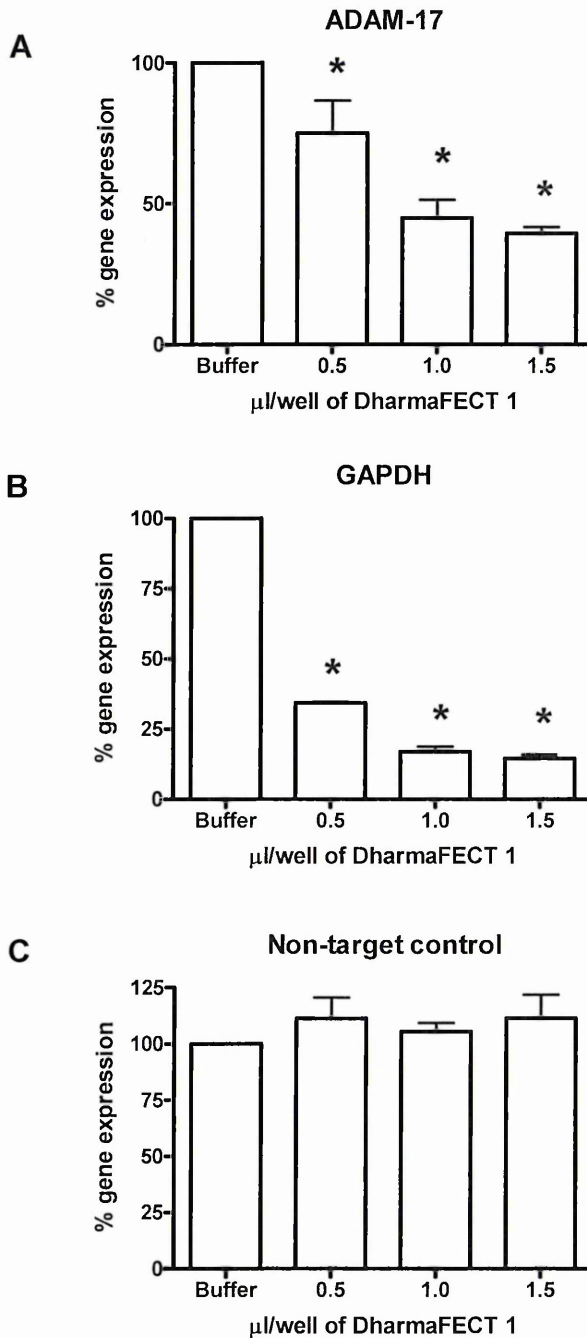


Figure 4.4: Determination of the optimal volume of transfection reagent, DharmaFECT 1, for gene knockdown of ADAM-17 in hCMEC/D3 cells using siRNA technology. Between 0.5 and 1.5 μl per well of transfection agent were used in combination with 100nM of siRNA against ADAM-17 (A), GAPDH (B) or a non-targeting scrambled RNA sequence (C), which were used as positive and negative controls, respectively. The cells were treated for 24 hours and then the RNA extracted and analysed by qRT-PCR. Data are represented as the mean ($n = 3$) \pm SEM. An asterisk indicates statistically significant differences of $p < 0.05$ (*) between treated samples and the control.

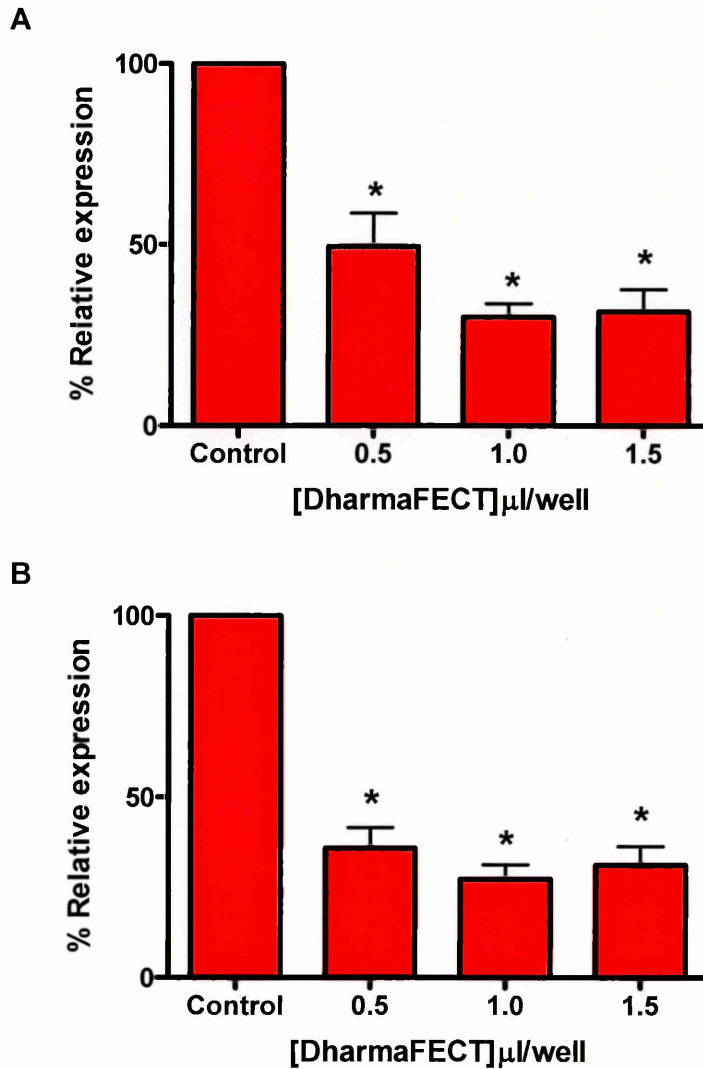


Figure 4.5: Time course study on the effects of different concentrations of DharmaFECT 1 transfection reagent on ADAM-17 mRNA expression in hCMEC/D3 cells using 100nM of siRNA. Cells were treated for either 24 (A) or 48 (B) hours with 0.5 to 1.5 $\mu\text{l}/\text{well}$ of DharmaFECT 1 reagent in combination with 100nM of ADAM-17 siRNA. The RNA was then extracted and analysed by qRT-PCR. Data are represented as the mean ($n = 3$) \pm SEM. An asterisk indicates statistically significant differences $p < 0.05$ (*) between treated samples and the control.

4.3.4 siRNA knockdown of ADAM-17, including all controls, following 48 hour treatment with siRNA and 1µl/well of DharmaFECT 1

The effects of knocking down ADAM-17 mRNA expression using 1µl/well of transfection reagent after 48 hours was repeated, including all controls for GAPDH, non-target control, and RISC-free control (Figure 4.6). After 48 hours treatment with siRNA and 1µl/well of DharmaFECT 1, ADAM-17 mRNA expression was significantly reduced by 61% ($p < 0.05$) and GAPDH significantly reduced by 96% ($p < 0.05$) (Figure 4.6). The mRNA levels of GAPDH following non-target control and RISC-free treatment were non-significantly reduced by 7% and 11%, respectively ($p > 0.05$) (Figure 4.6).

4.3.5 Knockdown of ADAM-17 protein expression in hCMEC/D3 cells following 72 hour treatment with siRNA

Protein expression following siRNA treatment was analysed after 72 hours (Figure 4.7). Following 72 hours treatment with siRNA against ADAM-17, the prominent 100 and 80kDa bands, which correspond to the pro- and mature form of ADAM-17, respectively, were reduced (Figure 4.7), indicating that protein knockdown was successful. GAPDH, RISC-free, non-target control, buffer only and media only controls had no effect on the level of protein expression of ADAM-17 (Figure 4.7). Expression of GAPDH was also determined by western blotting and showed a reduction in expression after 72 hours treatment with siRNA against GAPDH (Figure 4.7). Cells treated with siRNA against ADAM-17, RISC-free, or non-target control, and buffer-only and media only controls showed no altered expression levels in the amount of GAPDH protein (Figure 4.7).

4.3.6 Effects on ADAM-17 protein expression and fractalkine shedding following siRNA knockdown and TNF treatment in hCMEC/D3 cells

Following 72 hours siRNA treatment, and a further 24 hour treatment with TNF, ADAM-17 protein expression was reduced comparable to that obtained in the 72 hour time course (compare Figures 4.7 and 4.8). The controls, GAPDH, non-target control, buffer-only and media only elicited no effect on ADAM-17 protein expression. Protein levels of GAPDH were also examined at this time point and after TNF treatment and showed a reduction in expression following treatment with siRNA against GAPDH. No difference in expression levels of GAPDH were observed by the controls (Figure 4.8).

To determine the effects of knocking down ADAM-17 expression on the shedding of fractalkine, an ELISA assay on fractalkine levels in the cell supernatant was performed from cells, which had been treated for 72 hours with siRNA and then a subsequent 24 hours with TNF at 100ng/ml (Figure 4.9). Cells treated initially with

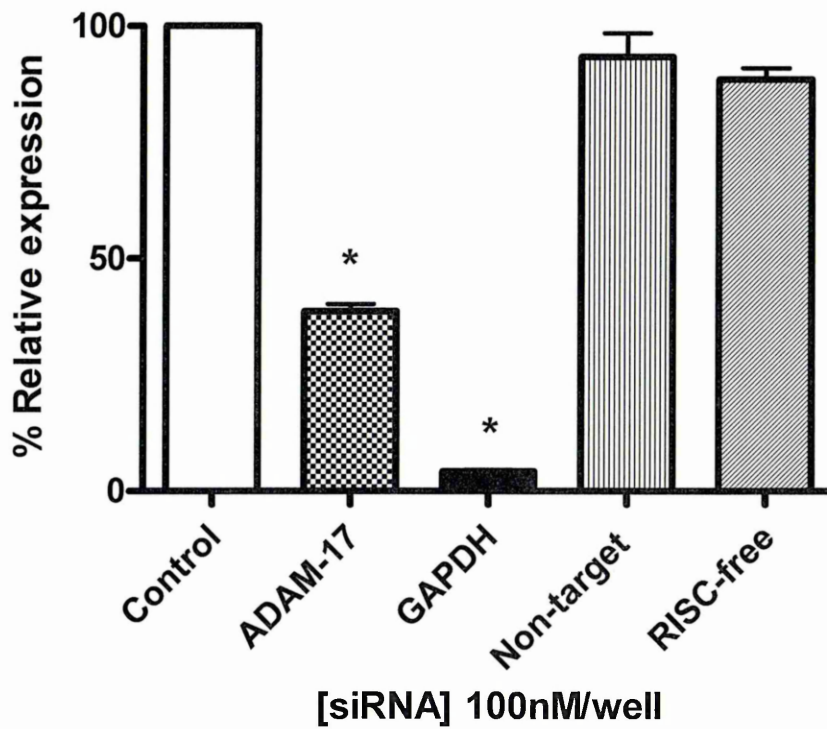


Figure 4.6: Knockdown of ADAM-17 gene expression in hCMEC/D3 cells using 1 μ l/well of DharmaFECT 1 reagent for 48 hours. GAPDH was used as a positive control and the non-target and RISC-free siRNAs were used as negative controls. Data are represented as the mean ($n = 3$) \pm SEM. An asterisk indicates statistically significant differences $p < 0.05$ (*) between treated samples and the control.

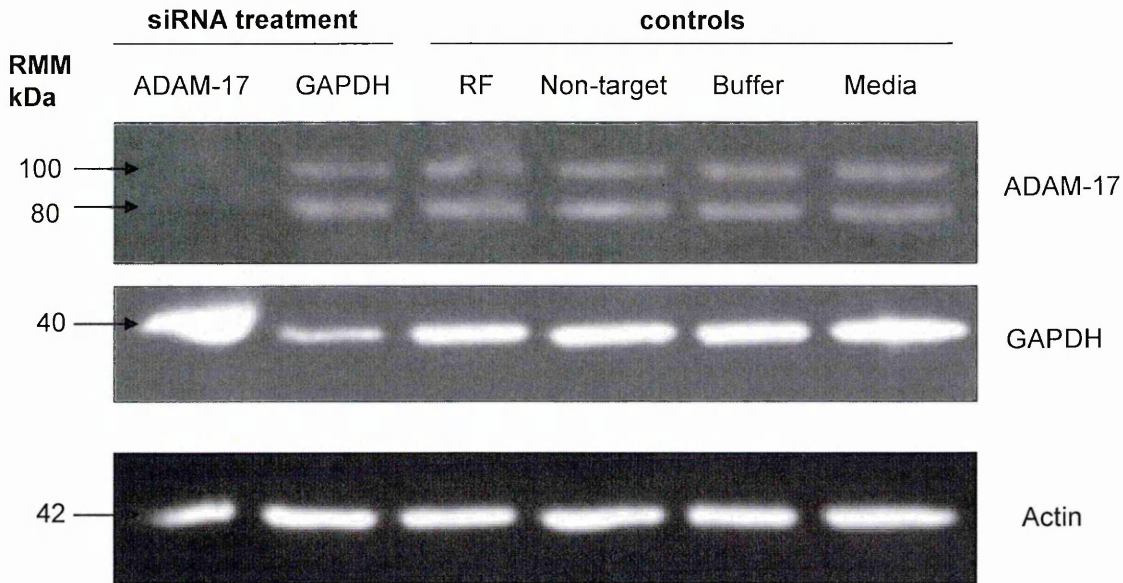


Figure 4.7: Protein expression in hCMEC/D3 cells following siRNA treatment or under control conditions. Cells were treated with siRNA (100nM) for 72 hours against ADAM-17 or GAPDH, or media with a RISC-free (RF), non-target control, buffer only or media only control. Following 72 hours siRNA knockdown total cell protein was extracted and immunoreactivity for ADAM-17 and GAPDH was carried out by western blotting. ADAM-17 immunoreactivity revealed bands at 100 and 80kDa, corresponding to the pro- and mature forms of the protein, respectively. Following ADAM-17 siRNA addition to the cells, a reduction in ADAM-17 at the protein level was observed. GAPDH siRNA addition to the cells, which acted as a positive control, resulted in a reduction of the housekeeping gene at the protein level. Protein expression levels of ADAM-17 and GAPDH were not altered under any of the control conditions (RF, non-target, buffer or media). Actin was used as a loading control. Data are representative of three replicate experiments.

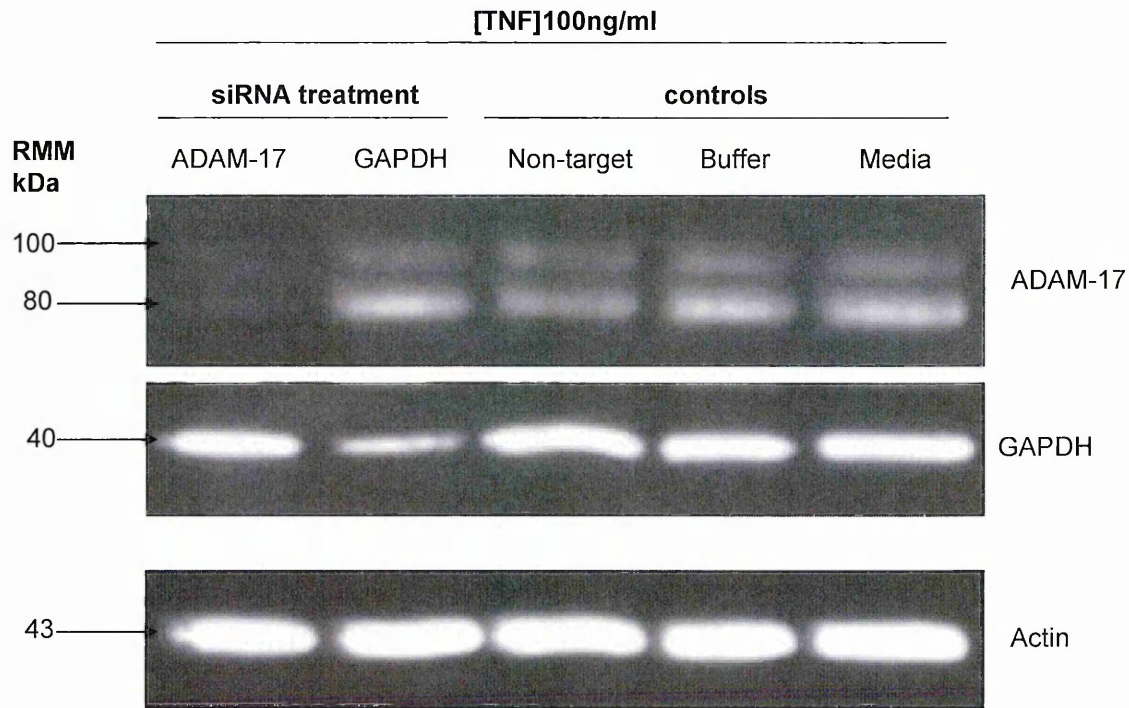


Figure 4.8: Protein expression in hCMEC/D3 cells following TNF treatment with siRNA knockdown or under control conditions. Cells were treated with siRNA (100nM) for 96 hours against ADAM-17 or GAPDH, or media with a non-target control, buffer only or media only control was added. In the last 24 hours of treatment TNF at 100ng/ml was added. ADAM-17 immunoreactivity revealed bands at 100 and 80kDa, corresponding to the pro- and mature forms of the protein, respectively. Following ADAM-17 siRNA addition to the cells, a reduction in ADAM-17 at the protein level was observed. GAPDH siRNA addition to the cells, which acted as a positive control, resulted in a reduction of the housekeeping gene at the protein level. Protein expression levels of ADAM-17 and GAPDH were not altered under any of the control conditions (Non-target, buffer or media). Actin was used as a loading control. Data are representative of three replicate experiments.

**Shedding of fractalkine under TNF treatment
following ADAM-17 knockdown**

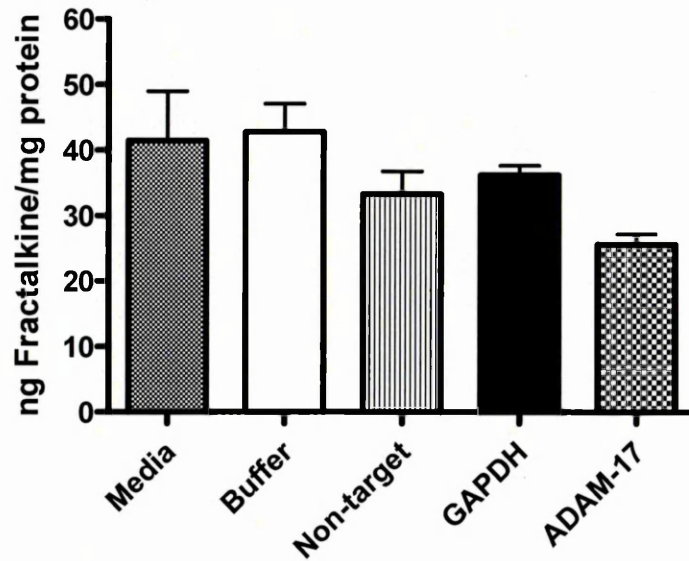


Figure 4.9: Effects on TNF-induced fractalkine shedding in hCMEC/D3 cells following siRNA knockdown of ADAM-17 expression. Cells were treated for 72 hours under control conditions (media or buffer-only control) or with siRNA against a non-target control (negative control), GAPDH (positive control) or ADAM-17. The media was then replaced with serum- and antibiotic-free media containing 100ng/ml of TNF and incubated for 24 hours. The cell supernatant was then removed and stored for later analysis by ELISA. Data are represented as the mean ($n = 3$) \pm SEM. No significant difference was observed between any of the groups ($p > 0.05$).

media or buffer only control media showed comparable concentrations of fractalkine in the cell supernatant following TNF application, at 41.5 and 42.8 ng fractalkine/mg protein, respectively (Figure 4.9). Cells treated with a non-target control or GAPDH siRNA produced reduced levels of fractalkine following TNF application, at 33.3 and 36.3 ng fractalkine/mg protein, respectively, in comparison to the media and buffer controls (Figure 4.9). However, cells treated with siRNA against ADAM-17 and subsequently with TNF showed a further reduction in the shedding of fractalkine at 25.7 ng fractalkine/mg protein in comparison to the controls (Figure 4.9). No significant difference was observed between the groups ($p > 0.05$).

4.4 Discussion

MS pathology is associated with both an increased expression of inflammatory cytokines within the serum and the inflammatory cuffs of patients, which can cause the activation of the endothelium and subsequently the up-regulation of adhesion molecules. Fractalkine expression in endothelial cells has been shown to be induced by a number of cytokines including TNF, IFN- γ and IL-1 (Bazan et al., 1997; Garcia et al., 2000; Imaizumi et al., 2000; Hatakeyama et al., 2004). However, there are few reports on the shedding of the chemokine following TNF treatment. Shedding of fractalkine by brain endothelial cells following TNF treatment was demonstrated in Chapter 3 (section 3.3.6), however, ADAM-17 expression and activity could not account for this following TNF treatment (Hurst et al., 2009). To fully elucidate the role of ADAM-17 in MS pathogenesis and in fractalkine shedding following pro-inflammatory cytokine treatment, siRNA knockdown of ADAM-17 was performed.

It was firstly important to establish the optimal conditions for knocking down ADAM-17. To this effect, the mRNA was examined following 24 hour treatment with 3 concentrations of DharmaFECT 1 transfection reagent. Following 24 hour treatment, none of the ADAM-17 levels were reduced by 70%, a level specified by the supplier to produce a functional effect. Therefore, a comparative study of 24 and 48 hours treatment was performed. Following 24 and 48 hour treatment with the siRNA, ADAM-17 levels were on this occasion reduced by 70% and 73%, respectively, when treated with 1 μ l/well of a 24-well plate, thus this concentration was chosen to study the protein levels. As the 48 hour incubation period produced a stronger reduction in ADAM-17 mRNA expression, it was decided to use the 48 hour incubation period for further analysis of mRNA. Reduced expression levels at the translational level should be evident between 72 and 96 hours of siRNA treatment. As fractalkine shedding is induced under TNF treatment, it was decided to knockdown ADAM-17 expression for 72 hours and then replace the media with media containing TNF at 100ng/ml and leave for a further 24 hours. Firstly, to determine whether ADAM-17 expression was indeed knocked down at the 72 hour time point, the protein expression at this time point was examined by western blotting. This revealed that ADAM-17 expression at the protein level was significantly reduced following 72 hours of siRNA knockdown. Following TNF treatment, ADAM-17 expression at the protein level was also knocked down. Fractalkine shedding into the cell supernatant was also examined, and revealed that although shedding of fractalkine is reduced upon knockdown of ADAM-17 it was not significantly so. This suggests that other proteases may contribute to the shedding of fractalkine under TNF treatment or that there is a residual amount of ADAM-17 which has not been knocked down, which is sufficient to maintain the shedding of fractalkine. The percentage of cells that were transfected with the siRNA was not determined in

this present study as equipment to facilitate the viewing of siGLO® fluorescent control reagents (fluorescent RNA duplexes, which allow visual inspection of transfection efficiency) was not available. Future studies could be performed using siGLO® to determine the efficiency of transfection should the equipment become available. It could also indicate that 70% knockdown of ADAM-17 is not sufficient to elicit a decrease in fractalkine shedding.

Ectodomain release of proteins can be mediated by a number of factors including, PMA (Dello Sbarba and Rovida, 2002), ionophore (Hundhausen et al., 2007), growth factor administration (Subramanian et al., 1997), and more recently cholesterol depletion (Matthews et al., 2003; Tellier et al., 2006; 2008). However, the shedding activities following cytokine treatment has received little attention (Ludwig et al., 2002; Singh et al., 2005). With regards to fractalkine, there are few studies to date which have investigated shedding and the sheddase responsible for this proteolytic activity under cytokine treatment. This is somewhat surprising given that TNF is expressed by T cells and macrophages within the perivascular cuff of MS lesions (Woodroffe and Cuzner, 1993) and fractalkine is found in significant levels in the serum of MS patients (Kastenbauer et al., 2003). ADAM-17 has been described as mediating the inducible shedding of fractalkine under PMA treatment (Garton et al., 2001; Tsou et al., 2001), whereas ADAM-10 mediates shedding of the chemokine under ionophore treatment (Hundhausen et al., 2003). Cathepsin S has also been shown to act as a protease for fractalkine in dorsal root ganglia neurons (Clark et al., 2007) and MMP-2 mediates the shedding of the chemokine in murine embryonic fibroblast cells (Dean and Overall, 2007). As knocking down ADAM-17 expression only slightly *reduced* fractalkine shedding following TNF treatment in endothelial cells, it is likely another protease(s) contributes to the release of the chemokine under TNF treatment, e.g. ADAM-10, cathepsin S or MMP-2. Future studies would need to be carried out to determine whether these enzymes mediate shedding of fractalkine in a cytokine environment, i.e. independent/combined siRNA knockdown of the proteases.

In addition as ADAM-17 is associated with the shedding of various other membrane-bound proteins associated with inflammation it will be necessary to expand this research and examine other proteins which may have been affected by the knockdown of ADAM-17. However, as the enzyme activity was not significantly changed following TNF treatment (Chapter 3 section 3.3.8) and siRNA treatment did not significantly reduce fractalkine shedding, it is likely other substrates of ADAM-17 may not be affected by ADAM-17 knockdown. Instead it appears likely TNF activates another protease responsible for fractalkine release. It has been shown that treatment of murine endothelial cells with siRNA that targets ADAM-17 show a significant reduction in the amount of soluble VCAM-1 (sVCAM-1) when treated with IL-1 β and

TNF (Singh et al., 2005). This could suggest that ADAM-17 activation requires co-treatment with multiple cytokines. This would also be more representative of the *in vivo* environment in the CNS in MS where many cytokines are differentially expressed within MS tissue and serum (Beck et al., 1988; Merrill, 1992; Lu et al., 1993; Woodroffe and Cuzner, 1993; Mokhtarian et al., 1994). It is also notable that the present work supports the previous work in chapter 3, whereby the increase in shedding of fractalkine under TNF treatment does not coincide with an increase in expression or activity of ADAM-17 and therefore it is likely another protease is responsible for this activity.

Recent studies using siRNA knockdown of ADAM-17 in HUVECs, to determine the enzyme's role in angiogenesis, have revealed that ADAM-17 plays a significant role in determining cell morphology, proliferation and *in vitro* angiogenesis (Gööz et al., 2009). siRNA induced ADAM-17 silencing, resulted in a significant reduction in cell proliferation and also under subconfluent conditions HUVECs appeared irregular in shape and avoided cell-cell contact. This behaviour was accounted for by lack of shedding of adhesions molecules by ADAM-17, e.g. VCAM-1 (Garton et al., 2003). This particular aspect of hCEMC/D3 cells was not investigated in this present study, however, the cells were seeded at 50% confluency, in-line with the guidelines of Dharmacon to facilitate transfection. When the cells reached confluency, it was not observed that cells avoided cell-cell contact. Further investigation into these aspects of ADAM-17 knockdown is required. It was also observed in the study by Gööz and colleagues (2009) that ADAM-17 can mediate the conversion of MMP-2 from an inactive form to an active form and MMP-2 has also been found to induce fractalkine cleavage (Dean and Overall, 2007). Inhibiting ADAM-17 in this present study did not have a significant effect upon fractalkine shedding, either through ADAM-17's direct action upon fractalkine or indirectly through MMP-2 activation. Thus, another enzyme such as ADAM-10 or cathepsin S could be facilitating fractalkine cleavage.

Reducing TNF bioavailability has long been an attractive treatment for autoimmune conditions and has been successful to a degree in RA and Crohn's disease. Inhibiting TNF proved successful in treating EAE (Ruddle et al., 1990; Selmaj et al., 1991; Selmaj et al., 1995). However, the administration of anti-TNF treatment elicited exacerbations in MS (van Oosten et al., 1996) and has even possibly resulted in the development of MS in a small number of patients who were being treated for RA (Sicotte and Voskuhl, 2001). Reduced bioavailability is associated with reduced remyelination ability, and prolonged responses from myelin-reactive T cells (Arnett et al., 2001; Kassiotis and Kollias, 2001). The pro-inflammatory effects of TNF are mediated through TNFR1 (Kassiotis and Kollias, 2001) and transgenic mice who cannot produce soluble TNF and thus only express transmembrane TNF show suppressed EAE onset and progression, while maintaining the autoimmune

suppressive properties of TNF (Alexopoulou et al, 2006). Thus it is thought that inhibiting the soluble TNF/TNFR1 pathway may be a more effective treatment for diseases such as MS. Inhibiting ADAM-17 would thus be an attractive treatment for MS, as this would prevent the solubilisation of TNF whilst retaining the membrane-bound form of the cytokine intact. However, it must also be noted that ADAM-10 can cleave TNF (Lunn et al., 1997; Rosendahl et al., 1997), and could possibly take over this activity if ADAM-17 is silenced. Inhibitors of ADAM-17 have already been produced to treat autoimmune diseases such as RA, however, either their efficacy was not sufficient or they resulted in hepatotoxicity due to the accumulation of transmembrane TNF, TNFR1 and TNFR2 (for review see Moss et al., 2008; McCoy and Tansey, 2008). In addition, it must also be noted that ADAM-17 is responsible for the cleavage of an array of membrane-bound substrates not only detrimentally implicated in disease but also beneficial; ADAM-17 is an α secretase which mediates the production of the non-amyloidgenic species of APP (Allinson et al., 2004). Thus, if ADAM-17 was inhibited within the brain this may result in the production of the amyloidgenic protein, causing AD.

In conclusion siRNA technology is a useful tool to examine the functional role of proteins, the application of which in this study, revealed that ADAM-17 knockdown does not significantly reduce the shedding of fractalkine from the human adult brain endothelial cell line, hCMEC/D3. This work and that described in Chapter 3 suggests that ADAM-17 does not account for the majority of fractalkine release under pro-inflammatory conditions and that other proteases must be involved. Future work is required to determine whether ADAM-10, cathepsin S, MMP-2 or an unidentified enzyme is responsible for this.

Chapter 5

Expression of ADAM-17 and fractalkine in post-mortem human control and MS brain tissue

5.1 Introduction

ADAM-17 has been found to be localised to various tissues of the body, including the normal human CNS (Goddard et al., 2001). Within the CNS it is restricted to endothelial cells and astrocytes (Goddard et al., 2001; Plumb et al., 2006). In MS white matter and the spinal cord of rats with EAE, the levels of ADAM-17 have been found to be up-regulated (Plumb et al., 2005; 2006). ADAM-17 mediates not only the release of soluble TNF, but also sheds fractalkine which has also been implicated in MS pathogenesis (Kastenbauer et al., 2003).

In the CNS fractalkine expression is restricted to endothelial cells, astrocytes and neurons (Bazan et al., 1997; Pan et al., 1997; Harrison et al., 1998; Nishiyori et al., 1998; Muehlhoefer et al., 2000; Hulshof et al., 2003). Fractalkine has been implicated in various pathologies, both within the CNS and also within the periphery. Increased levels of fractalkine have been detected intrathecally in HIV-infected patients, particularly those experiencing CNS complications, including HIV encephalopathy and myelopathy (Sporer et al., 2003). Fractalkine has been implicated in the inflammatory process of RA (Ruth et al., 2001), and atherosclerotic, diabetic and transplant vascular diseased arteries, all display positive immunogenicity for fractalkine, suggesting fractalkine may play a significant role in these diseases (Wong et al., 2002). Fractalkine has also been implicated in MS pathogenesis as it shows an increase in expression in the CSF and serum of patients with MS (Kastenbauer et al., 2003). However, in one study, expression levels of fractalkine in astrocytes in MS brains shows no altered regulation in comparison to control tissue. This was in spite of evidence that cultured human astrocytes show an increase in expression of fractalkine under pro-inflammatory conditions (Hulshof et al., 2003). Expression of fractalkine in the human brain endothelium in the latter study reported that: "fractalkine was moderately expressed on endothelial cells from normal control and MS patients" (Hulshof et al., 2003). Except for this report there are no comprehensive reports on the expression of fractalkine by endothelial cells in the human CNS in MS brain tissue. This work could provide an important insight into the role of fractalkine within the human CNS endothelium during MS pathogenesis. As the BBB acts as an interface between the blood and the brain, fractalkine's role as an adhesion molecule or a chemokine could be an important influence upon leukocyte recruitment within the CNS. The previous chapter (Chapter 3) reported that high levels of fractalkine were expressed and shed from human adult brain endothelial cells *in vitro* following TNF treatment, which would suggest that within the cytokine milieu of the perivascular cuff, fractalkine expression could be dysregulated dependent upon the extent of inflammation.

5.1.1 Aims of the study

The aims of this study were to undertake a preliminary investigation into the expression levels of fractalkine in control and MS patient post-mortem brains. In addition to this, the expression levels of ADAM-17 were also investigated to see whether fractalkine and ADAM-17 showed any relationship in their expression levels and/or co-localisation.

5.2 Materials and methods

5.2.1 Suppliers used in this chapter

Leica Microsystems Ltd, Davy Avenue, Knowlhill, Milton Keynes, MK5 8LB, Buckinghamshire, UK; **Novocastra Laboratories**, Balliol Business Park, Benton Lane, Newcastle Upon Tyne, NE12 8EW, UK; **R A Lamb Ltd.**, Units 4 & 5 Parkview Industrial Estate, Alder Close, Lottbridge Drove, Eastbourne, East Sussex, BN23 6QE; or as otherwise stated in Chapter 2 (2.2.1), Chapter 3 (3.2.1) and Chapter 4 (4.2.1).

5.2.2 Tissue

15 blocks of snap frozen autopsy brain tissue from 5 MS patients and 5 normal control patients were obtained from The UK Multiple Sclerosis Tissue Bank, Charing Cross, London, UK (registered charity no. 207495) for use in this study. From the MS patients, 10 blocks were obtained: 5 macroscopically determined lesional blocks and 5 macroscopically determined NAWM blocks (Table 5.1). Informed consent and ethical approval for this study was obtained through the Multi-Centre Research Ethics Committee (MREC) (see Appendix I). All MS tissue was obtained from patients who were diagnosed with SPMS, and who had a mean disease course of 27 years (range 8-39). Mean ages at the time of death were: MS, 58 years (range 46-64); controls, 81 years (range 64-92) (Table 5.1). MS was confirmed clinically and neuropathologically.

The UK Multiple Sclerosis Tissue Bank prepared the tissue for this part of the study by dividing the brain tissue into grid reference sections. Tissue blocks were prepared by the tissue bank by first cutting the whole brain into an anterior and posterior portion by dissecting through the mamillary bodies (Figure 5.1). One centimetre coronal slices were then cut through the entire brain. Slices were numbered based upon whether the slice was derived anteriorly to the mamillary bodies and therefore from the frontal pole, or posteriorly to the mamillary bodies and therefore from the occipital pole. The former were numbered A1, A2 etc and the latter were numbered P1, P2 etc. The coronal slices were then laid on a grid and divided into 2cm² blocks, frozen by immersion in isopentane, pre-cooled on dry-ice and then stored in air-tight containers at -85°C (Dr. Abhi Vora, The UK Multiple Sclerosis Tissue Bank). Each patient is given an ID code and the four digits following that pertain to the coronal section and the grid reference where the tissue block was taken from, e.g. MS130 P2D3, is patient ID: MS130, and the coronal section is P2 and therefore derived from the second section posterior to the mamillary bodies, and the block was taken from grid co-ordinates D3 (Figure 5.1).

10µm cryostat (Leica) sections from each block were cut at -20°C and mounted onto PolysineTM coated slides and stored at -80°C until further histological and immunohistochemical analysis was performed.

Table 5.1: Patient details of CNS tissue used in this study. Tissue was supplied by The UK Multiple Sclerosis Tissue Bank (Charing Cross, London, UK). In each case the age, sex, MS type/control, disease duration, cause of death and death to tissue preservation time is given.

Case ID	Block IDs	Age (Yrs)	Sex	MS type/control	Disease duration (Yrs)	Cause of death	Death to tissue preservation interval (hrs)
MS 074	A1C6* A1E7*	64	Female	SPMS	36	Gastrointestinal bleed/obstruction, aspiration pneumonia	7
MS 090	P2E3 P2B3	62	Male	SPMS	39	Multiple sclerosis	17
MS 100	A2D2 A2C2	46	Male	SPMS	8	Pneumonia	7
MS 109	A1C2 A1D1	60	Female	SPMS	25	Myocardial infarct	22
MS 130	P2D3 P2F4	57	Female	SPMS	Unknown	Multiple sclerosis	22
C 011	A1B5*	77	Male	Control	N/A	Carcinoma of the lung metastasised	26
C 014	P2C3*	64	Female	Control	N/A	Cardiac failure	18
C 016	A2D1*	92	Male	Control	N/A	Congestion cardiac failure, old age	13
C 019	P1B2*	90	Female	Control	N/A	Old age	15
C 020	P2B2*	84	Female	Control	N/A	Congestive cardiac failure, ischaemic heart disease, atrial fibrillation	24

Key: SPMS, secondary progressive MS

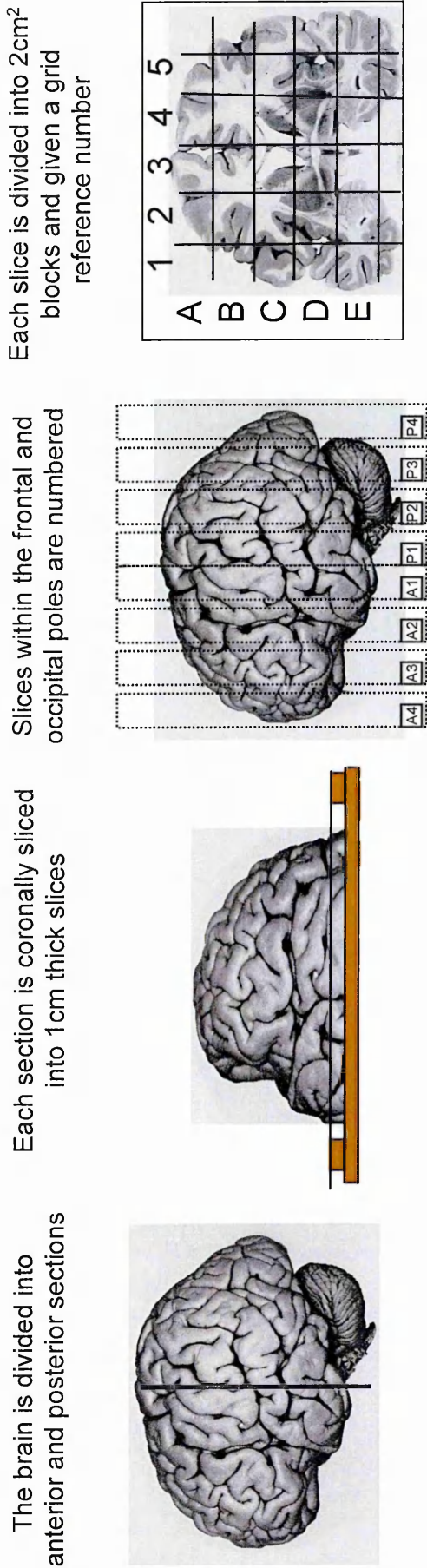


Figure 5.1: Schematic diagram explaining coronal slicing and block preparation of the cerebrum by The UK Multiple Sclerosis Tissue Bank.

The whole brain is divided into the frontal and occipital portion and then each portion is sliced into 1cm thick slices. Depending upon where the slice was derived in relation to the mamillary bodies determines the code allotted to the brain slice. Slices from the frontal part are termed A1, A2 etc and slices from the occipital portion are termed P1, P2 etc. Each slice is then placed on a grid and 2cm² blocks are cut from the slices. The co-ordinates from where the block is taken act as a reference code for the tissue. Images courtesy of The UK Multiple Sclerosis Tissue Bank.

5.2.3 Tissue characterisation

To determine the extent of inflammation, demyelination and cellular reactivity, various stains were employed. To determine the extent of inflammation haematoxylin and eosin (H&E) stain was performed. Demyelination was determined using Oil red O (ORO) positivity and MOG immunoreactivity. An antibody directed against HLA-DR was used to determine the activation status of microglia, macrophages, T cells and B cells. Stains for these markers and for the target proteins of interest were carried out on serial sections from each block and examined within the white matter regions of the tissue.

5.2.3.1 Haematoxylin and eosin staining (H&E)

H&E stain is a method commonly used in histology. Haematoxylin stains cell nuclei a black/purple colour. Eosin Y, which is a pink/red dye stains cytoplasmic components of the cell (Stevens and Lowe, 1997).

10µm frozen sections were allowed to air dry for 30 minutes at RT, fixed in 4% PFA (see Chapter 3 section 3.2.4.5) at RT for 5 minutes, washed, and then placed in filtered Harris's haematoxylin for 1 minute. Slides were then rinsed in running tap water until the water ran clear and then placed in eosin Y for 2 minutes. Following another wash step in tap water, the sections were dehydrated in a series of graded ethanol at the following concentrations: 50%, 70%, 80% and 95%. Slides were placed in each ethanol grade for 2 minutes. Following 4 changes of xylene (Sigma-Aldrich, UK), the sections were mounted in DPX mountant (Sigma, Aldrich, UK).

5.2.3.2 Oil red O staining (ORO)

ORO stain is a fat soluble dye (lysochrome) used to stain neutral triglycerides and lipids dark red on frozen sections. ORO is commonly employed to identify lipid-laden macrophages that have engulfed myelin and areas of demyelination, a characteristic of MS (Kirk et al., 2003; Plumb et al., 2006). Other techniques involve using luxol fast blue (LFB) or periodic acid-Schiff (PAS) reaction staining to delineate areas of demyelination and the presence of phagocytic macrophages (Boyle and McGeer, 1990; De Groot et al., 2001). ORO solution was prepared by dissolving 1g of ORO powder (Sigma-Aldrich, U.K) in 60% triethyl phosphate (TEP) (Sigma-Aldrich, UK) and heating to 100°C on a hot plate for 5 minutes. The mixture was stirred continuously using a magnetic stirrer, and the temperature not allowed to exceed 110°C. The resulting mixture was filtered through filter paper (Whatman) whilst it was hot and then again when it had cooled. The mixture was stored at RT for up to a month.

Frozen sections were prepared for ORO staining in the same manner as for H&E staining, except they were fixed in 4% PFA for 1 hour at 4°C. Following the fixation step, the sections were rinsed in tap water, rinsed briefly in 60% TEP, and then

placed in filtered ORO solution for 10-15 minutes at RT. The sections were then rinsed briefly in 60% TEP, followed by tap water. Nuclei were counterstained with Harris's haematoxylin (20% v/v) for 30 seconds, washed in deionised H₂O (dH₂O), and mounted in aqueous mountant, glycerol gelatin (Sigma-Aldrich, UK).

5.2.3.3 Sudan black B staining (SBB)

SBB is a stain which, like ORO, is a fat soluble dye (lysochrome) that stains neutral triglycerides and lipids blue-black. SBB can be used to quench autofluorescence, which in brain tissue is normally a product of lipofuscin, a break-down product of old red blood cells (Goddard et al., 2001). Autofluorescence from this source is usually visible between the excitation range 360-647nm, and appears as small punctate, intracellular structures (<http://www.uhnresearch.ca/facilities/wcif>).

SBB solution was prepared by dissolving 1g of SBB powder in 70% ethanol, continuously stirred at RT in the dark for 2 hours, and then filtered through filter paper (Whatman). The mixture was stored at 4°C for a maximum of 2 months.

5.2.4 Tissue grading

5.2.4.1 H&E and ORO stains

To determine the extent of inflammation and demyelination, H&E and ORO tissue stains, respectively, were observed and graded on a + to +++ (ORO) or to +++++ (H&E) scale. For H&E, grade + was interpreted as few immune cell infiltrates around the blood vessels and grade +++++ had a large burden of immune cell infiltrates around the vessel (Figure 5.2). For ORO, grade + was interpreted as the presence of a few ORO positive cells and grade +++ had a large number of ORO positive cells (not seen in the tissue blocks used in this thesis) (Figure 5.3). If the tissue lacked inflammatory or ORO positive cells the tissue was graded as negative.

5.2.4.2 HLA-DR reactivity

To determine the type of inflammatory activity within the tissue blocks a HLA-DR staining was employed. HLA-DR is a cell surface receptor encoded by the human leukocyte antigen complex on chromosome 6 region 6p21.31. It is a major histocompatibility complex (MHC) class II (Delves et al., 2006). There are very low levels of MHC class II detected in normal brains and thus any reactivity in this tissue type was graded + (Figure 5.4 A and B), however, in autoimmune disease expression is increased particularly in and around active MS lesions (Boyle and McGreer, 1990; Bö et al., 1994). To determine the type of activity within the tissue samples, the Bö et al. (1994) system of MHC class II classification was used. Whereby, in actively demyelinating lesions, the distribution of HLA-DR is evenly distributed and was graded

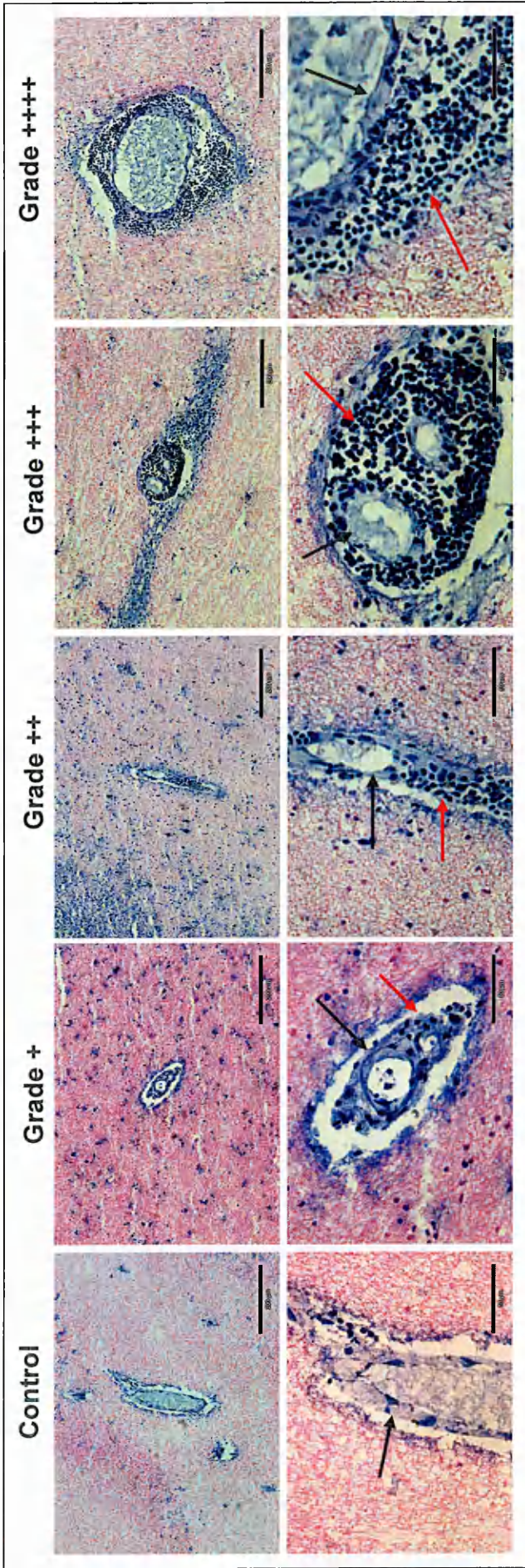


Figure 5.2: Haematoxylin and eosin (H&E) staining showing the grades of inflammation seen in CNS white matter in this study. Control tissue (CO11 A1B5) showed no inflammation, whereas most of the MS tissue was graded as having an inflammatory burden of + (MS100 A2C2) or ++ (MS074 A1E7), and in one patient (MS130 P2F4) an inflammatory burden of +++ and +++++ was observed. The black arrows indicate the blood vessel endothelium wall and the red arrows show the leukocytes that have breached the blood-brain barrier. The upper panel shows a lower magnification, whereas the lower panel shows a higher magnification of the same region. Scale bar for the upper panel is 200µm, and 50µm for the lower panel.

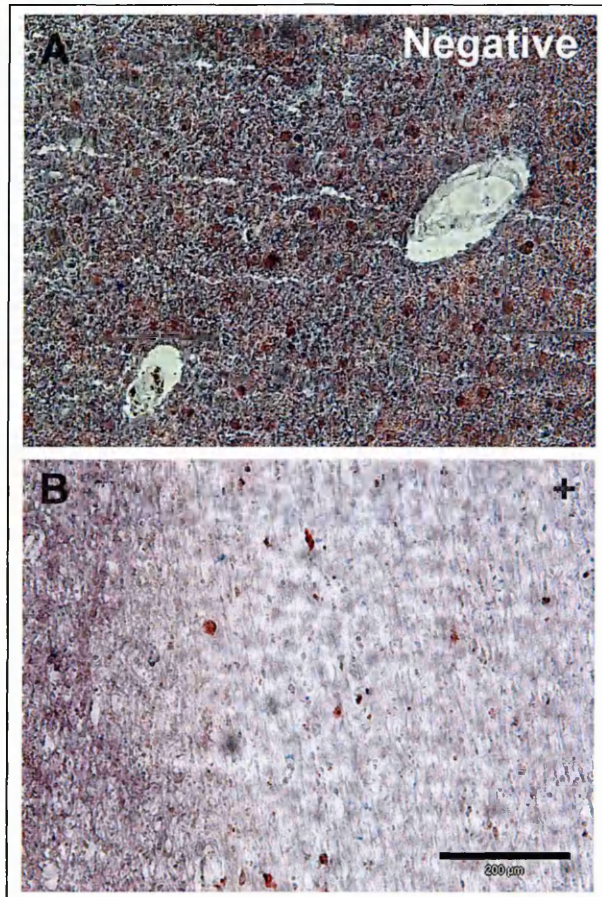


Figure 5.3: Oil red O (ORO) staining showing the grades of lipid-laden macrophages observed in the white matter tissue used in this study. Either no ORO positive cells were observed (A) (MS100 A2C2) or a few ORO positive cells graded as + were diffusely scattered in areas of demyelination (B) (MS090 P2B3). Scale bar is 200µm.

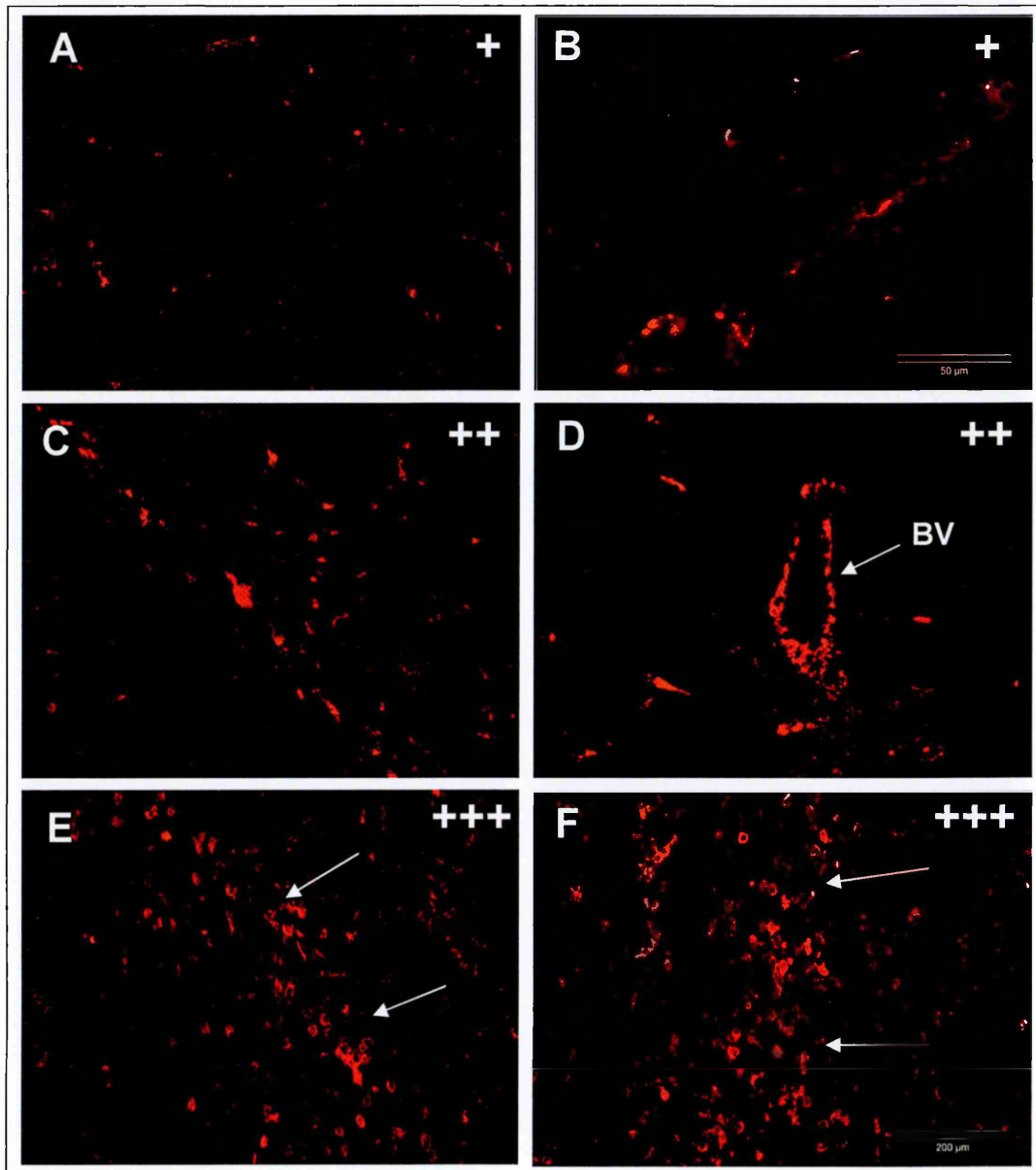


Figure 5.4: HLA-DR staining of white matter tissue showing the different grades of cellular activation. Grade + shows a low level of expression of HLA-DR positivity (A (CO20 P2B2) and B (CO14 P2C3)); grade ++ shows an even distribution of HLA-DR reactivity, which is increased compared to control tissue (C (MS109 A1C2) and D (MS109 A1D1)), and which was also increased in the region of blood vessels (BV) due to perivascular inflammatory cells surrounding the BV (D); grade +++ showed increased HLA-DR reactivity (E (MS090 P2B3) and F (MS090 P2B3)), which was increased at the lesional edge (arrows), these types of lesions were typically classified as chronic-active lesions. *Note that A and C-F images were taken at the same magnification and have a scale bar of 200 μ m. The scale bar in image B is 50 μ m.*

++ (Fig 5.4 C and D); in chronic-active lesions HLA-DR positive cells are restricted to the lesional edge rather than centrally and were graded +++ (Fig 5.4 E and F); whereas in chronic-inactive lesions there is little/no HLA-DR reactivity within the lesion, at the edges, or outside the demyelinated region (not seen in this study) (Bö et al., 1994).

5.2.4.3 MOG reactivity

MOG staining was also employed to determine the extent of demyelination in the tissue blocks (Fig 5.5). MOG is a glycoprotein that is specific to the CNS and is expressed on the surface of myelin sheaths and oligodendrocytes (Brunner et al., 1989). Immunohistochemical examination of MOG can reveal the extent of demyelination/remyelination in CNS tissue, and thus be an indicator of the type of lesion. For example in the chronic plaque there is no evidence of active myelin breakdown, whereas in active plaques marked pallor of myelin is evident (Lucchinetti et al., 2005).

5.2.4.4 Classification criteria using all markers

Using H&E, ORO, HLA-DR and MOG staining, MS lesions were classified into two distinct subclasses, either active or chronic-active. Using MOG as a marker for demyelination it could be determined whether there was complete absence of MOG in the lesion, or whether there was partial loss. If the tissue fitted the former criteria the tissue was classified as chronic, however, if there was partial loss the lesion was classed as active if there was inflammation, as determined using H&E, as well. In addition to this the cellular reactivity was assessed using HLA-DR: in the case of the chronic lesion if the lesion had positive HLA-DR staining at the lesional edge, the tissue was classed as active; in the case of the active lesion, the HLA-DR staining was seen throughout the tissue. This classification was also made using the presence of lipid-laden macrophages, which were witnessed at the lesion edge in chronic-active lesions.

5.2.5 Immunohistochemistry

5.2.5.1 Single immunofluorescence

Immunohistochemistry was carried out as previously described (Plumb et al., 2006), but with some modifications. Briefly, for each antibody the optimal concentration was determined by trying a range of dilutions in line with the recommendations of the manufacturer, except anti-vWF and HLA-DR, which were previously optimised within the laboratory by Dr. H. Denney, and also the anti-MOG antibody which was provided as a gift by Dr. S. McQuaid and used at his recommended dilution. In addition, different concentrations of goat serum were used to prevent non-specific binding, and eventually

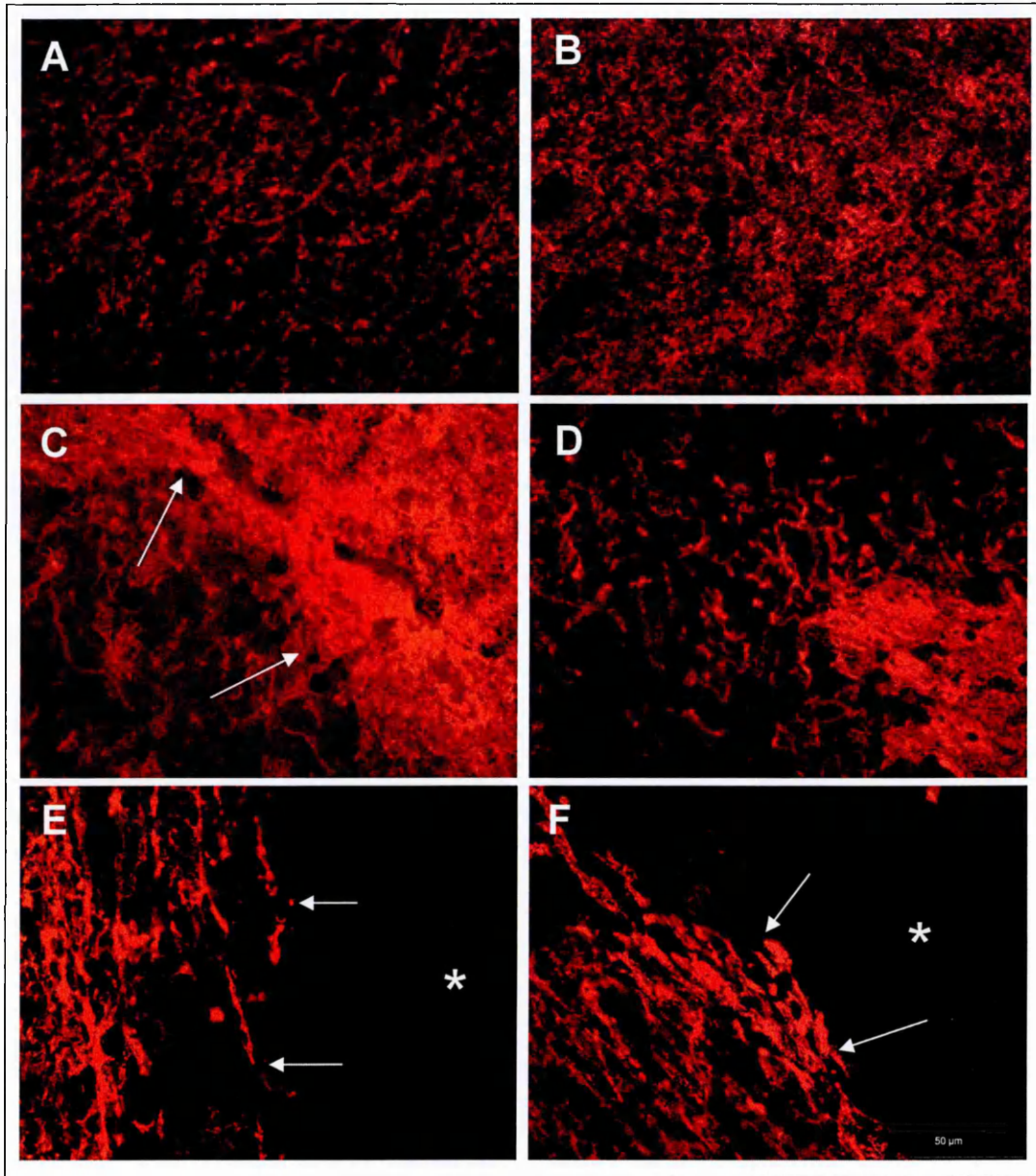


Figure 5.5: Myelin oligodendrocyte glycoprotein (MOG) staining of control (A and B) and MS (C-F) tissue to determine the extent of demyelination. Control tissue showed a uniform pattern of expression of MOG (A (CO11A1B5) and B (CO19 P1B2)). Active lesions (C (MS074 A1C6) and D (MS074 A1C6)) showed a disrupted MOG staining pattern with clearly demarcated lesional borders (arrow, C) but not complete MOG breakdown. Chronic-active lesions (E (MS090 P2B3) and F (MS090 P2B3)) had complete MOG loss in the lesional centre (asterisk) and clearly demarcated lesional borders (arrows, E and F). *Scale bar is 50µm.*

a concentration was used that was recommended by G. Arnott (Sheffield Hallam University). Slides were removed from the -80°C freezer and allowed to thaw and dry for 30 minutes at RT. Slides were then placed in ice cold acetone for 10 minutes to fix the tissue. The sections were then allowed to dry for 15 minutes at RT. A wax pen (Vector Laboratories, U.K.) was used to retain the antibody on the tissue. The primary antibody was applied in 125µl of 0.3% normal goat serum in PBS and allowed to incubate overnight at 4°C (see Table 5.2 for individual antibody concentrations). For HLA-DR and MOG staining, the primary antibody was diluted in PBS without goat serum. The following day, sections were washed three times for 5 minutes with PBS with shaking, and the secondary antibody applied and allowed to incubate for 1 hour at RT in the dark (see Table 5.2 for individual antibody concentrations). After another wash step, slides were incubated in SBB for 5 minutes at RT, rinsed with PBS eight times and mounted in Vectashield hardset mounting media with DAPI (Vector Laboratories, UK) using a coverslip (22x50mm). All incubations were performed in a humidified immunochamber (R A Lamb Ltd., U.K.). At no point after re-hydration were the tissue sections allowed to dry out. For controls, the primary antibody was substituted with an isotype/class control or omission of the primary antibody, and the procedure carried out as described above to determine the extent of non-specific staining.

5.2.5.2 Dual immunofluorescence

The first part of the staining procedure was carried out as described above, however, following the addition of the secondary antibody and the subsequent wash step, the second primary antibody was applied and allowed to incubate at RT for 1 hour in the dark. Following another wash step, the slides were then incubated with the appropriate secondary antibody for 1 hour at RT in the dark, washed, stained with SBB, rinsed and then mounted in Vectashield hardset mounting media with DAPI (as above). Controls were run in parallel, whereby an isotype control, class control or omission of the primary antibody was used as the primary antibody and then the secondary antibody applied, as described above. Either the control antibodies were applied in correct order or the primary antibody controls were swapped around to determine any cross-reactivity of the secondary antibodies with the primary antibodies.

5.2.5.3 Image analysis and capture

Tissue grading was carried out on an Olympus BX60 microscope which had a light and fluorescence function. For lesion classification, images were captured using a ColorView Soft Imaging system camera on an Olympus BX51 microscope and using the software cell[^]D version 2.3. Other images were captured using a Zeiss 510 CLSM.

Table 5.2: Details of the antibodies used in this study. Each antibody (Ab) was initially optimised or was used at a concentration previously reported or used in another study in this laboratory. As negative controls, either an isotype or class of Ab was substituted for the 1°Ab at the same concentration. Where no suitable isotype control was available, omission of the 1°Ab served as a negative control.

Antibody	Monoclonal/polyclonal	Catalogue no.	Company	Dilution
ADAM-17	Polyclonal (IgG)	ab2051	abcam	1 in 20 (25µg/ml) 1 in 50 (10µg/ml) 1 in 100 (5µg/ml) 1 in 200 (2.5µg/ml)
ADAM-17	Monoclonal (IgG1)	MAB9302	R&D Systems	1 in 60 (8µg/ml)
Fractalkine	Polyclonal (IgG)	ab25088	abcam	1 in 100 (10µg/ml) 1 in 500 (2µg/ml)
Fractalkine	Monoclonal (IgG ₁)	MAB3651	R&D Systems	1:20 (25µg/ml) 1:60 (8.3µg/ml) 1:100 (5µg/ml) 1:200 (2.5µg/ml)
vWF	Monoclonal (IgG1 kappa)	M0616	Dako	1 in 100 (3.15µg/ml)
HLA-DR	Monoclonal (IgG2b)	NCL-LN3	Novocastra	1:50 (500ng/ml)
MOG	Monoclonal (clone z12)	gift from Dr. Stephen McQuaid (Queen's University Belfast)	N/A	1 in 100 (unknown)
Rabbit IgG	Polyclonal	ab27478	abcam	1 in 20 (10µg/ml)
Mouse IgG1 kappa	Monoclonal	ab18448	abcam	1 in 159 (3.15µg/ml)
Mouse IgG2b	Monoclonal	ab18428	abcam	1 in 2000 (500ng/ml)
Alexa fluor® 488 goat anti-rabbit	N/A	A-11011	Molecular Probes	1 in 500
Alexa fluor® 568 goat anti-mouse	N/A	A-11004	Molecular Probes	1 in 500

5.3 Results

5.3.1 Tissue classification

All MS patient blocks displayed varying degrees of perivascular cuffs (Table 5.3). Most patients displayed cuffs graded at +/++, except one patient block (MS130 P2F4), which had perivascular cuffs of grade +++/++++ (Table 5.3). Only one patient block (MS090 P2B3) showed ORO positive lipid-laden macrophages at the lesion border, but these were very sparse and the block was graded + (Table 5.3). Only 2 patient blocks displayed chronic-active lesions, i.e. MOG loss and a rim of HLA-DR positive cells bordering the lesion (MS090 P2B3 and MS130 P2D3). The other blocks had MOG loss but did not display ORO positive macrophages, HLA-DR reactivity was increased but these cells did not form a hypercellular rim bordering the lesion, these blocks were thus classified as active lesions (Table 5.3). As such there was no NAWM to make a comparison with, and thus areas that were approximately, and at least, 1cm away from the demyelinated region were examined for the expression of ADAM-17 and fractalkine in a peri-lesional area as a comparison to the lesional area.

5.3.2 Determining the level of background staining

In order to determine the level of background staining from the controls, each antibody that was used in this study was examined in peri-lesional white matter and the corresponding antibody control was then examined within the same region. HLA-DR reactivity was observed within discrete regions, whereas its respective isotype control (IgG2b) showed no reactivity with the tissue (Fig 5.6 A and B). The anti-MOG antibody showed a homogenous staining pattern, whereas omission of the primary antibody control showed no background staining from the secondary antibody (Fig 5.6 C and D). vWF localised to blood vessels, whereas its isotype control (IgG1 kappa) tended to show a homogenous red hue over the whole of the tissue but did not stain any areas which would resemble blood vessels (Fig 5.6 E and F). The polyclonal antibodies for both ADAM-17 and fractalkine were of the same class, thus the same IgG class was used as a control. No isotype control was available for the monoclonal antibodies for ADAM-17 and fractalkine, so omission of the primary antibody served as a negative control. The monoclonal antibody for ADAM-17 tended to localise to blood vessels but showed a little astrocytic staining within the parenchyma, as did the polyclonal antibody (Fig 5.7 A and B). The monoclonal antibody showed more staining for the parenchymal cells and the polyclonal antibody for fractalkine localised to blood vessels (Fig 5.7 C and D). Again omission of the primary antibody did not show any background staining from the secondary antibody for the monoclonal antibodies (Fig 5.7 E). The rabbit IgG controls showed some staining within the tissue, but this was of a lesser degree than the positive staining (Fig 5.7 F).

Table 5.3: Tissue classification of MS and control blocks based upon H&E, ORO, HLA-DR and MOG stainings. For each block the brain bank classification is given and then the score for each of the staining criteria is shown with the eventual outcome for the lesion type. Tissue was graded on a + to +++ scale (++++ for H&E) in terms of ORO and HLA-DR activity. MOG staining was analysed and assessed based upon whether it was absent in the lesion. Tissue was either classed as an active lesion or as a chronic-active lesion. No block was classed as normal appearing white matter (NAWM) as there was some activity in each of these blocks.

Patient ID	Block	Brain bank classification	H&E	ORO	HLA-DR	MOG	Re-classification of lesion type
MS 074	A1C6	Lesion	++	Negative	++	Disrupted	Active
MS 074	A1E7	NAWM	++	Negative	++	Disrupted	Active
MS 090	P2E3	Lesion	+	Negative	++	Disrupted	Active
MS 090	P2B3	NAWM	+	+	+++	Absent	Chronic-active
MS 100	A2D2	Lesion	+	Negative	++	Disrupted	Active
MS 100	A2C2	NAWM	+/+++	Negative	+	Disrupted	Active
MS 109	A1C2	Lesion	+	+	++	Disrupted	Active
MS 109	A1D1	NAWM	+	+	+/++	Disrupted	Active
MS 130	P2D3	Lesion	+	+	+++	Absent	Chronic-active
MS 130	P2F4	NAWM	++++	Negative	++	Disrupted	Active
CO 11	A1B5	Control	Negative	Negative	+	Even distribution	N/A
CO 14	P2C3	Control	Negative	Negative	+	Even distribution	N/A
CO 16	A2D1	Control	Negative	Negative	++	Even distribution	N/A
CO 19	P1B2	Control	Negative	Negative	+	Even distribution	N/A
CO 20	P2B2	Control	Negative	Negative	+/++	Irregular	N/A

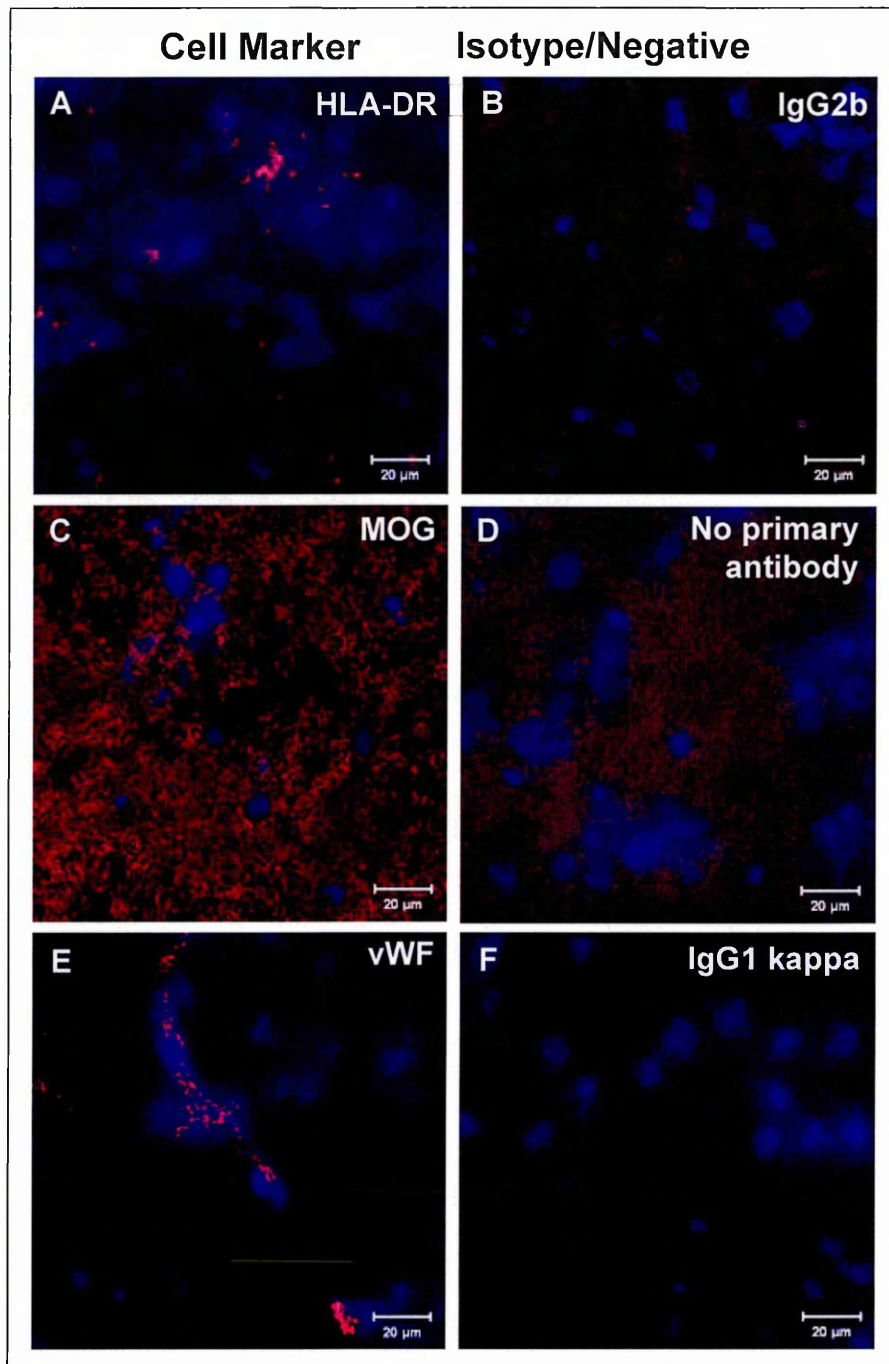


Figure 5.6: Peri-lesional white matter (MS109 A1D1) showing the cell markers used to characterise the tissue and their respective isotype/negative controls. HLA-DR (A) was used to demonstrate cellular activation, MOG (C) was used to determine the extent of myelination and von Willebrand Factor (vWF) (E) was used to identify blood vessels. For HLA-DR (B) and vWF (F), isotype controls were used at the same concentration as the primary antibody. Omission of the primary antibody served as a negative control for the MOG staining (D). Immunohistochemical examination of each protein was carried out on serial sections from each tissue block. *Scale bar is 20μm.*

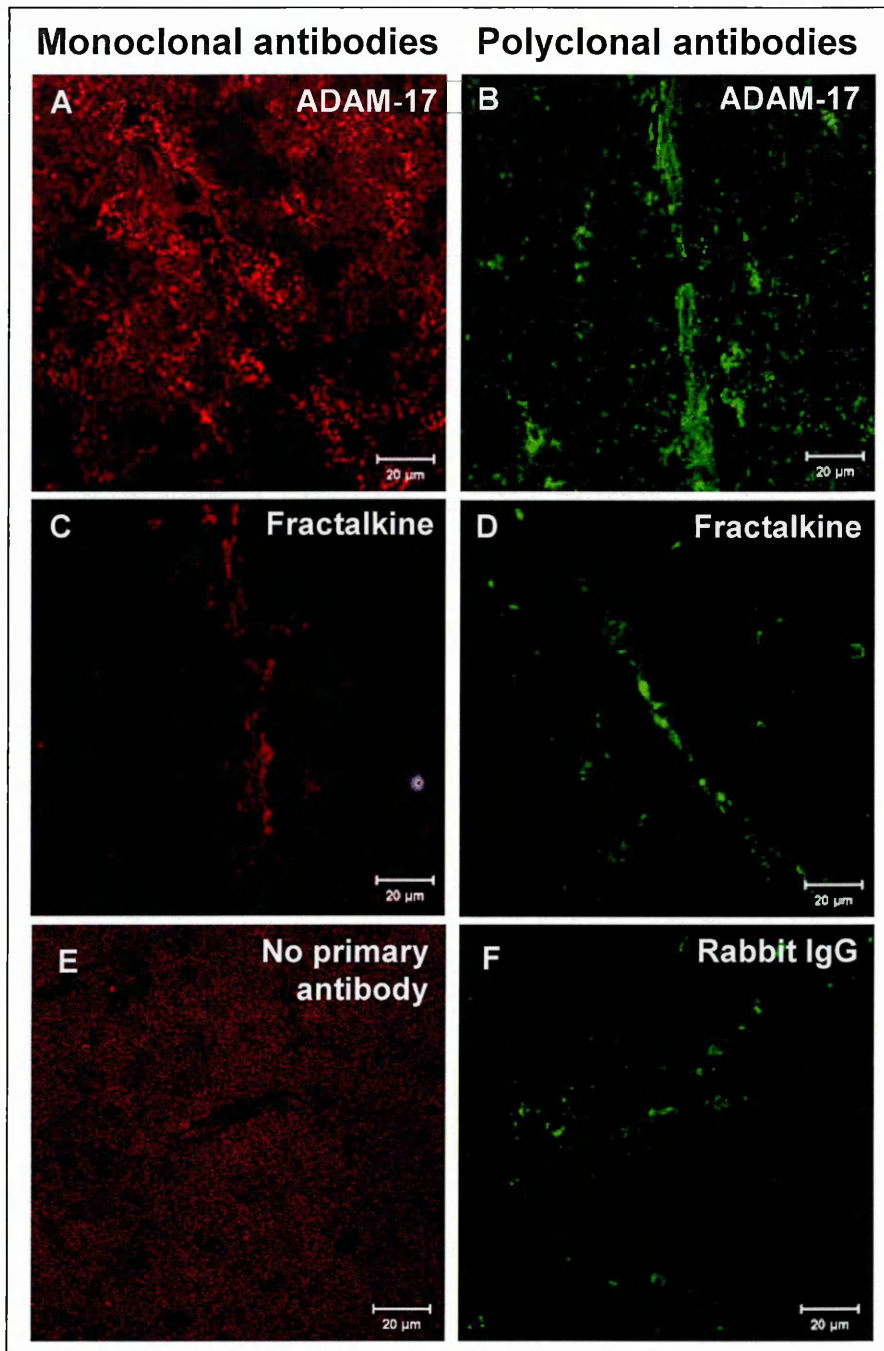


Figure 5.7: Peri-lesional white matter (MS109 A1D1) showing the different antibody combinations to demonstrate ADAM-17 and fractalkine expression. ADAM-17 expression was determined using a monoclonal (A) and polyclonal antibody (B), and fractalkine expression using a monoclonal (C) and polyclonal antibody (D). Omission of the primary antibody was used as a control for the monoclonal antibody (E), whereas a rabbit polyclonal IgG was used as a control for the polyclonal antibody (F). Immunohistochemical examination of each protein was carried out on serial sections from each tissue block. *Scale bar is 20 μ m.*

5.3.3 Selection of appropriate antibodies to study expression of ADAM-17 and fractalkine

To determine which antibody combination to use for examining the dual expression of ADAM-17 and fractalkine, the monoclonal and polyclonal antibodies for both proteins was examined in each tissue type. Within the control tissue, monoclonal anti-ADAM-17 staining appeared to more readily stain astrocytic processes (Figure 5.8 A) whereas the polyclonal antibody tended to stain cell bodies (Figure 5.8 B). The monoclonal antibody against fractalkine tended to also stain parenchymal structures such as astrocytic processes whereas the polyclonal antibody against fractalkine more visibly stained blood vessels. The same patterns were observed in peri-lesional white matter tissue, whereby the monoclonal antibodies stained the astrocytic processes but the polyclonal antibodies tended to stain cell bodies and blood vessels (refer back to Figure 5.7 A-D). The same patterns were seen in lesional tissue (Figure 5.9 A-D) and within perivascular cuffs (Figure 5.10 A-D).

As ADAM-17 has been reported to localise within astrocytes, endothelial cells and macrophages (Goddard et al., 2001; Plumb et al., 2006) and fractalkine was seen more readily in blood vessels, which was of interest due to the *in vitro* studies on hCMEC/D3 endothelial cells in the previous chapters, it was decided to study ADAM-17 using the monoclonal antibody and fractalkine using the polyclonal antibody.

5.3.4 Expression of ADAM-17 and fractalkine in blood vessels of MS and control CNS white matter using polyclonal antibodies

ADAM-17 expression within blood vessels of control white matter generally showed a homogenous pattern of distribution (Figure 5.11), but also appeared to aggregate at the basolateral regions of the endothelial cells of the blood vessel. The pattern of distribution did not usually show a preference for the luminal or abluminal surface of the vessel. In some instances, where the expression of ADAM-17 was increased on the abluminal side of the vessel, it appeared to be associated with the glial limitans. Fractalkine expression within blood vessels of control white matter also showed an even distribution (Figure 5.11), and did not aggregate at the basolateral interfaces of the endothelial cells. Fractalkine expression sometimes appeared as bright punctate vesicles within the cells. The chemokine/adhesion molecule was generally not observed to polarise to either the luminal or abluminal surfaces of the blood vessel.

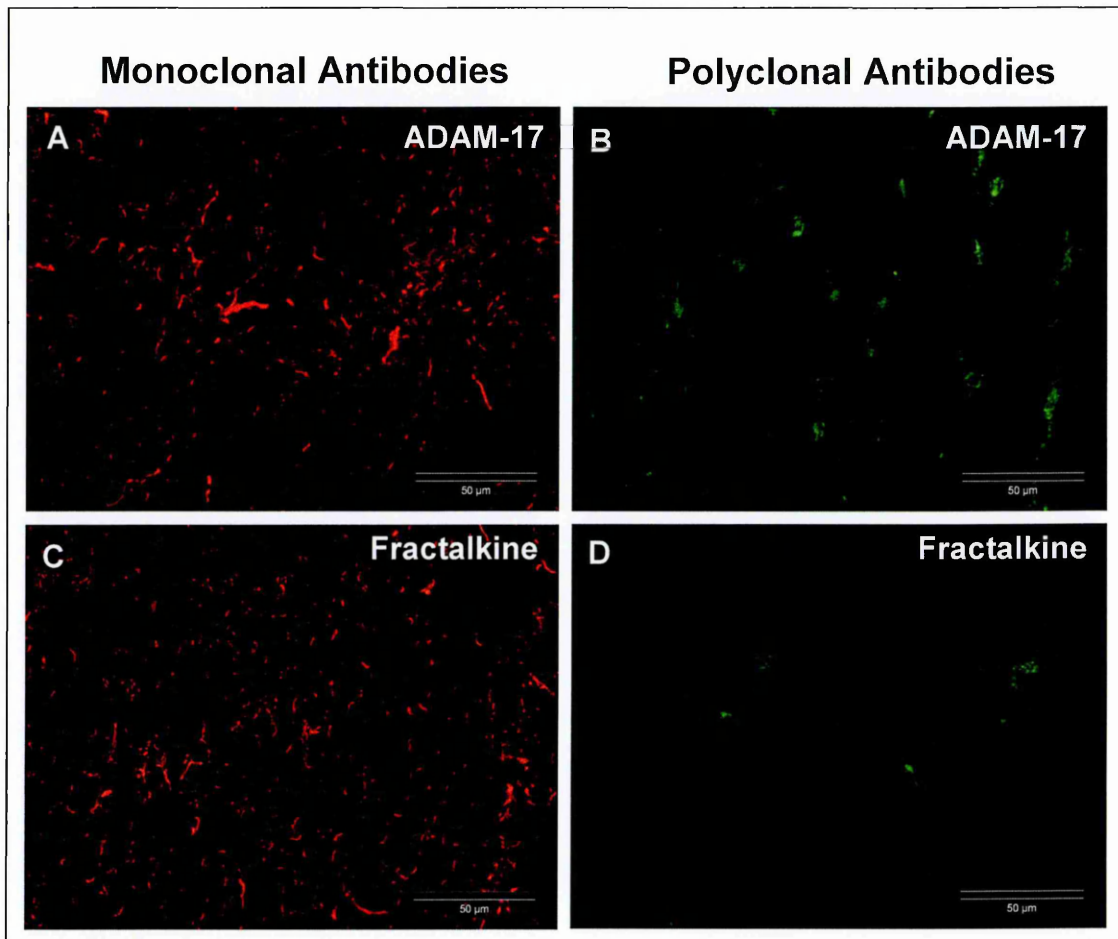


Figure 5.8: White matter control tissue (CO14 P2C3) showing the different antibody combinations to demonstrate ADAM-17 and fractalkine expression using monoclonal (red) and polyclonal (green) antibodies. ADAM-17 expression was determined using a monoclonal (A) and polyclonal antibody (B), and fractalkine expression using a monoclonal (C) and polyclonal antibody (D). Isotype and negative controls were run in parallel. Immunohistochemical examination of each protein was carried out on serial sections from each tissue block. Scale bar is 20 μ m.

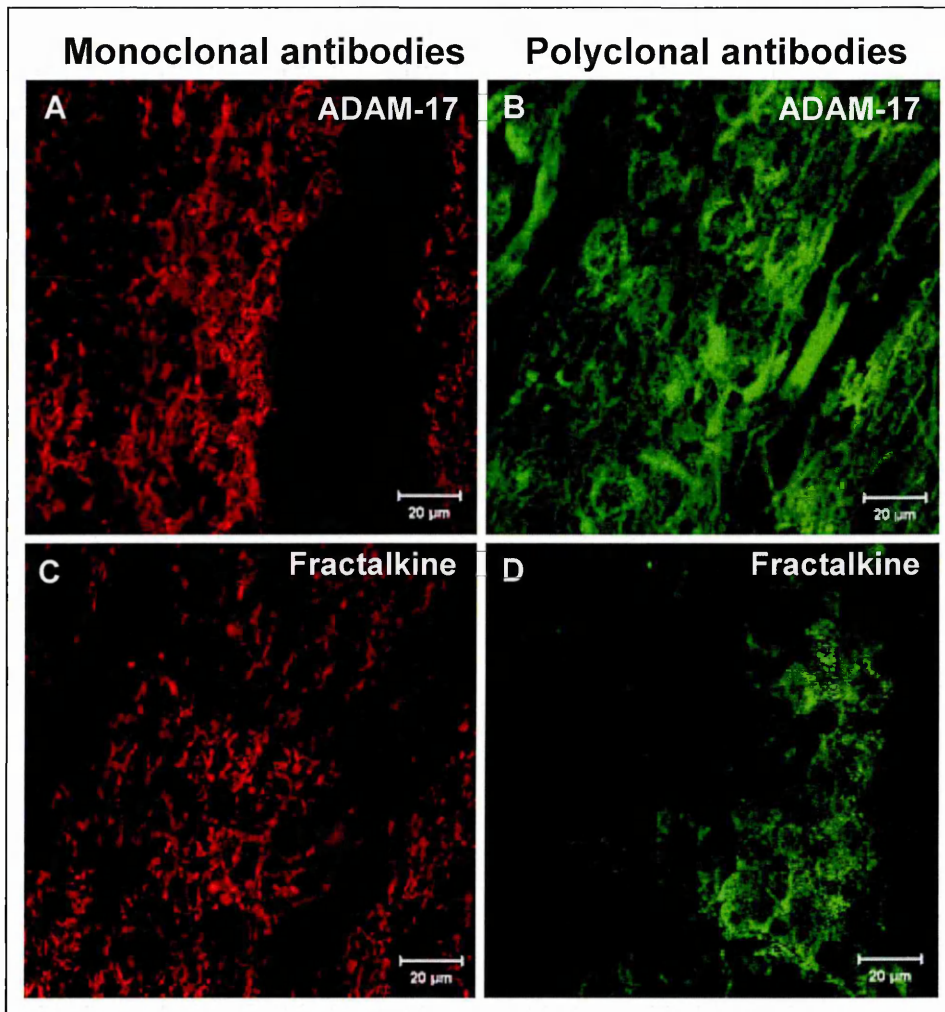


Figure 5.9: White matter lesional border (MS090 P2B3) showing ADAM-17 and fractalkine immunoreactivity using monoclonal (red) and polyclonal (green) antibodies. ADAM-17 expression was determined using a monoclonal (A) and polyclonal antibody (B), and fractalkine expression using a monoclonal (C) and polyclonal antibody (D). Isotype and negative controls were run in parallel. Immunohistochemical examination of each protein was carried out on serial sections from each tissue block. *Scale bar is 20 μ m.*

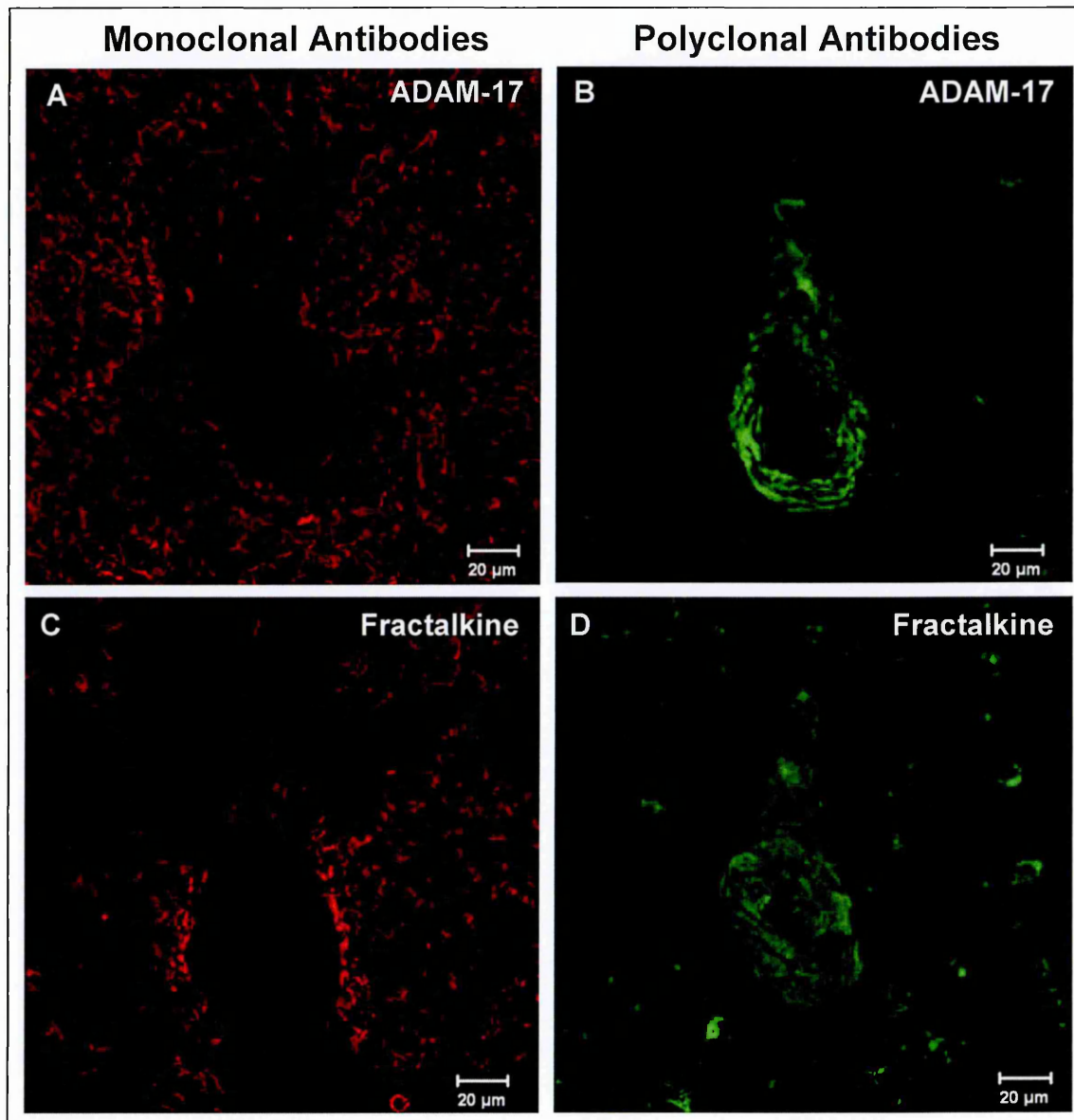


Figure 5.10: White matter perivascular cuff (MS130 P2F4) showing ADAM-17 and fractalkine immunoreactivity using monoclonal (red) and polyclonal (green) antibodies. ADAM-17 expression was determined using a monoclonal (A) and polyclonal antibody (B), and fractalkine expression using a monoclonal (C) and polyclonal antibody (D). Isotype and negative controls were run in parallel. Immunohistochemical examination of each protein was carried out on serial sections from each tissue block. *Scale bar is 20μm.*

The amount of perivascular cuffing around the blood vessels within the MS white matter tended to be of a grade + or ++ except for one case where grades of 3+ and 4+ were observed (MS130 P2F4). ADAM-17 expression in 1+/2+ blood vessels, using the polyclonal antibody, revealed that ADAM-17 showed a homogenous pattern of expression (Figure 5.12), which was not polarised to either the luminal or abluminal wall of the vessel. In some instances, ADAM-17's expression appeared increased with a heterogenous pattern of expression, which corresponded to the basolateral interfaces of the endothelial cells; this altered pattern of expression did not correspond to an altered expression of MOG and HLA-DR. Fractalkine expression also showed a homogenous, non-polarised expression pattern, and showed a stronger expression pattern within the cells of the cuff (Fig 5.12). The cuff that showed a heterogenous pattern of expression for ADAM-17 also showed a heterogenous expression pattern for fractalkine. Two inflammatory cuffs of +++/++++ were examined (MS130 P2F4), and revealed a very bright and intense ADAM-17 staining on the endothelium, which was not as homogenous as in the other vessels in this section. Fractalkine expression within this vessel was weakly expressed. The other vessel with a perivascular cuff showed a homogenous, less bright staining pattern for ADAM-17. The fractalkine staining within this cuff was dispersed and observed also within the lumen of the vessel.

Within the lesional tissue, ADAM-17 expression was homogenous and sometimes appeared increased (Figure 5.13). An increase in expression could not be found to be associated with an increase in HLA-DR reactivity however. Fractalkine was also homogeneously expressed (Figure 5.13). A similar homogenous pattern of expression of ADAM-17 and fractalkine was also observed within the peri-lesional white matter (Figure 5.14)

5.3.5 Expression of ADAM-17 and fractalkine in the parenchyma and perivascular cuffs using dual labelling

To determine dual expression of ADAM-17 and fractalkine, the expression of the proteins was examined using monoclonal and polyclonal antibodies, respectively. In control tissue, ADAM-17 expression within the parenchyma was mainly associated with astrocytic processes, and was increased in astrocytes of the glial limitans (Figure 5.15). Fractalkine expression within the white matter parenchyma tended to localise to cell bodies, which belonged to the ADAM-17 expressing cell processes; ADAM-17 was also observed in the same cell bodies but was less intense than the cell process staining (Figure 5.15). In addition, fractalkine was observed to stain axonal processes; these also faintly stained positive for ADAM-17, but not as intense as the astrocytic processes.

When ADAM-17 expression was examined in perivascular cuffs of grades +/++, using the monoclonal antibody, staining was evident in astrocytes and appeared increased in the glial limitans (Figure 5.16). In some instances astrocytic staining was more continuous and in others it was intermittent and difficult to determine whether it was astrocytic. Fractalkine expression was more homogenous and was increased within the cells of the cuff (Figure 5.16). In two inflammatory cuffs of +++/++++ (MS130 P2F4), ADAM-17 expression using the monoclonal antibody showed a bright, intense staining which was increased in the glial limitans whereas fractalkine expression within this vessel was weak. The other vessel showed a bright staining pattern for ADAM-17 but was difficult to distinguish endothelial cells from the cells in the perivascular cuff.

Within chronic-active lesions, ADAM-17 expression was visibly up-regulated in agreement with the previous report by Plumb et al., (2006), and was most prominent in astrocytes (Figure 5.17). Fractalkine expression within this type of lesion appeared to co-localise with macrophages in the active border, and was also seen within long processes adjacent to the lesion (Figure 5.17 and 5.18), which could correspond neuronal processes but cell-type specific markers would need to be utilised to confirm this statement. Fractalkine was also observed in other cell types but without cell-type specific markers it was difficult to distinguish the phenotype of these cells. Fractalkine appeared moderately expressed within this tissue type. Within the peri-lesional white matter, ADAM-17 staining was clearly reduced and fractalkine expression appeared to be mainly localised to blood vessels (Figure 5.19). The lack of macrophages within this area contributed to the decrease in expression of fractalkine.

Within active lesions, ADAM-17 expression was seen within astrocytes and appeared increased around the glial limitans. Fractalkine expression within this lesion type, however, was reduced and appeared to be mainly localised to blood vessels and other cell types, which were difficult to distinguish (Figure 5.20). Within the peri-lesional white matter of this tissue type, ADAM-17 expression within the parenchymal astrocytes sometimes was more interrupted and fractalkine expression showed the same pattern of distribution as within the chronic lesion (Figure 5.20).

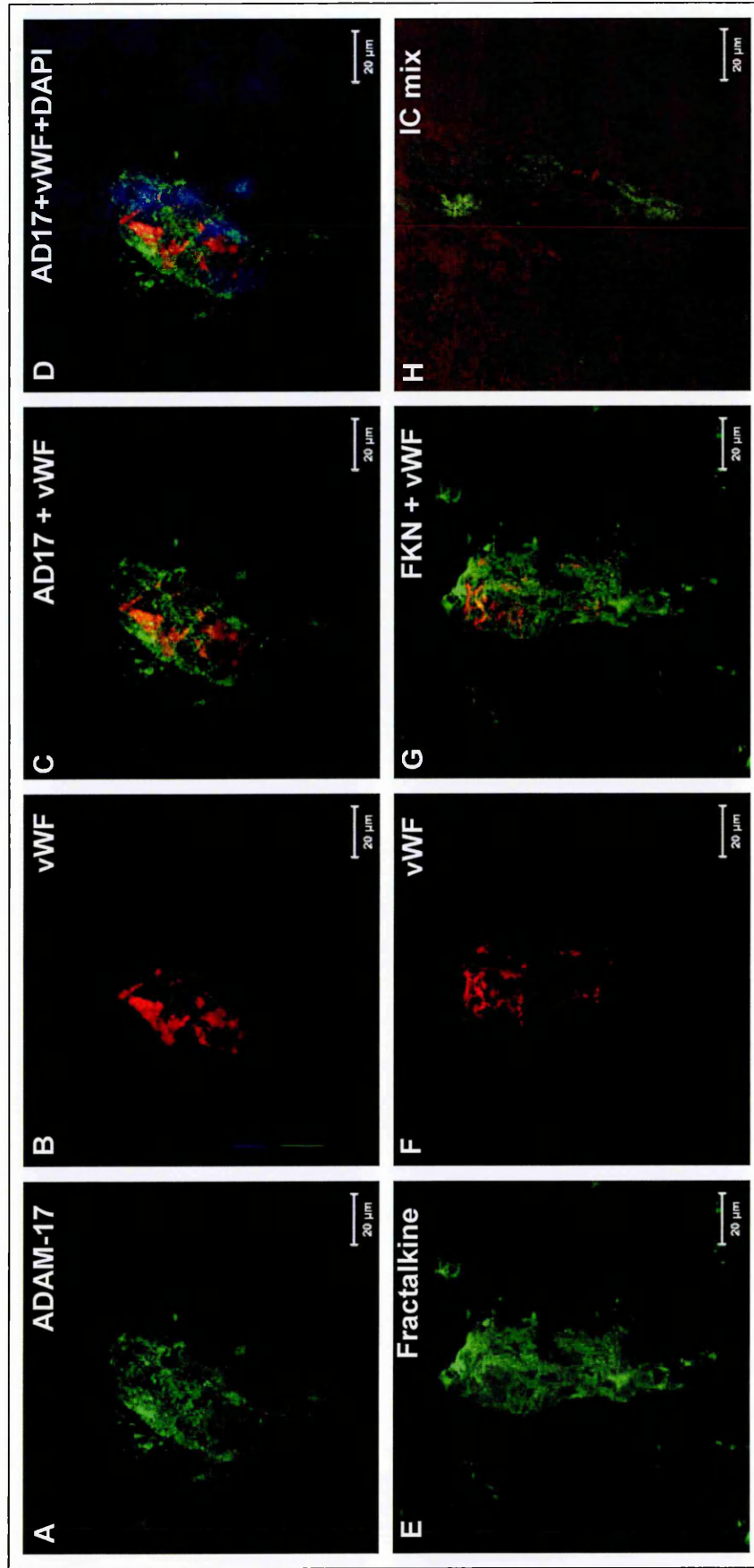


Figure 5.11: Expression of ADAM-17 and fractalkine in control white matter blood vessels (CO11 A1B5). ADAM-17 (AD17) (A) and von Willebrand Factor (vWF) (B) expression and the dual expression of the proteins (C). Fractalkine (FKN) (E) and vWF expression (F) and their co-localisation (G). ADAM-17 and vWF with DAPI as counterstain are shown (D). Isotype controls (IC) were processed in parallel to the positive stainings, either using the antibodies in the same order as the positives (not shown) or mixing the primary and secondary antibody combinations (H). Immunohistochemical examination of each protein was carried out on serial sections from each tissue block. Scale bar is 20μm.

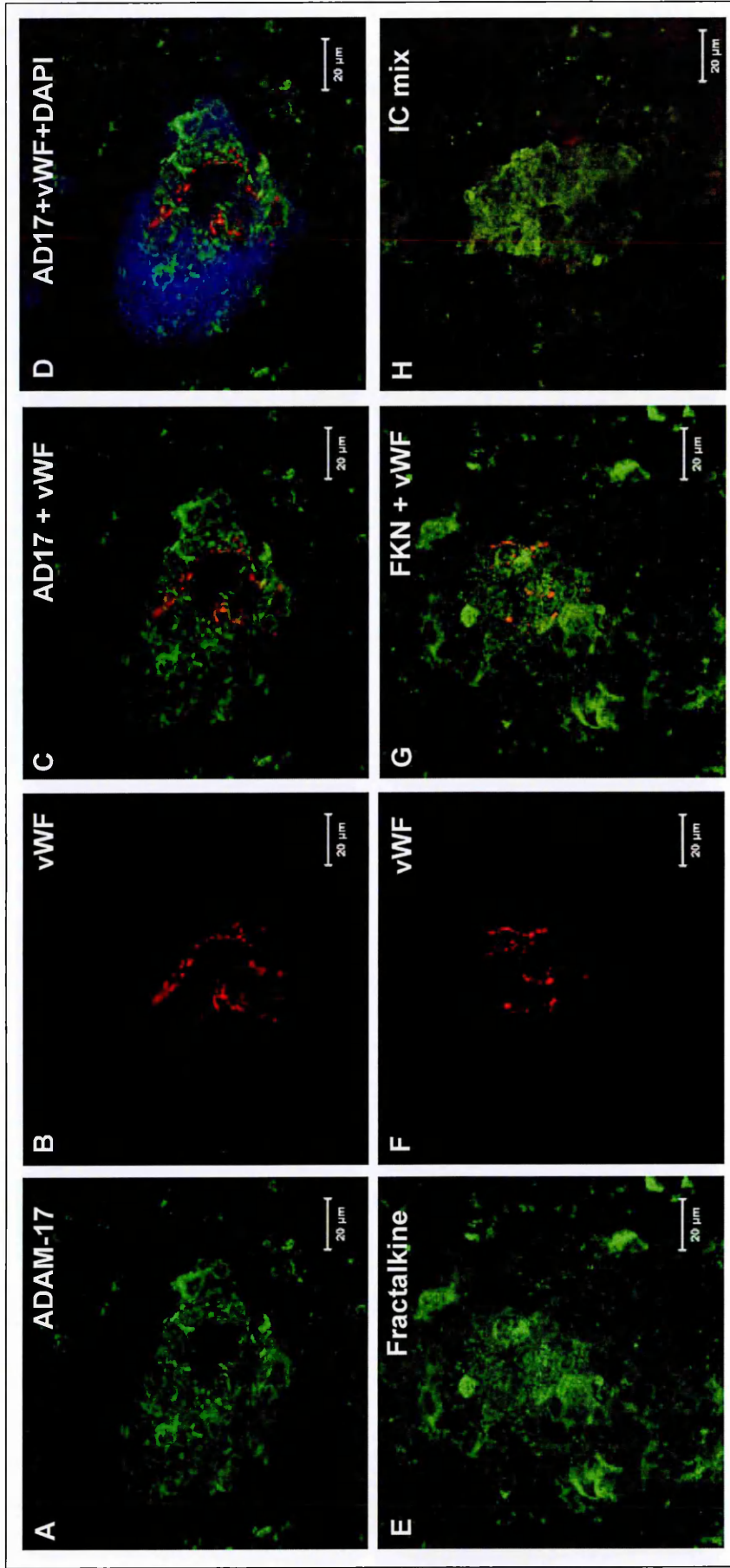


Figure 5.12: Expression of ADAM-17 and fractalkine in a white matter perivascular cuff (MS130 P2F4). ADAM-17 expression (AD17) (A) is localised both within the endothelium shown by the expression of von Willebrand Factor (vWF) (B and C) and also within small cells of the cuff. Fractalkine expression (FKN) (E) is localised to the endothelium as shown by the expression of vWF (F and G). ADAM-17 and vWF with DAPI as counterstain are shown (D). Isotype controls (IC) were processed in parallel to the positive stainings, either using the antibodies in the same order (not shown) as the positives or mixing the primary and secondary antibody combinations (H). Immunohistochemical examination of each protein was carried out on serial sections from each tissue block. Scale bar is 20µm.

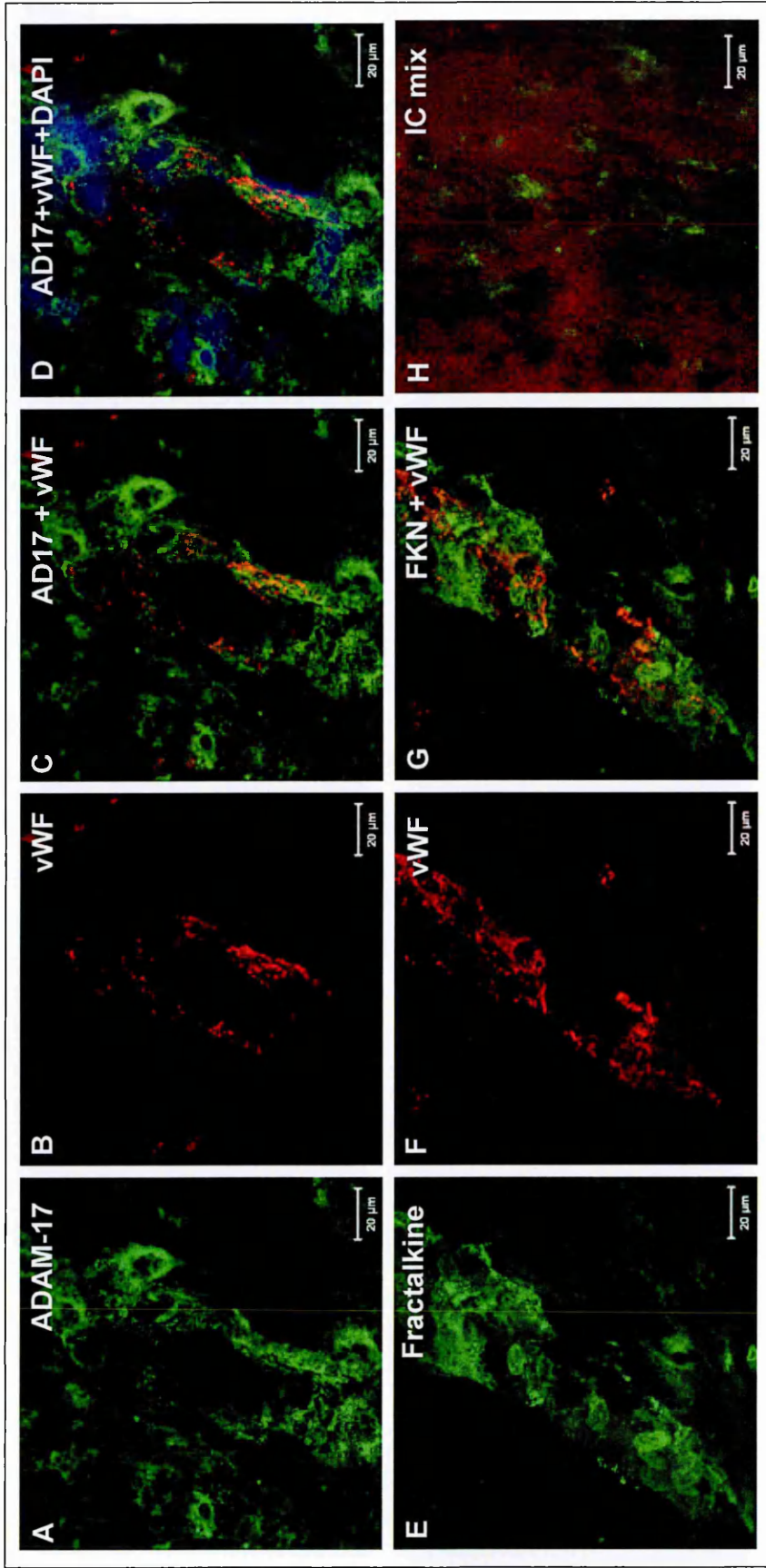


Figure 5.13: Expression of ADAM-17 and fractalkine in lesional white matter (MS090 P2B3). ADAM-17 (AD17) (A) and von Willebrand Factor (vWF) (B) expression and the dual expression of the proteins (C). Fractalkine (FKN) (E) and vWF expression (F) and their co-localisation (G). ADAM-17 and vWF with DAPI as counterstain are shown (D). Isotype controls (IC) were processed in parallel to the positive stainings, either using the antibodies in the same order as the positives (data not shown) or mixing the primary and secondary antibody combinations (H). Immunohistochemical examination of each protein was carried out on serial sections from each tissue block. *Scale bar is 20μm.*

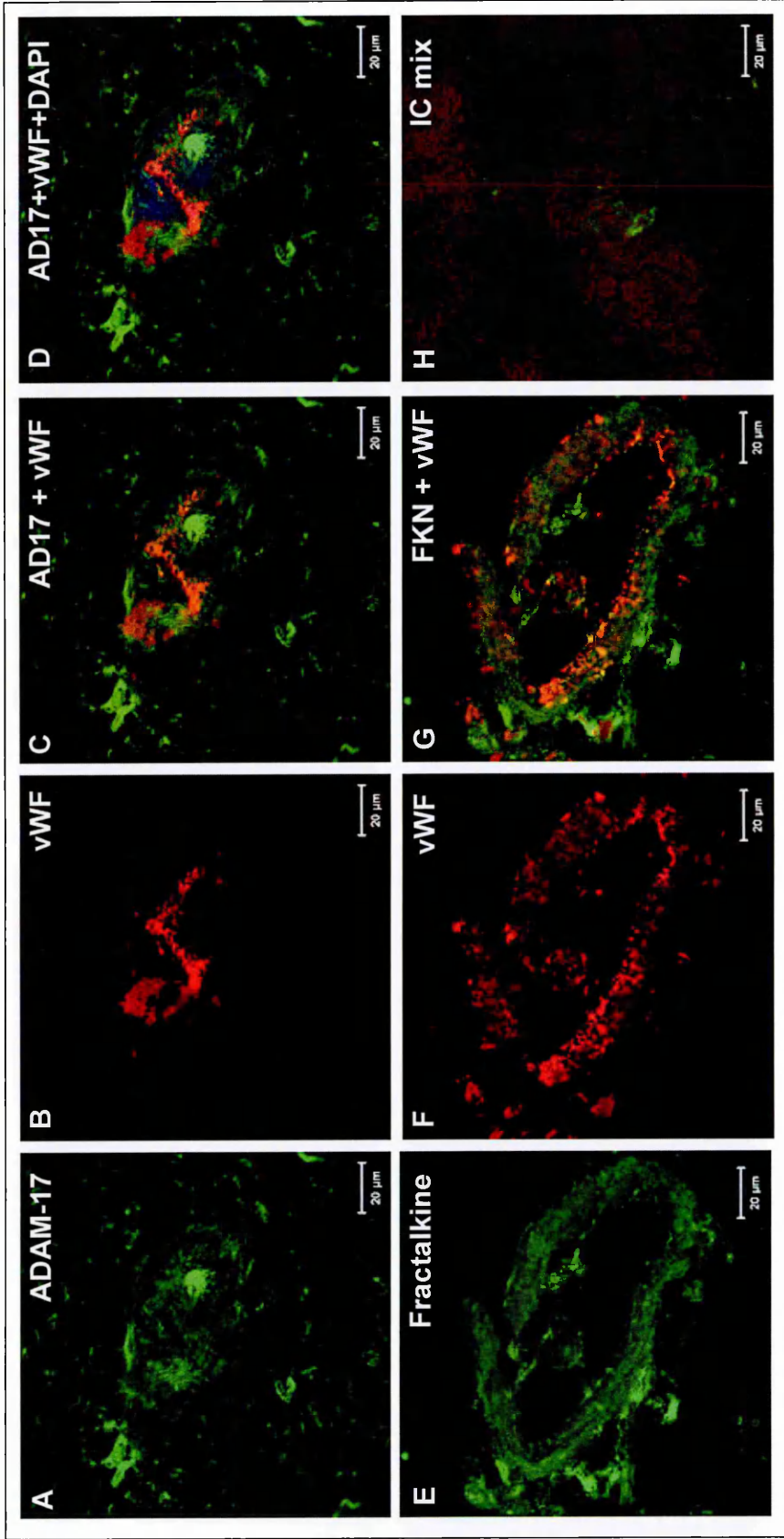


Figure 5.14: Expression of ADAM-17 and fractalkine in peri-lesional white matter (MS090 P2B3). ADAM-17 (AD17) (A) and von Willebrand Factor (vWF) (B) expression and the dual expression of the proteins (C). Fractalkine (FKN) (E) and vWF expression (F) and their co-localisation (G). ADAM-17 and vWF with DAPI as counterstain are shown (D). Isotype controls (data not shown) or mixing the primary and secondary antibody combinations (H). Immunohistochemical examination of each protein was carried out on serial sections from each tissue block. Scale bar is 20µm.

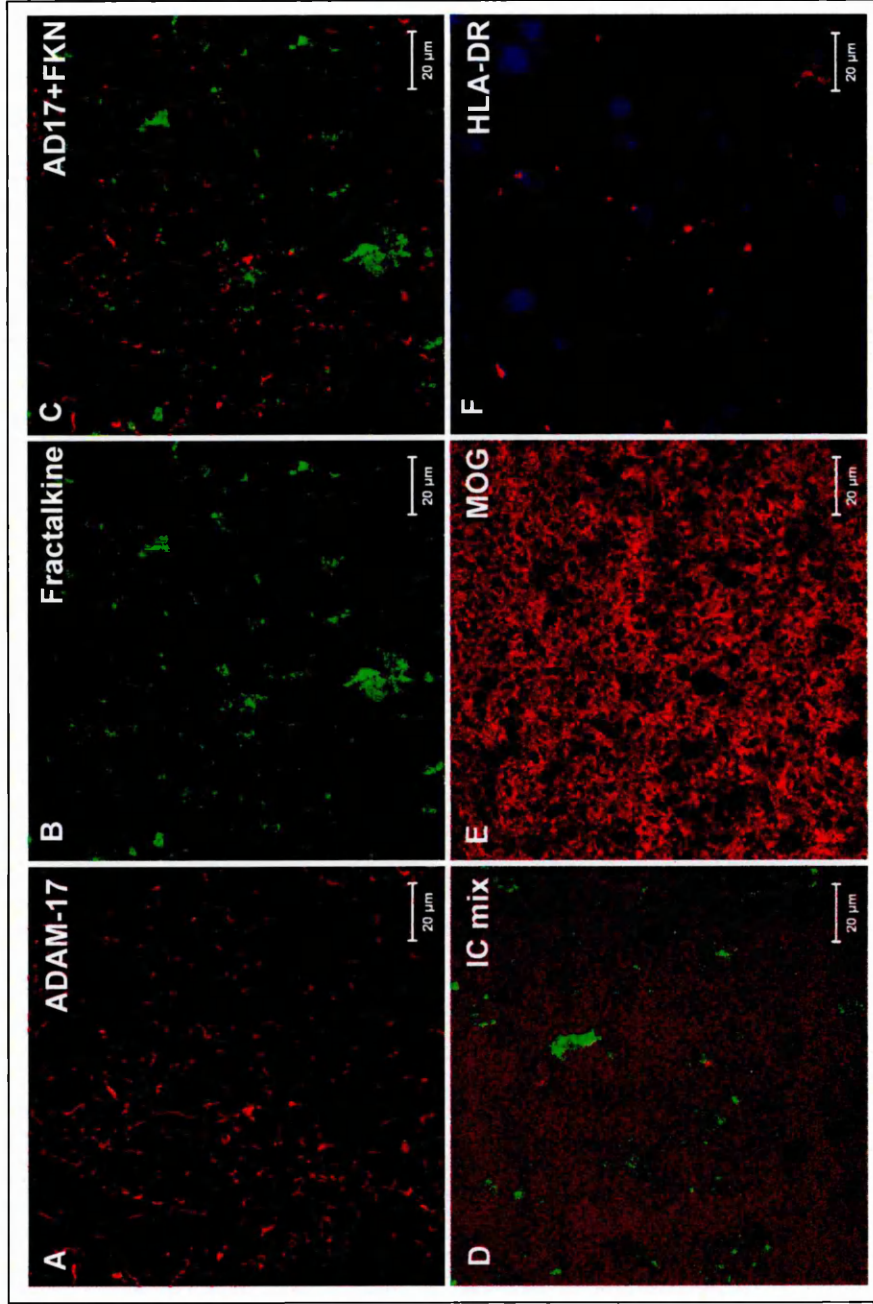


Figure 5.15: Dual expression of ADAM-17 and fractalkine in control white matter (CO16 A2D1). ADAM-17 (A) expression was examined using a monoclonal antibody and fractalkine (B) expression was examined using a polyclonal antibody. The composite images are shown (C). The levels of non-specific (IC, isotype control) (D), MOG (E) and HLA-DR (F) reactivity were also examined in parallel. DAPI was used as a counterstain (F). Immunohistochemical examination of each protein was carried out on serial sections from each tissue block. Scale bar is 20µm.

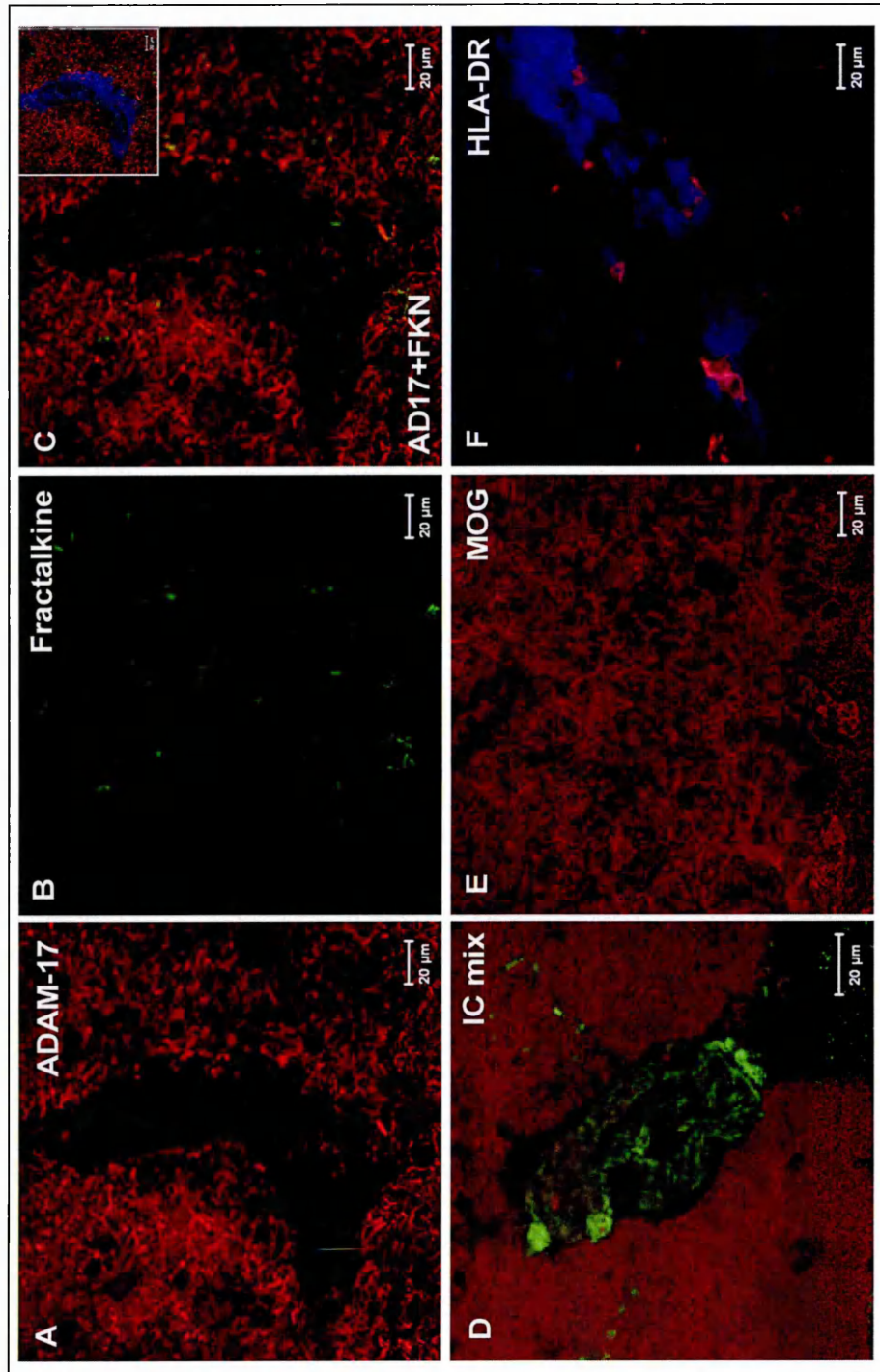


Figure 5.16: Dual expression of ADAM-17 and fractalkine in a white matter perivascular cuff (MS130 P2F4). ADAM-17 (A) expression was examined using a monoclonal antibody and fractalkine (B) expression was examined using a polyclonal antibody. The composite images are shown (C), highlighting the perivascular cuff (DAPI) (insert). The levels of non-specific (IC, isotype control) (D), MOG (E) and HLA-DR (F) reactivity were also examined in parallel. DAPI was used as a counterstain (F). Immunohistochemical examination of each protein was carried out on serial sections from each tissue block. *Scale bar is 20μm.*

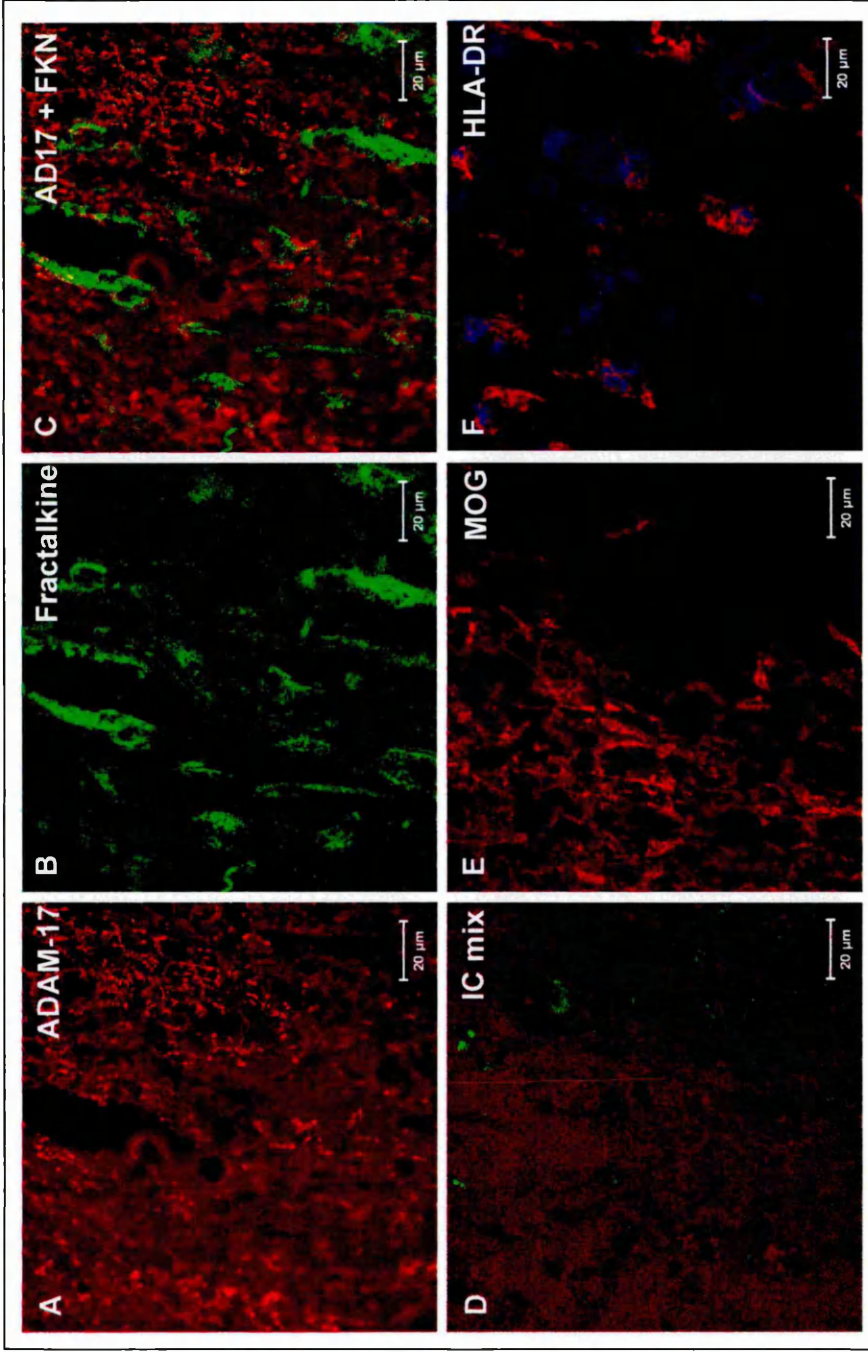


Figure 5.17: Dual expression of ADAM-17 and fractalkine in the white matter of an MS chronic-active lesion (MS090 P2B3). ADAM-17 (AD17) (A) expression was examined using a monoclonal antibody and fractalkine (FKN) (B) expression was examined using a polyclonal antibody. The composite images are shown (C). The levels of non-specific (IC, isotype control) (D), MOG (E) and HLA-DR (F) reactivity were also examined in parallel. DAPI was used as a counterstain (F). Immunohistochemical examination of each protein was carried out on serial sections from each tissue block. Scale bar is 20 μ m.

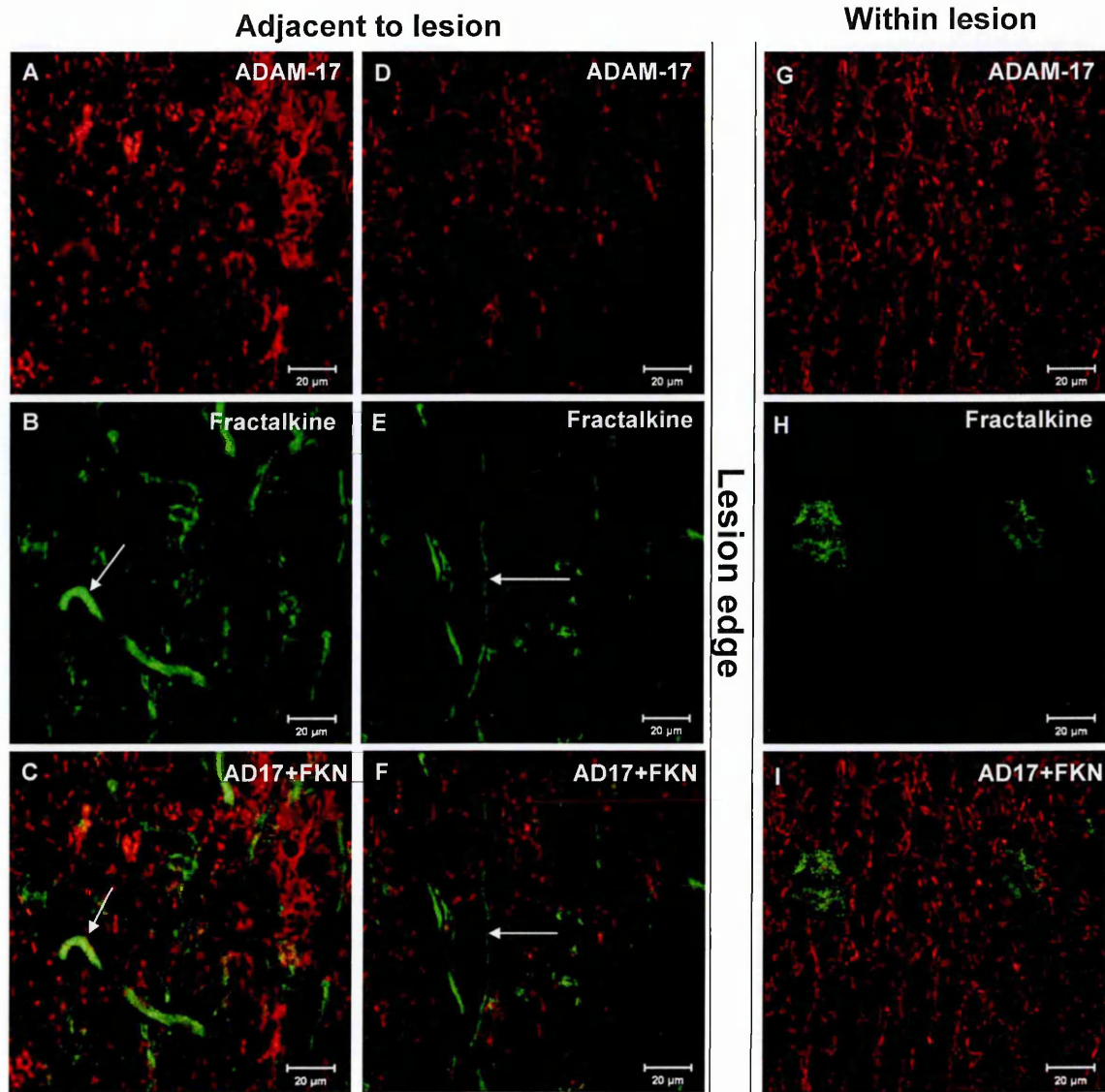


Figure 5.18: Dual expression of ADAM-17 and fractalkine next to and within the white matter MS lesion (MS090 P2B3). ADAM-17 (A, D and G) expression was examined using a monoclonal antibody and fractalkine (B, E and H) expression was examined using a polyclonal antibody. The composite images are shown (C, F and I). Adjacent to the MS plaque, fractalkine can be seen in axonal processes (B and E, arrows), whereas within the plaque, fractalkine was observed in cell bodies (H). Immunohistochemical examination of each protein was carried out on serial sections from each tissue block. *Scale bar is 20μm.*

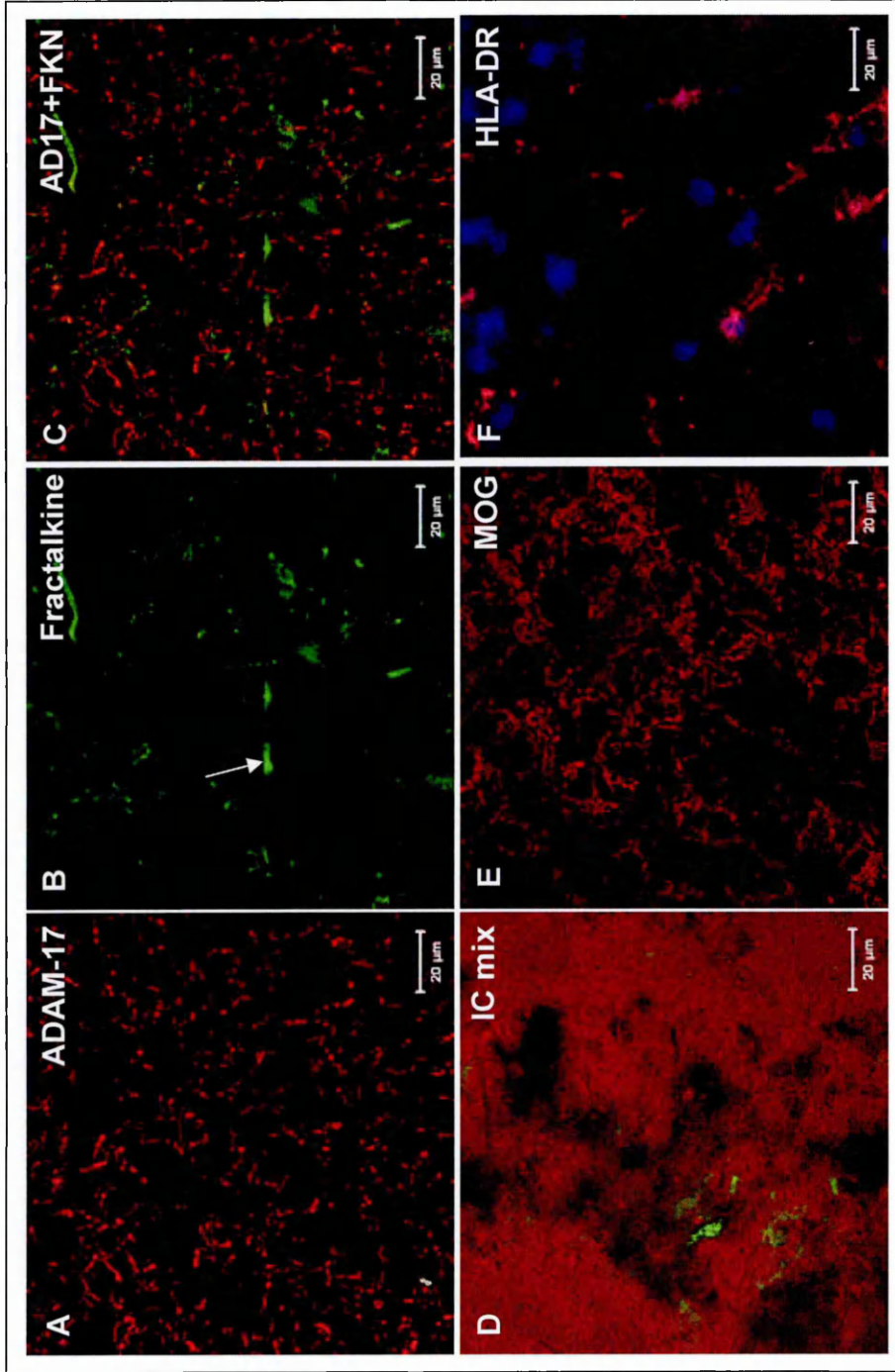


Figure 5.19: Dual expression of ADAM-17 and fractalkine in peri-lesional white matter (MS090 P2B3). ADAM-17 (A) expression was examined using a monoclonal antibody and fractalkine (B) expression was examined using a polyclonal antibody. The composite image is shown (C). The levels of non-specific (IC, isotype control) (D), MOG (E) and HLA-DR (F) reactivity were also examined in parallel. DAPI was used as a counterstain (F). Immunohistochemical examination of each protein was carried out on serial sections from each tissue block. Scale bar is 20µm.

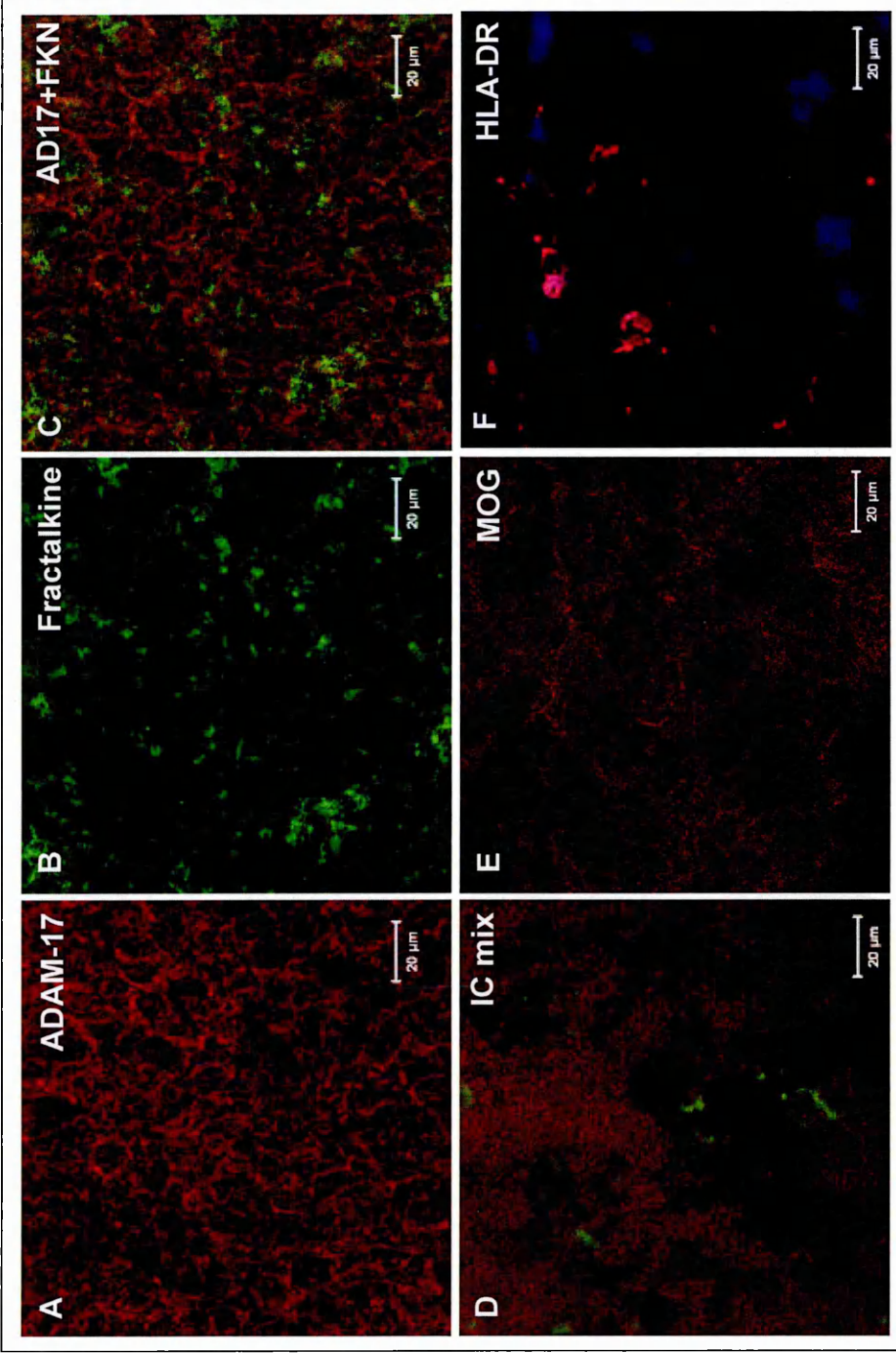


Figure 5.20: Dual expression of ADAM-17 and fractalkine in active white matter (MS130 P2F4). ADAM-17 (A) expression was examined using a monoclonal antibody and fractalkine (B) expression was examined using a polyclonal antibody. The composite image is shown (C). The levels of non-specific (IC, isotype control) (D), MOG (E) and HLA-DR (F) reactivity were also examined in parallel. DAPI was used as a counterstain (F). Immunohistochemical examination of each protein was carried out on serial sections from each tissue block. Scale bar is 20µm.

5.4 Discussion

Previous work has demonstrated that fractalkine is localised to various cells of the CNS, however, only one study has completed a comprehensive study of fractalkine expression in the human MS brain; this was restricted to studying astrocytic expression of the chemokine/adhesion molecule (Hulshof et al., 2003). ADAM-17 expression has also been studied within the MS brain and is increased in expression within lesions (Plumb et al., 2006).

Here, the expression of fractalkine in human control and MS brain tissue was studied in relation to ADAM-17 expression. Previous work has shown that fractalkine expression is expressed at the luminal side of the endothelium in coronary and in larger cerebral blood vessels (Harrison et al., 1999; Pan et al., 1997). This present study found that fractalkine is expressed homogenously throughout the blood vessel, sometimes showing a polarised distribution at the endothelium, but this was infrequent. This could be due to the fact that fractalkines expression was examined in post-capillary venules and not the larger cerebral blood vessels. Other studies have reported an up-regulation of fractalkine on cerebral endothelial cells during CNS inflammation, e.g. during EAE (Pan et al., 1997; Fischer et al., 2000). Fractalkine is also up-regulated in response to treatment with various pro-inflammatory cytokines that have been implicated with MS pathogenesis (Bazan et al., 1997; Garcia et al., 2000; Imaizumi et al., 2000; Hatakeyama et al., 2004). Fractalkine expression was moderately expressed in all tissue types and only showed a decrease in expression in active lesions in this study. Low expression levels of the chemokine/adhesion molecule have been reported in endothelial cells in the colon of Crohn's and ulcerative colitis patients (Lucas et al., 2001). Fractalkine was expressed constitutively both within the blood vessels and parenchyma of control tissue. This is interesting given that *in vitro* studies of endothelial expression of fractalkine reported it to only be induced by various cytokines (Bazan et al., 1997), suggesting the chemokine is only expressed under pathological conditions. Other cells of the parenchyma expressed fractalkine, but further dual labelling should be performed with various cell type specific markers, e.g. neurons, macrophages, etc, to determine their phenotype. Within the chronic-active lesion fractalkine appeared to stain cell bodies whereas adjacent to this area, and next to the lesion border, fractalkine was observed to stain neuronal processes. Cells at the active border of chronic-active lesions were also positive for fractalkine, which is in agreement with the previous study by Hulshof et al. (2003), which reported a weak immunoreactivity for fractalkine in macrophages in this region.

As expected ADAM-17 expression was increased in MS lesions, as this has already been reported (Plumb et al., 2006), however, the previous study quantified the data using an inclusion method, i.e. grade + corresponds to purely endothelial

expression; grade ++ endothelial and astrocytic expression; +++ abundant expression in the parenchyma (Plumb et al., 2006), however, in this present study increased expression was examined by comparing vessels alone. ADAM-17 expression within blood vessels was generally homogeneously expressed, occasionally showing an aggregation at what appeared to be the abluminal surface of the endothelial cells. When ADAM-17 expression was compared between the different grades of inflammation, in only one instance was ADAM-17 expression increased in an inflammatory cuff of +++/++++ (MS130 P2F4) compared to similar grades and +/-++ graded inflammatory cuffs. Suggesting this could be a localised phenomenon, or could signify that with increasing inflammatory burdens surrounding blood vessels, ADAM-17 is up-regulated. Due to restrictions in the study, e.g. focusing upon post-capillary venules, only 2 blood vessels of this grade were observed; the other vessel of this grade did not show an increase in ADAM-17 expression. Further tissue needs examining with varying grades of inflammation to determine whether this single observation is biologically significant. As ADAM-17 is responsible for the shedding of TNF (Black et al., 1997; Moss et al., 1997) and fractalkine (Garton et al., 2001) and both of these are involved in attraction and extravasation of leukocytes, it is reasonable to hypothesise that an increase in endothelial ADAM-17 expression could result in an increased shedding of these inflammatory mediators, which in turn would cause the attraction and migration of immune cells into the CNS. Thus, the level of ADAM-17 expression could be directly proportional to the extent of inflammation, i.e. amount of immune cells within the perivascular cuff.

To better understand the role of fractalkine in MS, research could be extended to the animal model of MS, EAE. Whereby, fractalkine expression could be knocked down. However, caution must be emphasised when interpreting experimental results from EAE with regard to fractalkine, as murine T cells are unresponsive to fractalkine, suggesting that they lack the CX3CR1 receptor (Haskell et al., 2001). Also it does not appear that fractalkine plays a prominent role in EAE as CX3CR1-deficient mice and wild-type litter mates have a similar disease severity (Haskell et al., 2001). However, altered peptide ligand (APL) treated mice show a decreased expression of fractalkine, which correlates with reduced inflammation in PLP-induced EAE mice (Fischer et al., 2000). The findings of Chapter 3 and that of other groups (Hulfshof et al., 2003; Kastenbauer et al., 2003) suggest that fractalkine may act more as a chemokine than an adhesion molecule in the CNS under pro-inflammatory and pathological conditions. Fractalkine could be acting on CNS cells if it was shed from the abluminal surface of the endothelium, however as has previously been reported, there is a greater amount of serum fractalkine than CSF fractalkine in MS patients (Kastenbauer et al., 2003). This highlights that endothelial cell secretion of fractalkine occurs predominantly into

the lumen of the blood vessel, but other cells could also contribute to the levels of fractalkine within serum. None-the-less, fractalkine expression is up-regulated in brain inflammation (Pan et al., 1997) and the brain has been shown to be the greatest "reservoir" for the chemokine, whereby aqueous brain extracts have been shown to contain greater than 3000pg/mg of the chemokine (Cardona et al., 2006; Pan et al., 1997). Secreted fractalkine in the CNS could be acting upon local microglia causing the secretion of MMPs which facilitate the breakdown of the BBB and also the destruction of MBP in MS as has previously been reported (Gijbels et al., 1993). Fractalkine has also been shown to mediate cell survival of microglia by inhibiting Fas ligand-induced cell death *in vitro* (Boehme et al., 2000).

Fractalkine expression within the brain is restricted to discrete regions, which include the cortex, hippocampus, caudate putamen, thalamus, and olfactory bulb, but is absent or significantly reduced in cerebellum, brainstem and white matter regions, including the corpus collosum and fimbria/fornix (Harrison et al., 1998). Fractalkine has been shown to stimulate chemotaxis and elevated intracellular calcium levels in microglia. Under pathological conditions, i.e. facial motor nerve axotomy, it was shown that microglia take up a perineuronal position, which is accompanied by a decrease in fractalkine mRNA by the motor neurons and the synthesis of different isoforms of the chemokine (Harrison et al., 1998). Fractalkine has been shown to be rapidly cleaved from cultured primary cortical neurons following glutamate excitotoxic stimuli. This preceded cell death by 2-3 hours and is thought to help mediate the migration of microglia and monocytes to the site of injury (Chapman et al., 2000a). Conversely, CX3CR1 knockout mice experience more extensive neuronal cell loss and microglial activation than their littermate controls in various neurodegenerative paradigms, suggesting that fractalkine signalling is an essential regulator of inflammatory neurotoxicity within the CNS. It is thought that fractalkine normally provides a tonic effect upon the microglia, limiting their activation in the healthy CNS (Cardona et al., 2006; Kerschensteiner et al., 2009). Microglia are thought to contribute to neurodegeneration upon their activation, which results in the production of various cytotoxic molecules, including proteases, reactive oxygen species, NO, prostaglandins and cytokines (for review see Gao et al., 2003), and are believed to be characteristic of certain neurodegenerative diseases, including AD, AIDS dementia and MS (Spranger and Fontana, 1996). Fractalkine has been shown to suppress NO, IL-6 and TNF production, and significantly reduce neuronal cell death, by LPS +/- IFN- γ activated microglia in a dose-dependent manner, suggesting fractalkine can act as an anti-inflammatory chemokine (Zujovic et al., 2000; Mizuno et al., 2003). Fractalkine is also thought to act directly on neurons to promote cell survival as hippocampal neurons exposed to the HIV-1 envelope protein, gp120_{III_B}, are rescued from cell death when

cultured with fractalkine (Meucci et al., 2000). In EAE, no significant difference in expression levels or distribution of fractalkine mRNA in neurons has been reported between affected and unaffected rodents brains (Schwaeble et al., 1998). The same unaltered transcription pattern has been observed in the rodent model of ischemic stroke, suggesting that neuronal fractalkine mRNA levels are impervious to neuroinflammatory processes (Chapman et al., 2000a). Fractalkine has been shown to increase the secretion of MMP-2 and TIMPs -1 and -2 following 24 hour treatment of human foetal microglial cell line, CHME3, with various concentrations of the chemokine (Cross and Woodroffe, 1999). It also increased MMP-9 secretion by primary rat brain microglia (Cross and Woodroffe, 1999). With regards to MMP-2 this is interesting given that MMP-2 mediates the cleavage of fractalkine in murine embryonic fibroblast cells (Dean and Overall, 2007), suggesting that fractalkine shedding provokes a positive feedback loop whereby it activates one of its proteases resulting in more release of the chemokine.

Other roles of fractalkine within MS could be as an angiogenic chemokine. MS lesions are typically centred on blood vessels (for review see Kirk et al., 2004) and fractalkine has been cited as being angiogenic in RA, whereby removal of fractalkine from synovial fluid from RA patients significantly inhibited angiogenic activity of human dermal microvascular endothelial cells in matrigel (Volin et al., 2001). Other angiogenic factors have also been implicated in playing a detrimental role in MS, such as VEGF, which is upregulated in acute and chronic MS plaques, and the administration of VEGF in MBP immunized rats provokes an inflammatory response in the brain (Proescholdt et al., 2002). In addition, a significant increase in the number of vessels in chronic, demyelinating EAE lesions, succeeds an increased expression of VEGF (Kirk and Karlik, 2003), and VEGF concentrations are significantly higher in MS patients in relapse, which coincides with spinal cord lesions on MRI (Su et al., 2006). Similar studies could be performed to determine whether there is a relationship with fractalkine, VEGF, and lesion formation in MS.

In conclusion, further experiments should be performed to fully elucidate the phenotype and expression levels of fractalkine expressing cells in relation to ADAM-17 in MS and control tissue. The study should be expanded to assess tissues with varying degrees of inflammation to determine whether ADAM-17 up-regulation corresponds with a larger inflammatory burden. Also, blocks with active demyelinating lesions, as characterised by the presence of lipid-laden macrophages, should be included to determine the expression levels of fractalkine within this tissue type.

6.1 General discussion

Previous work has demonstrated that ADAM-17 expression is increased in MS white matter lesions (Plumb et al., 2006) and that ADAM-17 mRNA expression is increased in the spinal cords of rats with EAE (Plumb et al., 2005). This present work sought to determine the functional role of an increased expression of ADAM-17 in the pathogenesis of MS. Using a newly developed *in vitro* model of the BBB, the human adult brain endothelial cell line, hCMEC/D3 (Weksler et al., 2005), the expression levels of ADAM-17, TIMP-3, and various substrates shed by the enzyme were studied at the molecular level under cytokine treatment regimes. This work revealed that of the substrates studied, only fractalkine was consistently significantly up-regulated at the mRNA level following TNF treatment. ADAM-17 and TIMP-3 expression were also increased, but not significantly so. In addition the expression of these three genes (ADAM-17, TIMP-3, and fractalkine) was studied at the translational level, which revealed only fractalkine was increased and this was accompanied by an increase in the shedding of the protein, but not an increase in the enzyme activity of ADAM-17. An increased expression of TNF has been observed in the perivascular cuffs (Woodroffe and Cuzner, 1993) and in the CSF (Hauser et al., 1990) of MS patients, however, this was also in conjunction with a number of other cytokines, including IFN- γ and IL-6 (Woodroffe and Cuzner, 1993). Thus, it cannot be assumed that the increase in ADAM-17 expression as witnessed in MS and EAE has been adequately replicated *in vitro*. Instead there are a number of cytokines expressed under inflammatory conditions in MS patients, which may contribute to the increased expression of ADAM-17 seen in the MS plaque, not merely the expression of one cytokine. It is also notable that the increase in ADAM-17 protein expression previously reported by Plumb et al. (2006), was quantitated using an inclusion method, whereby scores of ADAM-17 intensity was determined based upon cell types that expressed the protein. Thus, Plumb et al. (2006) did not *per se* say there was an increased expression of ADAM-17 within endothelial cells rather that more cell types expressed ADAM-17 within the inflammatory lesions.

None-the-less, the work of this thesis revealed an important observation: that under TNF cytokine treatment, fractalkine shedding is induced and increased in a dose-dependent manner, which cannot be accounted for by an increased expression or activity of ADAM-17. There are few studies examining ectodomain shedding of membrane-bound proteins under cytokine inducible conditions (Ludwig et al., 2002; Singh et al., 2005), instead most studies have used PMA, the physiological counterpart of which is unknown, to study this phenomenon. However, given that MS is an inflammatory disease and that a number of adhesion molecules and chemokines are found within the serum and CSF of these patients it is important to understand what role cytokines may play in inducing enzyme mediated ectodomain shedding. This

finding was also of interest due to the lack of involvement of ADAM-17, which has been cited as being responsible for the inducible cleavage of fractalkine following PMA treatment (Garton et al., 2001; Tsou et al., 2001). Thus, this raises questions as to whether other enzymes involved in fractalkine shedding, e.g. ADAM-10 (Hundhausen et al., 2003), cathepsin S (Clark et al., 2007), MMP-2 (Dean and Overall, 2007) or as yet an unidentified enzyme, could instead be activated under TNF treatment. Cellular expressed ADAM-17 is proposed to respond to PMA stimulation by showing an increase in enzyme activity and not an increase in protein expression (Doedens et al., 2003), however, this was not observed in this current study following cytokine activation. Other mechanisms of regulation could be involved in mediating the activity of enzymes and shedding of their cognate proteins. ADAM-17 has been found to co-localise within lipid-rafts, where it is thought ectodomain shedding is regulated (Tellier et al., 2006). Fractalkine, however, does not associate with these cholesterol-rich domains and upon cholesterol depletion fractalkine does not redistribute, unlike ADAM-17 (Durkan et al., 2006; Tellier et al., 2006). In intestinal epithelial cells, fractalkine is found to associate with caveolae, which are vesicular invaginations of the plasma membrane that are associated with a number of signalling pathways (Muehlhoefer et al., 2000). It is also notable that an increase in the substrate concentration could be enough to favour enzymatic activity and shedding of the membrane-bound proteins as this will alter the reaction rate. With increasing substrate concentrations, there would be an increase in the reaction rate of the enzyme until saturated: an increase in fractalkine protein expression was observed by ICC and ELISA in Chapter 3, which could have been enough to favour shedding of the protein instead of an increase in the activity of ADAM-17. It was also observed that knocking down or silencing ADAM-17 using siRNA technology (Chapter 4) did not completely abolish or significantly reduce shedding of fractalkine, suggesting another protease or mechanism is involved with the release of the chemokine/adhesion molecule.

Fractalkine is expressed on neurons (Pan et al., 1997; Nishiyori et al., 1998; Harrison et al., 1998), astrocytes (Hulshof et al., 2003) and endothelial cells (Bazan et al., 1997; Muehlhoefer et al., 2000) within the CNS whereas its receptor is expressed on T cells (Bazan et al., 1997; Imai et al., 1997), NK cells (Imai et al., 1997), monocytes (Bazan et al., 1997; Imai et al., 1997), microglia (Nishiyori et al., 1998), astrocytes (Maciejewski-Lenoir et al., 1999) and neurons (Meucci et al., 2000). These expression patterns both within the CNS and immune systems, between the ligand and its cognate receptor, strongly suggest fractalkine plays a significant role in neuro-immune cross talk, particularly in CNS disorders (Kerschensteiner et al., 2009).

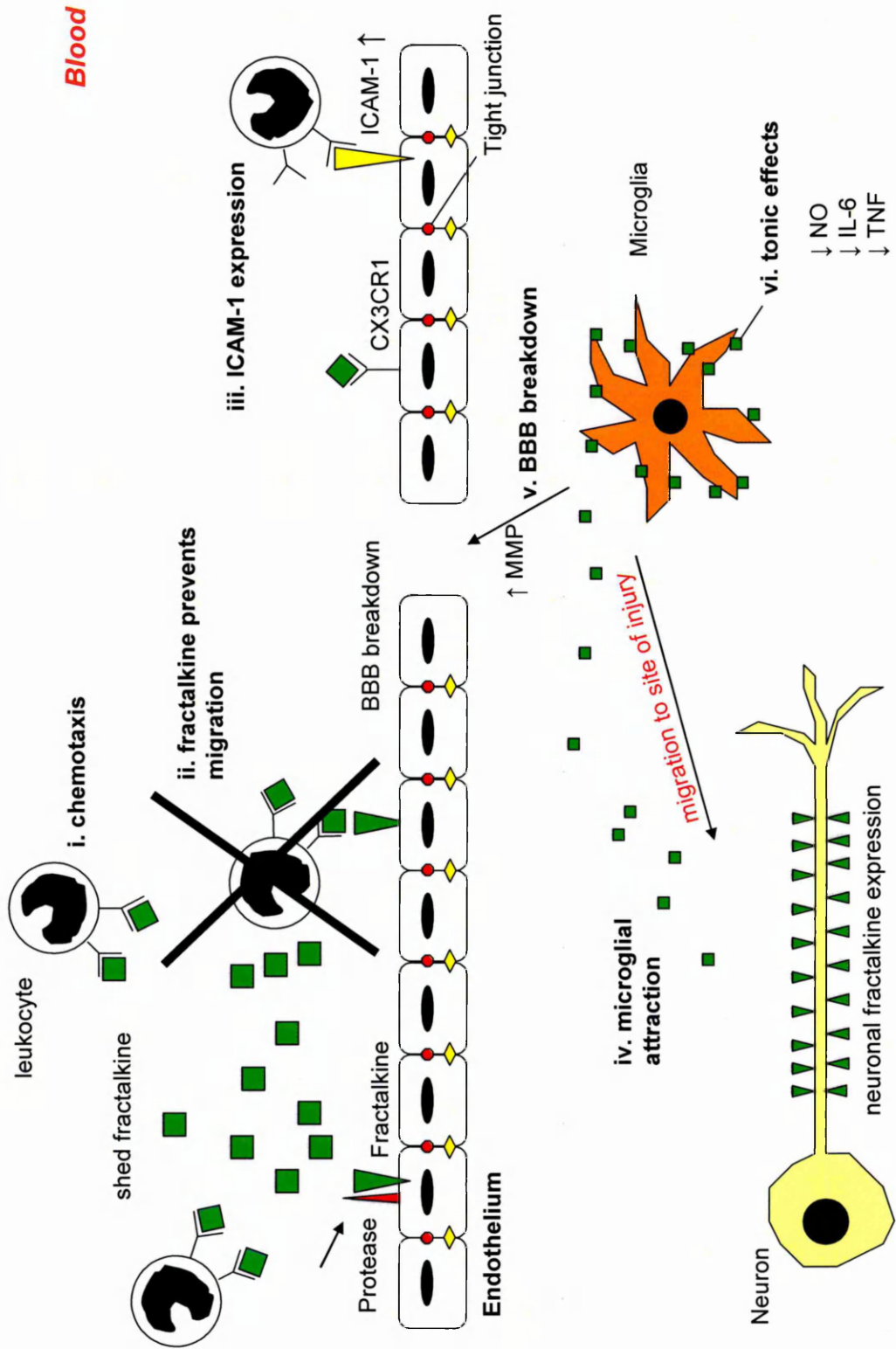
As fractalkine is expressed on the endothelium and various immune cells, fractalkine has been cited as being important in regulating leukocyte trafficking into the

CNS. Fractalkine is a potent chemoattractant (Bazan et al., 1997) and blocking the interaction of fractalkine with its receptor has been shown to be beneficial at reducing or preventing disease in animal models of stroke and idiopathic inflammatory myopathy (Soriano et al., 2002; Suzuki et al., 2005) (Figure 6.1). In addition, the autocrine effects of fractalkine, acting back upon the CX3CR1-expressing endothelium, results in the expression of ICAM-1 which facilitates neutrophil recruitment (Yang et al., 2007) (Figure 6.1), suggesting fractalkine has pro-inflammatory properties. Alternatively, shed fractalkine can act to saturate CX3CR1 preventing further attachment of immune cells to the fractalkine expressing endothelium and preventing CX3CR1-expressing cells from migrating into the CNS (Ancuta et al., 2003; Chapman et al., 2000b; Imai et al., 1997) (Figure 6.1), suggesting a protective function. Fractalkine has also been found to have angiogenic properties (Volin et al., 2001) and could also play a role in blood vessel formation in MS, which could be detrimental to the disease.

Within the CNS, fractalkine possesses anti-inflammatory properties by reducing the microglial production of inflammatory cytokines (Zujovic et al., 2000; Mizuno et al., 2003) and providing a tonic effect upon microglia preventing their activation (Cardona et al., 2006) (Figure 6.1), ultimately preventing neurodegeneration. However, fractalkine also stimulates the release of MMPs by microglia (Cross and Woodroffe, 1999), which could contribute to breakdown of the BBB, facilitating leukocyte infiltration (Figure 6.1). Fractalkine also causes the chemoattraction of microglia to site of injury (Chapman et al., 2000a) (Figure 6.1). Fractalkine is increased in the serum and CSF (Kastenbauer et al., 2003) of MS patients, however, no dysregulation has been observed in the CNS tissue of MS patients (Hulshof et al., 2003). Studies performed to elucidate the role of fractalkine in MS pathogenesis using EAE, suggest fractalkine is important for recruitment of NK cells. The lack of CX3CR1-expressing NK results in CNS haemorrhages, lack of functional recovery and a higher mortality rate (Huang et al., 2006). In agreement with this finding is the observation that MS patients are deficient in circulating CX3CR1⁺ NK cells, however MRI activity levels increase in association with the number of circulating CX3CR1⁺ NK cells, suggesting the role of NK in MS is complex (Infante-Duarte et al., 2005).

TNF has long been implicated in MS (Brosnan et al., 1988), however it has been shown that administering anti-TNF treatment to patients with MS exacerbates rather than ameliorates the disease course (Van Oosten et al., 1996). Inhibition of localised TNF production may be an effective method of preventing the harmful effects of TNF. One strategy to reduce TNF bioavailability might be to modulate ADAM-17 activity. Reducing the bioavailability of TNF by knocking down ADAM-17 expression and therefore activity might be a possible target to treat MS as this will prevent the

Figure 6.1: Schematic representation of the role of fractalkine in MS pathogenesis. i. Chemotaxis: fractalkine is a potent chemokine which when shed, will attract various leukocytes that express the receptor, CX3CR1. ii. Fractalkine prevents migration: studies have shown that if monocytes are pre-incubated with fractalkine they cannot attach onto the fractalkine expressing endothelium and cross the endothelial layer. iii. ICAM-1 expression: fractalkine can act in an autocrine fashion and bind to the CX3CR1-expressing endothelium, which in turn causes an increase in expression of ICAM-1, facilitating immune cell attachment and hence extravasation. iv. Microglial attraction: cleavage of fractalkine from neurons has been shown to cause the migration of microglia to sites of injury. v. BBB breakdown: activation of microglia by fractalkine has been shown to cause the synthesis of MMPs which facilitate BBB breakdown. vi. Tonic effects: action of fractalkine upon microglia produces tonic effects, which prevent the cells activation and include the suppressed expression of cytotoxic molecules, including NO, IL-6 and TNF.



production of soluble TNF, implicated in the detrimental effects of the cytokine seen in MS, whilst retaining the membrane-bound form of the cytokine, which may be protective (Alexopoulou et al, 2006).

However the functional role of ADAM-17 in the pathogenesis of MS is as yet still unknown; it has many properties that are indicative of both a pathogenic and neuroprotective role. On the negative side it mediates the solubilisation of membrane-bound TNF (Black et al., 1997; Moss et al., 1997), however it is also a sheddase for a number of other membrane proteins including the TNF receptors (Peschon et al., 1998; Reddy et al., 2000), which could act to sequester soluble TNF and thereby prevent cellular activation. It is also a sheddase for fractalkine which when administered in its soluble form to monocytes prevents the arrest of these cells onto endothelial cells (Ancuta et al., 2003). Thus, up-regulation of ADAM-17 could inhibit both the adhesion and extravasation of cells of the immune system into the CNS by blocking the interaction of these cells and the endothelium via solubilisation of fractalkine. However, fractalkine is also a potent chemokine (Bazan et al., 1997) and would therefore also recruit immune cells. ADAM-17 has also been implicated in other neurological processes and deemed to have a neuroprotective role as it has been shown to be involved in the processing of APP along the α -pathway, although this is not thought to be a constitutive role of ADAM-17 (Allinson et al., 2004). Conversely it has been shown to be up-regulated in EAE (Plumb et al., 2005), but its actual role in the pathogenesis in EAE is unknown. Due to this dual functionality of ADAM-17 and the fact that it has a vast array of substrates any attempts at utilizing this protease as a therapeutic tool for MS must be viewed with some trepidation. Hence, further investigations into the functional role of ADAM-17 and fractalkine both in physiological and pathological conditions are necessary.

6.2 Addressing the hypothesis of the thesis

The original hypothesis of this thesis was that an increased expression ratio of ADAM-17 to TIMP-3 as observed in MS and EAE (Plumb et al., 2005;2006) would favour the shedding of various substrates of ADAM-17 (Chapter 1, Figure 1.14). This thesis determined that the inflammatory conditions experienced in MS favour the shedding of fractalkine, however, this is not related to an increase in expression or activity of ADAM-17 or a decreased expression of TIMP-3. To further elucidate the role of ADAM-17 and fractalkine in MS, the following work could be carried out.

6.3 Future work

6.3.1 *In vitro* work using hCMEC/D3

The work of this thesis has tried to recapitulate the *in vivo* expression of ADAM-17 in endothelial cells using a novel endothelial cell line, hCMEC/D3. To further determine the control of expression of this enzyme, experiments using combinatorial administration of cytokines to the cells to determine whether this alters the expression of ADAM-17, TIMP-3 and substrates shed by the protease further should be performed. This may better replicate the *in vivo* situation where a number of cytokines are expressed by T cells within the perivascular cuff, which act upon the endothelium.

To elucidate the protease responsible for fractalkine shedding following TNF treatment the expression of ADAM-10, cathepsin S and MMP-2 could be studied at the mRNA and protein level, and siRNA knockdown of the proteins performed to determine what effect this has upon fractalkine shedding, following TNF treatment.

In addition, it will be important to determine the shedding mechanism of ADAM-17 and/or another protease, e.g. whether proteins associate within lipid-rafts to carry out their shedding activities. This association should also be examined under control and TNF treatment to determine whether inflammation affects this localisation.

6.3.2 *In vivo* work using post-mortem human brain tissue from The UK Multiple Sclerosis tissue Bank

Preliminary findings of this thesis cannot conclusively determine whether fractalkine expression is altered in MS patients' brains. The level of demyelination as determined by the presence of lipid-laden macrophages within the MS blocks was not extensive nor was the level of inflammation. Tissue blocks containing varying degrees of inflammation and demyelination should be studied to determine whether this reveals any differences in fractalkine expression. Certain aspects of the expression of ADAM-17 and fractalkine within MS tissue warrant further investigation. Such as an increased expression of ADAM-17 in the endothelium of grade +++/++++ perivascular cuffs, and the expression of fractalkine in axons next to the active border and also within macrophages of the active rim. Dual immunofluorescence for fractalkine using neuronal and macrophage markers should be performed to conclusively determine the phenotype of these positive cells. In light of the relationship between neuronal fractalkine and microglial CX3CR1, further studies should also investigate the microglial expression of CX3CR1.

As ADAM-17 does not mediate the cleavage of fractalkine under TNF treatment *in vitro*, this suggest another protease could be responsible for this. Further investigation into the expression of other proteases associated with fractalkine release,

such as ADAM-10, cathepsin S and MMP-2, in control and MS CNS tissue should be performed to determine their relationship to the chemokine/adhesion molecule.

6.3.3 Patient samples

To determine the functional role fractalkine might play in immune cell recruitment across the endothelium in MS, human blood samples from control and MS patients could be obtained. Fractalkine expression in hCMEC/D3 cells could be induced by cytokine treatment and the leukocytes from the patient samples could be allowed to attach to the fractalkine expressing endothelium. This would help determine whether MS patients show an increased propensity for their lymphocytes to attach to fractalkine expressing endothelial cells, and also the phenotypes of the cells, e.g. NK, T cells, which do attach. Pre-incubation of the leukocytes with fractalkine could be carried out to determine whether this prevents attachment of the cells to the endothelium. This work could also be extended to carry out migration assays on the patient samples towards fractalkine. Assays with and without siRNA knockdowns of the protease responsible for fractalkine release could also be carried out to determine the effects this has on leukocyte attachment and migration.

6.4 Summary

Increased expression of ADAM-17 in MS and EAE suggests that the protease plays a significant role in MS pathogenesis. ADAM-17 cleaves approximately 50 membrane-bound proteins, which have various physiological and pathological properties, e.g. in inflammation. The chemokine and adhesion molecule, fractalkine, has also been implicated in MS pathogenesis and is proteolytically cleaved by ADAM-17. Fractalkine expression and shedding was increased in this study following pro-inflammatory cytokine treatment in human endothelial cells, but this was not accompanied by an increase in the expression or activity of ADAM-17, suggesting the protease may not be responsible for this role under inflammatory conditions. Further investigation into the function of ADAM-17 using siRNA knockdowns of the protein confirmed the previous findings, showing that silencing ADAM-17 expression in endothelial cells does not significantly affect fractalkine shedding. *In vivo* analysis of ADAM-17 and fractalkine in human MS brain tissue revealed that fractalkine is not altered in the CNS endothelium in MS, but further investigation using CNS tissue with different degrees of activity (inflammation and demyelination) tissue is required before a firm conclusion can be made. This thesis has highlighted fractalkine as a major chemokine expressed by CNS endothelium under inflammatory conditions. Further work on the function of endothelial derived fractalkine are warranted to elucidate its role in MS pathogenesis.

- Abbott, N.J., L. Ronnback, and E. Hansson. 2006. Astrocyte-endothelial interactions at the blood-brain barrier. *Nat.Rev.Neurosci.* **7**:41-53.
- Afonso, P.V., S. Ozden, M.C. Prevost, C. Schmitt, D. Seilhean, B. Weksler, P.O. Couraud, A. Gessain, I.A. Romero, and P.E. Ceccaldi. 2007. Human blood-brain barrier disruption by retroviral-infected lymphocytes: role of myosin light chain kinase in endothelial tight-junction disorganization. *J.Immunol.* **179**:2576-2583.
- Agrawal, S., P. Anderson, M. Durbeej, N. van Rooijen, F. Ivars, G. Opdenakker, and L.M. Sorokin. 2006. Dystroglycan is selectively cleaved at the parenchymal basement membrane at sites of leukocyte extravasation in experimental autoimmune encephalomyelitis. *J.Exp.Med.* **203**:1007-1019.
- Agrawal, S.M., L. Lau, and V.W. Yong. 2008. MMPs in the central nervous system: where the good guys go bad. *Semin.Cell Dev.Biol.* **19**:42-51.
- Ahn, S.Y., C.H. Cho, K.G. Park, H.J. Lee, S. Lee, S.K. Park, I.K. Lee, and G.Y. Koh. 2004. Tumor necrosis factor-alpha induces fractalkine expression preferentially in arterial endothelial cells and mithramycin A suppresses TNF-alpha-induced fractalkine expression. *Am.J.Pathol.* **164**:1663-1672.
- Alexopoulou, L., K. Kranidioti, S. Xanthoulea, M. Denis, A. Kotanidou, E. Douni, P.J. Blakeshear, D.L. Kontoyiannis, and G. Kollias. 2006. Transmembrane TNF protects mutant mice against intracellular bacterial infections, chronic inflammation and autoimmunity. *Eur.J.Immunol.* **36**:2768-2780.
- Allan, S.M., and N.J. Rothwell. 2001. Cytokines and acute neurodegeneration. *Nat.Rev.Neurosci.* **2**:734-744.
- Allinson, T.M., E.T. Parkin, T.P. Condon, S.L. Schwager, E.D. Sturrock, A.J. Turner, and N.M. Hooper. 2004. The role of ADAM10 and ADAM17 in the ectodomain shedding of angiotensin converting enzyme and the amyloid precursor protein. *Eur.J.Biochem.* **271**:2539-2547.
- Amour, A., C.G. Knight, A. Webster, P.M. Slocombe, P.E. Stephens, V. Knauper, A.J. Docherty, and G. Murphy. 2000. The in vitro activity of ADAM-10 is inhibited by TIMP-1 and TIMP-3. *FEBS Lett.* **473**:275-279.
- Amour, A., P.M. Slocombe, A. Webster, M. Butler, C.G. Knight, B.J. Smith, P.E. Stephens, C. Shelley, M. Hutton, V. Knauper, A.J. Docherty, and G. Murphy. 1998. TNF-alpha converting enzyme (TACE) is inhibited by TIMP-3. *FEBS Lett.* **435**:39-44.
- Ancuta, P., R. Rao, A. Moses, A. Mehle, S.K. Shaw, F.W. Luscinskas, and D. Gabuzda. 2003. Fractalkine preferentially mediates arrest and migration of CD16+ monocytes. *J.Exp.Med.* **197**:1701-1707.
- Anthony, D.C., B. Ferguson, M.K. Matyzak, K.M. Miller, M.M. Esiri, and V.H. Perry. 1997. Differential matrix metalloproteinase expression in cases of multiple sclerosis and stroke. *Neuropathol.Appl.Neurobiol.* **23**:406-415.
- Argaw, A.T., Y. Zhang, B.J. Snyder, M.L. Zhao, N. Kopp, S.C. Lee, C.S. Raine, C.F. Brosnan, and G.R. John. 2006. IL-1beta regulates blood-brain barrier permeability via reactivation of the hypoxia-angiogenesis program. *J.Immunol.* **177**:5574-5584.

- Arnett, H.A., J. Mason, M. Marino, K. Suzuki, G.K. Matsushima, and J.P. Ting. 2001. TNF alpha promotes proliferation of oligodendrocyte progenitors and remyelination. *Nat.Neurosci.* **4**:1116-1122.
- Astier, A.L., G. Meiffren, S. Freeman, and D.A. Hafler. 2006. Alterations in CD46-mediated Tr1 regulatory T cells in patients with multiple sclerosis. *J.Clin.Invest.* **116**:3252-3257.
- Avasarala, J. R., A. H. Cross, J. L. Trotter. 2001. Oligoclonal band number as a marker for the prognosis of multiple sclerosis. *Arch Neurol.* **58** (12): 2044-2045.
- Avolio, C., F. Giuliani, G.M. Liuzzi, M. Ruggieri, D. Paolicelli, P. Riccio, P. Livrea, and M. Trojano. 2003. Adhesion molecules and matrix metalloproteinases in multiple sclerosis: effects induced by Interferon-beta. *Brain Res.Bull.* **61**:357-364.
- Balashov, K.E., J.B. Rottman, H.L. Weiner, and W.W. Hancock. 1999. CCR5(+) and CXCR3(+) T cells are increased in multiple sclerosis and their ligands MIP-1alpha and IP-10 are expressed in demyelinating brain lesions. *Proc.Natl.Acad.Sci.U.S.A.* **96**:6873-6878.
- Ballabh, P., A. Braun, and M. Nedergaard. 2004. The blood-brain barrier: an overview: structure, regulation, and clinical implications. *Neurobiol.Dis.* **16**:1-13.
- Banks, W.A., S.R. Plotkin, and A.J. Kastin. 1995. Permeability of the blood-brain barrier to soluble cytokine receptors. *Neuroimmunomodulation.* **2**:161-165.
- Baraczka, K., T. Pozsonyi, M. Szongoth, K. Nekam, A. Megyeri, Z. Balogh, and L. Jakab. 1999. A study of increased levels of soluble vascular cell adhesion molecule-1 (sVCAM-1) in the cerebrospinal fluid of patients with multiple sclerosis and systemic lupus erythematosus. *Acta Neurol.Scand.* **99**:95-99.
- Bazan, J.F., K.B. Bacon, G. Hardiman, W. Wang, K. Soo, D. Rossi, D.R. Greaves, A. Zlotnik, and T.J. Schall. 1997. A new class of membrane-bound chemokine with a CX3C motif. *Nature.* **385**:640-644.
- Beck, J., P. Rondot, L. Catinot, E. Falcoff, H. Kirchner, and J. Wietzerbin. 1988. Increased production of interferon gamma and tumor necrosis factor precedes clinical manifestation in multiple sclerosis: do cytokines trigger off exacerbations? *Acta Neurol.Scand.* **78**:318-323.
- Bielekova, B., B. Goodwin, N. Richert, I. Cortese, T. Kondo, G. Afshar, B. Gran, J. Eaton, J. Antel, J. A. Frank, H. F. McFarland, R. Martin. 2000. Encephalitogenic potential of the myelin basic protein peptide (amino acids 83-99) in multiple sclerosis: Results of a phase II clinical trial with an altered peptide ligand. *Nat Med.* **6** (10): 1167-1175.
- Bielekova, B., M.H. Sung, N. Kadom, R. Simon, H. McFarland, and R. Martin. 2004. Expansion and functional relevance of high-avidity myelin-specific CD4+ T cells in multiple sclerosis. *J.Immunol.* **172**:3893-3904.
- Bitsch, A., J. Schuchardt, S. Bunkowski, T. Kuhlmann, and W. Bruck. 2000. Acute axonal injury in multiple sclerosis. Correlation with demyelination and inflammation. *Brain.* **123** (6):1174-1183.
- Black, J.A., P. Felts, K.J. Smith, J.D. Kocsis, and S.G. Waxman. 1991. Distribution of sodium channels in chronically demyelinated spinal cord axons: immuno-ultrastructural localization and electrophysiological observations. *Brain Res.* **544**:59-70.

- Black, J.A., J. Newcombe, B.D. Trapp, and S.G. Waxman. 2007. Sodium channel expression within chronic multiple sclerosis plaques. *J.Neuropathol.Exp.Neurol.* **66**:828-837.
- Black, R.A. 2002. Tumor necrosis factor-alpha converting enzyme. *Int.J.Biochem.Cell Biol.* **34**:1-5.
- Black, R.A., J.R. Doedens, R. Mahimkar, R. Johnson, L. Guo, A. Wallace, D. Virca, J. Eisenman, J. Slack, B. Castner, S.W. Sunnarborg, D.C. Lee, R. Cowling, G. Jin, K. Charrier, J.J. Peschon, and R. Paxton. 2003. Substrate specificity and inducibility of TACE (tumour necrosis factor alpha-converting enzyme) revisited: the Ala-Val preference, and induced intrinsic activity. *Biochem.Soc.Symp.* (**70**):39-52.
- Black, R.A., C.T. Rauch, C.J. Kozlosky, J.J. Peschon, J.L. Slack, M.F. Wolfson, B.J. Castner, K.L. Stocking, P. Reddy, S. Srinivasan, N. Nelson, N. Boiani, K.A. Schooley, M. Gerhart, R. Davis, J.N. Fitzner, R.S. Johnson, R.J. Paxton, C.J. March, and D.P. Cerretti. 1997. A metalloproteinase disintegrin that releases tumour-necrosis factor-alpha from cells. *Nature.* **385**:729-733.
- Bö, L., J.J. Geurts, S.J. Mork, and P. van der Valk. 2006. Grey matter pathology in multiple sclerosis. *Acta Neurol.Scand.Suppl.* **183**:48-50.
- Bö, L., S. Mork, P.A. Kong, H. Nyland, C.A. Pardo, and B.D. Trapp. 1994. Detection of MHC class II-antigens on macrophages and microglia, but not on astrocytes and endothelia in active multiple sclerosis lesions. *J.Neuroimmunol.* **51**:135-146.
- Bö, L., J.W. Peterson, S. Mork, P.A. Hoffman, W.M. Gallatin, R.M. Ransohoff, and B.D. Trapp. 1996. Distribution of immunoglobulin superfamily members ICAM-1, -2, -3, and the beta 2 integrin LFA-1 in multiple sclerosis lesions. *J.Neuropathol.Exp.Neurol.* **55**:1060-1072.
- Boehme, S.A., F.M. Lio, D. Maciejewski-Lenoir, K.B. Bacon, and P.J. Conlon. 2000. The chemokine fractalkine inhibits Fas-mediated cell death of brain microglia. *J.Immunol.* **165**:397-403.
- Bolton, S.J., D.C. Anthony, and V.H. Perry. 1998. Loss of the tight junction proteins occludin and zonula occludens-1 from cerebral vascular endothelium during neutrophil-induced blood-brain barrier breakdown in vivo. *Neuroscience.* **86**:1245-1257.
- Bond, M., G. Murphy, M.R. Bennett, A.C. Newby, and A.H. Baker. 2002. Tissue inhibitor of metalloproteinase-3 induces a Fas-associated death domain-dependent type II apoptotic pathway. *J.Biol.Chem.* **277**:13787-13795.
- Borland, G., G. Murphy, and A. Ager. 1999. Tissue inhibitor of metalloproteinases-3 inhibits shedding of L-selectin from leukocytes. *J.Biol.Chem.* **274**:2810-2815.
- Boyle, E.A., and P.L. McGeer. 1990. Cellular immune response in multiple sclerosis plaques. *Am.J.Pathol.* **137**:575-584.
- Breij, E.C., B.P. Brink, R. Veerhuis, C. van den Berg, R. Vloet, R. Yan, C.D. Dijkstra, P. van der Valk, and L. Bo. 2008. Homogeneity of active demyelinating lesions in established multiple sclerosis. *Ann.Neurol.* **63**:16-25.

- Brew, K., D. Dinakarpanian, and H. Nagase. 2000. Tissue inhibitors of metalloproteinases: evolution, structure and function. *Biochim.Biophys.Acta.* **1477**:267-283.
- Brosnan, C.F., B. Cannella, L. Battistini, and C.S. Raine. 1995. Cytokine localization in multiple sclerosis lesions: correlation with adhesion molecule expression and reactive nitrogen species. *Neurology.* **45**:S16-21.
- Brosnan, C.F., K. Selmaj, and C.S. Raine. 1988. Hypothesis: a role for tumor necrosis factor in immune-mediated demyelination and its relevance to multiple sclerosis. *J.Neuroimmunol.* **18**:87-94.
- Brown, D., and J.L. Stow. 1996. Protein trafficking and polarity in kidney epithelium: from cell biology to physiology. *Physiol.Rev.* **76**:245-297.
- Brown, H., T.T. Hien, N. Day, N.T. Mai, L.V. Chuong, T.T. Chau, P.P. Loc, N.H. Phu, D. Bethell, J. Farrar, K. Gatter, N. White, and G. Turner. 1999. Evidence of blood-brain barrier dysfunction in human cerebral malaria. *Neuropathol.Appl.Neurobiol.* **25**:331-340.
- Bruck, W., P. Porada, S. Poser, P. Rieckmann, F. Hanefeld, H.A. Kretzschmar, and H. Lassmann. 1995. Monocyte/macrophage differentiation in early multiple sclerosis lesions. *Ann.Neurol.* **38**:788-796.
- Bruck, W., M. Schmied, G. Suchanek, Y. Bruck, H. Breitschopf, S. Poser, S. Piddlesden, and H. Lassmann. 1994. Oligodendrocytes in the early course of multiple sclerosis. *Ann.Neurol.* **35**:65-73.
- Brueckmann, M., A.S. Nahrup, S. Lang, T. Bertsch, K. Fukudome, V. Liebe, J.J. Kaden, U. Hoffmann, M. Borggreffe, and G. Huhle. 2006. Recombinant human activated protein C upregulates the release of soluble fractalkine from human endothelial cells. *Br.J.Haematol.* **133**:550-557.
- Brunner, C., H. Lassmann, T.V. Waehneltdt, J.M. Matthieu, and C. Linington. 1989. Differential ultrastructural localization of myelin basic protein, myelin/oligodendroglial glycoprotein, and 2',3'-cyclic nucleotide 3'-phosphodiesterase in the CNS of adult rats. *J.Neurochem.* **52**:296-304.
- Brynskov, J., P. Foegh, G. Pedersen, C. Ellervik, T. Kirkegaard, A. Bingham, and T. Saermark. 2002. Tumour necrosis factor alpha converting enzyme (TACE) activity in the colonic mucosa of patients with inflammatory bowel disease. *Gut.* **51**:37-43.
- Bugno, M., B. Witek, J. Bereta, M. Bereta, D.R. Edwards, and T. Kordula. 1999. Reprogramming of TIMP-1 and TIMP-3 expression profiles in brain microvascular endothelial cells and astrocytes in response to proinflammatory cytokines. *FEBS Lett.* **448**:9-14.
- Bullard, D.C., X. Hu, T.R. Schoeb, R.G. Collins, A.L. Beaudet, and S.R. Barnum. 2007. Intercellular adhesion molecule-1 expression is required on multiple cell types for the development of experimental autoimmune encephalomyelitis. *J.Immunol.* **178**:851-857.
- Bulman, D.E., and G.C. Ebers. 1992. The geography of MS reflects genetic susceptibility. *Journal of Tropical and Geographical Neurology.* **2**:66-72.
- Butt, A.M., H.C. Jones, and N.J. Abbott. 1990. Electrical resistance across the blood-brain barrier in anaesthetized rats: a developmental study. *J.Physiol.* **429**:47-62.

- Buxbaum, J.D., K.N. Liu, Y. Luo, J.L. Slack, K.L. Stocking, J.J. Peschon, R.S. Johnson, B.J. Castner, D.P. Cerretti, and R.A. Black. 1998. Evidence that tumor necrosis factor alpha converting enzyme is involved in regulated alpha-secretase cleavage of the Alzheimer amyloid protein precursor. *J.Biol.Chem.* **273**:27765-27767.
- Bzowska, M., N. Jura, A. Lassak, R.A. Black, and J. Bereta. 2004. Tumour necrosis factor-alpha stimulates expression of TNF-alpha converting enzyme in endothelial cells. *Eur.J.Biochem.* **271**:2808-2820.
- Calabresi, P.A., A. Prat, K. Biernacki, J. Rollins, and J.P. Antel. 2001. T lymphocytes conditioned with Interferon beta induce membrane and soluble VCAM on human brain endothelial cells. *J.Neuroimmunol.* **115**:161-167.
- Calabresi, P.A., L.R. Tranquill, J.M. Dambrosia, L.A. Stone, H. Maloni, C.N. Bash, J.A. Frank, and H.F. McFarland. 1997. Increases in soluble VCAM-1 correlate with a decrease in MRI lesions in multiple sclerosis treated with interferon beta-1b. *Ann.Neurol.* **41**:669-674.
- Canault, M., E. Tellier, B. Bonardo, E. Mas, M. Aumailley, I. Juhan-Vague, G. Nalbone, and F. Peiretti. 2006. FHL2 interacts with both ADAM-17 and the cytoskeleton and regulates ADAM-17 localization and activity. *J.Cell.Physiol.* **208**:363-372.
- Cannella, B., and C.S. Raine. 1995. The adhesion molecule and cytokine profile of multiple sclerosis lesions. *Ann.Neurol.* **37**:424-435.
- Cardenas, A., M.A. Moro, J.C. Leza, E. O'Shea, A. Davalos, J. Castillo, P. Lorenzo, and I. Lizasoain. 2002. Upregulation of TACE/ADAM17 after ischemic preconditioning is involved in brain tolerance. *J.Cereb.Blood Flow Metab.* **22**:1297-1302.
- Cardona, A.E., E.P. Piro, M.E. Sasse, V. Kostenko, S.M. Cardona, I.M. Dijkstra, D. Huang, G. Kidd, S. Dombrowski, R. Dutta, J.C. Lee, D.N. Cook, S. Jung, S.A. Lira, D.R. Littman, and R.M. Ransohoff. 2006. Control of microglial neurotoxicity by the fractalkine receptor. *Nat.Neurosci.* **9**:917-924.
- Carton, H., R. Vlietinck, J. Debruyne, J. De Keyser, M.B. D'Hooghe, R. Loos, R. Medaer, L. Truyen, I.M. Yee, and A.D. Sadovnick. 1997. Risks of multiple sclerosis in relatives of patients in Flanders, Belgium. *J.Neurol.Neurosurg.Psychiatry.* **62**:329-333.
- Castillo, J., A. Davalos, J. Naveiro, and M. Noya. 1996. Neuroexcitatory amino acids and their relation to infarct size and neurological deficit in ischemic stroke. *Stroke.* **27**:1060-1065.
- Chapman, G.A., K. Moores, D. Harrison, C.A. Campbell, B.R. Stewart, and P.J. Strijbos. 2000a. Fractalkine cleavage from neuronal membranes represents an acute event in the inflammatory response to excitotoxic brain damage. *J.Neurosci.* **20**:RC87.
- Chapman, G.A., K.E. Moores, J. Gohil, T.A. Berkhout, L. Patel, P. Green, C.H. Macphee, and B.R. Stewart. 2000b. The role of fractalkine in the recruitment of monocytes to the endothelium. *Eur.J.Pharmacol.* **392**:189-195.
- Chen, A., P. Engel, and T.F. Tedder. 1995. Structural requirements regulate endoproteolytic release of the L-selectin (CD62L) adhesion receptor from the cell surface of leukocytes. *J.Exp.Med.* **182**:519-530.

- Choi, D.W., and S.M. Rothman. 1990. The role of glutamate neurotoxicity in hypoxic-ischemic neuronal death. *Annu.Rev.Neurosci.* **13**:171-182.
- Chong, N.H., A. Kvanta, S. Seregard, A.C. Bird, P.J. Luthert, and B. Steen. 2003. TIMP-3 mRNA is not overexpressed in Sorsby fundus dystrophy. *Am.J.Ophthalmol.* **136**:954-955.
- Cimini, A., A. Bernardo, M.G. Cifone, L. Di Marzio, and S. Di Loreto. 2003. TNFalpha downregulates PPARdelta expression in oligodendrocyte progenitor cells: implications for demyelinating diseases. *Glia.* **41**:3-14.
- Clark, A.K., P.K. Yip, J. Grist, C. Gentry, A.A. Staniland, F. Marchand, M. Dehvari, G. Wotherspoon, J. Winter, J. Ullah, S. Bevan, and M. Malcangio. 2007. Inhibition of spinal microglial cathepsin S for the reversal of neuropathic pain. *Proc.Natl.Acad.Sci.U.S.A.* **104**:10655-10660.
- Claudio, L., C.S. Raine, and C.F. Brosnan. 1995. Evidence of persistent blood-brain barrier abnormalities in chronic-progressive multiple sclerosis. *Acta Neuropathol.* **90**:228-238.
- Clerici, M., M. Saresella, D. Trabattoni, L. Speciale, S. Fossati, S. Ruzzante, R. Cavaretta, M. Filippi, D. Caputo, and P. Ferrante. 2001. Single-cell analysis of cytokine production shows different immune profiles in multiple sclerosis patients with active or quiescent disease. *J.Neuroimmunol.* **121**:88-101.
- Colon, A.L., L.A. Menchen, O. Hurtado, J. De Cristobal, I. Lizasoain, J.C. Leza, P. Lorenzo, and M.A. Moro. 2001. Implication of TNF-alpha convertase (TACE/ADAM17) in inducible nitric oxide synthase expression and inflammation in an experimental model of colitis. *Cytokine.* **16**:220-226.
- Comabella, M., C. Romera, M. Camina, H. Perkal, M.A. Moro, J.C. Leza, I. Lizasoain, M. Castillo, and X. Montalban. 2006. TNF-alpha converting enzyme (TACE) protein expression in different clinical subtypes of multiple sclerosis. *J.Neurol.* **253**:701-706.
- Compston, A., and A. Coles. 2008. Multiple sclerosis. *Lancet.* **372**:1502-1517.
- Contin, C., V. Pitard, T. Itai, S. Nagata, J.F. Moreau, and J. Dechanet-Merville. 2003. Membrane-anchored CD40 is processed by the tumor necrosis factor-alpha-converting enzyme. Implications for CD40 signaling. *J.Biol.Chem.* **278**:32801-32809.
- Correale, J., W. Gilmore, M. McMillan, S. Li, K. McCarthy, T. Le, and L.P. Weiner. 1995. Patterns of cytokine secretion by autoreactive proteolipid protein-specific T cell clones during the course of multiple sclerosis. *J.Immunol.* **154**:2959-2968.
- Crocker, S.J., A. Pagenstecher, and I.L. Campbell. 2004. The TIMPs tango with MMPs and more in the central nervous system. *J.Neurosci.Res.* **75**:1-11.
- Cross, A.K., and M.N. Woodroffe. 1999. Chemokine modulation of matrix metalloproteinase and TIMP production in adult rat brain microglia and a human microglial cell line in vitro. *Glia.* **28**:183-189.
- Crowe, P.D., B.N. Walter, K.M. Mohler, C. Otten-Evans, R.A. Black, and C.F. Ware. 1995. A metalloprotease inhibitor blocks shedding of the 80-kD TNF receptor and TNF processing in T lymphocytes. *J.Exp.Med.* **181**:1205-1210.

- Cucullo, L., M. Hossain, E. Rapp, T. Manders, N. Marchi, and D. Janigro. 2007. Development of a humanized in vitro blood-brain barrier model to screen for brain penetration of antiepileptic drugs. *Epilepsia*. **48**:505-516.
- Dallasta, L.M., L.A. Pisarov, J.E. Esplen, J.V. Werley, A.V. Moses, J.A. Nelson, and C.L. Achim. 1999. Blood-brain barrier tight junction disruption in human immunodeficiency virus-1 encephalitis. *Am.J.Pathol.* **155**:1915-1927.
- Daubener, W., S. Nockemann, M. Gutsche, and U. Hadding. 1995. Heparin inhibits the antiparasitic and immune modulatory effects of human recombinant interferon-gamma. *Eur.J.Immunol.* **25**:688-692.
- Davie, C.A., G.J. Barker, A.J. Thompson, P.S. Tofts, W.I. McDonald, and D.H. Miller. 1997. ¹H magnetic resonance spectroscopy of chronic cerebral white matter lesions and normal appearing white matter in multiple sclerosis. *J.Neurol.Neurosurg.Psychiatry.* **63**:736-742.
- De Groot, C.J., E. Bergers, W. Kamphorst, R. Ravid, C.H. Polman, F. Barkhof, and P. van der Valk. 2001. Post-mortem MRI-guided sampling of multiple sclerosis brain lesions: increased yield of active demyelinating and (p)reactive lesions. *Brain*. **124**:1635-1645.
- De Stefano, N., S. Narayanan, G.S. Francis, R. Arnaoutelis, M.C. Tartaglia, J.P. Antel, P.M. Matthews, and D.L. Arnold. 2001. Evidence of axonal damage in the early stages of multiple sclerosis and its relevance to disability. *Arch.Neurol.* **58**:65-70.
- Dean, G., T.W. Yeo, A. Goris, C.J. Taylor, R.S. Goodman, M. Elian, A. Galea-Debono, A. Aquilina, A. Felice, M. Vella, S. Sawcer, and D.A. Compston. 2008. HLA-DRB1 and multiple sclerosis in Malta. *Neurology*. **70**:101-105.
- Dean, R.A., and C.M. Overall. 2007. Proteomics discovery of metalloproteinase substrates in the cellular context by iTRAQ labeling reveals a diverse MMP-2 substrate degradome. *Mol.Cell.Proteomics*. **6**:611-623.
- Dello Sbarba, P., and E. Rovida. 2002. Transmodulation of cell surface regulatory molecules via ectodomain shedding. *Biol.Chem.* **383**:69-83.
- Delves, P., S. Martin, D. Burton, and I. Roitt. 2006. Essential Immunology. 11th Ed. Blackwell Publishing Ltd.
- Diamond, M.S., R. Alon, C.A. Parkos, M.T. Quinn, and T.A. Springer. 1995. Heparin is an adhesive ligand for the leukocyte integrin Mac-1 (CD11b/CD1). *J.Cell Biol.* **130**:1473-1482.
- Diaz-Rodriguez, E., J.C. Montero, A. Esparis-Ogando, L. Yuste, and A. Pandiella. 2002. Extracellular signal-regulated kinase phosphorylates tumor necrosis factor alpha-converting enzyme at threonine 735: a potential role in regulated shedding. *Mol.Biol.Cell.* **13**:2031-2044.
- Dittmer, A., and J. Dittmer. 2006. Beta-actin is not a reliable loading control in Western blot analysis. *Electrophoresis*. **27**:2844-2845.
- Dobbie, M.S., R.D. Hurst, N.J. Klein, and R.A. Surtees. 1999. Upregulation of intercellular adhesion molecule-1 expression on human endothelial cells by tumour necrosis factor-alpha in an in vitro model of the blood-brain barrier. *Brain Res.* **830**:330-336.
- Doedens, J.R., and R.A. Black. 2000. Stimulation-induced down-regulation of tumor necrosis factor-alpha converting enzyme. *J.Biol.Chem.* **275**:14598-14607.

- Doedens, J.R., R.M. Mahimkar, and R.A. Black. 2003. TACE/ADAM-17 enzymatic activity is increased in response to cellular stimulation. *Biochem.Biophys.Res.Commun.* **308**:331-338.
- Dopp, J.M., A. Mackenzie-Graham, G.C. Otero, and J.E. Merrill. 1997. Differential expression, cytokine modulation, and specific functions of type-1 and type-2 tumor necrosis factor receptors in rat glia. *J.Neuroimmunol.* **75**:104-112.
- Dore-Duffy, P., W. Newman, R. Balabanov, R.P. Lisak, E. Mainolfi, R. Rothlein, and M. Peterson. 1995. Circulating, soluble adhesion proteins in cerebrospinal fluid and serum of patients with multiple sclerosis: correlation with clinical activity. *Ann.Neurol.* **37**:55-62.
- Droogan, A.G., S.A. McMillan, J.P. Douglas, and S.A. Hawkins. 1996. Serum and cerebrospinal fluid levels of soluble adhesion molecules in multiple sclerosis: predominant intrathecal release of vascular cell adhesion molecule-1. *J.Neuroimmunol.* **64**:185-191.
- Drulovic, J., M. Mostarica-Stojkovic, Z. Levic, N. Stojavljevic, V. Pravica, and S. Mesaros. 1997. Interleukin-12 and tumor necrosis factor-alpha levels in cerebrospinal fluid of multiple sclerosis patients. *J.Neurol.Sci.* **147**:145-150.
- Duan, J.J., Z. Lu, C.B. Xue, X. He, J.L. Seng, J.J. Roderick, Z.R. Wasserman, R.Q. Liu, M.B. Covington, R.L. Magolda, R.C. Newton, J.M. Trzaskos, and C.P. Decicco. 2003. Discovery of N-hydroxy-2-(2-oxo-3-pyrrolidinyl)acetamides as potent and selective inhibitors of tumor necrosis factor-alpha converting enzyme (TACE). *Bioorg.Med.Chem.Lett.* **13**:2035-2040.
- Durkan, A., M., Alexander, R. T., Liu, G. Y., Rui, M., Femia, G., Robinson, L. A. 2007. Expression and targeting of CX3CL1 (fractalkine) in renal tubular epithelial cells. *J. Am. Soc. Nephrol.* **18** (1): 74-83
- Ebers, G.C., A.D. Sadovnick, and N.J. Risch. 1995. A genetic basis for familial aggregation in multiple sclerosis. Canadian Collaborative Study Group. *Nature.* **377**:150-151.
- Ebers, G.C., I.M. Yee, A.D. Sadovnick, and P. Duquette. 2000. Conjugal multiple sclerosis: population-based prevalence and recurrence risks in offspring. Canadian Collaborative Study Group. *Ann.Neurol.* **48**:927-931.
- Engelhardt, B., and L. Kappos. 2008. Natalizumab: targeting alpha4-integrins in multiple sclerosis. *Neurodegener Dis.* **5**:16-22.
- Fabis, M.J., G.S. Scott, R.B. Kean, H. Koprowski, and D.C. Hooper. 2007. Loss of blood-brain barrier integrity in the spinal cord is common to experimental allergic encephalomyelitis in knockout mouse models. *Proc.Natl.Acad.Sci.U.S.A.* **104**:5656-5661.
- Fainardi, E., M. Castellazzi, T. Bellini, M.C. Manfrinato, E. Baldi, I. Casetta, E. Paolino, E. Granieri, and F. Dalocchio. 2006. Cerebrospinal fluid and serum levels and intrathecal production of active matrix metalloproteinase-9 (MMP-9) as markers of disease activity in patients with multiple sclerosis. *Mult.Scler.* **12**:294-301.
- Fan, H., and R. Derynck. 1999. Ectodomain shedding of TGF-alpha and other transmembrane proteins is induced by receptor tyrosine kinase activation and MAP kinase signaling cascades. *EMBO J.* **18**:6962-6972.

- Fan, H., C.W. Turck, and R. Derynck. 2003. Characterization of growth factor-induced serine phosphorylation of tumor necrosis factor-alpha converting enzyme and of an alternatively translated polypeptide. *J.Biol.Chem.* **278**:18617-18627.
- Feghali, C.A., and T.M. Wright. 1997. Cytokines in acute and chronic inflammation. *Front.Biosci.* **2**:d12-26.
- Ferguson, B., M.K. Matyszak, M.M. Esiri, and V.H. Perry. 1997. Axonal damage in acute multiple sclerosis lesions. *Brain.* **120** (3):393-399.
- Ferrara, N. 1995. The role of vascular endothelial growth factor in pathological angiogenesis. *Breast Cancer Res.Treat.* **36**:127-137.
- Ferrari, C.C., A.M. Depino, F. Prada, N. Muraro, S. Campbell, O. Podhajcer, V.H. Perry, D.C. Anthony, and F.J. Pitossi. 2004. Reversible demyelination, blood-brain barrier breakdown, and pronounced neutrophil recruitment induced by chronic IL-1 expression in the brain. *Am.J.Pathol.* **165**:1827-1837.
- Filippi, M., M. Bozzali, M. Rovaris, O. Gonen, C. Kesavadas, A. Ghezzi, V. Martinelli, R.I. Grossman, G. Scotti, G. Comi, and A. Falini. 2003. Evidence for widespread axonal damage at the earliest clinical stage of multiple sclerosis. *Brain.* **126**:433-437.
- Filippi, M., A. Campi, V. Dousset, C. Baratti, V. Martinelli, N. Canal, G. Scotti, and G. Comi. 1995. A magnetization transfer imaging study of normal-appearing white matter in multiple sclerosis. *Neurology.* **45**:478-482.
- Fischer, F.R., L. Santambrogio, Y. Luo, M.A. Berman, W.W. Hancock, and M.E. Dorf. 2000. Modulation of experimental autoimmune encephalomyelitis: effect of altered peptide ligand on chemokine and chemokine receptor expression. *J.Neuroimmunol.* **110**:195-208.
- Forster, C., M. Burek, I.A. Romero, B. Weksler, P.O. Couraud, and D. Drenckhahn. 2008. Differential effects of hydrocortisone and TNFalpha on tight junction proteins in an in vitro model of the human blood-brain barrier. *J.Physiol.* **586**:1937-1949.
- Franciotta, D., R. Bergamaschi, G. Martino, E. Zardini, G. Desina, and V. Cosi. 1999. Tumor necrosis factor-alpha and its soluble receptors in plasma and cerebrospinal fluid of multiple sclerosis patients treated with methylprednisolone. *Eur.Cytokine Netw.* **10**:431-436.
- Franciotta, D.M., L.M. Grimaldi, G.V. Martino, G. Piccolo, R. Bergamaschi, A. Citterio, and G.V. Melzi d'Eril. 1989. Tumor necrosis factor in serum and cerebrospinal fluid of patients with multiple sclerosis. *Ann.Neurol.* **26**:787-789.
- Francis, K., J. van Beek, C. Canova, J.W. Neal, and P. Gasque. 2003. Innate immunity and brain inflammation: the key role of complement. *Expert Rev.Mol.Med.* **5**:1-19.
- Frohman, E.M., M.K. Racke, and C.S. Raine. 2006. Multiple sclerosis--the plaque and its pathogenesis. *N.Engl.J.Med.* **354**:942-955.
- Furlan, R., E. Brambilla, F. Ruffini, P.L. Poliani, A. Bergami, P.C. Marconi, D.M. Franciotta, G. Penna, G. Comi, L. Adorini, and G. Martino. 2001. Intrathecal delivery of IFN-gamma protects C57BL/6 mice from chronic-progressive experimental autoimmune encephalomyelitis by increasing apoptosis of central nervous system-infiltrating lymphocytes. *J.Immunol.* **167**:1821-1829.

- Gaillard, P.J., L.H. Voorwinden, J.L. Nielsen, A. Ivanov, R. Atsumi, H. Engman, C. Ringbom, A.G. de Boer, and D.D. Breimer. 2001. Establishment and functional characterization of an in vitro model of the blood-brain barrier, comprising a co-culture of brain capillary endothelial cells and astrocytes. *Eur.J.Pharm.Sci.* **12**:215-222.
- Gale, C.R., and C.N. Martyn. 1995. Migrant studies in multiple sclerosis. *Prog.Neurobiol.* **47**:425-448.
- Galustian, C., J. Dye, L. Leach, P. Clark, and J.A. Firth. 1995. Actin cytoskeletal isoforms in human endothelial cells in vitro: alteration with cell passage. *In Vitro Cell.Dev.Biol.Anim.* **31**:796-802.
- Gao, H.M., B. Liu, W. Zhang, and J.S. Hong. 2003. Novel anti-inflammatory therapy for Parkinson's disease. *Trends Pharmacol.Sci.* **24**:395-401.
- Garcia, G.E., Y. Xia, S. Chen, Y. Wang, R.D. Ye, J.K. Harrison, K.B. Bacon, H.G. Zerwes, and L. Feng. 2000. NF-kappaB-dependent fractalkine induction in rat aortic endothelial cells stimulated by IL-1beta, TNF-alpha, and LPS. *J.Leukoc.Biol.* **67**:577-584.
- Garton, K.J., P.J. Gough, C.P. Blobel, G. Murphy, D.R. Greaves, P.J. Dempsey, and E.W. Raines. 2001. Tumor necrosis factor-alpha-converting enzyme (ADAM17) mediates the cleavage and shedding of fractalkine (CX3CL1). *J.Biol.Chem.* **276**:37993-38001.
- Garton, K.J., P.J. Gough, J. Philalay, P.T. Wille, C.P. Blobel, R.H. Whitehead, P.J. Dempsey, and E.W. Raines. 2003. Stimulated shedding of vascular cell adhesion molecule 1 (VCAM-1) is mediated by tumor necrosis factor-alpha-converting enzyme (ADAM 17). *J.Biol.Chem.* **278**:37459-37464.
- Gay, D., and M. Esiri. 1991. Blood-brain barrier damage in acute multiple sclerosis plaques. An immunocytological study. *Brain.* **114**:557-572.
- Gechtman, Z., J.L. Alonso, G. Raab, D.E. Ingber, and M. Klagsbrun. 1999. The shedding of membrane-anchored heparin-binding epidermal-like growth factor is regulated by the Raf/mitogen-activated protein kinase cascade and by cell adhesion and spreading. *J.Biol.Chem.* **274**:28828-28835.
- Gerritsen, M.E., J.E. Tomlinson, C. Zlot, M. Ziman, and S. Hwang. 2003. Using gene expression profiling to identify the molecular basis of the synergistic actions of hepatocyte growth factor and vascular endothelial growth factor in human endothelial cells. *Br.J.Pharmacol.* **140**:595-610.
- Geurts, J.J., L. Bo, P.J. Pouwels, J.A. Castelijns, C.H. Polman, and F. Barkhof. 2005. Cortical lesions in multiple sclerosis: combined postmortem MR imaging and histopathology. *AJNR Am.J.Neuroradiol.* **26**:572-577.
- Gijbels, K., P. Proost, S. Masure, H. Carton, A. Billiau, and G. Opdenakker. 1993. Gelatinase B is present in the cerebrospinal fluid during experimental autoimmune encephalomyelitis and cleaves myelin basic protein. *J.Neurosci.Res.* **36**:432-440.
- Goddard, D.R., R.A. Bunning, and M.N. Woodroffe. 2001. Astrocyte and endothelial cell expression of ADAM 17 (TACE) in adult human CNS. *Glia.* **34**:267-271.

- Gomis-Ruth, F.X., K. Maskos, M. Betz, A. Bergner, R. Huber, K. Suzuki, N. Yoshida, H. Nagase, K. Brew, G.P. Bourenkov, H. Bartunik, and W. Bode. 1997. Mechanism of inhibition of the human matrix metalloproteinase stromelysin-1 by TIMP-1. *Nature*. **389**:77-81.
- Gooz, P., M. Gooz, A. Baldys, and S. Hoffman. 2009. ADAM-17 regulates endothelial cell morphology, proliferation, and in vitro angiogenesis. *Biochem.Biophys.Res.Commun.* **380**:33-38.
- Goto, F., K. Goto, K. Weindel, and J. Folkman. 1993. Synergistic effects of vascular endothelial growth factor and basic fibroblast growth factor on the proliferation and cord formation of bovine capillary endothelial cells within collagen gels. *Lab.Invest.* **69**:508-517.
- Goumans, M.J., Z. Liu, and P. ten Dijke. 2009. TGF-beta signaling in vascular biology and dysfunction. *Cell Res.* **19**:116-127.
- Greaves, D.R., T. Hakkinen, A.D. Lucas, K. Liddiard, E. Jones, C.M. Quinn, J. Senaratne, F.R. Green, K. Tyson, J. Boyle, C. Shanahan, P.L. Weissberg, S. Gordon, and S. Yla-Hertualla. 2001. Linked chromosome 16q13 chemokines, macrophage-derived chemokine, fractalkine, and thymus- and activation-regulated chemokine, are expressed in human atherosclerotic lesions. *Arterioscler.Thromb.Vasc.Biol.* **21**:923-929.
- Gregory, S.G., S. Schmidt, P. Seth, J.R. Oksenberg, J. Hart, A. Prokop, S.J. Caillier, M. Ban, A. Goris, L.F. Barcellos, R. Lincoln, J.L. McCauley, S.J. Sawcer, D.A. Compston, B. Dubois, S.L. Hauser, M.A. Garcia-Blanco, M.A. Pericak-Vance, J.L. Haines, and Multiple Sclerosis Genetics Group. 2007. Interleukin 7 receptor alpha chain (IL7R) shows allelic and functional association with multiple sclerosis. *Nat.Genet.* **39**:1083-1091.
- Grell, M., E. Douni, H. Wajant, M. Lohden, M. Clauss, B. Maxeiner, S. Georgopoulos, W. Lesslauer, G. Kollias, K. Pfizenmaier, and P. Scheurich. 1995. The transmembrane form of tumor necrosis factor is the prime activating ligand of the 80 kDa tumor necrosis factor receptor. *Cell.* **83**:793-802.
- Grell, M., H. Wajant, G. Zimmermann, and P. Scheurich. 1998. The type 1 receptor (CD120a) is the high-affinity receptor for soluble tumor necrosis factor. *Proc.Natl.Acad.Sci.U.S.A.* **95**:570-575.
- Grell, M., G. Zimmermann, D. Hulser, K. Pfizenmaier, and P. Scheurich. 1994. TNF receptors TR60 and TR80 can mediate apoptosis via induction of distinct signal pathways. *J.Immunol.* **153**:1963-1972.
- Grenett, H.E., R.L. Benza, X.N. Li, M.L. Aikens, J.R. Grammer, S.L. Brown, and F.M. Booyse. 1999. Expression of plasminogen activator inhibitor type I in genotyped human endothelial cell cultures: genotype-specific regulation by insulin. *Thromb.Haemost.* **82**:1504-1509.
- Gumbiner, B. 1987. Structure, biochemistry, and assembly of epithelial tight junctions. *Am.J.Physiol.* **253**:C749-58.
- Haas, J., A. Hug, A. Viehover, B. Fritzsching, C.S. Falk, A. Filser, T. Vetter, L. Milkova, M. Korporal, B. Fritz, B. Storch-Hagenlocher, P.H. Krammer, E. Suri-Payer, and B. Wildemann. 2005. Reduced suppressive effect of CD4+CD25high regulatory T cells on the T cell immune response against myelin oligodendrocyte glycoprotein in patients with multiple sclerosis. *Eur.J.Immunol.* **35**:3343-3352.

- Haddock, G., A.K. Cross, J. Plumb, J. Surr, D.J. Buttle, R.A. Bunning, and M.N. Woodroffe. 2006. Expression of ADAMTS-1, -4, -5 and TIMP-3 in normal and multiple sclerosis CNS white matter. *Mult.Scler.* **12**:386-396.
- Hafler, D.A. 2004. Multiple sclerosis. *J.Clin.Invest.* **113**:788-794.
- Hafler, D.A., A. Compston, S. Sawcer, E.S. Lander, M.J. Daly, P.L. De Jager, P.I. de Bakker, S.B. Gabriel, D.B. Mirel, A.J. Iverson, M.A. Pericak-Vance, S.G. Gregory, J.D. Rioux, J.L. McCauley, J.L. Haines, L.F. Barcellos, B. Cree, J.R. Oksenberg, and S.L. Hauser. 2007. International Multiple Sclerosis Genetics Consortium. Risk alleles for multiple sclerosis identified by a genomewide study. *N.Engl.J.Med.* **357**:851-862.
- Hannon, G.J. 2002. RNA interference. *Nature.* **418**:244-251.
- Haorah, J., S.H. Ramirez, K. Schall, D. Smith, R. Pandya, and Y. Persidsky. 2007. Oxidative stress activates protein tyrosine kinase and matrix metalloproteinases leading to blood-brain barrier dysfunction. *J.Neurochem.* **101**:566-576.
- Harkness, K.A., P. Adamson, J.D. Sussman, G.A. Davies-Jones, J. Greenwood, and M.N. Woodroffe. 2000. Dexamethasone regulation of matrix metalloproteinase expression in CNS vascular endothelium. *Brain.* **123** (4):698-709.
- Harkness, K.A., J.D. Sussman, G.A. Davies-Jones, J. Greenwood, and M.N. Woodroffe. 2003. Cytokine regulation of MCP-1 expression in brain and retinal microvascular endothelial cells. *J.Neuroimmunol.* **142**:1-9.
- Harrison, J.K., Y. Jiang, S. Chen, Y. Xia, D. Maciejewski, R.K. McNamara, W.J. Streit, M.N. Salafranca, S. Adhikari, D.A. Thompson, P. Botti, K.B. Bacon, and L. Feng. 1998. Role for neuronally derived fractalkine in mediating interactions between neurons and CX3CR1-expressing microglia. *Proc.Natl.Acad.Sci.U.S.A.* **95**:10896-10901.
- Harrison, J.K., Y. Jiang, E.A. Wees, M.N. Salafranca, H.X. Liang, L. Feng, and L. Belardinelli. 1999. Inflammatory agents regulate in vivo expression of fractalkine in endothelial cells of the rat heart. *J.Leukoc.Biol.* **66**:937-944.
- Haskell, C.A., W.W. Hancock, D.J. Salant, W. Gao, V. Csizmadia, W. Peters, K. Faia, O. Fituri, J.B. Rottman, and I.F. Charo. 2001. Targeted deletion of CX(3)CR1 reveals a role for fractalkine in cardiac allograft rejection. *J.Clin.Invest.* **108**:679-688.
- Hatakeyama, M., T. Imaizumi, W. Tamo, K. Yamashita, H. Yoshida, I. Fukuda, and K. Satoh. 2004. Heparin inhibits IFN-gamma-induced fractalkine/CX3CL1 expression in human endothelial cells. *Inflammation.* **28**:7-13.
- Hauser, S.L., T.H. Doolittle, R. Lincoln, R.H. Brown, and C.A. Dinarello. 1990. Cytokine accumulations in CSF of multiple sclerosis patients: frequent detection of interleukin-1 and tumor necrosis factor but not interleukin-6. *Neurology.* **40**:1735-1739.
- Hayes, C.E., and E. Donald Acheson. 2008. A unifying multiple sclerosis etiology linking virus infection, sunlight, and vitamin D, through viral interleukin-10. *Med.Hypotheses.* **71**:85-90.
- Hewson, A.K., T. Smith, J.P. Leonard, and M.L. Cuzner. 1995. Suppression of experimental allergic encephalomyelitis in the Lewis rat by the matrix metalloproteinase inhibitor Ro31-9790. *Inflamm.Res.* **44**:345-349.

- Hillyer, P., E. Mordelet, G. Flynn, and D. Male. 2003. Chemokines, chemokine receptors and adhesion molecules on different human endothelia: discriminating the tissue-specific functions that affect leucocyte migration. *Clin.Exp.Immunol.* **134**:431-441.
- Hochmeister, S., R. Grundtner, J. Bauer, B. Engelhardt, R. Lyck, G. Gordon, T. Korosec, A. Kutzelnigg, J.J. Berger, M. Bradl, R.E. Bittner, and H. Lassmann. 2006. Dysferlin is a new marker for leaky brain blood vessels in multiple sclerosis. *J.Neuropathol.Exp.Neurol.* **65**:855-865.
- Hofman, F.M., D.R. Hinton, K. Johnson, and J.E. Merrill. 1989. Tumor necrosis factor identified in multiple sclerosis brain. *J.Exp.Med.* **170**:607-612.
- Holmoy, T. 2007. Immunopathogenesis of multiple sclerosis: concepts and controversies. *Acta Neurol.Scand.Suppl.* **187**:39-45.
- Holmoy, T., and A.L. Hestvik. 2008. Multiple sclerosis: immunopathogenesis and controversies in defining the cause. *Curr.Opin.Infect.Dis.* **21**:271-278.
- Howard, L., and P. Glynn. 1995. Membrane-associated metalloproteinase recognized by characteristic cleavage of myelin basic protein: assay and isolation. *Methods Enzymol.* **248**:388-395.
- Huang, D., F.D. Shi, S. Jung, G.C. Pien, J. Wang, T.P. Salazar-Mather, T.T. He, J.T. Weaver, H.G. Ljunggren, C.A. Biron, D.R. Littman, and R.M. Ransohoff. 2006. The neuronal chemokine CX3CL1/fractalkine selectively recruits NK cells that modify experimental autoimmune encephalomyelitis within the central nervous system. *FASEB J.* **20**:896-905.
- Hulshof, S., E.S. van Haastert, H.F. Kuipers, P.J. van den Elsen, C.J. De Groot, P. van der Valk, R. Ravid, and K. Biber. 2003. CX3CL1 and CX3CR1 expression in human brain tissue: noninflammatory control versus multiple sclerosis. *J.Neuropathol.Exp.Neurol.* **62**:899-907.
- Hundhausen, C., D. Misztela, T.A. Berkhout, N. Broadway, P. Saftig, K. Reiss, D. Hartmann, F. Fahrenholz, R. Postina, V. Matthews, K.J. Kallen, S. Rose-John, and A. Ludwig. 2003. The disintegrin-like metalloproteinase ADAM10 is involved in constitutive cleavage of CX3CL1 (fractalkine) and regulates CX3CL1-mediated cell-cell adhesion. *Blood.* **102**:1186-1195.
- Hundhausen, C., A. Schulte, B. Schulz, M.G. Andrzejewski, N. Schwarz, P. von Hundelshausen, U. Winter, K. Paliga, K. Reiss, P. Saftig, C. Weber, and A. Ludwig. 2007. Regulated shedding of transmembrane chemokines by the disintegrin and metalloproteinase 10 facilitates detachment of adherent leukocytes. *J.Immunol.* **178**:8064-8072.
- Hurst, L.A., R.A. Bunning, P.O. Couraud, I.A. Romero, B.B. Weksler, B. Sharrack, and M.N. Woodroffe. 2009. Expression of ADAM-17, TIMP-3 and fractalkine in the human adult brain endothelial cell line, hCMEC/D3, following pro-inflammatory cytokine treatment. *J.Neuroimmunol.* **210**: 108-112.
- Hutvagner, G., and P.D. Zamore. 2002. RNAi: nature abhors a double-strand. *Curr.Opin.Genet.Dev.* **12**:225-232.

Iba, K., R. Albrechtsen, B. Gilpin, C. Frohlich, F. Loechel, A. Zolkiewska, K. Ishiguro, T. Kojima, W. Liu, J.K. Langford, R.D. Sanderson, C. Brakebusch, R. Fassler, and U.M. Wewer. 2000. The cysteine-rich domain of human ADAM 12 supports cell adhesion through syndecans and triggers signaling events that lead to beta1 integrin-dependent cell spreading. *J. Cell Biol.* **149**:1143-1156.

Iba, K., R. Albrechtsen, B.J. Gilpin, F. Loechel, and U.M. Wewer. 1999. Cysteine-rich domain of human ADAM 12 (meltrin alpha) supports tumor cell adhesion. *Am.J.Pathol.* **154**:1489-1501.

Imai, T., K. Hieshima, C. Haskell, M. Baba, M. Nagira, M. Nishimura, M. Kakizaki, S. Takagi, H. Nomiyama, T.J. Schall, and O. Yoshie. 1997. Identification and molecular characterization of fractalkine receptor CX3CR1, which mediates both leukocyte migration and adhesion. *Cell.* **91**:521-530.

Imaizumi, T., T. Matsumiya, K. Fujimoto, K. Okamoto, X. Cui, U. Ohtaki, Hidemi, Yoshida, and K. Satoh. 2000. Interferon-gamma stimulates the expression of CX3CL1/fractalkine in cultured human endothelial cells. *Tohoku J.Exp.Med.* **192**:127-139.

Imaizumi, T., H. Yoshida, and K. Satoh. 2004. Regulation of CX3CL1/fractalkine expression in endothelial cells. *J.Atheroscler.Thromb.* **11**:15-21.

Infante-Duarte, C., A. Weber, K. Kratzschmar, T. Prozorovski, S. Pikol, I. Hamann, J. Bellmann-Strobl, O. Aktas, J. Dorr, J. Wuerfel, C. S. Sturzebecher, F. Zipp. *FASEB.* **19** (11): 1902+

Iwahashi, T., C.S. Koh, A. Inoue, and N. Yanagisawa. 1997. Tumor necrosis factor-alpha and transforming growth factor-beta production by isolated mononuclear cells from the spinal cords of Lewis rats with experimental autoimmune encephalomyelitis. *Tohoku J.Exp.Med.* **183**:123-133.

Jacobs, L.D., D.L. Cookfair, R.A. Rudick, R.M. Herndon, J.R. Richert, A.M. Salazar, J.S. Fischer, D.E. Goodkin, C.V. Granger, J.H. Simon, J.J. Alam, D.M. Bartoszak, D.N. Bourdette, J. Braiman, C.M. Brownschidle, M.E. Coats, S.L. Cohan, D.S. Dougherty, R.P. Kinkel, M.K. Mass, F.E. Munschauer 3rd, R.L. Priore, P.M. Pullicino, B.J. Scherokman, and R.H. Whitham. 1996. Intramuscular interferon beta-1a for disease progression in relapsing multiple sclerosis. The Multiple Sclerosis Collaborative Research Group (MSCRG). *Ann.Neurol.* **39**:285-294.

Jaworski, D.M., and N. Fager. 2000. Regulation of tissue inhibitor of metalloproteinase-3 (Timp-3) mRNA expression during rat CNS development. *J.Neurosci.Res.* **61**:396-408.

Jensen, J., M. Krakauer, and F. Sellebjerg. 2005. Cytokines and adhesion molecules in multiple sclerosis patients treated with interferon-beta1b. *Cytokine.* **29**:24-30.

Jin, G., X. Huang, R. Black, M. Wolfson, C. Rauch, H. McGregor, G. Ellestad, and R. Cowling. 2002. A continuous fluorimetric assay for tumor necrosis factor-alpha converting enzyme. *Anal.Biochem.* **302**:269-275.

Jinga, V.V., A. Gafencu, F. Antohe, E. Constantinescu, C. Heltianu, M. Raicu, I. Manolescu, W. Hunziker, and M. Simionescu. 2000. Establishment of a pure vascular endothelial cell line from human placenta. *Placenta.* **21**:325-336.

Jurewicz, A.M., A.K. Walczak, and K.W. Selmaj. 1999. Shedding of TNF receptors in multiple sclerosis patients. *Neurology.* **53**:1409-1414.

- Kahn, J., R.H. Ingraham, F. Shirley, G.I. Migaki, and T.K. Kishimoto. 1994a. Membrane proximal cleavage of L-selectin: identification of the cleavage site and a 6-kD transmembrane peptide fragment of L-selectin. *J.Cell Biol.* **125**:461-470.
- Kanazawa, N., T. Nakamura, K. Tashiro, M. Muramatsu, K. Morita, K. Yoneda, K. Inaba, S. Imamura, and T. Honjo. 1999. Fractalkine and macrophage-derived chemokine: T cell-attracting chemokines expressed in T cell area dendritic cells. *Eur.J.Immunol.* **29**:1925-1932.
- Karan, D., F.C. Lin, M. Bryan, J. Ringel, N. Moniaux, M.F. Lin, and S.K. Batra. 2003. Expression of ADAMs (a disintegrin and metalloproteases) and TIMP-3 (tissue inhibitor of metalloproteinase-3) in human prostatic adenocarcinomas. *Int.J.Oncol.* **23**:1365-1371.
- Karpus, W.J., and R.M. Ransohoff. 1998. Chemokine regulation of experimental autoimmune encephalomyelitis: temporal and spatial expression patterns govern disease pathogenesis. *J.Immunol.* **161**:2667-2671.
- Kashiwagi, M., M. Tortorella, H. Nagase, and K. Brew. 2001. TIMP-3 is a potent inhibitor of aggrecanase 1 (ADAM-TS4) and aggrecanase 2 (ADAM-TS5). *J.Biol.Chem.* **276**:12501-12504.
- Kassiotis, G., and G. Kollias. 2001. Uncoupling the proinflammatory from the immunosuppressive properties of tumor necrosis factor (TNF) at the p55 TNF receptor level: implications for pathogenesis and therapy of autoimmune demyelination. *J.Exp.Med.* **193**:427-434.
- Kastenbauer, S., U. Koedel, M. Wick, B.C. Kieseier, H.P. Hartung, and H.W. Pfister. 2003. CSF and serum levels of soluble fractalkine (CX3CL1) in inflammatory diseases of the nervous system. *J.Neuroimmunol.* **137**:210-217.
- Katz, D., J.K. Taubenberger, B. Cannella, D.E. McFarlin, C.S. Raine, and H.F. McFarland. 1993. Correlation between magnetic resonance imaging findings and lesion development in chronic, active multiple sclerosis. *Ann.Neurol.* **34**:661-669.
- Kebir, H., K. Kreymborg, I. Ifergan, A. Dodelet-Devillers, R. Cayrol, M. Bernard, F. Giuliani, N. Arbour, B. Becher, and A. Prat. 2007. Human TH17 lymphocytes promote blood-brain barrier disruption and central nervous system inflammation. *Nat.Med.* **13**:1173-1175.
- Kermode, A.G., A.J. Thompson, P. Tofts, D.G. MacManus, B.E. Kendall, D.P. Kingsley, I.F. Moseley, P. Rudge, and W.I. McDonald. 1990. Breakdown of the blood-brain barrier precedes symptoms and other MRI signs of new lesions in multiple sclerosis. Pathogenetic and clinical implications. *Brain.* **113** (Pt 5):1477-1489.
- Kerschensteiner, M., E. Meinl, and R. Hohlfeld. 2009. Neuro-immune crosstalk in CNS diseases. *Neuroscience.* **158**:1122-1132.
- Khoury, S.J., C.R. Guttmann, E.J. Orav, M.J. Hohol, S.S. Ahn, L. Hsu, R. Kikinis, G.A. Mackin, F.A. Jolesz, and H.L. Weiner. 1994. Longitudinal MRI in multiple sclerosis: correlation between disability and lesion burden. *Neurology.* **44**:2120-2124.
- Kidd, D., F. Barkhof, R. McConnell, P.R. Algra, I.V. Allen, and T. Revesz. 1999. Cortical lesions in multiple sclerosis. *Brain.* **122** (1):17-26.
- Kieseier, B.C., H. Pischel, E. Neuen-Jacob, W.W. Tourtellotte, and H.P. Hartung. 2003. ADAM-10 and ADAM-17 in the inflamed human CNS. *Glia.* **42**:398-405.

Killar, L., J. White, R. Black, and J. Peschon. 1999. Adamalysins. A family of metzincins including TNF-alpha converting enzyme (TACE). *Ann.N.Y.Acad.Sci.* **878**:442-452.

Kirk, J., J. Plumb, M. Mirakhur, and S. McQuaid. 2003. Tight junctional abnormality in multiple sclerosis white matter affects all calibres of vessel and is associated with blood-brain barrier leakage and active demyelination. *J.Pathol.* **201**:319-327.

Kirk, S., J.A. Frank, and S. Karlik. 2004. Angiogenesis in multiple sclerosis: is it good, bad or an epiphenomenon? *J.Neurol.Sci.* **217**:125-130.

Kirk, S.L., and S.J. Karlik. 2003. VEGF and vascular changes in chronic neuroinflammation. *J.Autoimmunity.* **21**:353-363.

Kjellen, L., and U. Lindahl. 1991. Proteoglycans: structures and interactions. *Annu.Rev.Biochem.* **60**:443-475.

Koenig, A., K. Norgard-Sumnicht, R. Linhardt, and A. Varki. 1998. Differential interactions of heparin and heparan sulfate glycosaminoglycans with the selectins. Implications for the use of unfractionated and low molecular weight heparins as therapeutic agents. *J.Clin.Invest.* **101**:877-889.

Kojro, E., and F. Fahrenholz. 2005. The non-amyloidogenic pathway: structure and function of alpha-secretases. *Subcell.Biochem.* **38**:105-127.

Kornek, B., and H. Lassmann. 1999. Axonal pathology in multiple sclerosis. A historical note. *Brain Pathol.* **9**:651-656.

Kraus, J., P. Oschmann, B. Engelhardt, C. Schiel, C. Hornig, R. Bauer, A. Kern, H. Traupe, and W. Dorndorf. 1998. Soluble and cell surface ICAM-1 as markers for disease activity in multiple sclerosis. *Acta Neurol.Scand.* **98**:102-109.

Kraus, J., K. Voigt, A.M. Schuller, M. Scholz, K.S. Kim, M. Schilling, W.R. Schabitz, P. Oschmann, and B. Engelhardt. 2008. Interferon-beta stabilizes barrier characteristics of the blood-brain barrier in four different species in vitro. *Mult.Scler.* **14**:843-852.

Kuhlmann, T., G. Lingfeld, A. Bitsch, J. Schuchardt, and W. Bruck. 2002. Acute axonal damage in multiple sclerosis is most extensive in early disease stages and decreases over time. *Brain.* **125**:2202-2212.

Kutzelnigg, A., C.F. Lucchinetti, C. Stadelmann, W. Bruck, H. Rauschka, M. Bergmann, M. Schmidbauer, J.E. Parisi, and H. Lassmann. 2005. Cortical demyelination and diffuse white matter injury in multiple sclerosis. *Brain.* **128**:2705-2712.

Kwon, E.E., and J.W. Prineas. 1994. Blood-brain barrier abnormalities in longstanding multiple sclerosis lesions. An immunohistochemical study. *J.Neuropathol.Exp.Neurol.* **53**:625-636.

Laing, K.J., and C.J. Secombes. 2004. Chemokines. *Dev.Comp.Immunol.* **28**:443-460.

Lang, H.L., H. Jacobsen, S. Ikemizu, C. Andersson, K. Harlos, L. Madsen, P. Hjorth, L. Sondergaard, A. Svejgaard, K. Wucherpfennig, D.I. Stuart, J.I. Bell, E.Y. Jones, and L. Fugger. 2002. A functional and structural basis for TCR cross-reactivity in multiple sclerosis. *Nat.Immunol.* **3**:940-943.

- Langholz, E., P. Munkholm, M. Davidsen, and V. Binder. 1994. Course of ulcerative colitis: analysis of changes in disease activity over years. *Gastroenterology*. **107**:3-11.
- Lassmann, H., W. Bruck, and C. Lucchinetti. 2001. Heterogeneity of multiple sclerosis pathogenesis: implications for diagnosis and therapy. *Trends Mol.Med.* **7**:115-121.
- Lee, M.A., J. Palace, G. Stabler, J. Ford, A. Gearing, and K. Miller. 1999. Serum gelatinase B, TIMP-1 and TIMP-2 levels in multiple sclerosis. A longitudinal clinical and MRI study. *Brain*. **122** (2):191-197.
- Leech, S., J. Kirk, J. Plumb, and S. McQuaid. 2007. Persistent endothelial abnormalities and blood-brain barrier leak in primary and secondary progressive multiple sclerosis. *Neuropathol.Appl.Neurobiol.* **33**:86-98.
- Lewis, M., L.A. Tartaglia, A. Lee, G.L. Bennett, G.C. Rice, G.H. Wong, E.Y. Chen, and D.V. Goeddel. 1991. Cloning and expression of cDNAs for two distinct murine tumor necrosis factor receptors demonstrate one receptor is species specific. *Proc.Natl.Acad.Sci.U.S.A.* **88**:2830-2834.
- Li, X., and H. Fan. 2004. Loss of ectodomain shedding due to mutations in the metalloprotease and cysteine-rich/disintegrin domains of the tumor necrosis factor-alpha converting enzyme (TACE). *J.Biol.Chem.* **279**:27365-27375.
- Li, X., L. Perez, Z. Pan, and H. Fan. 2007. The transmembrane domain of TACE regulates protein ectodomain shedding. *Cell Res.* **17**:985-998.
- Liedtke, W., B. Cannella, R.J. Mazzaccaro, J.M. Clements, K.M. Miller, K.W. Wucherpfennig, A.J. Gearing, and C.S. Raine. 1998. Effective treatment of models of multiple sclerosis by matrix metalloproteinase inhibitors. *Ann.Neurol.* **44**:35-46.
- Lindert, R.B., C.G. Haase, U. Brehm, C. Linington, H. Wekerle, and R. Hohlfeld. 1999. Multiple sclerosis: B- and T-cell responses to the extracellular domain of the myelin oligodendrocyte glycoprotein. *Brain*. **122** (Pt 11):2089-2100.
- Liu, G.Y., V. Kulasingam, R.T. Alexander, N. Touret, A.M. Fong, D.D. Patel, and L.A. Robinson. 2005. Recycling of the membrane-anchored chemokine, CX3CL1. *J.Biol.Chem.* **280**:19858-19866.
- Livak, K.J., and T.D. Schmittgen. 2001. Analysis of relative gene expression data using real-time quantitative PCR and the 2(-Delta Delta C(T)) Method. *Methods*. **25**:402-408.
- Loddick, S.A., and N.J. Rothwell. 1999. Mechanisms of tumor necrosis factor alpha action on neurodegeneration: interaction with insulin-like growth factor-1. *Proc.Natl.Acad.Sci.U.S.A.* **96**:9449-9451.
- Lortat-Jacob, H., and J.A. Grimaud. 1992. Binding of interferon-gamma to heparan sulfate is restricted to the heparin-like domains and involves carboxylic--but not N-sulfated--groups. *Biochim.Biophys.Acta.* **1117**:126-130.
- Lu, C.Z., M.A. Jensen, and B.G. Arnason. 1993. Interferon gamma- and interleukin-4-secreting cells in multiple sclerosis. *J.Neuroimmunol.* **46**:123-128.
- Lublin, F.D. 2005. Clinical features and diagnosis of multiple sclerosis. *Neurol.Clin.* **23**:1-15.

- Lucas, A.D., N. Chadwick, B.F. Warren, D.P. Jewell, S. Gordon, F. Powrie, and D.R. Greaves. 2001. The transmembrane form of the CX3CL1 chemokine fractalkine is expressed predominantly by epithelial cells in vivo. *Am.J.Pathol.* **158**:855-866.
- Lucchinetti, C., W. Bruck, J. Parisi, B. Scheithauer, M. Rodriguez, and H. Lassmann. 2000. Heterogeneity of multiple sclerosis lesions: implications for the pathogenesis of demyelination. *Ann.Neurol.* **47**:707-717.
- Lucchinetti, C.F., J. Parisi, and W. Bruck. 2005. The pathology of multiple sclerosis. *Neurol.Clin.* **23**:77-105, vi.
- Ludwig, A., T. Berkhout, K. Moores, P. Groot, and G. Chapman. 2002. Fractalkine is expressed by smooth muscle cells in response to IFN-gamma and TNF-alpha and is modulated by metalloproteinase activity. *J.Immunol.* **168**:604-612.
- Lum, L., M.S. Reid, and C.P. Blobel. 1998. Intracellular maturation of the mouse metalloprotease disintegrin MDC15. *J.Biol.Chem.* **273**:26236-26247.
- Lum, L., B.R. Wong, R. Josien, J.D. Becherer, H. Erdjument-Bromage, J. Schlondorff, P. Tempst, Y. Choi, and C.P. Blobel. 1999. Evidence for a role of a tumor necrosis factor-alpha (TNF-alpha)-converting enzyme-like protease in shedding of TRANCE, a TNF family member involved in osteoclastogenesis and dendritic cell survival. *J.Biol.Chem.* **274**:13613-13618.
- Lundmark, F., K. Duvefelt, E. Iacobaeus, I. Kockum, E. Wallstrom, M. Khademi, A. Oturai, L.P. Ryder, J. Saarela, H.F. Harbo, E.G. Celius, H. Salter, T. Olsson, and J. Hillert. 2007. Variation in interleukin 7 receptor alpha chain (IL7R) influences risk of multiple sclerosis. *Nat.Genet.* **39**:1108-1113.
- Lunn, C.A., X. Fan, B. Dalie, K. Miller, P.J. Zavodny, S.K. Narula, and D. Lundell. 1997. Purification of ADAM 10 from bovine spleen as a TNFalpha convertase. *FEBS Lett.* **400**:333-335.
- Luster, A.D. 1998. Chemokines-chemotactic cytokines that mediate inflammation. *N.Engl.J.Med.* **338**:436-445.
- Lycke, J.N., J.E. Karlsson, O. Andersen, and L.E. Rosengren. 1998. Neurofilament protein in cerebrospinal fluid: a potential marker of activity in multiple sclerosis. *J.Neurol.Neurosurg.Psychiatry.* **64**:402-404.
- MacEwan, D.J. 2002. TNF receptor subtype signalling: differences and cellular consequences. *Cell.Signal.* **14**:477-492.
- Maciejewski-Lenoir, D., S. Chen, L. Feng, R. Maki, and K.B. Bacon. 1999. Characterization of fractalkine in rat brain cells: migratory and activation signals for CX3CR-1-expressing microglia. *J.Immunol.* **163**:1628-1635.
- Magliozzi, R., O. Howell, A. Vora, B. Serafini, R. Nicholas, M. Puopolo, R. Reynolds, and F. Aloisi. 2007. Meningeal B-cell follicles in secondary progressive multiple sclerosis associate with early onset of disease and severe cortical pathology. *Brain.* **130**:1089-1104.
- Maimone, D., S. Gregory, B.G. Arnason, and A.T. Reder. 1991. Cytokine levels in the cerebrospinal fluid and serum of patients with multiple sclerosis. *J.Neuroimmunol.* **32**:67-74.

- Majka, S., P.G. McGuire, and A. Das. 2002. Regulation of matrix metalloproteinase expression by tumor necrosis factor in a murine model of retinal neovascularization. *Invest. Ophthalmol. Vis. Sci.* **43**:260-266.
- Man, S., E.E. Ubogu, and R.M. Ransohoff. 2007. Inflammatory cell migration into the central nervous system: a few new twists on an old tale. *Brain Pathol.* **17**:243-250.
- Man, S., E.E. Ubogu, K.A. Williams, B. Tucky, M.K. Callahan, and R.M. Ransohoff. 2008. Human brain microvascular endothelial cells and umbilical vein endothelial cells differentially facilitate leukocyte recruitment and utilize chemokines for T cell migration. *Clin. Dev. Immunol.* 2008:384982.
- Mann, C.L., M.B. Davies, V.L. Stevenson, S.M. Leary, M.D. Boggild, C. Ko Ko, P.W. Jones, A.A. Fryer, R.C. Strange, A.J. Thompson, and C.P. Hawkins. 2002. Interleukin 1 genotypes in multiple sclerosis and relationship to disease severity. *J. Neuroimmunol.* **129**:197-204.
- Marrie, R.A. 2004. Environmental risk factors in multiple sclerosis aetiology. *Lancet Neurol.* **3**:709-718.
- Marrosu, M.G., M. Lai, E. Cocco, V. Loi, G. Spinicci, M.P. Pischedda, S. Massole, G. Marrosu, and P. Contu. 2002. Genetic factors and the founder effect explain familial MS in Sardinia. *Neurology.* **58**:283-288.
- Marrosu, M.G., M.R. Murru, G. Costa, R. Murru, F. Muntoni, and F. Cucca. 1998. DRB1-DQA1-DQB1 loci and multiple sclerosis predisposition in the Sardinian population. *Hum. Mol. Genet.* **7**:1235-1237.
- Martin, D., and S.L. Near. 1995. Protective effect of the interleukin-1 receptor antagonist (IL-1ra) on experimental allergic encephalomyelitis in rats. *J. Neuroimmunol.* **61**:241-245.
- Martino, G., A. Consiglio, D.M. Franciotta, A. Corti, M. Filippi, K. Vandebroek, F.L. Sica, G. Comi, and L.M. Grimaldi. 1997. Tumor necrosis factor alpha and its receptors in relapsing-remitting multiple sclerosis. *J. Neurol. Sci.* **152**:51-61.
- Maskos, K., C. Fernandez-Catalan, R. Huber, G.P. Bourenkov, H. Bartunik, G.A. Ellestad, P. Reddy, M.F. Wolfson, C.T. Rauch, B.J. Castner, R. Davis, H.R. Clarke, M. Petersen, J.N. Fitzner, D.P. Cerretti, C.J. March, R.J. Paxton, R.A. Black, and W. Bode. 1998. Crystal structure of the catalytic domain of human tumor necrosis factor-alpha-converting enzyme. *Proc. Natl. Acad. Sci. U. S. A.* **95**:3408-3412.
- Mason, J.L., K. Suzuki, D.D. Chaplin, and G.K. Matsushima. 2001. Interleukin-1beta promotes repair of the CNS. *J. Neurosci.* **21**:7046-7052.
- Matthews, V., B. Schuster, S. Schutze, I. Bussmeyer, A. Ludwig, C. Hundhausen, T. Sadowski, P. Saftig, D. Hartmann, K.J. Kallen, and S. Rose-John. 2003a. Cellular cholesterol depletion triggers shedding of the human interleukin-6 receptor by ADAM10 and ADAM17 (TACE). *J. Biol. Chem.* **278**:38829-38839.
- Matthews, V., B. Schuster, S. Schutze, I. Bussmeyer, A. Ludwig, C. Hundhausen, T. Sadowski, P. Saftig, D. Hartmann, K.J. Kallen, and S. Rose-John. 2003b. Cellular cholesterol depletion triggers shedding of the human interleukin-6 receptor by ADAM10 and ADAM17 (TACE). *J. Biol. Chem.* **278**:38829-38839.

- Matzner, Y., G. Marx, R. Drexler, and A. Eldor. 1984. The inhibitory effect of heparin and related glycosaminoglycans on neutrophil chemotaxis. *Thromb.Haemost.* **52**:134-137.
- Mayhan, W.G. 2002. Cellular mechanisms by which tumor necrosis factor-alpha produces disruption of the blood-brain barrier. *Brain Res.* **927**:144-152.
- McCandless, E.E., Q. Wang, B.M. Woerner, J.M. Harper, and R.S. Klein. 2006. CXCL12 limits inflammation by localizing mononuclear infiltrates to the perivascular space during experimental autoimmune encephalomyelitis. *J.Immunol.* **177**:8053-8064.
- McCoy, M.K., and M.G. Tansey. 2008. TNF signaling inhibition in the CNS: implications for normal brain function and neurodegenerative disease. *J.Neuroinflammation.* **5**:45.
- McDonnell, G.V., S.A. McMillan, J.P. Douglas, A.G. Droogan, and S.A. Hawkins. 1999. Serum soluble adhesion molecules in multiple sclerosis: raised sVCAM-1, sICAM-1 and sE-selectin in primary progressive disease. *J.Neurol.* **246**:87-92.
- McFarlin, D.E., and P.J. Lachmann. 1989. Multiple sclerosis. Hopeful genes and immunology. *Nature.* **341**:693-694.
- McManus, M.T., and P.A. Sharp. 2002. Gene silencing in mammals by small interfering RNAs. *Nat.Rev.Genet.* **3**:737-747.
- Merrill, J.E. 1992. Proinflammatory and antiinflammatory cytokines in multiple sclerosis and central nervous system acquired immunodeficiency syndrome. *J.Immunother.* **12**:167-170.
- Meucci, O., A. Fatatis, A.A. Simen, and R.J. Miller. 2000. Expression of CX3CR1 chemokine receptors on neurons and their role in neuronal survival. *Proc.Natl.Acad.Sci.U.S.A.* **97**:8075-8080.
- Mezyk, R., M. Bzowska, and J. Bereta. 2003. Structure and functions of tumor necrosis factor-alpha converting enzyme. *Acta Biochim.Pol.* **50**:625-645.
- Migaki, G.I., J. Kahn, and T.K. Kishimoto. 1995. Mutational analysis of the membrane-proximal cleavage site of L-selectin: relaxed sequence specificity surrounding the cleavage site. *J.Exp.Med.* **182**:549-557.
- Milla, M.E., M.A. Leesnitzer, M.L. Moss, W.C. Clay, H.L. Carter, A.B. Miller, J.L. Su, M.H. Lambert, D.H. Willard, D.M. Sheeley, T.A. Kost, W. Burkhart, M. Moyer, R.K. Blackburn, G.L. Pahel, J.L. Mitchell, C.R. Hoffman, and J.D. Becherer. 1999. Specific sequence elements are required for the expression of functional tumor necrosis factor-alpha-converting enzyme (TACE). *J.Biol.Chem.* **274**:30563-30570.
- Miller, D.H., S.R. Hammond, J.G. McLeod, G. Purdie, and D.C. Skegg. 1990. Multiple sclerosis in Australia and New Zealand: are the determinants genetic or environmental? *J.Neurol.Neurosurg.Psychiatry.* **53**:903-905.
- Miller, M.D., and M.S. Krangel. 1992. Biology and biochemistry of the chemokines: a family of chemotactic and inflammatory cytokines. *Crit.Rev.Immunol.* **12**:17-46.
- Millward, J.M., M. Caruso, I.L. Campbell, J. Gauldie, and T. Owens. 2007. IFN-gamma-induced chemokines synergize with pertussis toxin to promote T cell entry to the central nervous system. *J.Immunol.* **178**:8175-8182.

- Mitic, L.L., and J.M. Anderson. 1998. Molecular architecture of tight junctions. *Annu.Rev.Physiol.* **60**:121-142.
- Mizuno, T., J. Kawanokuchi, K. Numata, and A. Suzumura. 2003. Production and neuroprotective functions of fractalkine in the central nervous system. *Brain Res.* **979**:65-70.
- Mohler, K.M., P.R. Sleath, J.N. Fitzner, D.P. Cerretti, M. Alderson, S.S. Kerwar, D.S. Torrance, C. Otten-Evans, T. Greenstreet, and K. Weerawarna. 1994. Protection against a lethal dose of endotoxin by an inhibitor of tumour necrosis factor processing. *Nature.* **370**:218-220.
- Mokhtarian, F., Y. Shi, D. Shirazian, L. Morgante, A. Miller, and D. Grob. 1994. Defective production of anti-inflammatory cytokine, TGF-beta by T cell lines of patients with active multiple sclerosis. *J.Immunol.* **152**:6003-6010.
- Moll, C., C. Mourre, M. Lazdunski, and J. Ulrich. 1991. Increase of sodium channels in demyelinated lesions of multiple sclerosis. *Brain Res.* **556**:311-316.
- Montero, J.C., L. Yuste, E. Diaz-Rodriguez, A. Esparis-Ogando, and A. Pandiella. 2002. Mitogen-activated protein kinase-dependent and -independent routes control shedding of transmembrane growth factors through multiple secretases. *Biochem.J.* **363**:211-221.
- Moon, S.O., W. Kim, M.J. Sung, S. Lee, K.P. Kang, D.H. Kim, S.Y. Lee, J.N. So, and S.K. Park. 2006. Resveratrol suppresses tumor necrosis factor-alpha-induced fractalkine expression in endothelial cells. *Mol.Pharmacol.* **70**:112-119.
- Moore, K.W., R. de Waal Malefyt, R.L. Coffman, and A. O'Garra. 2001. Interleukin-10 and the interleukin-10 receptor. *Annu.Rev.Immunol.* **19**:683-765.
- Moss, M.L., S.L. Jin, M.E. Milla, D.M. Bickett, W. Burkhart, H.L. Carter, W.J. Chen, W.C. Clay, J.R. Didsbury, D. Hassler, C.R. Hoffman, T.A. Kost, M.H. Lambert, M.A. Leesnitzer, P. McCauley, G. McGeehan, J. Mitchell, M. Moyer, G. Pahel, W. Rocque, L.K. Overton, F. Schoenen, T. Seaton, J.L. Su, and J.D. Becherer. 1997. Cloning of a disintegrin metalloproteinase that processes precursor tumour-necrosis factor-alpha. *Nature.* **385**:733-736.
- Moss, M.L., L. Sklair-Tavron, and R. Nudelman. 2008. Drug insight: tumor necrosis factor-converting enzyme as a pharmaceutical target for rheumatoid arthritis. *Nat.Clin.Pract.Rheumatol.* **4**:300-309.
- Muehlhoefer, A., L.J. Saubermann, X. Gu, K. Luedtke-Heckenkamp, R. Xavier, R.S. Blumberg, D.K. Podolsky, R.P. MacDermott, and H.C. Reinecker. 2000. Fractalkine is an epithelial and endothelial cell-derived chemoattractant for intraepithelial lymphocytes in the small intestinal mucosa. *J.Immunol.* **164**:3368-3376.
- Mullis, K.B., and F.A. Faloona. 1987. Specific synthesis of DNA in vitro via a polymerase-catalyzed chain reaction. *Methods Enzymol.* **155**:335-350.
- Mumford, C.J., N.W. Wood, H. Kellar-Wood, J.W. Thorpe, D.H. Miller, and D.A. Compston. 1994. The British Isles survey of multiple sclerosis in twins. *Neurology.* **44**:11-15.

- Muraguchi, T., Y. Takegami, T. Ohtsuka, S. Kitajima, E.P. Chandana, A. Omura, T. Miki, R. Takahashi, N. Matsumoto, A. Ludwig, M. Noda, and C. Takahashi. 2007. RECK modulates Notch signaling during cortical neurogenesis by regulating ADAM10 activity. *Nat.Neurosci.* **10**:838-845.
- Murray, J.M. 2005. Confocal microscopy, deconvolution, and structured illumination methods. In *Live cell imaging: a laboratory manual*. Cold Spring Harbor Laboratory Press; Pap/Dvdr edition. Chapter 14: pp239-279.
- Nadeau, S., and S. Rivest. 1999. Effects of circulating tumor necrosis factor on the neuronal activity and expression of the genes encoding the tumor necrosis factor receptors (p55 and p75) in the rat brain: a view from the blood-brain barrier. *Neuroscience*. **93**:1449-1464.
- Newcombe, J., C.P. Hawkins, C.L. Henderson, H.A. Patel, M.N. Woodroffe, G.M. Hayes, M.L. Cuzner, D. MacManus, E.P. du Boulay, and W.I. McDonald. 1991. Histopathology of multiple sclerosis lesions detected by magnetic resonance imaging in unfixed postmortem central nervous system tissue. *Brain*. **114** (2):1013-1023.
- Niino, M., C. Bodner, M.L. Simard, S. Alatab, D. Gano, H.J. Kim, M. Trigueiro, D. Racicot, C. Guerette, J.P. Antel, A. Fournier, F. Grand'Maison, and A. Bar-Or. 2006. Natalizumab effects on immune cell responses in multiple sclerosis. *Ann.Neurol.* **59**:748-754.
- Nishiyori, A., M. Minami, Y. Ohtani, S. Takami, J. Yamamoto, N. Kawaguchi, T. Kume, A. Akaike, and M. Satoh. 1998. Localization of fractalkine and CX3CR1 mRNAs in rat brain: does fractalkine play a role in signaling from neuron to microglia? *FEBS Lett.* **429**:167-172.
- Olerup, O., and J. Hillert. 1991. HLA class II-associated genetic susceptibility in multiple sclerosis: a critical evaluation. *Tissue Antigens*. **38**:1-15.
- Ollier, W., and D.P.M. Symmons. 1992. Clinical consequences: predominantly one organ disease. In *Autoimmunity*. Bios Scientific Publishers Ltd. pp111.
- Oppenheim, J.J. 2001. Cytokines: past, present, and future. *Int.J.Hematol.* **74**:3-8.
- Owens, G.P., K.M. Wings, A.M. Ritchie, S. Edwards, M.P. Burgoon, L. Lehnhoff, K. Nielsen, J. Corboy, D.H. Gilden, and J.L. Bennett. 2007. VH4 gene segments dominate the intrathecal humoral immune response in multiple sclerosis. *J.Immunol.* **179**:6343-6351.
- Pagenstecher, A., A.K. Stalder, C.L. Kincaid, S.D. Shapiro, and I.L. Campbell. 1998. Differential expression of matrix metalloproteinase and tissue inhibitor of matrix metalloproteinase genes in the mouse central nervous system in normal and inflammatory states. *Am.J.Pathol.* **152**:729-741.
- Pan, W., and A.J. Kastin. 2002. TNFalpha transport across the blood-brain barrier is abolished in receptor knockout mice. *Exp.Neurol.* **174**:193-200.
- Pan, Y., C. Lloyd, H. Zhou, S. Dolich, J. Deeds, J.A. Gonzalo, J. Vath, M. Gosselin, J. Ma, B. Dussault, E. Woolf, G. Alperin, J. Culpepper, J.C. Gutierrez-Ramos, and D. Gearing. 1997. Neurotactin, a membrane-anchored chemokine upregulated in brain inflammation. *Nature*. **387**:611-617.
- Pandiella, A., and J. Massague. 1991. Multiple signals activate cleavage of the membrane transforming growth factor-alpha precursor. *J.Biol.Chem.* **266**:5769-5773.

- Panitch, H.S., R.L. Hirsch, A.S. Haley, and K.P. Johnson. 1987. Exacerbations of multiple sclerosis in patients treated with gamma interferon. *Lancet*. **1**:893-895.
- Papadopoulos, E.J., C. Sasseti, H. Saeki, N. Yamada, T. Kawamura, D.J. Fitzhugh, M.A. Saraf, T. Schall, A. Blauvelt, S.D. Rosen, and S.T. Hwang. 1999. Fractalkine, a CX3C chemokine, is expressed by dendritic cells and is up-regulated upon dendritic cell maturation. *Eur.J.Immunol*. **29**:2551-2559.
- Pei, Y., and T. Tuschl. 2006. On the art of identifying effective and specific siRNAs. *Nat.Methods*. **3**:670-676.
- Peiretti, F., M. Canault, P. Deprez-Beauclair, V. Berthet, B. Bonardo, I. Juhan-Vague, and G. Nalbone. 2003. Intracellular maturation and transport of tumor necrosis factor alpha converting enzyme. *Exp.Cell Res*. **285**:278-285.
- Pepper, M.S., N. Ferrara, L. Orci, and R. Montesano. 1992. Potent synergism between vascular endothelial growth factor and basic fibroblast growth factor in the induction of angiogenesis in vitro. *Biochem.Biophys.Res.Commun*. **189**:824-831.
- Peress, N.S., E. Perillo, and R.J. Seidman. 1996. Glial transforming growth factor (TGF)-beta isotypes in multiple sclerosis: differential glial expression of TGF-beta 1, 2 and 3 isotypes in multiple sclerosis. *J.Neuroimmunol*. **71**:115-123.
- Peschon, J.J., J.L. Slack, P. Reddy, K.L. Stocking, S.W. Sunnarborg, D.C. Lee, W.E. Russell, B.J. Castner, R.S. Johnson, J.N. Fitzner, R.W. Boyce, N. Nelson, C.J. Kozlosky, M.F. Wolfson, C.T. Rauch, D.P. Cerretti, R.J. Paxton, C.J. March, and R.A. Black. 1998. An essential role for ectodomain shedding in mammalian development. *Science*. **282**:1281-1284.
- Pestka, S., C.D. Krause, and M.R. Walter. 2004. Interferons, interferon-like cytokines, and their receptors. *Immunol.Rev*. **202**:8-32.
- Peter, J.B., F.N. Boctor, and W.W. Tourtellotte. 1991. Serum and CSF levels of IL-2, sIL-2R, TNF-alpha, and IL-1 beta in chronic progressive multiple sclerosis: expected lack of clinical utility. *Neurology*. **41**:121-123.
- Petereit, H.F., R. Pukrop, F. Fazekas, S.U. Bamborschke, S. Ropele, H.W. Kolmel, S. Merkelsbach, G. Japp, P.J. Jongen, H.P. Hartung, and O.R. Hommes. 2003. Low interleukin-10 production is associated with higher disability and MRI lesion load in secondary progressive multiple sclerosis. *J.Neurol.Sci*. **206**:209-214.
- Petty, M.A., and E.H. Lo. 2002. Junctional complexes of the blood-brain barrier: permeability changes in neuroinflammation. *Prog.Neurobiol*. **68**:311-323.
- Pillai, R.S. 2005. MicroRNA function: multiple mechanisms for a tiny RNA? *RNA*. **11**:1753-1761.
- Plumb, J., A.K. Cross, J. Surr, G. Haddock, T. Smith, R.A. Bunning, and M.N. Woodroffe. 2005. ADAM-17 and TIMP3 protein and mRNA expression in spinal cord white matter of rats with acute experimental autoimmune encephalomyelitis. *J.Neuroimmunol*. **164**:1-9.
- Plumb, J., S. McQuaid, A.K. Cross, J. Surr, G. Haddock, R.A. Bunning, and M.N. Woodroffe. 2006. Upregulation of ADAM-17 expression in active lesions in multiple sclerosis. *Mult.Scler*. **12**:375-385.

Powell, D.W. 1981. Barrier function of epithelia. *Am.J.Physiol.* **241**:G275-88.

PRISMS (Prevention of Relapses and Disability by Interferon beta-1a Subcutaneously in Multiple Sclerosis) Study Group. 1998. Randomised double-blind placebo-controlled study of interferon beta-1a in relapsing/remitting multiple sclerosis. *Lancet.* **352**: 1498-1504.

Probert, L., K. Akassoglou, M. Pasparakis, G. Kontogeorgos, and G. Kollias. 1995. Spontaneous inflammatory demyelinating disease in transgenic mice showing central nervous system-specific expression of tumor necrosis factor alpha. *Proc.Natl.Acad.Sci.U.S.A.* **92**:11294-11298.

Proescholdt, M.A., S. Jacobson, N. Tresser, E.H. Oldfield, and M.J. Merrill. 2002. Vascular endothelial growth factor is expressed in multiple sclerosis plaques and can induce inflammatory lesions in experimental allergic encephalomyelitis rats. *J.Neuropathol.Exp.Neurol.* **61**:914-925.

Qi, J.H., Q. Ebrahem, N. Moore, G. Murphy, L. Claesson-Welsh, M. Bond, A. Baker, and B. Anand-Apte. 2003. A novel function for tissue inhibitor of metalloproteinases-3 (TIMP3): inhibition of angiogenesis by blockage of VEGF binding to VEGF receptor-2. *Nat.Med.* **9**:407-415.

Qin, Y., P. Duquette, Y. Zhang, P. Talbot, R. Poole, and J. Antel. 1998. Clonal expansion and somatic hypermutation of V(H) genes of B cells from cerebrospinal fluid in multiple sclerosis. *J.Clin.Invest.* **102**:1045-1050.

Raine, C.S. 1995. Multiple sclerosis: TNF revisited, with promise. *Nat.Med.* **1**:211-214.

Ramagopalan, S.V., A.P. Morris, D.A. Dymont, B.M. Herrera, G.C. DeLuca, M.R. Lincoln, S.M. Orton, M.J. Chao, A.D. Sadovnick, and G.C. Ebers. 2007. The inheritance of resistance alleles in multiple sclerosis. *PLoS Genet.* **3**:1607-1613.

Ramsden, L., and C.C. Rider. 1992. Selective and differential binding of interleukin (IL)-1 alpha, IL-1 beta, IL-2 and IL-6 to glycosaminoglycans. *Eur.J.Immunol.* **22**:3027-3031.

Reddy, H., S. Narayanan, P.M. Matthews, R.D. Hoge, G.B. Pike, P. Duquette, J. Antel, and D.L. Arnold. 2000a. Relating axonal injury to functional recovery in MS. *Neurology.* **54**:236-239.

Reddy, P., J.L. Slack, R. Davis, D.P. Cerretti, C.J. Kozlosky, R.A. Blanton, D. Shows, J.J. Peschon, and R.A. Black. 2000b. Functional analysis of the domain structure of tumor necrosis factor-alpha converting enzyme. *J.Biol.Chem.* **275**:14608-14614.

Reiss, K., and P. Saftig. 2009. The "A Disintegrin And Metalloprotease" (ADAM) family of sheddases: Physiological and cellular functions. *Semin.Cell Dev.Biol.* **20**:126-137.

Revesz, T., D. Kidd, A.J. Thompson, R.O. Barnard, and W.I. McDonald. 1994. A comparison of the pathology of primary and secondary progressive multiple sclerosis. *Brain.* **117** (4):759-765.

Rieckmann, P., U. Michel, M. Albrecht, W. Bruck, L. Wockel, and K. Felgenhauer. 1995. Soluble forms of intercellular adhesion molecule-1 (ICAM-1) block lymphocyte attachment to cerebral endothelial cells. *J.Neuroimmunol.* **60**:9-15.

Robertson, N.P., D. Clayton, M. Fraser, J. Deans, and D.A. Compston. 1996. Clinical concordance in sibling pairs with multiple sclerosis. *Neurology.* **47**:347-352.

- Robertson, N.P., J.I. O'Riordan, J. Chataway, D.P. Kingsley, D.H. Miller, D. Clayton, and D.A. Compston. 1997. Offspring recurrence rates and clinical characteristics of conjugal multiple sclerosis. *Lancet*. **349**:1587-1590.
- Rocks, N., G. Paulissen, M. El Hour, F. Quesada, C. Crahay, M. Gueders, J.M. Foidart, A. Noel, and D. Cataldo. 2008. Emerging roles of ADAM and ADAMTS metalloproteinases in cancer. *Biochimie*. **90**:369-379.
- Roghani, M., J.D. Becherer, M.L. Moss, R.E. Atherton, H. Erdjument-Bromage, J. Arribas, R.K. Blackburn, G. Weskamp, P. Tempst, and C.P. Blobel. 1999. Metalloprotease-disintegrin MDC9: intracellular maturation and catalytic activity. *J.Biol.Chem*. **274**:3531-3540.
- Romera, C., O. Hurtado, S.H. Botella, I. Lizasoain, A. Cardenas, P. Fernandez-Tome, J.C. Leza, P. Lorenzo, and M.A. Moro. 2004. In vitro ischemic tolerance involves upregulation of glutamate transport partly mediated by the TACE/ADAM17-tumor necrosis factor-alpha pathway. *J.Neurosci*. **24**:1350-1357.
- Roncarolo, M.G., R. Bacchetta, C. Bordignon, S. Narula, and M.K. Levings. 2001. Type 1 T regulatory cells. *Immunol.Rev*. **182**:68-79.
- Rooke, J., D. Pan, T. Xu, and G.M. Rubin. 1996. KUZ, a conserved metalloprotease-disintegrin protein with two roles in Drosophila neurogenesis. *Science*. **273**:1227-1231.
- Rosendahl, M.S., S.C. Ko, D.L. Long, M.T. Brewer, B. Rosenzweig, E. Hedl, L. Anderson, S.M. Pyle, J. Moreland, M.A. Meyers, T. Kohno, D. Lyons, and H.S. Lichenstein. 1997. Identification and characterization of a pro-tumor necrosis factor-alpha-processing enzyme from the ADAM family of zinc metalloproteases. *J.Biol.Chem*. **272**:24588-24593.
- Rovida, E., A. Paccagnini, M. Del Rosso, J. Peschon, and P. Dello Sbarba. 2001. TNF-alpha-converting enzyme cleaves the macrophage colony-stimulating factor receptor in macrophages undergoing activation. *J.Immunol*. **166**:1583-1589.
- Rubin, L.L., D.E. Hall, S. Porter, K. Barbu, C. Cannon, H.C. Horner, M. Janatpour, C.W. Liaw, K. Manning, and J. Morales. 1991. A cell culture model of the blood-brain barrier. *J.Cell Biol*. **115**:1725-1735.
- Ruddle, N.H., C.M. Bergman, K.M. McGrath, E.G. Lingenheld, M.L. Grunnet, S.J. Padula, and R.B. Clark. 1990. An antibody to lymphotoxin and tumor necrosis factor prevents transfer of experimental allergic encephalomyelitis. *J.Exp.Med*. **172**:1193-1200.
- Ruth, J.H., M.V. Volin, G.K. Haines 3rd, D.C. Woodruff, K.J. Katschke Jr, J.M. Woods, C.C. Park, J.C. Morel, and A.E. Koch. 2001. Fractalkine, a novel chemokine in rheumatoid arthritis and in rat adjuvant-induced arthritis. *Arthritis Rheum*. **44**:1568-1581.
- Saitoh, T., and K.R. Dobkins. 1986. Protein kinase C in human brain and its inhibition by calmodulin. *Brain Res*. **379**:196-199.
- Schafer, A., C. Schulz, M. Eigenthaler, D. Fraccarollo, A. Kobsar, M. Gawaz, G. Ertl, U. Walter, and J. Bauersachs. 2004. Novel role of the membrane-bound chemokine fractalkine in platelet activation and adhesion. *Blood*. **103**:407-412.
- Schlondorff, J., J.D. Becherer, and C.P. Blobel. 2000. Intracellular maturation and localization of the tumour necrosis factor alpha convertase (TACE). *Biochem.J*. **347** (1):131-138.

- Schlondorff, J., and C.P. Blobel. 1999. Metalloprotease-disintegrins: modular proteins capable of promoting cell-cell interactions and triggering signals by protein-ectodomain shedding. *J. Cell. Sci.* **112** (21):3603-3617.
- Schlondorff, J., L. Lum, and C.P. Blobel. 2001. Biochemical and pharmacological criteria define two shedding activities for TRANCE/OPGL that are distinct from the tumor necrosis factor alpha convertase. *J. Biol. Chem.* **276**:14665-14674.
- Schulz, B., J. Pruessmeyer, T. Maretzky, A. Ludwig, C.P. Blobel, P. Saftig, and K. Reiss. 2008. ADAM10 regulates endothelial permeability and T-Cell transmigration by proteolysis of vascular endothelial cadherin. *Circ. Res.* **102**:1192-1201.
- Schulz, C., A. Schafer, M. Stolla, S. Kerstan, M. Lorenz, M.L. von Bruhl, M. Schiemann, J. Bauersachs, T. Gloe, D.H. Busch, M. Gawaz, and S. Massberg. 2007. Chemokine fractalkine mediates leukocyte recruitment to inflammatory endothelial cells in flowing whole blood: a critical role for P-selectin expressed on activated platelets. *Circulation.* **116**:764-773.
- Schwaeble, W.J., C.M. Stover, T.J. Schall, D.J. Dairaghi, P.K. Trinder, C. Linington, A. Iglesias, A. Schubart, N.J. Lynch, E. Weihe, and M.K. Schafer. 1998. Neuronal expression of fractalkine in the presence and absence of inflammation. *FEBS Lett.* **439**:203-207.
- Seifert, T., B.C. Kieseier, S. Ropele, S. Strasser-Fuchs, F. Quehenberger, F. Fazekas, and H.P. Hartung. 2002. TACE mRNA expression in peripheral mononuclear cells precedes new lesions on MRI in multiple sclerosis. *Mult. Scler.* **8**:447-451.
- Selmaj, K., W. Papierz, A. Glabinski, and T. Kohno. 1995. Prevention of chronic relapsing experimental autoimmune encephalomyelitis by soluble tumor necrosis factor receptor I. *J. Neuroimmunol.* **56**:135-141.
- Selmaj, K.W., and C.S. Raine. 1988. Tumor necrosis factor mediates myelin and oligodendrocyte damage in vitro. *Ann. Neurol.* **23**:339-346.
- Selmaj, K. W., C.S. Raine, and A.H. Cross. 1991. Anti-tumor necrosis factor therapy abrogates autoimmune demyelination. *Ann. Neurol.* **30**:694-700.
- Senger, D.R., L. Van de Water, L.F. Brown, J.A. Nagy, K.T. Yeo, T.K. Yeo, B. Berse, R.W. Jackman, A.M. Dvorak, and H.F. Dvorak. 1993. Vascular permeability factor (VPF, VEGF) in tumor biology. *Cancer Metastasis Rev.* **12**:303-324.
- Serafini, B., B. Rosicarelli, D. Franciotta, R. Magliozzi, R. Reynolds, P. Cinque, L. Andreoni, P. Trivedi, M. Salvetti, A. Faggioni, and F. Aloisi. 2007. Dysregulated Epstein-Barr virus infection in the multiple sclerosis brain. *J. Exp. Med.* **204**:2899-2912.
- Sharief, M.K., and R. Hentges. 1991. Association between tumor necrosis factor-alpha and disease progression in patients with multiple sclerosis. *N. Engl. J. Med.* **325**:467-472.
- Sharief, M.K., M.A. Noori, M. Ciardi, A. Cirelli, and E.J. Thompson. 1993. Increased levels of circulating ICAM-1 in serum and cerebrospinal fluid of patients with active multiple sclerosis. Correlation with TNF-alpha and blood-brain barrier damage. *J. Neuroimmunol.* **43**:15-21.
- Sharp, P.A. 2001. RNA interference--2001. *Genes Dev.* **15**:485-490.

- Sicotte, N.L., and R.R. Voskuhl. 2001. Onset of multiple sclerosis associated with anti-TNF therapy. *Neurology*. **57**:1885-1888.
- Simi, A., N. Tsakiri, P. Wang, and N.J. Rothwell. 2007. Interleukin-1 and inflammatory neurodegeneration. *Biochem.Soc.Trans.* **35**:1122-1126.
- Simpson, J.E., J. Newcombe, M.L. Cuzner, and M.N. Woodroffe. 2000. Expression of the interferon-gamma-inducible chemokines IP-10 and Mig and their receptor, CXCR3, in multiple sclerosis lesions. *Neuropathol.Appl.Neurobiol.* **26**:133-142.
- Singh, R.J., J.C. Mason, E.A. Lidington, D.R. Edwards, R.K. Nuttall, R. Khokha, V. Knauper, G. Murphy, and J. Gavrilovic. 2005. Cytokine stimulated vascular cell adhesion molecule-1 (VCAM-1) ectodomain release is regulated by TIMP-3. *Cardiovasc.Res.* **67**:39-49.
- Sipe, K.J., D. Srisawasdi, R. Dantzer, K.W. Kelley, and J.A. Weyhenmeyer. 1996. An endogenous 55 kDa TNF receptor mediates cell death in a neural cell line. *Brain Res.Mol.Brain Res.* **38**:222-232.
- Sippy, B.D., F.M. Hofman, D. Wallach, and D.R. Hinton. 1995. Increased expression of tumor necrosis factor-alpha receptors in the brains of patients with AIDS. *J.Acquir.Immune Defic.Syndr.Hum.Retrovirol.* **10**:511-521.
- Skegg, D.C., P.A. Corwin, R.S. Craven, J.A. Malloch, and M. Pollock. 1987. Occurrence of multiple sclerosis in the north and south of New Zealand. *J.Neurol.Neurosurg.Psychiatry.* **50**:134-139.
- Skinner, M.P., C.M. Lucas, G.F. Burns, C.N. Chesterman, and M.C. Berndt. 1991. GMP-140 binding to neutrophils is inhibited by sulfated glycans. *J.Biol.Chem.* **266**:5371-5374.
- Skovronsky, D.M., S. Fath, V.M. Lee, and M.E. Milla. 2001. Neuronal localization of the TNFalpha converting enzyme (TACE) in brain tissue and its correlation to amyloid plaques. *J.Neurobiol.* **49**:40-46.
- Skovronsky, D.M., D.B. Moore, M.E. Milla, R.W. Doms, and V.M. Lee. 2000. Protein kinase C-dependent alpha-secretase competes with beta-secretase for cleavage of amyloid-beta precursor protein in the trans-Golgi network. *J.Biol.Chem.* **275**:2568-2575.
- Slack, B.E., L.K. Ma, and C.C. Seah. 2001. Constitutive shedding of the amyloid precursor protein ectodomain is up-regulated by tumour necrosis factor-alpha converting enzyme. *Biochem.J.* **357**:787-794.
- Smith, S.S., M. Ludwig, J.E. Wohler, D.C. Bullard, A.J. Szalai, and S.R. Barnum. 2008. Deletion of both ICAM-1 and C3 enhances severity of experimental autoimmune encephalomyelitis compared to C3-deficient mice. *Neurosci.Lett.* **442**:158-160.
- Snove, O., Jr, and J.J. Rossi. 2006. Expressing short hairpin RNAs in vivo. *Nat.Methods.* **3**:689-695.
- Sobel, R., A, and W. Moore G. R. 2008. Demyelinating diseases. *In Greenfield's Neuropathology*. 8th Ed. S. Love, D. Louis N and D. Ellison W, editors.
- Sobel, R.A., M.E. Mitchell, and G. Fondren. 1990. Intercellular adhesion molecule-1 (ICAM-1) in cellular immune reactions in the human central nervous system. *Am.J.Pathol.* **136**:1309-1316.

- Soderstrom, M., J. Hillert, J. Link, V. Navikas, S. Fredrikson, and H. Link. 1995. Expression of IFN-gamma, IL-4, and TGF-beta in multiple sclerosis in relation to HLA-Dw2 phenotype and stage of disease. *Mult.Scler.* **1**:173-180.
- Sorensen, T.L., M. Tani, J. Jensen, V. Pierce, C. Lucchinetti, V.A. Folcik, S. Qin, J. Rottman, F. Sellebjerg, R.M. Strieter, J.L. Frederiksen, and R.M. Ransohoff. 1999. Expression of specific chemokines and chemokine receptors in the central nervous system of multiple sclerosis patients. *J.Clin.Invest.* **103**:807-815.
- Soriano, S.G., L.S. Amaravadi, Y.F. Wang, H. Zhou, G.X. Yu, J.R. Tonra, V. Fairchild-Huntress, Q. Fang, J.H. Dunmore, D. Huszar, and Y. Pan. 2002. Mice deficient in fractalkine are less susceptible to cerebral ischemia-reperfusion injury. *J.Neuroimmunol.* **125**:59-65.
- Sporer, B., S. Kastenbauer, U. Koedel, G. Arendt, and H.W. Pfister. 2003. Increased intrathecal release of soluble fractalkine in HIV-infected patients. *AIDS Res.Hum.Retroviruses.* **19**:111-116.
- Spranger, M., Fontana, A. 1996. Activation of microglia: a dangerous interlude in immune function in the brain. *Neuroscientist.* **2**:293.
- Stephan, C.C., and T.A. Brock. 1996. Vascular endothelial growth factor, a multifunctional polypeptide. *P.R.Health Sci.J.* **15**:169-178.
- Stephens, D.J., and V.J. Allan. 2003. Light microscopy techniques for live cell imaging. *Science.* **300**:82-86.
- Stevens, A., and J. Lowe. 1997. Histology: don't switch off! Techniques used in histology and cell biology. In *Human Histology*. Mosby, an imprint of Times Mirror International Publishers Limited, Grafos SA, Arte sobre papel, Barcelona, Spain: pp1-8.
- Stevenson, B.R., and B.H. Keon. 1998. The tight junction: morphology to molecules. *Annu.Rev.Cell Dev.Biol.* **14**:89-109.
- Stoddart, J.H., Jr, R.R. Jasuja, M.A. Sikorski, U.H. von Andrian, and J.W. Mier. 1996. Protease-resistant L-selectin mutants. Down-modulation by cross-linking but not cellular activation. *J.Immunol.* **157**:5653-5659.
- Strunk, R., and H.R. Colten. 1976. Inhibition of the enzymatic activity of the first component of complement (C1) by heparin. *Clin.Immunol.Immunopathol.* **6**:248-255.
- Stuve, O., C.M. Marra, P.D. Cravens, M.P. Singh, W. Hu, A. Lovett-Racke, N.L. Monson, J.T. Phillips, J.W. Cohen Tervaert, R.A. Nash, H.P. Hartung, B.C. Kieseier, M.M. Racke, E.M. Frohman, and B. Hemmer. 2007. Potential risk of progressive multifocal leukoencephalopathy with natalizumab therapy: possible interventions. *Arch.Neurol.* **64**:169-176.
- Su, J.J., M. Osoegawa, T. Matsuoka, M. Minohara, M. Tanaka, T. Ishizu, F. Mihara, T. Taniwaki, and J. Kira. 2006. Upregulation of vascular growth factors in multiple sclerosis: correlation with MRI findings. *J.Neurol.Sci.* **243**:21-30.
- Subramanian, S.V., M.L. Fitzgerald, and M. Bernfield. 1997. Regulated shedding of syndecan-1 and -4 ectodomains by thrombin and growth factor receptor activation. *J.Biol.Chem.* **272**:14713-14720.

- Sunnemark, D., S. Eltayeb, M. Nilsson, E. Wallstrom, H. Lassmann, T. Olsson, A.L. Berg, and A. Ericsson-Dahlstrand. 2005. CX3CL1 (fractalkine) and CX3CR1 expression in myelin oligodendrocyte glycoprotein-induced experimental autoimmune encephalomyelitis: kinetics and cellular origin. *J.Neuroinflammation*. **2**:17.
- Suzuki, F., T. Nanki, T. Imai, H. Kikuchi, S. Hirohata, H. Kohsaka, and N. Miyasaka. 2005. Inhibition of CX3CL1 (fractalkine) improves experimental autoimmune myositis in SJL/J mice. *J.Immunol*. **175**:6987-6996.
- Svejgaard, A. 2008. The immunogenetics of multiple sclerosis. *Immunogenetics*. **60**:275-286.
- Takeda, S., T. Igarashi, H. Mori, and S. Araki. 2006. Crystal structures of VAP1 reveal ADAMs' MDC domain architecture and its unique C-shaped scaffold. *EMBO J*. **25**:2388-2396.
- Tartaglia, L.A., and D.V. Goeddel. 1992. Two TNF receptors. *Immunol.Today*. **13**:151-153.
- Tellier, E., M. Canault, M. Poggi, B. Bonardo, A. Nicolay, M.C. Alessi, G. Nalbone, and F. Peiretti. 2008. HDLs activate ADAM17-dependent shedding. *J.Cell.Physiol*. **214**:687-693.
- Tellier, E., M. Canault, L. Rebsomen, B. Bonardo, I. Juhan-Vague, G. Nalbone, and F. Peiretti. 2006. The shedding activity of ADAM17 is sequestered in lipid rafts. *Exp.Cell Res*. **312**:3969-3980.
- The IFN- β Multiple Sclerosis Study Group and The University of British Columbia MS/MRI Analysis Group. 1995. Interferon beta-1b in the treatment of multiple sclerosis: final outcome of the randomized controlled trial. *Neurology*. **45** (7): 1277-1285.
- Thomas, K.A. 1996. Vascular endothelial growth factor, a potent and selective angiogenic agent. *J.Biol.Chem*. **271**:603-606.
- Thompson, A.J., C.H. Polman, D.H. Miller, W.I. McDonald, B. Brochet, X. Filippi M Montalban, and J. De Sa. 1997. Primary progressive multiple sclerosis. *Brain*. **120** (6):1085-1096.
- Toft-Hansen, H., A.A. Babcock, J.M. Millward, and T. Owens. 2007. Downregulation of membrane type-matrix metalloproteinases in the inflamed or injured central nervous system. *J.Neuroinflammation*. **4**:24.
- Toft-Hansen, H., R. Buist, X.J. Sun, A. Schellenberg, J. Peeling, and T. Owens. 2006. Metalloproteinases control brain inflammation induced by pertussis toxin in mice overexpressing the chemokine CCL2 in the central nervous system. *J.Immunol*. **177**:7242-7249.
- Toft-Hansen, H., R.K. Nuttall, D.R. Edwards, and T. Owens. 2004. Key metalloproteinases are expressed by specific cell types in experimental autoimmune encephalomyelitis. *J.Immunol*. **173**:5209-5218.
- Trapp, B.D., and K.A. Nave. 2008. Multiple sclerosis: an immune or neurodegenerative disorder? *Annu.Rev.Neurosci*. **31**:247-269.
- Trapp, B.D., J. Peterson, R.M. Ransohoff, R. Rudick, S. Mork, and L. Bo. 1998. Axonal transection in the lesions of multiple sclerosis. *N.Engl.J.Med*. **338**:278-285.

Traugott, U., and P. Lebon. 1988. Interferon-gamma and Ia antigen are present on astrocytes in active chronic multiple sclerosis lesions. *J.Neurol.Sci.* **84**:257-264.

Trojano, M., C. Avolio, I.L. Simone, G. Defazio, C. Manzari, F. De Robertis, A. Calo, and P. Livrea. 1996. Soluble intercellular adhesion molecule-1 in serum and cerebrospinal fluid of clinically active relapsing-remitting multiple sclerosis: correlation with Gd-DTPA magnetic resonance imaging-enhancement and cerebrospinal fluid findings. *Neurology.* **47**:1535-1541.

Tsou, C.L., C.A. Haskell, and I.F. Charo. 2001. Tumor necrosis factor-alpha-converting enzyme mediates the inducible cleavage of fractalkine. *J.Biol.Chem.* **276**:44622-44626.

Tsukada, N., M. Matsuda, K. Miyagi, and N. Yanagisawa. 1993. Increased levels of intercellular adhesion molecule-1 (ICAM-1) and tumor necrosis factor receptor in the cerebrospinal fluid of patients with multiple sclerosis. *Neurology.* **43**:2679-2682.

Tuschl, T. 2001. RNA interference and small interfering RNAs. *Chembiochem.* **2**:239-245.

Tzartos, J.S., M.A. Friese, M.J. Craner, J. Palace, J. Newcombe, M.M. Esiri, and L. Fugger. 2008. Interleukin-17 production in central nervous system-infiltrating T cells and glial cells is associated with active disease in multiple sclerosis. *Am.J.Pathol.* **172**:146-155.

Ubogu, E.E., M.B. Cossoy, and R.M. Ransohoff. 2006. The expression and function of chemokines involved in CNS inflammation. *Trends Pharmacol.Sci.* **27**:48-55.

Ukkonen, M., K. Wu, B. Reipert, P. Dastidar, and I. Elovaara. 2007. Cell surface adhesion molecules and cytokine profiles in primary progressive multiple sclerosis. *Mult.Scler.* **13**:701-707.

Vaillant, C., M. Didier-Bazes, A. Hutter, M.F. Belin, and N. Thomasset. 1999. Spatiotemporal expression patterns of metalloproteinases and their inhibitors in the postnatal developing rat cerebellum. *J.Neurosci.* **19**:4994-5004.

Vaknin-Dembinsky, A., K. Balashov, and H.L. Weiner. 2006. IL-23 is increased in dendritic cells in multiple sclerosis and down-regulation of IL-23 by antisense oligos increases dendritic cell IL-10 production. *J.Immunol.* **176**:7768-7774.

van der Valk, P., and C.J. De Groot. 2000. Staging of multiple sclerosis (MS) lesions: pathology of the time frame of MS. *Neuropathol.Appl.Neurobiol.* **26**:2-10.

Van Der Voorn, P., J. Tekstra, R.H. Beelen, C.P. Tensen, P. Van Der Valk, and C.J. De Groot. 1999. Expression of MCP-1 by reactive astrocytes in demyelinating multiple sclerosis lesions. *Am.J.Pathol.* **154**:45-51.

van Horssen, J., L. Bo, C.M. Vos, I. Virtanen, and H.E. de Vries. 2005. Basement membrane proteins in multiple sclerosis-associated inflammatory cuffs: potential role in influx and transport of leukocytes. *J.Neuropathol.Exp.Neurol.* **64**:722-729.

van Noort, J.M., J.J. Bajramovic, A.C. Plomp, and M.J. van Stipdonk. 2000. Mistaken self, a novel model that links microbial infections with myelin-directed autoimmunity in multiple sclerosis. *J.Neuroimmunol.* **105**:46-57.

- van Oosten, B.W., F. Barkhof, L. Truyen, J.B. Boringa, F.W. Bertelsmann, B.M. von Blomberg, J.N. Woody, H.P. Hartung, and C.H. Polman. 1996. Increased MRI activity and immune activation in two multiple sclerosis patients treated with the monoclonal anti-tumor necrosis factor antibody cA2. *Neurology*. **47**:1531-1534.
- van Waesberghe, J.H., W. Kamphorst, C.J. De Groot, M.A. van Walderveen, J.A. Castelijns, R. Ravid, G.J. Lycklama a Nijeholt, P. van der Valk, C.H. Polman, A.J. Thompson, and F. Barkhof. 1999. Axonal loss in multiple sclerosis lesions: magnetic resonance imaging insights into substrates of disability. *Ann.Neurol*. **46**:747-754.
- van Walderveen, M.A., W. Kamphorst, P. Scheltens, J.H. van Waesberghe, R. Ravid, J. Valk, C.H. Polman, and F. Barkhof. 1998. Histopathologic correlate of hypointense lesions on T1-weighted spin-echo MRI in multiple sclerosis. *Neurology*. **50**:1282-1288.
- Venken, K., N. Hellings, K. Hensen, J.L. Rummens, R. Medaer, M.B. D'hooghe, B. Dubois, J. Raus, and P. Stinissen. 2006. Secondary progressive in contrast to relapsing-remitting multiple sclerosis patients show a normal CD4+CD25+ regulatory T-cell function and FOXP3 expression. *J.Neurosci.Res*. **83**:1432-1446.
- Venken, K., N. Hellings, M. Thewissen, V. Somers, K. Hensen, J.L. Rummens, R. Medaer, R. Hupperts, and P. Stinissen. 2008. Compromised CD4+ CD25(high) regulatory T-cell function in patients with relapsing-remitting multiple sclerosis is correlated with a reduced frequency of FOXP3-positive cells and reduced FOXP3 expression at the single-cell level. *Immunology*. **123**:79-89.
- Vercellino, M., F. Plano, B. Votta, R. Mutani, M.T. Giordana, and P. Cavalla. 2005. Grey matter pathology in multiple sclerosis. *J.Neuropathol.Exp.Neurol*. **64**:1101-1107.
- Viglietta, V., C. Baecher-Allan, H.L. Weiner, and D.A. Hafler. 2004. Loss of functional suppression by CD4+CD25+ regulatory T cells in patients with multiple sclerosis. *J.Exp.Med*. **199**:971-979.
- Vilcek, J., and M. Feldmann. 2004. Historical review: Cytokines as therapeutics and targets of therapeutics. *Trends Pharmacol.Sci*. **25**:201-209.
- Volin, M.V., J.M. Woods, M.A. Amin, M.A. Connors, L.A. Harlow, and A.E. Koch. 2001. Fractalkine: a novel angiogenic chemokine in rheumatoid arthritis. *Am.J.Pathol*. **159**:1521-1530.
- Vos, C.M., J.J. Geurts, L. Montagne, E.S. van Haastert, L. Bo, P. van der Valk, F. Barkhof, and H.E. de Vries. 2005. Blood-brain barrier alterations in both focal and diffuse abnormalities on postmortem MRI in multiple sclerosis. *Neurobiol.Dis*. **20**:953-960.
- Walsh, S.V., A.M. Hopkins, and A. Nusrat. 2000. Modulation of tight junction structure and function by cytokines. *Adv.Drug Deliv.Rev*. **41**:303-313.
- Wang, W., W.L. Dentler, and R.T. Borchardt. 2001. VEGF increases BMEC monolayer permeability by affecting occludin expression and tight junction assembly. *Am.J.Physiol.Heart Circ.Physiol*. **280**:H434-40.
- Wang, X., G.Z. Feuerstein, L. Xu, H. Wang, W.A. Schumacher, M.L. Ogletree, R. Taub, J.J. Duan, C.P. Decicco, and R.Q. Liu. 2004. Inhibition of tumor necrosis factor-alpha-converting enzyme by a selective antagonist protects brain from focal ischemic injury in rats. *Mol.Pharmacol*. **65**:890-896.

- Washington, R., J. Burton, R.F. Todd 3rd, W. Newman, L. Dragovic, and P. Dore-Duffy. 1994. Expression of immunologically relevant endothelial cell activation antigens on isolated central nervous system microvessels from patients with multiple sclerosis. *Ann.Neurol.* **35**:89-97.
- Watt, S.M., J. Williamson, H. Genevier, J. Fawcett, D.L. Simmons, A. Hatzfeld, S.A. Nesbitt, and D.R. Coombe. 1993. The heparin binding PECAM-1 adhesion molecule is expressed by CD34+ hematopoietic precursor cells with early myeloid and B-lymphoid cell phenotypes. *Blood.* **82**:2649-2663.
- Waubant, E., D.E. Goodkin, L. Gee, P. Bacchetti, R. Sloan, T. Stewart, P.B. Andersson, G. Stabler, and K. Miller. 1999. Serum MMP-9 and TIMP-1 levels are related to MRI activity in relapsing multiple sclerosis. *Neurology.* **53**:1397-1401.
- Waxman, S.G. 2008. Mechanisms of disease: sodium channels and neuroprotection in multiple sclerosis-current status. *Nat.Clin.Pract.Neurol.* **4**:159-169.
- Waxman, S.G. 2006. Axonal conduction and injury in multiple sclerosis: the role of sodium channels. *Nat.Rev.Neurosci.* **7**:932-941.
- Waxman, S.G. 1997. Molecular remodeling of neurons in multiple sclerosis: what we know, and what we must ask about brain plasticity in demyelinating diseases. *Adv.Neurol.* **73**:109-120.
- Weber, B.H., G. Vogt, R.C. Pruett, H. Stohr, and U. Felbor. 1994. Mutations in the tissue inhibitor of metalloproteinases-3 (TIMP3) in patients with Sorsby's fundus dystrophy. *Nat.Genet.* **8**:352-356.
- Wej, S., M. Kashiwagi, S. Kota, Z. Xie, H. Nagase, and K. Brew. 2005. Reactive site mutations in tissue inhibitor of metalloproteinase-3 disrupt inhibition of matrix metalloproteinases but not tumor necrosis factor-alpha-converting enzyme. *J.Biol.Chem.* **280**:32877-32882.
- Weksler, B.B., E.A. Subileau, N. Perriere, P. Charneau, K. Holloway, M. Leveque, H. Tricoire-Leignel, A. Nicotra, S. Bourdoulous, P. Turowski, D.K. Male, F. Roux, J. Greenwood, I.A. Romero, and P.O. Couraud. 2005. Blood-brain barrier-specific properties of a human adult brain endothelial cell line. *FASEB J.* **19**:1872-1874.
- Wetzel, M., G.A. Rosenberg, and L.A. Cunningham. 2003. Tissue inhibitor of metalloproteinases-3 and matrix metalloproteinase-3 regulate neuronal sensitivity to doxorubicin-induced apoptosis. *Eur.J.Neurosci.* **18**:1050-1060.
- Wild-Bode, C., K. Fellerer, J. Kugler, C. Haass, and A. Capell. 2006. A basolateral sorting signal directs ADAM10 to adherens junctions and is required for its function in cell migration. *J.Biol.Chem.* **281**:23824-23829.
- Willenborg, D.O., S.A. Fordham, M.A. Staykova, I.A. Ramshaw, and W.B. Cowden. 1999. IFN-gamma is critical to the control of murine autoimmune encephalomyelitis and regulates both in the periphery and in the target tissue: a possible role for nitric oxide. *J.Immunol.* **163**:5278-5286.
- Willer, C.J., D.A. Dymont, N.J. Risch, A.D. Sadovnick, G.C. Ebers, and Canadian Collaborative Study Group. 2003. Twin concordance and sibling recurrence rates in multiple sclerosis. *Proc.Natl.Acad.Sci.U.S.A.* **100**:12877-12882.

- Winges, K.M., D.H. Gilden, J.L. Bennett, X. Yu, A.M. Ritchie, and G.P. Owens. 2007. Analysis of multiple sclerosis cerebrospinal fluid reveals a continuum of clonally related antibody-secreting cells that are predominantly plasma blasts. *J.Neuroimmunol.* **192**:226-234.
- Wisniewska, M., P. Goettig, K. Maskos, E. Belouski, D. Winters, R. Hecht, R. Black, and W. Bode. 2008. Structural determinants of the ADAM inhibition by TIMP-3: crystal structure of the TACE-N-TIMP-3 complex. *J.Mol.Biol.* **381**:1307-1319.
- Wolburg, H., K. Wolburg-Buchholz, and B. Engelhardt. 2005. Diapedesis of mononuclear cells across cerebral venules during experimental autoimmune encephalomyelitis leaves tight junctions intact. *Acta Neuropathol.* **109**:181-190.
- Wong, B.W., D. Wong, and B.M. McManus. 2002. Characterization of fractalkine (CX3CL1) and CX3CR1 in human coronary arteries with native atherosclerosis, diabetes mellitus, and transplant vascular disease. *Cardiovasc.Pathol.* **11**:332-338.
- Wong, D., and K. Dorovini-Zis. 1995. Expression of vascular cell adhesion molecule-1 (VCAM-1) by human brain microvessel endothelial cells in primary culture. *Microvasc.Res.* **49**:325-339.
- Woodroffe, M.N., and M.L. Cuzner. 1993. Cytokine mRNA expression in inflammatory multiple sclerosis lesions: detection by non-radioactive in situ hybridization. *Cytokine.* **5**:583-588.
- Yang, S., K. Toy, G. Ingle, C. Zlot, P.M. Williams, G. Fuh, B. Li, A. de Vos, and M.E. Gerritsen. 2002. Vascular endothelial growth factor-induced genes in human umbilical vein endothelial cells: relative roles of KDR and Flt-1 receptors. *Arterioscler.Thromb.Vasc.Biol.* **22**:1797-1803.
- Yang, X.P., S. Mattagajasingh, S. Su, G. Chen, Z. Cai, K. Fox-Talbot, K. Irani, and L.C. Becker. 2007. Fractalkine upregulates intercellular adhesion molecule-1 in endothelial cells through CX3CR1 and the Jak Stat5 pathway. *Circ.Res.* **101**:1001-1008.
- Yednock, T.A., C. Cannon, L.C. Fritz, F. Sanchez-Madrid, L. Steinman, and N. Karin. 1992. Prevention of experimental autoimmune encephalomyelitis by antibodies against alpha 4 beta 1 integrin. *Nature.* **356**:63-66.
- Yeo, T.W., P.L. De Jager, S.G. Gregory, L.F. Barcellos, A. Walton, A. Goris, C. Fenoglio, M. Ban, C.J. Taylor, R.S. Goodman, E. Walsh, C.S. Wolfish, R. Horton, J. Traherne, S. Beck, J. Trowsdale, S.J. Caillier, A.J. Iverson, T. Green, S. Pobywajlo, E.S. Lander, M.A. Pericak-Vance, J.L. Haines, M.J. Daly, J.R. Oksenberg, S.L. Hauser, A. Compston, D.A. Hafler, J.D. Rioux, and S. Sawcer. 2007. A second major histocompatibility complex susceptibility locus for multiple sclerosis. *Ann.Neurol.* **61**:228-236.
- Yong, V.W., C. Power, P. Forsyth, and D.R. Edwards. 2001. Metalloproteinases in biology and pathology of the nervous system. *Nat.Rev.Neurosci.* **2**:502-511.
- Yong, V.W., R.K. Zabad, S. Agrawal, A. Goncalves Dasilva, and L.M. Metz. 2007. Elevation of matrix metalloproteinases (MMPs) in multiple sclerosis and impact of immunomodulators. *J.Neurol.Sci.* **259**:79-84.
- Yu, W.H., S. Yu, Q. Meng, K. Brew, and J.F. Woessner Jr. 2000. TIMP-3 binds to sulfated glycosaminoglycans of the extracellular matrix. *J.Biol.Chem.* **275**:31226-31232.

Zaffaroni, M. 2003. Biological indicators of the neurodegenerative phase of multiple sclerosis. *Neurol.Sci.* **24** Suppl 5:S279-82.

Zamore, P.D. 2001. RNA interference: listening to the sound of silence. *Nat.Struct.Biol.* **8**:746-750.

Zhang, X.P., T. Kamata, K. Yokoyama, W. Puzon-McLaughlin, and Y. Takada. 1998. Specific interaction of the recombinant disintegrin-like domain of MDC-15 (metargidin, ADAM-15) with integrin alphavbeta3. *J.Biol.Chem.* **273**:7345-7350.

Zhao, L., M. Shey, M. Farnsworth, and M.O. Dailey. 2001. Regulation of membrane metalloproteolytic cleavage of L-selectin (CD62I) by the epidermal growth factor domain. *J.Biol.Chem.* **276**:30631-30640.

Zhong, H., and J.W. Simons. 1999. Direct comparison of GAPDH, beta-actin, cyclophilin, and 28S rRNA as internal standards for quantifying RNA levels under hypoxia. *Biochem.Biophys.Res.Commun.* **259**:523-526.

Zozulya, A.L., E. Reinke, D.C. Baiu, J. Karman, M. Sandor, and Z. Fabry. 2007. Dendritic cell transmigration through brain microvessel endothelium is regulated by MIP-1alpha chemokine and matrix metalloproteinases. *J.Immunol.* **178**:520-529.

Zujovic, V., J. Benavides, X. Vige, C. Carter, and V. Taupin. 2000. Fractalkine modulates TNF-alpha secretion and neurotoxicity induced by microglial activation. *Glia.* **29**:305-315.

The London Multi-Centre Research Ethics Committee

10th June 2002
pw/lc/02-39

The Old Refectory
Central Middlesex Hospital
Acton Lane
London
NW10 7NS

Professor Richard Reynolds
Professor of Cellular Neurobiology
Department of Neuroinflammation
Division of Neuroscience
Imperial College of Faculty of Medicine
Charing Cross Campus
Fulham Palace Road
London W6 8RF

Tel: 020 8453 2336
Fax: 020 8961 0012
Email: louise.cox@nwlh.nhs.uk

Dear Professor Reynolds

Application Reference Number MREC/02/2/39
Title The UK Multiple Sclerosis Tissue Bank

The Chairman of the London Multicentre Research Ethics Committee has considered the amendments submitted in response to the Committee's earlier review of your application on 24th April 2002 as set out in our letter dated 1st May 2002. The documents considered were as follows:

<i>Letter from Professor Reynolds</i>	<i>(received 6th June 2002)</i>
<i>MREC Application Form</i>	<i>(dated 21st February 2002)</i>
<i>Protocol (Appendix 1)</i>	<i>(Version 1, dated 21st February 2002)</i>
<i>Information Sheet</i>	<i>(Version 3, dated June 2002)</i>
<i>Consent Form</i>	<i>(Version 1, dated 21st February 2002)</i>
<i>Agreement of Next-of-Kin or Legal Representative to the Donation of Tissue Form</i>	<i>(Version 1, dated 21st February 2002)</i>
<i>Agreement of Next-of-Kin or Legal Representative to Consult the Medical Records of a Tissue Donor</i>	<i>(Version 1, dated 21st February 2002)</i>
<i>Advertisement</i>	<i>(Version 1, dated 21st February 2002)</i>
<i>The Bank Statement Newsletter</i>	<i>(Issue 1)</i>
<i>Article: "A Very Special Bank"</i>	<i>(Frontiers)</i>

The Chairman, acting under delegated authority, is satisfied that these accord with the decision of the Committee and has agreed that there is no objection on ethical grounds to the proposed study. I am, therefore, happy to give you our approval on the understanding that you will follow the conditions of the approval set out below. A full record of the review undertaken by the MREC is contained in the attached MREC Response Form. The project must be started within three years of the date on which MREC approval is given.

While undertaking the review of your application the MREC noted the research involves the establishment of a new disease or patient database for research purposes / the use of an existing database collected for previous research or other purposes with subsequent patient contact. For this reason you are asked to read carefully the sections concerning LREC involvement and local NHS management set out below as there are specific requirements involved when undertaking such research.

MREC Conditions of Approval

- No research procedures are undertaken until the appropriate local research ethics committees is informed of the research including the name of the local clinician involved.
- The local clinician must inform his/her NHS organisation of their co-operation in the research project.
- The protocol approved by the MREC is followed and any changes to the protocol are undertaken only after MREC approval.
- If projects are approved before funding is received, the MREC must see, and approve, any major changes made by the funding body. The MREC would expect to see a copy of the final questionnaire before it is used.
- You must promptly inform the MREC of:
 - (i) any changes that increase the risk to subjects and/or affect significantly the conduct of the research;
 - (ii) any new information that may affect adversely the safety or welfare of the subjects or the conduct of the trial.
- You must complete and return to the MREC the annual review form that will be sent to you once a year, and the final report form when your research is completed.

LREC involvement

When undertaking the review of your project the MREC observed that there is/ limited patient contact involving the performance of a technical procedures or additional data collection as described in the MREC approved protocol/ initial contact by a local clinician for purposes of recruitment. It is felt that these tasks appear well within his/her routine professional competence and adequate facilities for such procedure are available as part of his/her normal professional practice.

For this reason you are asked to only inform the appropriate LREC of the project by sending a copy of this letter and also **giving the name and contact details of the local clinician involved and what procedures will be undertaken by this person.** If (unusually) the LREC has any reason to doubt that the local clinician is competent to carry out the tasks required, it will inform the clinician and the MREC that gave ethical approval giving full reasons.

When such tasks are performed by centrally based researchers it should be assumed that the MREC has reviewed their competence to undertake the tasks and it is not necessary to inform the LREC of the contact details but only that the research will take place.

You are not required to wait for confirmation from the LREC before starting your research.

Local NHS Management

The local clinician must inform his/her NHS organisation of their co-operation in the research project and the nature of their involvement. Care should be taken to ensure with the NHS organisation that local indemnity arrangements are adequate.

Legal and Regulatory Requirements

It remains your responsibility to ensure in the subsequent collection, storage or use of data or research sample you are not contravening the legal or regulatory requirements of any part of the UK in which the research material is collected, stored or used. If data is transferred outside the UK you should be aware of the requirements of the Data Protection Act 1998.

ICH GCP Compliance

The MRECs are fully compliant with the International Conference on Harmonisation/Good Clinical Practice (ICH GCP) Guidelines for the Conduct of Trials Involving the Participation of Human Subjects as they relate to the responsibilities, composition, function, operations and records of an Independent Ethics Committee/Independent Review Board. To this end it undertakes to adhere as far as is consistent with its Constitution, to the relevant clauses of the ICH Harmonised Tripartite Guideline for Good Clinical Practice, adopted by the Commission of the European Union on 17 January 1997. The Standing Orders and a Statement of Compliance were included on the computer disk containing the guidelines and application form and are available on request or on the Internet at www.corec.org.uk

Yours sincerely



Louise Cox
Administrator
The London Multicentre Research Ethics Committee

Enc